Structural and Geochronological Constraints on the Ductile Deformation Observed Along the Gaoligong Shan And Chong Shan Shear Zones, Yunnan (China)

by

Sinan Osman Akciz

B.S. Geology
Istanbul Technical University, Turkey, 1997

Submitted to the Department of Earth, Atmospheric, and Planetary Sciences in partial fulfillment of the requirements for the degree of

Doctor of Philosophy
at the

MASSACHUSETTS INSTITUTE OF TECHNOLOGY
September 2004

Signature of Author .....
Department of Earth, Atmospheric, and Planetary Sciences
August, 2004

Certified by .....
B. Clark Burchfiel
Schlumberger Professor of Geology
Thesis Supervisor

Accepted by .....
Maria T. Zuber
E.A. Griswold Professor of Geophysics and Planetary Science
Department Head

Structural and Geochronological Constraints on the Ductile Deformation Observed Along the Gaoligong Shan And Chong Shan Shear Zones, Yunnan (China)

by
Sinan Osman Akciz
B.S. Geology
Istanbul Technical University, Turkey, 1997

Submitted to the Department of Earth, Atmospheric, and Planetary Sciences on September 09, 2004, in partial fulfillment of the requirements for the degree of Doctor of Philosophy

Abstract

The mechanism by which the Cenozoic post-collisional northward motion of India relative to Eurasia and South China was accommodated along its eastern boundary is still a poorly understood aspect of the tectonic evolution of SE Asia. This thesis focuses on a critically important area within the India-Eurasia collision zone, a region known as the Three Rivers area, and presents the first structural and geochronological data from several transects across two poorly documented linear metamorphic belts located in between the Sagaing fault and the Ailao Shan Shear Zone: the Gaoligong Shan Shear Zone (GSSZ) and the Chong Shan Shear Zone (CSSZ) in Yunnan, China. The presently inactive GSSZ is an important dextral Cenozoic (and possibly latest Mesozoic) ductile shear zone and appears to be the only right-lateral shear zone with the appropriate orientation to accommodate major pre- ca. 11 Ma northward movement of India relative to Eurasia. The previously unknown CSSZ is a long (>300 km) and wide (10-20 km) metamorphic belt containing an assemblage low- to high-grade rocks from possibly several tectonic units which contain a prominent sub-vertical foliation and a sub-horizontal stretching lineation. Preliminary U/Pb results indicate that the ductile dextral shearing terminated by ~18 Ma. Our regional map compilations indicate that the GSSZ and its proposed conjugate, the ASSZ, likely terminate within the Bangong Co-Nujiang suture zone. This thesis documents the dextral GSSZ as the conjugate pair to the sinistral ASSZ, and thus constrains the limits of the crustal fragments that extruded to the southeast. Based on our reinterpretations of the geological maps of Tibet and the Three Rivers area, however, we propose that the extruded crustal material originated east of the easternmost corner of the Indian indentor, and did not create space for the penetration of India;. while at least limited extrusion did occur, there is no compelling geological evidence to indicate large-scale eastward movement of crustal material from directly north of the India indentor. Data presented in this thesis also indicate that extruded region was dismembered into at least two major crustal fragments, separated by the CSSZ.

Thesis Supervisor: Dr. B. Clark Burchfiel

Title: Schlumberger Professor of Geology

Acknowledgements

Seven Years at EAPS does not sound as appealing or exciting as "Seven Years in Tibet", but it has definitely been at least as adventuresome and emotional as the movie itself. Questions and answers are what life at MIT seems to be about. "Extrusion or no extrusion?" is the question I tried to answer in this thesis, but I would not have been able to do it without the help of many people who have been a part of my graduate education and my life, and it is now my great pleasure to take this opportunity to thank them.

First and foremost, I want to thank my thesis supervisor, B. Clark Burchfiel, for bringing me to MIT. You have given me enormous freedom to pursue my own interests while at the same time providing just the right amount of guidance. I am also deeply grateful for your encouragement and generous financial support these many years.

A very special word of thanks to a great friend, colleague and mentor, A.M. Celal Sengor, for sharing with me his unique way of seeing the world. Your passion for geology and enthusiasm will always be inspirational.

Many thanks go to the members of my doctoral advisory committee for their guidance and for contributing valuable insights to my thesis work.: Sam Bowring (Chair), Kip Hodges, Nafi Toksoz, and David Rowley. In particular I want to thank Sam and Kip for letting me use their labs. Special thanks go to David for listening to all my talks at geological meetings and for coming all the way from the University of Chicago to serve as my external examiner. I also thank Robert King and John Geissmann for their interest in my thesis work. My ever-smiling colleague Yin Jiyun, resourceful Institute contact Mr. Chen, and superb drivers Mr. Kou and Mr. Zhang made my long and wet field seasons run very smoothly and safely. I am looking forward to working on other outstanding questions with them.

Long hours at the Green building would not have been bearable if I were not surrounded by knowledgeable friends who helped me daily. I would like to acknowledge all of my fellow graduate students for their support and friendship over the years at MIT. Jahan Ramezani and James Crowley deserve special thanks for helping me immensely with the U-Pb analyses. Lindsay Schoenbohm and Alexis Ault read through the last minute drafts of this thesis, and I thank them for that. It was always enjoyable to chat with Daniel Sheehan, Arthur White and Bill Hutchison. I thank my officemate, Ben Crosby, for bearing with me and my mess for all these years. I owe a great deal to Marin Clark and Constantine Giannitsis. Life at MIT, however, would not have been the same without Simon Brocklehurst. Your generous nature and considerateness are deeply appreciated by this foreign driver!

I am grateful to Karen Garofalo, Roberta Bennett-Calorio, Carol Sprague and the EAPS librarians, Kathy Keefe and Joe Hankins, for helping me out and taking care of me during all these seven years of my MIT life. I am very grateful to have met Tony and to have seen him almost every night while I was finishing my thesis. Thank you for the delicious lentil soups and nightly chats.

I wish to thank Dilek Aydas, Emine Fetvaci Zach Magoon and Marcy Michaud, for helping me get through the difficult times, and for all the emotional support, adventure, entertainment, and caring they provided. Can Mardin, Berfin Seyhan, Gokhan Oguz and Neslihan Gok kept me up-to-date with Turkish news, rumors and humor. Thank you all for making me laugh and feel less homesick. I owe more than thanks to Alp and Hatice Kantarci, for their friendship, hospitality and care. Thank you for being there for me, "Pirim".

I cannot conclude without thanking Jessica Neu. Your patience and liveliness beats my stubbornness by far. I could not have finished this thesis without your support and love.

Lastly, and most importantly, I wish to thank my parents, Filiz and Suha Akciz. We went through a lot together, in these past seven years, even though we were a continent and an ocean apart. Thank you for sharing my "distant" life. Your patience and understanding made my MIT life much easier. To You, I dedicate this thesis.

The work in this thesis was supported by NSF grants #EAR-9706630 and #EAR-0003571.

Table of Contents

Chapter 1. INTRODUCTION

"Scientists still do not appear to understand sufficiently that all earth sciences must contribute evidence toward unveiling the state of our planet in earlier times, and that the truth of the matter can only be reached by combing all this evidence. . . It is only by combing the information furnished by all the earth sciences that we can hope to determine 'truth' here, that is to say, to find the picture that sets out all the known facts in the best arrangement and that therefore has the highest degree of probability. Further, we have to be prepared always for the possibility that each new discovery, no matter what science furnishes it, may modify the conclusions we draw."

Alfred Wegener. The Origins of Continents and Oceans (4th edition)

Chapter 1. INTRODUCTION

Since the collision between Eurasia and India at ~45 Ma (Rowley 1996, 1998) there has been between ~2,000 and ~3,500 km of convergence between India and Eurasia from the western to eastern Himalayan syntaxes, respectively, as shown by palaeomagnetic data (e.g. Patriat, 1983) and seafloor-spreading reconstructions (e.g. Molnar and Tapponnier, 1975; Patriat and Achache, 1984; Stock and Molnar, 1987). Much of this convergence appears to have been accommodated by internal deformation within Asia as southernmost Tibet has moved northwards by 2000(±900) km (Molnar and Tapponnier, 1975; Patriat and Achache, 1984). However, the mechanism by which the Cenozoic post-collisional northward motion of India relative to Eurasia and South China was accommodated along its eastern boundary is still a poorly understood component of the tectonic evolution of SE Asia. Models for the tectonic evolution range from southeastward extrusion of the region between the right-lateral Sagaing Fault in Burma and the left-lateral Ailao Shan Shear Zone (ASSZ) in Yunnan, China, as a single lithospheric block with minimal internal deformation and minor rotation (e.g. Tapponnier et al., 1982, 1986), to lateral spreading of thickened viscous lithosphere with little eastward extrusion (Houseman and England, 1993). Alternate models argue for eastward flow of lower crust accompanied by large-scale clockwise rotation and crustal thickening (Royden et al., 1997) and extrusion of crustal material accompanied by significant internal deformation and large-scale rotation of smaller crustal fragments (Wang and Burchfiel, 1997).

The concept of lateral extrusion in Cenozoic time (Figure 1), in particular, has played an important role in tectonic interpretations of Asia, especially since the publication of numerous detailed works conducted along the ASSZ (e.g. Tapponnier et al., 1982, 1986; Harrison et al.,

1992, 1996; Leloup et al., 1993, 1995; Schärer et al., 1990, 1994; Gilley et al., 2003). The ASSZ is interpreted to have accommodated 700±200 km of displacement of Indochina to the southeast relative to South China (Leloup et al., 1995) since at least 34 Ma, based on dating of monazite inclusions in syn-kinematic garnet (Gilley et al., 2003). U-Pb ages of accessory minerals from late syntectonic leucogranites parallel to the foliation and affected by left-lateral shearing cluster around 24 Ma (Leloup et al., 1995) indicate that the left-lateral shearing continued at least until this time. The $^{40}Ar/^{39}Ar$ data indicate that the ASSZ mylonites rapidly cooled during the lower Miocene, before the end of left-lateral motion (Harrison et al., 1992, 1996; Leloup et al., 1993). However, numerous important questions still remain unanswered regarding the nature and the style of deformation induced by the indentation of India into Asia: (1) Where is the right-lateral conjugate shear system to the left-lateral ASSZ, since the proposed Sagaing fault is only ~13 Ma old (Curray et al., 1979, Lawver et al., 1976) ? (2) Did the older shear system continue to be active once the Sagaing fault was initiated? (3) Has extrusion tectonics been largely accomplished by rigid block motion (Leloup et al., 1995), or by a series of internally deformed crustal fragments that translated and rotated differentially (Wang and Burchfiel, 1997) (Figure 2)? (4) How far can the ASSZ and its conjugate pair be followed to the north? Did they help crustal fragments to extrude from in front of India to the southeast in order to accommodate the indentation, or were they active only within the broad right-lateral accommodation zone east of India? (5) Did crustal anisotropies play a role in localizing the deformation associated with the indentation? (6) Could older zones of weaknesses, far field collisional events, and temporal changes in lithospheric rheologies contribute to the determination of the style of deformation resulting from the India – Eurasia collision, or should we still continue to perform analogue and numerical experiments assuming a temporal continuity in the style of deformation. The answers

to these questions are not only important in understanding how continental SE Asia evolved in the Cenozoic times, but also in understanding

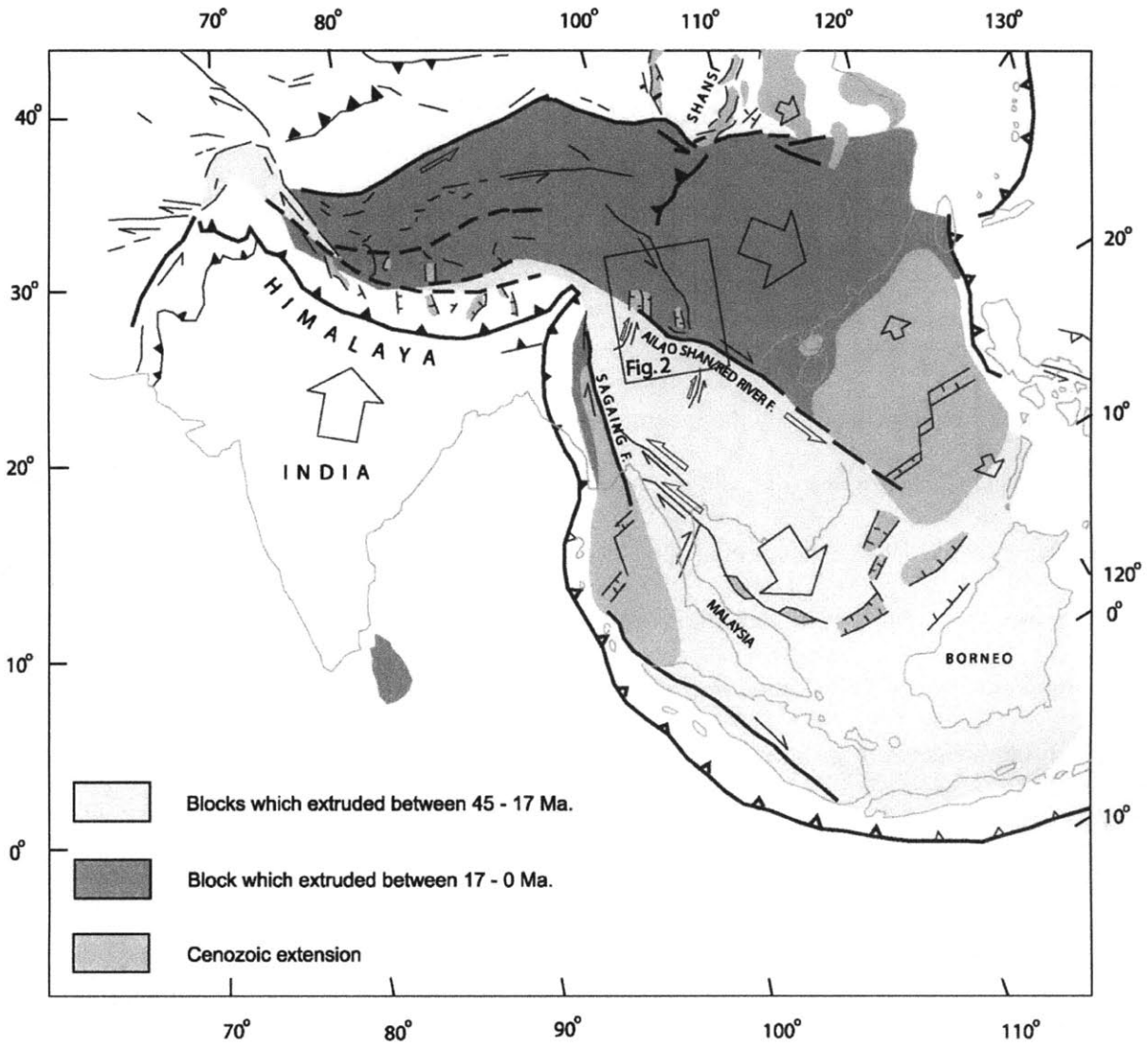

Figure 1. Schematic map of Cenozoic extrusion and large faults in Eastern Asia (modified after Tapponnier et al., 1986). Heavy lines indicate major faults or plate boundaries. Small arrows show senses of finite motion on strike-slip faults. Open arrows represent the sense of motion from Eocene until mid-Miocene, Solid arrows indicate the present day senses of motion, deduced from morphological offsets and seismicity. Shaded areas represent the regions affected by the different extrusion phases. Large open arrows represent the major block motions with respect to Siberia since the Eocene.

the kinematic and dynamic processes operating within regions of intracontinental convergence, which still remains one of the most challenging and important problems in tectonics.

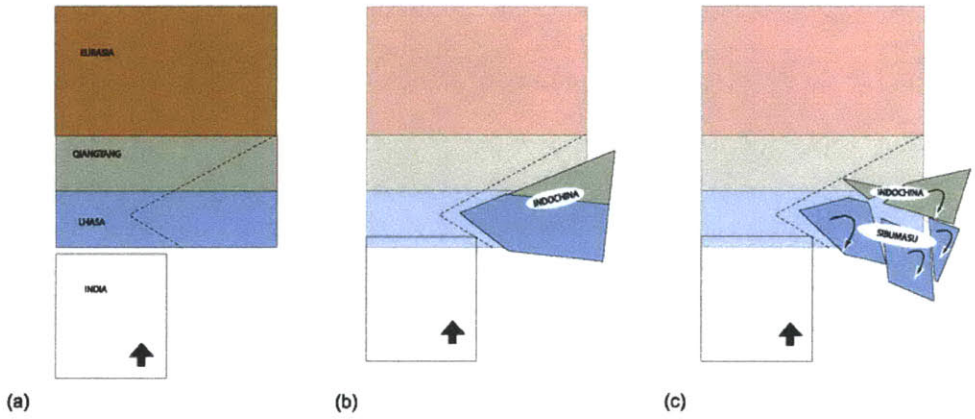

Figure 2. A schematic diagram which demonstrates two possible extrusion styles. (a) Undeformed Eurasia continent prior to the collision of India. (b) Extrusion of a single rigid block, with minor clockwise rotation. (c) Extrusion of dismembered crustal blocks which also rotate clockwise.

This thesis focuses on a critically important area within the India-Eurasia collision zone, a region known as the Three Rivers area. The bedrock geology of the region around the eastern Himalayan syntaxis has been insufficiently studied to evaluate these outstanding questions, particularly for the early Cenozoic part of the deformational history, since seismological, neotectonic, and geodetic studies cannot be used.

A large part of this study was devoted to fieldwork. During three field seasons that lasted a total of 7 months , a preliminary geological map of the Gaoligongshan Shear Zone (GSSZ) and the Chongshan Shear Zone (CSSZ) was made at 1:25,000 (Appendix A). The mapped zone covers an area of about six hundred and fifty square kilometers between Binzhongluo and LiuKu, Yunnan, China. Additional mapping was done along four transects across the southern

part of the Chongshan Shear Zone (see chapter 4 for details) and four transects across the Gaoligongshan Shear Zone, south of LiuKu.

Field studies show that the GSSZ is the major right-lateral shear zone that accommodated early Cenozoic displacement between India and Eurasia. It consists of two distinct units: an orthogneiss unit to the west, composed mainly of mylonitic granite, and a metasedimentary unit to the east. Most of the foliation in the GSSZ metamorphic rocks dips steeply ($\geq 60°$) both to the west and east and the rocks show well-developed mylonitic textures and a prominent subhorizontal lineation interpreted as a stretching lineation formed by the elongation of quartz, feldspar, and biotite, In all the sections and sites we studied along ~400 km length of the GSSZ, the foliation and stretching lineation appear to result from a single phase of non-coaxial deformation. Kinematic shear criteria observed in horizontal sections perpendicular to the foliation and parallel to the lineation, indicate a consistant right-lateral sense of shear.

Syn- to post-tectonic pegmatite dikes and tourmaline-bearing micaceous leucogranites are concentrated in the metasedimentary part of the GSSZ. They form concordant veins, layers and lens-shaped bodies with a foliation defined by micas. Boudinage is widespread and affects both the mylonitized leucogranitic sills that are interpreted to have formed during earlier stages of deformation as well as some of the unfoliated leucogranites and pegmatites which are interpreted to have emplaced during later stages of deformation. Boudin axes are both horizontal and vertical and indicate both horizontal and vertical stretching even though the vertically stretched boudins are not associated with a vertical lineation. Chapters 2 and 3 focus on the GSSZ and contain detailed descriptions of the lithologies and their protoliths, as well as structural evidence documenting that GSSZ is a major, ductile strike-slip shear zone.

The geochronological analyses of syn- to post-kinematic leucocratic intrusives are also part of the present study. Biotite and muscovite separated from these six granitic intrusions were analyzed in Chapter 2 in an effort to determine (1) the time during which the right-lateral shearing along the GSSZ was coming to an end, (2) the age of the termination of the shearing along the GSSZ and (3) a basis for the ongoing effort to explore the cooling history of the GSSZ. $^{40}Ar/^{39}Ar$ cooling ages from granitic dikes which cross-cut the right-lateral ductile fabrics of the GSSZ indicate that movement on the GSSZ ceased before ca.12 Ma, after which the right-lateral motion between India and the Sibumasu crustal fragment was accommodated along the Sagaing fault zone in Burma.

Preliminary U/Pb results, presented in Chapter 3, indicate that the ductile dextral shearing on the GSSZ terminated by ~18 Ma. The limited number of U/Pb dates from 3 syn-kinematic granitic sills, however are all older than 50 Ma, the generally accepted time of the collision between India and Eurasia. The significance of these old ages is currently being investigated and may yield important data on when the collision at the eastern Himalayan syntaxis occurred.

The Chong Shan Shear zone (hereafter, CSSZ), which is described in Chapter 4, is the least known of the three linear metamorphic belts of the Three Rivers region. This study demonstrates that it is mainly a left-lateral shear zone of regional importance during early Cenozoic extrusion and that extrusion of at least two major crustal fragments, the Sibumasu and Indochina, occurred. Lithological and structural descriptions of the CSSZ shear zone are presented for the first time, along with the results of the preliminary geochronological work. The CSSZ consists of a collective assemblage of migmatite, quartz-feldspar-biotite-bearing paragneiss, mica-schist, impure quartzite, calc-silicate rocks, marble, augen gneiss and mylonitic granite, from possibly several tectonic units. Most of the rocks contain a prominent sub-vertical

foliation and a sub-horizontal stretching lineation. Seven structural sections across the CSSZ were studied that had varying exposure quality. The rock units that form the CSSZ change from south to north and cannot be easily connected between cross-sections, probably due to different protoliths in different parts of the shear zone.

Preliminary U/Pb analyses indicate that the CSSZ has been active since at least ~34 Ma, and perhaps as early as 41 Ma. The mostly left-lateral strike-slip shearing continued at least until ~29 Ma, and perhaps as late as ~24 Ma, and terminated by ~17 Ma. This new data from the CSSZ along with the data from the GSSZ (chapters 2 and 3) indicate that the region between the GSSZ and ASSZ was not a single rigid block (Tapponnier et al., 1982, 1986), but was dismembered into at least two major fragments, the Sibumasu and the Indochina continental fragments, with different styles of internal deformation.

The GSSZ and CSSZ are separated by the Baoshan crustal fragment, with a distinctive Paleozoic stratigraphic succession, in the south, but merge to the north where the Baoshan fragment pinches out. There is no equivalent of the Baoshan fragment farther north and thus we interpret that this crustal fragment ended where the two shear zones coalesced. The Baoshan fragment continues south into Indochina where it forms part of the larger Sibumasu fragment. The kinematics of the CSSZ indicate the Baoshan fragment moved to the SE relative to the Indochina fragment that lies to the NE. Where the two shears zones merge, the CSSZ contains right-lateral shear sense indicators along its western side, suggesting that shearing in the GSSZ influenced the CSSZ after they merged and shows the complexity of movements of these two crustal fragments during extrusion.

The close spatial correlation between the location of the Gaoligongshan and Chongshan strike-slip shear zones and the Bangong-Nujiang and the Lancangjiang-Raub suture zones

inspired Chapter 5, which is a review of the currently available geological data from the Bangong-Nujiang and Lancangjiang-Raub suture zones and the re-interpretation of the relations of these suture zones to the younger shear zones, the CSSZ and GSSZ, along the northernmost section of the Sibumasu tectonic element based on our field and laboratory studies. The re-interpretation of these suture zone leads to several important conclusions that include: 1) the Sibumasu tectonic element pinches out in western Yunnan, and does not continue into Tibet, 2) the Qiangtang tectonic element pinches out in eastern Tibet and does not continue into Yunnan, 3) The Bangong-Nujiang ocean separated the Lhasa crustal fragment from both the Qiangtang and the Sibumasu tectonic elements, 4) Cenozoic right-lateral shearing along the Gaoligongshan shear zone, re-activated a cryptic suture between the Qiangtang and the Sibumasu blocks. 5) The Chengling-Mengliang suture and the Lancangjiang suture are presently separated by the left-lateral CSSZ, but were likely connected prior to India-Eurasia collision ~50 Ma. A better documentation of the exact location of the various segments of these suture zones by detailed fieldwork and determination of the duration of their deformational histories by detailed geochronological studies will undoubtly vastly improve our understanding of the Cenozoic tectonic evolution of SE Asia. But what is documented in our work is that the shear zones in the northern part of the study area contain two cryptic major suture zones

The lithological and structural descriptions, as well as the geochronological results presented in this thesis will no doubt require considerable refinement as tectonic studies in the area proceed. Figure 3 is a demonstration of the vastness of Asia in comparison to the USA, as well as the minute size of my field area, which is labeled as a red rectangle inside Louisiana. Interested readers, who chose to read the remainder of this dissertation, should keep Figure 3 in their minds at all times.

All of the chapters in this dissertation, were written as independent manuscripts, and as such they contain some redundancy.

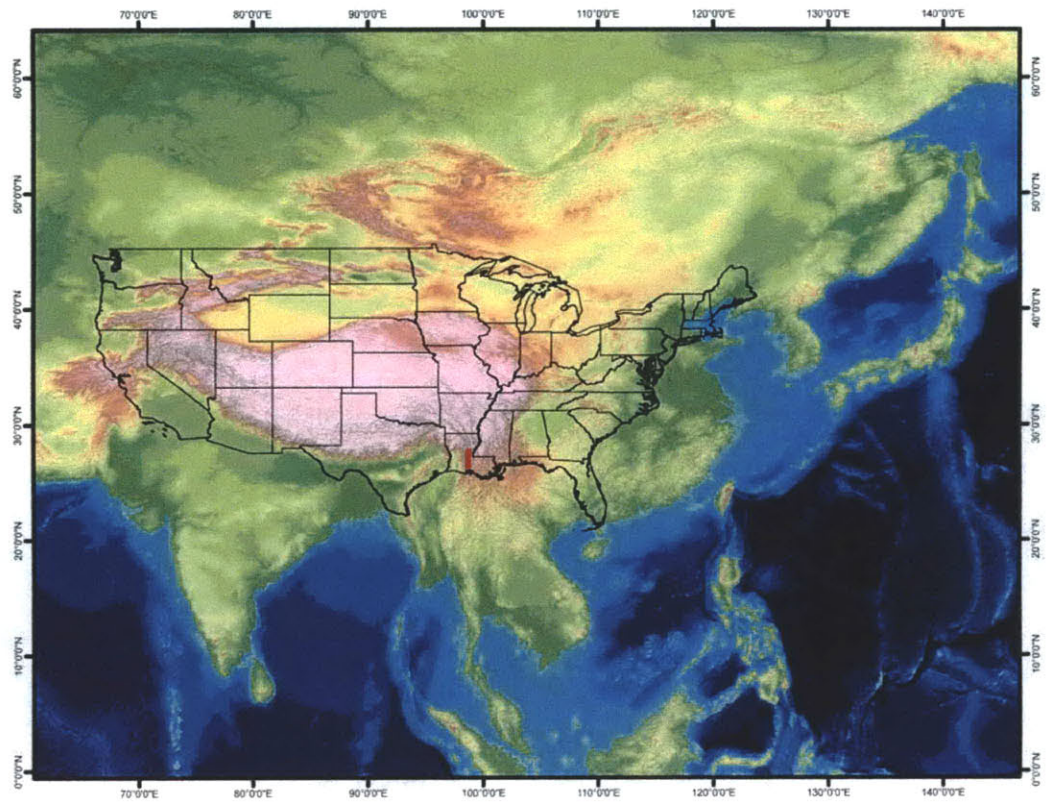

Figure 3 A thematic map that compares the size of the Tibetan Plateau and eastern Asia, the regions effected by the India – Eurasia collision, and the size of USA and its states. The red rectangle within the state of Louisiana is the field area that contains the GSSZ and part of the CSSZ, described in detail in this dissertation.

REFERENCES:

Curray, J.R., Moore, D.G., Lawver, L.A., Emmel, F.J., Raitt, R.W., Henry, M., Kieckhefer, R., 1979, Tectonics of the Andaman sea and Burma, in Watkins, T.S. et al., eds., Geological and geophysical investigations of continental margins: AAPG Memoir no. 29, p.189-198.

Gilley, L.D., Harrison, T.M., Leloup, P. H., Ryerson, F. J., Lovera, O. M., Wang, J.-H., 2003, Direct dating of left-lateral deformation along the Red River shear zone, China and Vietnam: Journal of Geophysical Research, v. 108, no. B2, p ECV 14-1 to 14-21.

Harrison, T. M., Chen Wenji, Leloup, P.H., Ryerson, F.J., Tapponnier, P., 1992, An early Miocene transition in deformation regime within the Red River fault zone, Yunnan, and

its significance for Indo-Asian tectonics: Journal of Geophysical Research, v. 97, p. 7,159-7,182.

Harrison T.M., Leloup, P.H., Ryerson, F.J., Tapponnier, P., Lacassin, R., Chen Wenji, 1996, Diachronous initiation of Transtension along the Ailao Shan-Red River Shear zone, Yunnan and Vietnam, in Yin, A. and Harrison, T.M., eds., The Tectonics of Asia: New York, Cambridge University Press, p. 208-226.

Houseman, G., England, P., 1993, Crustal thickening versus lateral expulsion in the Indian-Asian continental collision: JGR, v.98, p. 12,233-12,249.

Lawver, L.A., Curray J.R., Moore, D.G., 1976, Tectonic evolution of the Andaman Sea: EOS, v. 57, p. 333-334.

Le Dain A.Y., Tapponier P., Molnar, P., 1984, Active faulting and tectonics of Burma and surrounding regions: Journal of Geophysical Research, v. 89, p. 453–472.

Leloup, P. H., Kienast, J.R., 1993, High-temperature metamorphism in a major strike-slip shear zone: the Ailao Shan-Red River, People's Republic of China: Earth and Planetary Science Letters, v. 118, p. 213-234.

Leloup, P. H., Lacassin, R., Tapponnier, P., Zhong Dalai, Liu Xiaohan, Zhang Lianshang, Ji Shaocheng, Phan Trong Trinh, 1995, The Ailao Shan-Red River shear zone (Yunnan, China), Tertiary transform boundary of Indochina: Tectonophysics, v. 251, p. 3-84.

Molnar, P., Tapponnier, P., 1975, Cenozoic tectonics of Asia; effects of a continental collision: Science, v. 189, p. 419-426.

Patriat, P., 1983, Evolution du systeme de dorsales de l'Ocean Indien [Ph.D. thesis], Universite´ Pierre et Marie Curie, Paris.

Patriat, P., Achache, J., 1984, India-Eurasia collision chronology has implications for crustal shortening and driving mechanism of plates: Nature, v. 311, p. 615-621.

Royden, L.H., Burchfiel, B. C., King, R. W., Wang, E., Chen Zhiliang, Shen Feng, Liu Yuping, 1997, Surface deformation and lower crustal flow in eastern Tibet: Science, v. 276, p. 788-790.

Schärer, U., Zhang Lian-Sheng, Tapponnier, P., 1994, Duration of strike-slip movements in large shear zones: The Red River belt, China : Earth and Planetary Science Letters, v. 126, p. 379-397.

Tapponnier, P., Peltzer, G., Le Dain, A.Y., Armijo, R., Cobbold, P., 1982, Propagating extrusion tectonics in Asia: new insights from simple experiments with plasticine: Geology, v. 10, p. 611-616.

Tapponnier, P., Peltzer, G., Armijo, R., 1986, On the mechanics of the collision between India and Asia: Coward, M.P., and Ries, A.C., eds., Collision Tectonics: London, Geological Society, Geological Society Special Publication, no. 19, p. 115-157.

Wang, E., Burchfiel, B.C., 1997, Interpretation of Cenozoic tectonics in the right-lateral accommodation zone between the Ailao Shan shear zone and the Eastern Himalayan Syntaxis: International Geology Review, v. 39, p. 191-219.

Termination of ductile strike-slip shearing along the Gaoligong Shan Shear Zone, western Yunnan, China, and its relations to the tectonics of the eastern Himalayan syntaxis.

Sinan Akciz[1]*
B. Clark Burchfiel[1]
Yin Jiyun[2]
Chen Liangzhong[2]

[1]Massachusetts Institute of Technology, Dept. of Earth, Atmospheric and Planeary Sciences, 77 Massachusetts Ave., Cambridge, MA 02139
[2]Yunnan Institute of Geological Sciences, 131 Baita Rd., Kunming, Yunnan, China.
*E-mail: akciz@mit.edu

Chapter 2- Termination of shearing along the Gaoligong Shan Shear Zone

ABSTRACT:

The concept of lateral extrusion in Cenozoic time, has played an important role in tectonic interpretations of Asia, even though the right-lateral conjugate shear system to the left-lateral ASSZ, has not yet been documented. The Gaoligong Shan metarmorphic belt in Yunnan, Southwestern China, is a right-lateral ductile shear zone that accommodated much of the motion between India and the Sibumasu tectonic unit (Indochina) prior to the initiation of the presently active Sagaing fault in Burma. For more than 500 km, penetrative ductile right-shear is marked by a steep foliation and subhorizontal lineation that affected rocks of dominantly igneous protoliths in the west and dominantly sedimentary protoliths in the east. The igneous protoliths are the continuation of the Gangdese batholith and the sedimentary protoliths are probably dominantly upper Paleozoic rocks of the Lhasa crustal fragment. Muscovite and biotite from late kinematic anatectic melts in the shear zone yield $^{40}Ar/^{39}Ar$ dates from ~18 to ~12 Ma; the youngest age coming from a cross-cutting dike that postdates the right-lateral deformation within the GSSZ. The data indicate that deformation within the GSSZ ended by ~ 12 Ma and the right-lateral motion between India and Sibumasu began to be accommodated along the Sagaing fault zone in Burma. The change in location of the shear between India and Sibumasu to have been caused by the change in orientation of the GSSZ with time so that it was no longer properly oriented to continue to accommodate motion between the two crustal fragments. Change in the orientation of the GSSZ occurred by clockwise bending of the shear zone resulting from fragmentation of part of the Sibumasu crust and possible clockwise rotation of the shear zone.

INTRODUCTION:

Since the collision between Eurasia and India at ~45 Ma (Rowley 1996, 1998) there has been between ~2,000 and ~3,500 km of convergence from the western to eastern Himalayan syntaxes, respectively, as shown by palaeomagnetic data (e.g. Klootwick et al., 1992) and seafloor-spreading reconstructions (e.g. Molnar and Tapponnier, 1975; Patriat, 1983; Patriat and Achache, 1984; Stock and Molnar, 1987). Much of this convergence appears to have been accommodated by internal deformation within Asia as southernmost Tibet has moved northwards by 2000(±900) km (Molnar and Tapponnier, 1975; Patriat and Achache, 1984). According to the widely referenced extrusion model proposed by Tapponnier and coworkers in the early 1980's, a significant fraction of post-collisional deformation in Asia was taken up by successive extrusions of large, coherent blocks with little internal deformation along major strike-slip faults (Figure 1). In all the versions of this model, the right-lateral Sagaing fault in Burma is assumed to accommodate the northward motion of India into Eurasia east of the eastern Himalayan syntaxis (Figure 1). However, the movement on the Sagaing fault probably started during spreading in the Andaman Sea, from ca. 11 Ma (Curray et al., 1979) to ca. 13 Ma

(Lawver et al., 1976). Therefore, how and where indentation was accommodated in the region east of the India indenter between ca. 11 and ca. 45 Ma are still subject to speculation, mainly due to lack of geological investigations carried out in the region.

Our field studies show that the Gaoligong Shan (Akciz et al., 2000 , Akciz et al. in prep.) and Chong Shan (Akciz et al., 2000, 2001, Akciz et al., in prep.) metamorphic belts (Figure 2) of western Yunnan, China, are not belts of Precambrian-aged metamorphic basement rocks (Bureau of Geology and Mineral Resources of Yunnan Province, 1990) as previously mapped, but rather sub-vertically foliated and sub-horizontally stretched amphibolite-grade paragneiss and orthogneiss mylonitic strike-slip zones with right- and left-lateral shear sense indicators, respectively. We, therefore, prefer to refer to them as the Gaoligongshan Shear Zone (GSSZ) and Chong Shan Shear Zone (CSSZ). Both of these shear zones have been intruded by networks of foliation-parallel sills and dikes of granitic composition. Most of the sills are syn-deformational, while the dikes are unambiguously post-deformational.

The presently inactive GSSZ appears to be the only right-lateral shear zone with the appropriate orientation to accommodate major pre- ca. 11 Ma northward movement of India relative to Eurasia. However, whether these belts are related to the India-Eurasia collision, as postulated by Wang and Burchfiel (1997), and how they are related to the Sagaing fault to the west and the well-documented Cenozoic Ailao Shan Shear Zone (ASSZ) to the east (e.g. Leloup et al., 1995) remain as unresolved questions.

One important barrier to unraveling the tectonics of the eastern Himalayan syntaxis has been the paucity of reliable geochronological dating of deformation, with the exception of the work carried out along the Ailao Shan shear zone (e.g. Harrison et al., 1992; Leloup et al., 1993, 1995; Schärer et al., 1994, 1996; Harrison et al., 1996; Gilley et al., 2003). Most of the geochronological studies in the region, despite the presence of abundant granitic intrusives, which can be grouped as syn- and post-deformational, have focused on age of magmatic rocks using Rb-Sr whole rock or mineral K-Ar and U-Pb methods. Biotite and muscovite samples from the mylonites of GSSZ have yielded K-Ar dates of 14.4, 15.0, and 23.8 Ma, and a single $^{40}Ar/^{39}Ar$ analysis yielded a date of 11.6 Ma (Zhong and Wang, 1991). A date of 17 to 20 Ma was also reported by Zhong and Wang (1991) on a migmatite from mylonitic rocks, but no information regarding the analysis has been published.

To begin to address the role of the GSSZ, and to better understand the role of extrusion tectonics in the Cenozoic evolution of SE Asia, we present here recently obtained $^{40}Ar/^{39}Ar$ data from syn-deformational leucogranite sills and also granitic and pegmatite dikes that cross-cut the ductile right-lateral shear fabrics of the GSSZ, and discuss their significance. This work forms part of a larger structural and reconnaissance geochronological study that aims to date the period during which deformation within the GSSZ and CSSZ was active.

GEOLOGICAL BACKGROUND:

The Three Rivers region of western Yunnan lies east of the eastern Himalayan syntaxis and consists of a tectonic collage of continental fragments of Gondwana and Cathaysian affinities and magmatic arcs formed by subduction within Palaeo-Tethys (e.g. Şengör, 1984; Hutchison, 1989). During intracontinental deformation following the India/Eurasia collision, the collage was modified by post-collisional Cenozoic deformation characterized by fragmentation and rotation of crustal blocks (Wang and Burchfiel, 1997) and displacement along major faults and shear zones as India moved northward relative to Indochina and South China.

The Tengchong crustal fragment (these pieces of crust are often referred to as blocks which incorrectly implies rigid behavior of the deformed crust) is here interpreted as the southeastern continuation of the Lhasa crustal fragment of southern Tibet and is bounded on the east by the GSSZ (Figure 2). Its sedimentary sequence within China lacks dated exposures of early Palaeozoic sedimentary rocks and is characterized by upper Carboniferous to lower Permian marine carbonate and clastic strata containing cold water fauna that indicate that the fragment was part of the Gondwana domain (Chenjun, 1994). All the strata were extensively intruded and metamorphosed by Mesozoic and Cenozoic(?) plutonic rocks and are partially covered by Upper Tertiary and Quaternary intermediate to basic volcanic rocks. High-grade metamorphic and igneous rocks crop out in the eastern part of the Tengchong fragment along the west side of the Nujiang (Salween) River and form a narrow structural high that continues south into Burma as the Mogok Metamorphic Belt (Chibber, 1934). These high-grade rocks have been considered to be Middle Proterozoic in age and have been interpreted as an upthrust slice of the basement of the Tengchong crustal fragment prior to this study (Bureau of Geology and Mineral Resources of Yunnan Province, 1990). Our study, however, indicates these rocks are part of a Mesozoic batholith and their metasedimentary wall rocks are of probable Paleozoic age. The

Mesozoic plutonic rocks are the southeastward continuation of the Gangdese batholilth of southern Tibet and at least some of the high-grade metasedimentary rocks are part of the Lhasa crustal fragment. In support of this interpretation, both the less metamorphosed quartzite and limestone interbedded with fine-grained sandstone of mainly Carboniferous and Permian (?) age along with the large plutons that intrude them can be traced from the Lhasa crustal fragment into the Tengchong crustal fragment in the map area.

The Baoshan crustal fragment lies to the east of the GSSZ and forms the northernmost continuation of the more regional Sibumasu continental fragment as defined by Metcalfe (1984, 1988) (Figure 2). Upper Proterozoic to Middle Cambrian slightly metamorphosed diamictites and carbonate rocks form the basal part of the Baoshan stratigraphic sequence in the study area. The Silurian and Ordovician units consist mainly of fossiliferous shallow-water siliciclastics rocks and some argillaceous limestone and shale. From the Middle Devonian to the end of Early Carboniferous time, various fossiliferous carbonate units were deposited. The lower part of the Upper Carboniferous strata contains diamictites, along with turbidite, conglomeratic sandstone, and siltstone (Jin, 1994). The upper part comprises black mudstones and siltstones, which are regarded as periglacial deposits. Basaltic lava flows (Woniusi basalt) with pillow lavas and tuffaceous intercalations terminate Palaeozoic sedimentation in the early Permian (Bureau of Geology and Mineral Resources of Yunnan Province, 1990). These basalts may be related to rifting and the beginning of separation of the Baoshan continental fragment from the Gondwana margin (Jin, 1994), although few data supporting this interpretation are described in the literature. Lower Permian(?) red beds lie disconformably above the Woniusi Basalts. The Mesozoic strata consist of Triassic limestone and Jurassic marine strata and red beds that are generally restricted to the margins of the Baoshan unit. Cenozoic rocks are rare and are characterized by upper Eocene-Oligocene conglomerate and sandstone that rest unconformably on deformed older rocks.

The sedimentary sequences for the Tengchong and Baoshan crustal fragments are very different and belong to two different crustal fragments that are separated by a major suture, the probable SE continuation of the Bangong – Nujiang suture (Jin, 1994). Most of the rocks of the GSSZ belong to the Lhasa tectonic unit, although some rocks in its eastern part may belong to the Baoshan tectonic unit. Thus, the Bangong – Nujiang suture is expressed as a cryptic suture within the eastern part of the GSSZ.

THE GAOLIGONGSHAN SHEAR ZONE (GSSZ):

Our field studies show that the GSSZ (Figures 3 and 4) consists of two distinct units: an orthogneiss unit to the west, composed mainly of mylonitic granite of presumably Cretaceous (and younger) age, and a metasedimentary unit to the east that consists of quartz-feldspar-biotite (QFB) paragneiss, impure quartzite, calcsilicate rocks, marble, and biotite schist. The metasedimentary rocks contain garnet, K-feldspar and sillimanite, indicating they were metamorphosed at amphibolite grade. The calcsilicate rocks are composed of alternating green and gray bands, and contain quartz, plagioclase, calcite, diopside ±wollastonite, ±muscovite, and ±biotite. The interlayering of siliciclastic rocks, calcsiliate and marble at all scales supports a metasedimentary origin for the QFB-gneiss. The rarity of marble and the lack of amphibolite that would be indicative of metamorphosed basalt indicate the protoliths of these metamorphic rocks in the GGSZ are not from the Baoshan tectonic unit. Some of these rocks can be traced northward into lower grade rocks of the Lhasa crustal fragment, thus much of the high-grade metasedimentary rocks in the shear zone belong to the Lhasa crustal fragment.

Most of the foliation in the GSSZ metamorphic rocks dips steeply ($\geq 60°$) both to the west and east and shows well-developed mylonitic textures (Figure 5). Syn- to post-tectonic pegmatite dikes and tourmaline-bearing micaceous leucogranites are concentrated in the metasedimentary part of the GSSZ. They form concordant veins, layers and lens-shaped bodies with a foliation defined by micas. They also have been affected by same ductile deformation as their host mylonitic metamorphic rocks.

Outcrop surfaces polished by the Nujiang River and its tributaries provide well-exposed horizontal sections, parallel with the lineations and close to the XZ plane of the finite strain ellipsoid (i.e. perpendicular to the foliation and parallel to lineation). The schistosity is marked by biotite, and quartz and/or feldspar ribbons. This schistosity contains a prominent lineation interpreted as a stretching lineation formed by the elongation of quartz, feldspar, and biotite, although intersection lineations (formed by the intersection of foliation and compositional layering) are also present at numerous outcrops mainly within folded quartzite and calcsilicate units. Sheath folds and folds with axes parallel to lineation are present and are marked by intersection lineations that parallel the mylonitic stretching lineation. Boudinage is widespread and affects both the mylonitized leucogranitic sills that are interpreted to have formed during earlier stages of deformation as well as some of the unfoliated leucogranites and pegmatites

which are interpreted to have emplaced during later stages of deformation. Boudin axes are both horizontal and vertical and indicate both horizontal and vertical stretching even though the vertically stretched boudins are not associated with a vertical lineation. In all the sections and sites we studied along ~400 km length of the GSSZ, the steep foliation and horizontal stretching lineation appear to result from a single phase of non-coaxial, horizontal right-lateral shear. Consistent shear criteria, such as asymmetric tails on deformed feldspar porphyroclasts, S-C surfaces, asymmetric boudins, cm.- to dm.-scale asymmetric folds observed in horizontal sections perpendicular to the foliation and parallel to the lineation, indicate a right-lateral sense of shear (Figure 5).

Data from microstructural analysis of oriented thin sections confirm observations at the mesoscopic scale within the GSSZ. In thin section, the foliation is marked by metamorphic minerals (biotite, muscovite, ±chlorite, and ±sillimanite) and by quartz and feldspar ribbons, and the lineation is formed by quartz, feldspar and biotite. The most common mineral defining the lineation is quartz that forms long polycrystalline ribbons generally made of recrystallized grains. The grains have an irregular shape, sutured boundaries, often with undulatory extinction, subgrains and deformation bands. Plastic deformation combined with dynamic recrystallization thus appears to have been the dominant deformation mechanism in the quartz. None of the K-feldspar grains have plastic deformation features. Some feldspar grains, especially plagioclase, show brittle fractures. The contrast between quartz and feldspar deformation indicates temperatures were probably between 350° and ~500° C. Many feldspar grains have sigma-type tail structures that yield right-lateral sense of shear. Augens of quartz and feldspar crystals are wrapped by fine-grained quartz and feldspar. The foliation formed by various mica minerals is deflected around the augens and garnets.

$^{40}Ar/^{39}Ar$ THERMOCHRONOLOGY:

All of the units forming the metasedimentary section of the GSSZ, except for the marble and the calc-silicate rocks, have been intruded by cm- to dm-scale leucogranite and pegmatite sills. The mineralogy of the leucogranites and pegmatites is dominated by quartz, sodic plagioclase, ±microcline, ±garnet, ±muscovite, ±biotite and tourmaline. Most sills are either undeformed or exhibit a very weak foliation, compared to the strongly foliated host rocks.

Samples 98JN14.4 and 99M28.1 are unfoliated pegmatites, and sample 98JN12.2 is a foliated leucogranite without lineations. We have also analyzed two pegmatite dikes (98JN15.9 and 00JN5.3) and one granitic intrusion (98JL14.2) which are undeformed and cross-cut the high-temperature ductile shear fabric. All of these three samples unambiguously post-date major ductile movements in the GSSZ.

We analyzed biotite and muscovite separated from these six granitic intrusions, in an effort to determine (1) the time during which the right-lateral shearing along the GSSZ was coming to an end, (2) the age of the termination of the shearing along the GSSZ and (3) a basis for the ongoing effort to explore the cooling history of the GSSZ.

Muscovite and biotite were analyzed by the $^{40}Ar/^{39}Ar$ incremental heating method for the GSSZ samples (99M28.1, 98JN14.4, 99M28.1, 98JN15.9, 00JN5.3 and 98JL14.2). Sample locations and schematic block diagrams showing their structural setting are shown in Figure 3. Details of our $^{40}Ar/^{39}Ar$ analytical procedure are given in Appendix A. Analytical results are listed in Table 1, and the corresponding isochrons and age spectra diagrams are given in Figure 6.

The one deformed leucogranite dike sample we have analyzed yielded a cooling age ca. 17.5 Ma, whereas the undeformed dikes consistently yielded younger dates of ca. 12 – 13.5 Ma. Of the two cross-cutting pegmatite samples, muscovite from 98JN15.9 yielded a date of 11.83±0.18 Ma and biotite from sample 00JN5.3 yielded a date of 12.01±0.26 Ma. Muscovite from the granite sample 98JL14.2 yielded a date of 11.61±0.37 Ma.

DISCUSSION:

All of these preliminary ages support our field observations, which we have used to group the samples based on their degree of deformation: the cross-cutting dikes are younger than the unfoliated sills which are younger than the sheared sills. While the ages of the cross-cutting dikes indicate the minimum age of when the right-lateral shearing along the GSSZ terminated, the data from the syn-deformational sills, can be interpreted in at least two different ways. In the first interpretation, the sills were intruded during the later stages of the right-lateral shearing and so they experienced very little if any strike-slip shearing. In this case, these ages can be interpreted as the time during which the right-lateral shearing was coming to an end. As an alternative interpretation, because the GSSZ is at least 1,500 km long along with the Mogok Metamorphic Belt and is as wide as 40 km, the sampled sill may not have experienced any

deformation due to slip partitioning. Therefore, the $^{40}Ar/^{39}Ar$ dates only constrain the cooling of the GSSZ, and cannot be used in determining the termination of the shearing unequivocally. We, therefore, base the following discussion on the $^{40}Ar/^{39}Ar$ dates of the three cross-cutting dikes, which are ca. 12 Ma. We interpret all our $^{40}Ar/^{39}Ar$ results as cooling ages, so our results are interpreted as minimum ages.

The GSSZ is the only recognized right-lateral structure with the appropriate orientation in the region between the ASSZ and the Sagaing fault, along which a significant amount of the indentation of India into Eurasia could have been accommodated during early Cenozoic time (Figure 2). While our work on determining the initiation and duration of shearing along the GSSZ is ongoing, the $^{40}Ar/^{39}Ar$ data from two pegmatite dikes and a granitic intrusive body that cross-cut the ductile right-lateral shear fabrics of the GSSZ show that the shearing on the GSSZ ended by at least ca.12 Ma. Interestingly, the termination of the shearing along the GSSZ is almost coincident with the initiation of the Sagaing fault (Curray et al., 1979). Why and how this right-lateral shearing ended along the GSSZ and began to be accommodated along the Sagaing fault, however, are unresolved questions.

A growing number of palaeomagnetic studies demonstrate the importance of large clockwise rotations, up to 90°, within the northern part of the Indochina tectonic element (Lanping/Simao fold and thrust belt) since Jurassic times (e.g. Huang and Opdike, 1993; Funahara et al., 1992, 1993; Chen et al., 1995; Geissman 1999, 2001). Palaeomagnetic evidence from the Khorat Plateau, however, indicates a net rotation of only ~ 14°±7° with respect to South China (Yang & Besse, 1993) since the Jurassic. Therefore, any tectonic model proposed for the evolution of the region since the Jurassic must account for both large clockwise rotations to the north and as little as 15° to the south.

In our interpretation, during Oligocene to approximately middle Miocene time, the Sibumasu/Indochina tectonic element, the region between the GSSZ and the ASSZ, was shortened and displaced to the southeast relative to South China and parts of eastern Tibet, as India penetrated into Eurasia. The initial orientation of these shear zones, as well as the orientation of the Indo-Burma section of the Indus-Tsangpo suture zone is unknown, but probably was NW-striking and likely was straighter than at present during and immediately following the collision. Continued indentation, however, ultimately caused the extrusion to terminate by modifying the internal structure of the extruding tectonic element, as well as its

margins to the north. Following the termination of shearing along the GSSZ by ca. 12 Ma (this study) and the ASSZ by sometime after 17 Ma (e.g. Harrison et al., 1992; Harrison et al., 1996), a new set of structures, including the Sagaing fault and the Xianshuihe-Xiaojiang fault system, formed. This modification was heterogeneous both spatially and temporally, and the interpretation will only grow more complicated as additional palaeomagnetic, geochronological and basic field data become available in the near future.

We discuss three of these possible deformational events, concentrating mainly on clockwise bending of the GSSZ. First, folding and thrusting within the Sibumasu/Indochina tectonic element caused a section of it to be pinched (Figure 2) and disrupted in contrast to otherwise linear and continuous eastern boundary, the ASSZ. Pinching of the Lanping section of the Indochina fragment is clear on geological maps of the region, but its degree of importance must be further investigated. However, we do not believe that it alone was significant enough to terminate the extrusion. Second, the Qamdo-Lanping-Simao belt (northern section of the Indochina fragment of the Sibumasu/Indochina tectonic element), the Jinsha suture, Yidun volcanic arc, and Garze-Litang suture all have arcuate trends (Figure 2). The present day orientations of these pre-existing structures may have been a result of the bending of the southern margin of Eurasia as India penetrated into it. Wang and Burchfiel (2000) show that some of this bending is at least 2-4 my. old, but the extent of Tertiary deformation remains to be investigated. The presumed Cenozoic bending, however, was not accommodated homogeneously. While the redbeds of the Qamdo-Lanping-Simao belt were folded and thrusted as well as being sheared in between the CSSZ and the ASSZ, the Sibumasu fragment of the Sibumasu/Indochina tectonic element was dismembered into numerous crustal fragments, bounded by numerous NE- and NW-oriented strike-slip faults. The bending and the dismemberment of this tectonic element and its margins, caused it to contain structures that were not compatible with further strike-slip movement and eventually terminated its extrusion. Third, clockwise bending of the GSSZ caused shearing along it to terminate, as it could no longer accommodate the Indian indentation (Wang and Burchfiel, 1997). According to the model of Wang and Burchfiel (1997), at that time a new fault, the northern part of the Sagaing fault, broke immediately west of the mylonitic GSSZ. They argue that the bending of the GSSZ is a consequence of left-slip on NE-trending strike-slip faults and clockwise rotation of eastern Tibet around the Eastern Himalayan Syntaxis. However, we prefer an alternative kinematic and dynamic interpretation which assumes that the structures

that accommodated the bending of the Sibumasu tectonic fragment also bend its boundaries, the GSSZ and the CSSZ (Figure 7).

The clockwise bend in the GSSZ is ~200 km long (Figure 8), yet there are no unambiguous geological markers which are offset by that magnitude. Geological maps (1:1,000,000 scale) of Thailand, Burma and SW China show that the Chiang Mai - Lincang belt in Thailand is bounded on the north and south by two strike-slip faults. This metamorphic belt is offset left-laterally along its northern edge by ~100 km along the western continuation of the Mengxing Fault, and by about the same amount left-laterally along the Wang Chao fault, along its southern edge (Lacassin et al., 1997). Of these faults, movement on the Wang Chao fault also distorted the post-Jurassic N-S trending fold axes through left-lateral bending (Le Dain et al., 1984; Tapponnier et al., 1986). The evidence for any geological offsets to the north is poorly constrained. However, while the Gangdese granites are generally restricted to the Lhasa tectonic element, there are at least two granitic bodies of unknown age which intruded the northern most part of the Sibumasu tectonic element east of the GSSZ (Figure 8), and are right-laterally offset by ca. 40 km by the Wanding Fault (Figure 8). No additional geological offsets are obvious, but this might be due to the lack of detailed mapping conducted near the borders of China – Burma and Thailand – Burma. To a first order, the total right-lateral offset of ~140 km can account for large part of the right-lateral bending of the GSSZ.

These faults are presently active as suggested by their sharp traces, the presence of river offsets on Landsat and CORONA images, as well as the fault plane solution of earthquakes (Le Dain et al., 1984). The present-day sense of slip deduced from such morphological offsets and geophysical calculations, however, is left-lateral and opposite to the geological offsets presented above (Lacassin et al., 1998).

While the geological evidence is limited, additional evidence for early right-lateral motion along the NE-trending faults might come from the study of the Salween River. The record of large sedimentary deposits in the Salween and Mekong deltas for at least the last 30 Ma suggest these rivers have been significant features of the southeast Asian landscape since at least Oligocene time (Métivier et al., 1999) A recent reinterpretation by Clark (2003) suggests a complicated drainage reorganization in Cenozoic time in this region, including capture of the upper Salween and Mekong rivers from their originally eastward draining courses by headward erosion along the lower Mekong and Salween rivers. This interpretation, however, does not

affect arguments for the antiquity of at least the lower portions of these rivers. The Salween River makes several right-lateral deflections along its course to the Andaman Sea (Figure 8). Two such major deflections also coincide with the Wanding and Mengxing faults (Figure 8). If we assume that at least the southern portions of Salween and Mekong have long been draining the southeastern portion of Tibet, then the ca.100 km right-stepping deflection along the Mengxing Fault and ca. 80 km right-lateral deflection along the Wanding Fault, further support the right-lateral motion along these faults. Alternatively, the right-stepping deflections of the Salween may have nothing to do with mid-Tertiary right-lateral motion along the Wanding and Mengxing faults. Pre-existing zones of weak and/or deformed rocks might have been followed by the developing Salween River and be responsible for these deflections. However, the pre-Cenozoic deformation of geology and geomorphology of the Sibumasu crustal fragment is so poorly known that this interpretation can not be tested at present. Even though this alternative view remains a possibility, which can only be resolved by further field work carried in the mostly unmapped region, we favor an early right-lateral motion along the NE-trending faults followed by a left lateral motion along the NW-trending faults from Oligocene to Miocene (ca. 30 Ma – ca.15 Ma), as was also suggested by Lacassin et al. (1998).

The geometry and kinematics of the three major shear zones of southeast Asia, the GSSZ, the CSSZ and the ASSZ, support and modify the kinematics of the extrusion model, however, quantitative estimates for the magnitude of extrusion are very difficult to determine because all three are positioned within or close to pre-Cenozoic suture zones (Figure 2) and thus parallel to geological elements. The GSSZ lies along the Bangong-Nujiang suture zone, the CSSZ follows the northern continuation of the Changning-Menglian suture zone (which is part of the Lancang Jiang - Changning-Menglian - Nan-Uttaradit – Sa Kaeo – Chantaburi - Bentong -Raub sutures, which will be referred to as Lanchangjiang suture for simplicity), and finally the ASSZ follows the Song Da – Anding suture zone (Sengor et al., 1988). Geological offsets across these shear zones have long been a subject of debate. While we did not observe any geological offsets for the GSSZ, several lines of evidence, summarized by Leloup et al. (1995), suggest left-lateral displacement in excess of 500 km along the ASSZ. Yang and Besse (1993) and Yang et al. (1995) have also concluded that as much as 1200 ± 500 km left-lateral displacement has occurred on the ASSZ based on palaeomagnetic studies. Briais et al. (1993) suggested a minimum left-lateral offset of about 540 ± 40 km based on the seafloor spreading data from the

South China Sea, even though a straightforward link between oceanic continuation of the shear zone and spreading in the South China Sea is still controversial. Additional palaeomagnetic studies currently being conducted in the Lanping/Simao belt also indicate <1000 km of southward displacement of at least part (Lanping-Simao fold belt) of the Indochina tectonic unit (Geissman, 2001). Right-lateral displacement along the GSSZ is, therefore, probably comparable to that of the displacement suggested for the ASSZ. However, identification of piercing point offsets are presently unrecognized; further, due to the tectonic fragmentation of the Sibumasu/Indochina tectonic element, any suggested magnitude of displacement remains poorly constrained.

IMPLICATIONS FOR ASIAN TECTONICS

The region between the eastern Himalayan syntaxis and the ASSZ records part of the post-collisional Cenozoic motion between India and South China. Three different interpretations of the style of deformation observed within this accommodation zone are possible. All are consistent with field observations, supported by geodetic, paleomagnetic and geochronologic data. The escape tectonics model for the Tibetan Plateau and SE Asia (e.g. Molnar and Tapponnier, 1975; Tapponnier et al., 1986) predict the extrusion of large rigid tectonic blocks along large strike-slip faults with very little or no internal deformation. Geochronologic data from the ASSZ (e.g. Harrison et al., 1992; Leloup et al., 1993, 1995; Schärer et al., 1994, 1996; Harrison et al., 1996; Gilley et al., 2003) support the first phase of the extrusion model as defined by Tapponnier et al. (1982). However, structural and temporal predictions of the second phase remain controversial (Allen et al., 1984; Leloup et al., 1995, Replumaz, 2001; Schoenbohm, 2004). Wang et al. (1998) present evidence for a second interpretation in which there is Pliocene-Quaternary rotation around the eastern Himalayan syntaxis of a region bounded to the east by the Xianshuihe - Xiaojiang fault system in China and Dien Bien Phu fault in Vietnam. This model is supported by various GPS campaigns carried out in the region (e.g. King et al., 1997; Wang et al., 1998; Chen et al., 2000), however, there is very limited evidence that a similar rotational deformation style was important between 45 and 10 Ma. Wang and Burchfiel (1997), alternatively suggested that extrusion may have occurred, but that the extruding block was not rigid, and rather was dismembered into numerous small, internally deformed crustal fragments that translated and rotated differentially.

We, however, favor an alternative kinematic interpretation which is based on our new field and geochronological data and the existing geological data from the region. According to our interpretation (Figure 9), deformation within the Sibumasu/Indochina tectonic element began in late Eocene time, shortly after the India-Eurasia collision. NE-SW shortening and both right-lateral and left-lateral strike slip deformation began in western Yunnan. During Oligocene to approximately middle Miocene time, the region between the GSSZ and the ASSZ was shortened and displaced to the southeast relative to South China and parts of eastern Tibet. The continued indentation, however, modified the extruding tectonic element, as well as its margins, and the deformation within the Sibumasu/Indochina block was heterogeneous. The Sibumasu fragment was dismembered it into numerous rhomb-shaped crustal blocks, bounded mainly by strike-slip faults, that ultimately caused the bending of the GSSZ. These fragments formed in order to facilitate the bending of the Sibumasu/Indochina tectonic element in front of the India indenter. The Indochina fragment, was folded and thrusted as well as sheared between the ASSZ and the CSSZ.

By at least ~12 Ma, the northern part of the GSSZ rotated until it was no longer favorably oriented to accommodate India's continued northward movement. At that time a new fault, the northern part of the Sagaing fault, broke immediately west of the mylonitic GSSZ (Figure 9). Our studies indicate that no ductile right-slip has occurred on the GSSZ at least since late Miocene time (~12 Ma). Other geochronological data from the CSSZ (Akciz et al., 2001) and the ASSZ (e.g. Leloup et al., 2001) also show that strike-slip motion along both of these left-lateral shear zones had ceased by ~17 Ma, even though the causes of those terminations are not clear.

Once extrusion of the Sibumasu/Indochina composite tectonic unit to the SE ceased, a new style of deformation began to affect the region, east of the Eastern Himalayan Syntaxis. Since Pliocene time, the Xianshuihe – Xiaojiang and Zongdian fault systems and their probable southward continuations bounded on the east by the Dien Bien Phu fault, gradually became the dominant structures accommodating indentation by the clockwise rotation of the southeastern Tibetan plateau (Wang and Burchfiel, 1997; King et al., 1997; Wang et al., 1998; Chen et al., 2000). The newly forming left-lateral structures probably reactivated some of the pre-Pliocene right-lateral faults resulting in a reversal of shear-sense along these faults (Lacassin et al., 1998). Thus, while the appropriately oriented pre-Cenozoic suture zones were reactivated as strike-slip faults during the early Cenozoic deformational phase, their Pliocene orientation was not

favorable for further reactivation. In contrast, the right-lateral faults which enabled the rotation of the northern section of the Sibumasu/Indochina tectonic element, were properly oriented to be reactivated as left-lateral faults. Although the right-lateral Red River fault developed since late Miocene or Pliocene time, along part of the older left-lateral Ailao Shan shear zone, the amount of right-lateral displacement is small, perhaps no larger than ~ 40 km (Allen et al., 1984; Replumaz et al., 2000; Wang et al., 1998; Schoenbohm 2004). Thus the amount of late Cenozoic eastward movement of the region between the Red River fault and the Altyn Tagh fault may be small and the extrusion of a large part of Tibet on individual faults may not have occurred as proposed by Tapponier et al. (1982, 1986). Rather, the right-lateral movement on the Red River fault may have been the result of the counterclockwise rotation of the ASSZ and differential extension north and south of the fault (Wang et al., 1998; Schoenbohm, 2004).

The major change in the deformational style from early to late Cenozoic time can be ascribed to significant changes in the rheological properties of the deforming crust. Early Cenozoic deformation was dominated by fragmentation of the crust and separation of extruding and rotating fragments by faults and locally mylonitic zones along which more ductile crust was extruded upward, whereas late Cenozoic deformation was dominated by the progressive development of a weak lower crust (Royden et al., 1997; Clark, et al., 2004) extruded from beneath Tibet. In this scenario a decoupling zone formed in the mid- to lower crust, above which the rotational deformation around the eastern Himalayan syntaxis has been accommodated in a broad zone since the Pliocene times.

CONCLUSIONS:

Preliminary $^{40}Ar/^{39}Ar$ cooling ages from syn-kinematic granitic sills, along with geochronological data from the CSSZ (e.g. Akciz et al., 2000, 2001) suggest that right-lateral movement on the GSSZ occurred, at least partly, contemporaneously with movement on the left-lateral CSSZ and ASSZ.

$^{40}Ar/^{39}Ar$ cooling ages from granitic dikes which cross-cut the right-lateral ductile fabrics of the GSSZ indicate that movement on the GSSZ ceased before ca.12 Ma. A series of NE-trending right-lateral, and NW-trending left-lateral strike-slip faults in association with bending caused clockwise rotation of the GSSZ. By ca.12 Ma, the GSSZ was significantly deformed. We suggest that, as a consequence, it was no longer properly orientated to accommodate the

northward indentation of India and a new fault, the northern part of the Sagaing fault, formed in order to accommodate further deformation.

Important internal deformation of crustal fragments accompanied the extrusion of the region between the GSSZ and the ASSZ during early Cenozoic time. Both the Indochina and Sibumasu section of this region were strongly deformed, though the style of deformation on either side of the intervening CSSZ is different and the internal deformation of each tectonic unit took place at different times. The Sibumasu section was broken into rhomb-shaped pieces by both left- and right-lateral faults, shortened, and superposed on pre-Cenozoic folds and thrust faults. The northern section of the Indochina element, however, was folded and thrusted, bent and smaller crustal pieces were shortened and differentially rotated clockwise up to 90° at least until ca.12 Ma. A combination of Oligo-Miocene oroclinal bending and post-mid-Cretaceous local block rotations can explain most of the paleomagnetic and geologic observations for the region.

The Cenozoic Gaoligong Shan, Chong Shan and Ailao Shan strike-slip shear zones are located either along or close to the Bangong – Nu Jiang, Lanchang Jiang, Jinshajiang and Song Da - Anding suture zones, respectively. Likewise, most of the present day left-lateral strike-slip fault systems of eastern Tibet also appear to have been active as right-lateral strike-slip faults from Oligocene until at least mid-Miocene time. Therefore, any dynamic model for the Cenozoic deformational history of the India – Eurasia collisional zone, must take into account the influence of pre-existing heterogeneities of the crust before collision of a continental block such as Sibumasu or India.

This work forms part of a larger structural and reconnaissance geochronological study which aims to date the period during which deformation within the Gaoligong and Chong Shan shear zones were active and provides the first detailed descriptions of these shear zones as well as the first reliable geochronological data from samples which have critical implications for our understanding of the accommodation of the post-collisional indentation of India into Eurasia. Our current results must be considered to be preliminary and will no doubt require considerable refinement as tectonic studies in the area proceed.

Appendix A: The $^{40}Ar/^{39}Ar$ Analytical Procedures

Minerals were hand-picked to increase purity of the separates and to ensure sample homogeneity. Final mineral separates varied in grain size from ca. 100 μm to several millimeters in diameter. Prior to packaging for irradiation, all mineral separates were cleaned in an ultrasonic bath with acetone, distilled water, and ethanol. 50 – 100 mg of material were sealed in ca. 1 cm^2 Al foil envelopes for irradiation in the research nuclear reactor at McMaster University, Ontario, Canada.

K, Ca, and Cl production factors during irradiation were determined by including packets of natural and synthetic K_2SO_4, CaF_2, and KCl salts with the samples. Taylor Creek Rhyolite sanidine (TCR-2; 27.87 Ma, Duffield & Dalrymple, 1990) for package clair-131 and Fish Canyon sanidine (28.02 Ma, Renne et al., 1998) for package clair-104 were used for the calculation of the fast neutron flux and the irradiation parameter, J, (e.g. McDougall and Harrison, 1999).

Gas extraction was accomplished by incremental heating in a double-vacuum resistance furnace. Additional details of the extraction line and gas purification are given by Hodges et al. (1994). The furnace contributes the dominant component of the operational blank which is therefore strongly temperature dependent. Furnace system blanks were measured as a function of temperature prior to each sample analysis.

$^{40}Ar/^{39}Ar$ model ages for each gas extraction step were calculated assuming an initial $^{40}Ar/^{39}Ar$ value of 295.5 and are assigned a 2σ uncertainty that reflects propagated errors in all correction factors and J. Release spectra illustrate model ages for incremental heating analyses as a function of the amount of $^{39}Ar_K$ in each step. Plateau ages determined from the release spectra are defined as the error-weighted mean age of at least three consequent increments that define 50% or more of the total ^{39}Ar released and have model ages that overlap the 2σ confidence level when the error in J is ignored. Age estimates also were derived from linear fits of the data on $^{36}Ar/^{40}Ar$ versus $^{39}Ar/^{40}Ar$ isotope correlation diagrams. For all samples, the two methods of data analysis yield dates that are indistinguishable at the 2σ confidence level. We have, therefore, chosen to use the plateau ages as the best estimate of the closure age of the sample since the errors associated with the plateau age are slightly smaller.

FIGURE CAPTIONS

Figure 1. Schematic map of Cenozoic extrusion tectonics and large faults in Eastern Asia (modified after Tapponnier et al., 1986). Heavy lines indicate major faults or plate boundaries. Small arrows show senses of finite motion on strike-slip faults. Open arrows represent the sense of motion from Eocene until mid-Miocene. Shaded areas represent the regions affected by the different extrusion phases. Large open arrows represent the major block motions with respect to Siberia since the Eocene. Boxed area refers to Figure 2.

Figure 2. Location of the four major tectonic elements within the Three Rivers area and the three ductile strike-slip shear zones: T = Tengchong (Lhasa); Q = Qiangtang; LS = Lanping/Simao; B = Baoshan (Sibumasu) Dashed line within the Baoshan element is the Late Palaeozoic Changling-Mengliang suture. Strike-slip shear zones are shown in black with white stripes. The stripes orientation does not refer to the orientation of the fabrics observed within all three of these shear zones. Abbreviations: ASSZ = Ailao Shan Shear Zone; CSSZ = Chong Shan Shear Zone; DSSZ = Dianchang Shan Shear Zone; GSSZ = Gaoligong Shan Shear Zone; XS = Xuelong Shan; M = Mangkang; S = Simao. Inset map shows location of Figure 2, in relation to the India/Eurasia collision zone and the major tectonic blocks that form Eurasia. Abbreviations: SG = Songpan – Garze flysch belt, BNS = Bangong-Nujiang suture zone, LS = Lanchangjiang suture zone, SAS = Song Da – Anning suture zone; Y = Yidun volcanic arc; GL = Garze-Litang suture zone.

Figure 3. Generalized geological map of the GSSZ and the CSSZ and the tectonic elements they separate. The two stereographic projection diagrams on the left show foliation and stretching lineation in mylonitic gneisses, measured along two nearly complete cross-sections (Schimidt diagrams, lower hemisphere projection). Numbers at the lower left hand corner of each diagram corresponds to the number of measurements. Location of dated samples are also shown.

Figure 4. The section of the Nujiang (Salween) valley where the GSSZ and CSSZ juxtapose against each other. (a) Nujiang morphology. View to the north. (b) A conceptual model for the style of deformation observed in the field. The GSSZ, a ductile dextral shear zone, is located to the west of another ductile, sinistral shear zone, the CSSZ. Horizontal shortening perpendicular to the shear zone boundaries (indicated by full arrows) results in vertical stretching of the rocks within the shear zones. The stretching lineations of the GSSZ, plunging <20° both to

the north and south, and the various shear sense indicators, observed on surfaces perpendicular to the foliation and parallel to these lineations, including folded porphyroclast tails, asymmetric folding of syntectonic sills and S-C fabrics indicate a very strong dextral strike-slip shearing along this mylonite zone. The CSSZ has similar shear sense indicator types, which are dominantly left-lateral, with a right-lateral overprint along the section where it is in contact with the GSSZ. The lower section of the block diagram is not drawn to scale

Figure 5. (a) Vertical foliation and (b) nearly horizontal stretching lineations in gneisses from the GSSZ. (c) Rotated feldspar porphyroclasts and (d) S-C mylonites indicate a right-lateral sense of shear. (e) Leucogranite dikes are mostly foliation parallel and undeformed. (d) Some of the leucogranitic sills are (f) vertically, and (g) horizontally stretched. (h) The outcrop picture of sample 98JN15.9. This is one of the few foliation cross-cutting dikes we observed in the field.

Figure 6. $^{40}Ar/^{39}Ar$ release spectra and inverse isochron diagrams for biotites and muscovites from the GSSZ granitic sills and dikes.

Figure 7. A schematic diagram which show the evolution of the Sibumasu/Indochina tectonic element following the India-Eurasia collision. (a) Continued indentation of India into Eurasia, causes oroclinal bending. The Sibumasu fragment of the Sibumasu/Indochina tectonic element accommodate this bending by braking into numerous rhomb-shaped crustal blocks, which ultimately cause the bending of its margins. (b) The Indochina fragment, however, mostly shortens. This style of deformation explains, why the northern Indochina fragment has rotated clockwise up to 90°, while the southern Indochina fragment has not.

Figure 8. A thematic map, which shows the location of the major rivers and the known and presumed locations of the granites and metamorphic rocks of the Three Rivers region. Note the spatial correlation between the largest right-lateral offsets of the Salween and the strike-slip faults which have been active since the early Tertiary (drawn in black color). Faults in red are currently active, but are not known to be active prior to 12 Ma.

Figure 9. Three stages, depicted schematically, in the evolution of the structures within the Sibumasu/Indochina tectonic element related to lateral extrusion and oroclinal bending. During Eocene to approximately middle Miocene time, the region between the GSSZ and the ASSZ was shortened and displaced to the southeast relative to South China and parts of eastern Tibet. The Sibumasu fragment was dismembered it into numerous rhomb-shaped crustal blocks, while the Indochina fragment, was mainly folded and thrusted. By at least ~12 Ma, the northern

part of the GSSZ rotated until it was no longer favorably oriented to accommodate India's continued northward movement. At that time a new fault, the northern part of the Sagaing fault, broke immediately west of the mylonitic GSSZ. Once extrusion of the Sibumasu/Indochina composite tectonic unit to the SE ceased, a new style of deformation began to affect the region, east of the Eastern Himalayan Syntaxis. Since Pliocene time, the Xianshuihe – Xiaojiang and Zongdian fault systems and their probable southward continuations bounded on the east by the Dien Bien Phu fault, gradually became the dominant structures accommodating indentation by the clockwise rotation of the southeastern Tibetan plateau.

REFERENCES:

Akciz, S., Burchfiel, B. C., Chen, Liangzhong, Yin, Jiyun, 2000, Gaoligong and Chong Shan Shear Zones, Yunnan, and accommodation of the northward movement of India relative to Indohina during mid-Cenozoic time: Geological Society of America Abstracts with Programs.

Akciz, S., Burchfiel, B. C., Chen, Liangzhong, Yin Jiyun, 2001, Geometry, Kinematics and Regional Significance of the Chong Shan Shear Zone, Yunnan, China. Geological Society of America Abstracts with Programs.

Briais, A., Patriat, P., Tapponnier, P., 1993, Updated interpretation of magnetic anomalies and seafloor spreading stages in the South China Sea: implications for the Tertiary tectonics of Southeast Asia: Journal of Geophysical Research, v. 98, p. 6,299-6,328.

Bureau of Geology and Mineral Resources of Yunnan Province, 1990, Regional Geology of Yunnan Province: Beijing, Geological Publishing House, 728 p.

Chen, H., Dobson, J., Heller, F., Jie Hao, 1995, Paleomagnetic evidence for clockwise rotation of the Simao region since the Cretaceous: A consequence of India-Asia collision: Earth and Planetary Science Letters, v. 134, p. 203-217.

Chen, Z., Burchfiel, B.C., Liu, Y., King, R.W., Royden, L.H., Tang, W., Wang, E., Zhao, J., Zhang, X., 2000, GPS measurements from eastern Tibet and their implications for India/Eurasia intracontinental deformation, Journal of Geophysical Research, v. 105, p. 16,215–16,227.

Chenjun, F., Zhang, Y., 1994, The structure and tectonics of Western Yunnan.: Journal of southeast Asian earth sciences, v. 9, p. 355-361.

Chhibber, H.L., 1934, The Geology of Burma: London, Macmillan & Co., 590 p.

Clark, M. K., Schoenbohm, L. M., Royden, L. H., Whipple, K. X., Burchfiel, B. C., Zhang, X., Tang, W., Wang, E., Chen, L., 2004, Surface uplift, tectonics and erosion of the Eastern Tibet from large-scale drainage patterns: Tectonics, v. 23, TC1006, doi:10.1029/2002TC001402.

Curray, J.R., Moore, D.G., Lawver, L.A., Emmel, F.J., Raitt, R.W., Henry, M., Kieckhefer, R., 1979, Tectonics of the Andaman sea and Burma, *in* Watkins, T.S. et al., eds., Geological and geophysical investigations of continental margins: AAPG Memoir no. 29, p.189-198.

Duffield, W.A., Dalrymple, G.B., 1990, The Taylor Creek Rhyolite of New Mexico: a rapidly emplaced field of lava domes and flows: Bulletin of Volcanology, v. 52, p. 475-487.

Funahara, S., Nishiwaki, N., Miki, M., Murata, F., Yo-ichiro Otofuji, Yi Zhao Wang, 1992, Paleomagnetic study of Cretaceous rocks from the Yangtze block, central Yunnan, China: implications for the India-Asia collision: Earth and Planetary Science Letters, v. 113, p. 77-91.

Funahara, S., Nishiwaki, N., Murata, F., Yo-ichiro Otofuji, Yi Zhao Wang, 1993, Clockwise rotation of the Red River fault inferred from paleomagnetic study of Cretaceous rocks in the Shan-Thai-Malay block of Western Yunnan, China: Earth and Planetary Science Letters, v. 117, p. 29-42.

Geissman, J.W., Burchfiel, B. C., Lianzhong, C., Harlan, S. S., Wawrzyniec, T. F., 1999, Paleomagnetic data from Upper Jurassic to lower Tertiary redbeds, western Yunnan, PRC; testing spatial variability in large-magnitude intracontinental deformation: Geological Society of America Abstracts with Programs, v. 7, p. 371.

Geissman, J.W., Burchfiel, B.C., Wang, E., Chen, L., Yin, J., 2001, Paleomagnetic data and Cenozoic tectonic rotations in northern Indochina, with implications for middle Cenozoic extrusion of crust south of the Ailao Shan shear zone: Geological Society of America Abstracts with Programs, Cordilleran Section, 97th annual meeting, v. 33, no. 3, p. 43.

Gilley, L.D., Harrison, T.M., Leloup, P. H., Ryerson, F. J., Lovera, O. M., Wang, J.-H., 2003, Direct dating of left-lateral deformation along the Red River shear zone, China and Vietnam: Journal of Geophysical Research, v. 108, no. B2, p ECV 14-1 to 14-21.

Hallet, B., Molnar, P., 2001, Distorted drainage basins as markers of crustal strain east of the Himalaya: Journal of Geophysical Research, v. 106, p. 13,697-13,709.

Harrison, T. M., Chen Wenji, Leloup, P.H., Ryerson, F.J., Tapponnier, P., 1992, An early Miocene transition in deformation regime within the Red River fault zone, Yunnan, and its significance for Indo-Asian tectonics: Journal of Geophysical Research, v. 97, p. 7,159-7,182.

Harrison T.M., Leloup, P.H., Ryerson, F.J., Tapponnier, P., Lacassin, R., Chen Wenji, 1996, Diachronous initiation of Transtension along the Ailao Shan-Red River Shear zone, Yunnan and Vietnam, in Yin, A. and Harrison, T.M., eds., The Tectonics of Asia: New York, Cambridge University Press, p. 208-226.

Hodges, K.V., Hames, W.E., Olszewski, W.J., Burchfiel, B.C., Royden L.H., Chen, Z., 1994, Thermobarometric and $^{40}Ar/^{39}Ar$ geochronologic constraints on Eohimalayan metamorphism in the Dinggye area, southern Tibet:: Contributions to Mineralogy and Petrography, v. 117, p. 151-163.

Huang, K., Opdike, N., 1993, Paleomagnetic results from Cretaceous and Jurassic rocks of South and Southwest Yunnan: evidence for large clockwise rotation in the Indochina and Shan-Tai-Malay terranes: Earth and Planetary Science Letters, v. 117, p. 507-524.

Hutchison, C.S., 1989, Geological evolution of South-east Asia: Oxford Monographs on Geology and Geophysics, Clarendon Press, Oxford, pp. 368.

Jin Xiaochi, 1994, Sedimentary and paleogeographic significance of Permo-Carboniferous sequences in western Yunnan, China. Geologisches Institut der Universitat zu Koln, Sonderveroefentlichungen, 136 p.

King, R.W., Shen, F., Burchfiel, B.C., Royden, L.H., Wang, E., Chen, Z., Liu, Y., Zhang, X.Y., Zhao, J.X. , Li, Y., 1997, Geodetic measurements of crustal motion in southwest China: Geology, v. 25, p. 179-182.

Klootwijk, C.T., Gee, J.S., Peirce, J.W., Smith, G.M., McFadden, P.L., 1992, An early India-Asia contact: Paleomagnetic constraints from Ninetyeast Ridge, ODP Leg 121: Geology v. 20, p. 395-398.

Lacassin R., Maluski, H., Leloup, P.H., Tapponnier, P., Hinthong, C., Siribhakdi, K., Chuaviroj, S., Charoenravat, A., 1997, Tertiary diachronic extrusion and deformation of western Indochina: structural and $^{40}Ar/^{39}Ar$ evidence from NW Thailand: Journal of Geophysical Research, v. 102, p. 10,013-10,037.

Lacassin, R., Replumaz, A., Leloup, P.H., 1998, Hairpin river loop and slip sense inversion on SE-Asian strike-slip faults: Geology, v. 26, p. 703-706.

Lawver, L.A., Curray J.R., Moore, D.G., 1976, Tectonic evolution of the Andaman Sea: EOS, v. 57, p. 333-334.

Le Dain A.Y., Tapponier P., Molnar, P., 1984, Active faulting and tectonics of Burma and surrounding regions: Journal of Geophysical Research, v. 89, p. 453–472.

Leloup, P. H., Kienast, J.R., 1993, High-temperature metamorphism in a major strike-slip shear zone: the Ailao Shan-Red River, People's Republic of China: Earth and Planetary Science Letters, v. 118, p. 213-234.

Leloup, P. H., Lacassin, R., Tapponnier, P., Zhong Dalai, Liu Xiaohan, Zhang Lianshang, Ji Shaocheng, Phan Trong Trinh, 1995, The Ailao Shan-Red River shear zone (Yunnan, China), Tertiary transform boundary of Indochina: Tectonophysics, v. 251, p. 3-84.

Leloup P.H., Arnaud N., Lacassin R., Kienast J.R., Harrison T.M., Phan Trong Trinh, Replumaz A., Tapponnier P, 2001, New constraints on the structure, thermochronology and timing of the Ailao Shan - Red River shear zone, SE Asia: Journal of Geophysical Research, v. 106, p. 6,657-6,671.

McDougall, I., Harrison, T.M., 1999, Geochronology and Thermochronology by the $^{40}Ar/^{39}Ar$ Method (2^{nd} Ed.): New York, Oxford University Press, 269 p.

Metcalfe, I., 1988, Origin and assembly of South-East Asian continental terranes, in Audley-Charles, M.G., and Hallam, A., eds., Gondwana & Tethys, Geological Society of London Special Publication No. 37, p. 101-118. Oxford University Press.

Metivier, F., Gaudemer, Y., Tapponnier, P., Klein, M., 1999, Mass accumulation rates in Asia during the Cenozoic: Geophysical Journal International, v. 137, p. 280-318.

Molnar, P., Tapponnier, P., 1975, Cenozoic tectonics of Asia; effects of a continental collision: Science, v. 189, p. 419-426.

Patriat, P., 1983, Evolution du systeme de dorsales de l'Ocean Indien [Ph.D. thesis], Universite´ Pierre et Marie Curie, Paris.

Patriat, P., Achache, J., 1984, India-Eurasia collision chronology has implications for crustal shortening and driving mechanism of plates: Nature, v. 311, p. 615-621.

Replumaz A., Lacassin, R., Tapponnier, P., Leloup, P.H., 2001. Large river offsets and Plio-Quaternary dextral slip rate on the Red River fault (Yunnan, China): Journal of Geophysical Research.,v. 106, p. 819-836.

Rowley, D.B., 1996, Age of initiation of collision between India and Asia: A Review of stratigraphic data: Earth and Planetary Science Letters, v. 145, p. 1-13.

Rowley, D.B., 1998, Minimum age of initiation of collision between India and Asia north of Everest based on the subsidence history of the Zhepure Mountain section: Journal of Geology, v. 106, p. 229-235.

Royden, L.H., Burchfiel, B. C., King, R. W., Wang, E., Chen Zhiliang, Shen Feng, Liu Yuping, 1997, Surface deformation and lower crustal flow in eastern Tibet: Science, v. 276, p. 788-790.

Schärer, U., Tapponnier, P., Lacassin, R., Leloup, P.H., Zhong Dalai, Ji Shaocheng, 1990, Intraplate tectonics in Asia: a precise age for large-scale Miocene movement along the Ailao Shan-Red River shear zone, China: Earth and Planetary Science Letters, v. *97*, p. 65-77.

Schärer, U., Zhang Lian-Sheng, Tapponnier, P., 1994, Duration of strike-slip movements in large shear zones: The Red River belt, China : Earth and Planetary Science Letters, v. 126, p. 379-397.

Schoenbohm, L., 2004, Cenozoic tectonic and geomorphic evolution of the Red River region, Yunnan Province, China [PhD Thesis] Boston, Massachusetts Institute of Technology, 235 p.

Şengör, A.M.C., 1984, The Cimmeride orogenic system and the tectonics of Eurasia: Geological Society of America, Special paper 195, xi+82 pp.

Şengör, A.M.C., Altiner, D., Cin, A., Ustaomer, T., and Hsu, K.J., 1988, Origin and assembly of the Tethyside orogenic collage at the expense of Gondwanaland, in Audley-Charles, M.G., and Hallam, A., eds, Gondwana and Tethys: Geological Society Special Publications, no. 37, p. 119-181.

Stock, J.M. Molnar, P., 1987, Revised history of the early Tertiary plate motion in the southwest Pacific: Nature, v. 325, p. 495-499.

Tapponnier, P., Peltzer, G., Le Dain, A.Y., Armijo, R., Cobbold, P., 1982, Propagating extrusion tectonics in Asia: new insights from simple experiments with plasticine: Geology, v. 10, p. 611-616.

Tapponnier, P., Peltzer, G., Armijo, R., 1986, On the mechanics of the collision between India and Asia: Coward, M.P., and Ries, A.C., eds., Collision Tectonics: London, Geological Society, Geological Society Special Publication, no. 19, p. 115-157.

Wang, E., Burchfiel, B.C., 1997, Interpretation of Cenozoic tectonics in the right-lateral accommodation zone between the Ailao Shan shear zone and the Eastern Himalayan Syntaxis: International Geology Review, v. 39, p. 191-219.

Wang, E., Burchfiel, B. C., Royden, L. H., Chen Liangzhong, Chen Jishen, Li Wenxin, Chen Zhiliang, 1998, Late Cenozoic Xianshuihe-Xiaojiang, Red River, and Dali fault systems of southwestern Sichuan and central Yunnan, China: Geological Society of America Special Paper, no. 327, 108 p.

Wang, E., Burchfiel, B. C., 2000, Late Cenozoic to Holocene deformation in southwestern Sichuan and adjacent Yunnan, China, and its role in formation of the southeastern part of the Tibetan Plateau: Geological Society of America Bulletin, v. 112, p. 413-423.

Yang, Z., Besse, J., 1993, Paleomagnetic study of Permian and Mesozoic sedimentary rocks from Northern Thailand supports the extrusion model for Indochina: Earth and Planetary Science Letters, v. 117, p. 525-552.

Yang, Z., Besse, J., Sutheetorn, V., Bassoulet, J.P., Fontaine, H., Buffetaut, E., 1995, Jurassic and Cretaceous paleomagnetic data for Indochina: paleogeographic evolution and deformation history of South Eastern Asia: Earth and Planetary Science Letters, v. *136*, p. 325-341.

Zhong, D., Wang, Y., 1991, Tertiary strike-slip fault and associated extensional structure, in Zhang, X., ed., Annual Report 1989-1990, Laboratory of Lithosphere Tectonic Evolution: Beijing, Chinese Science and Technology Press, p. 18-22 (in Chinese).

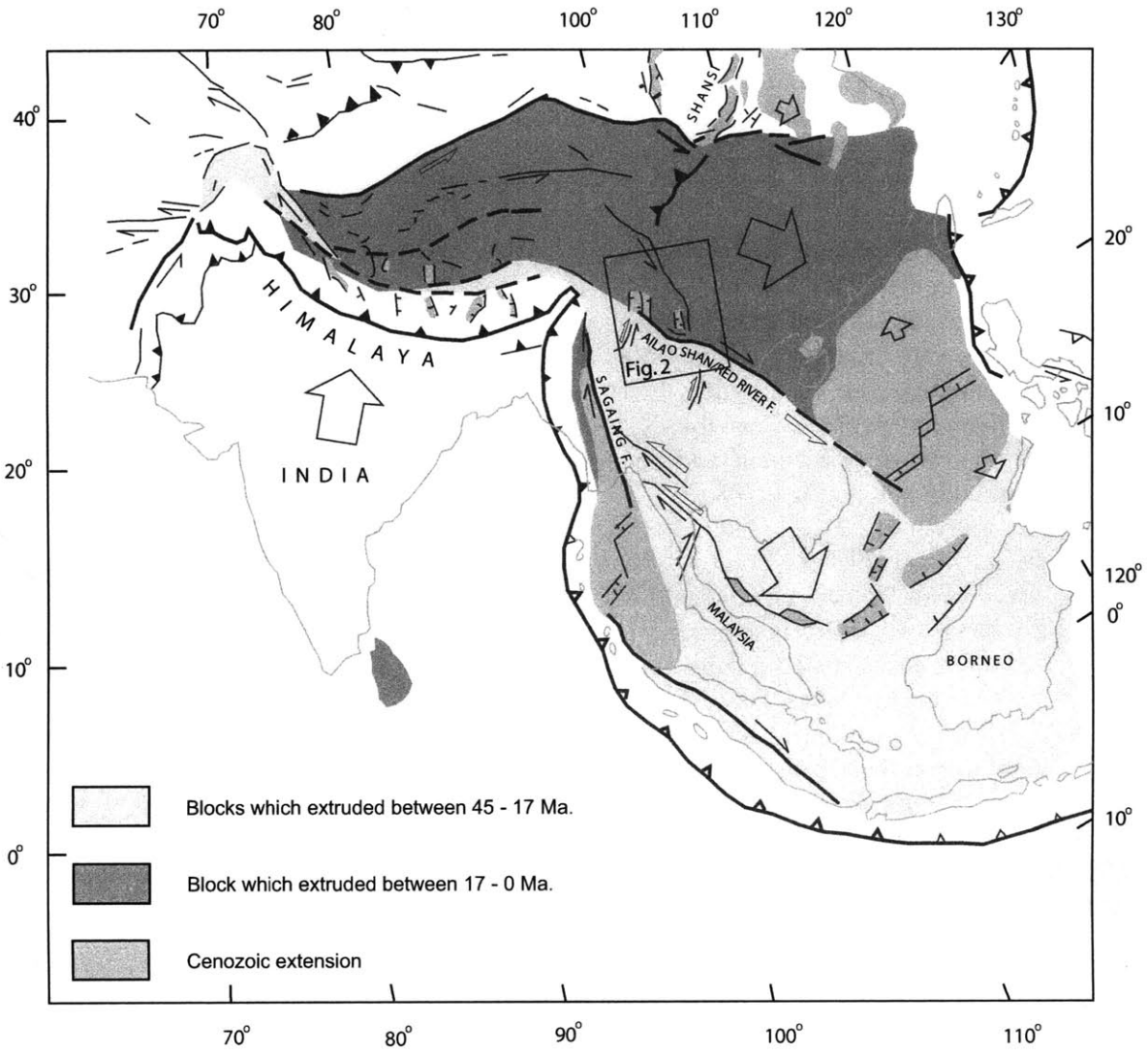
70°
80°
100°
110°
120°
130°
40°
30°
20°
10°
0°
SHANSI
HIMALAYA
INDIA
AILAO SHAN/RED RIVER F.
Fig. 2
SAGAING F.
MALAYSIA
BORNEO
Blocks which extruded between 45 - 17 Ma.
Block which extruded between 17 - 0 Ma.
Cenozoic extension
70°
80°
90°
100°
110°
20°
10°
120°
0°
10°

FIGURE 1

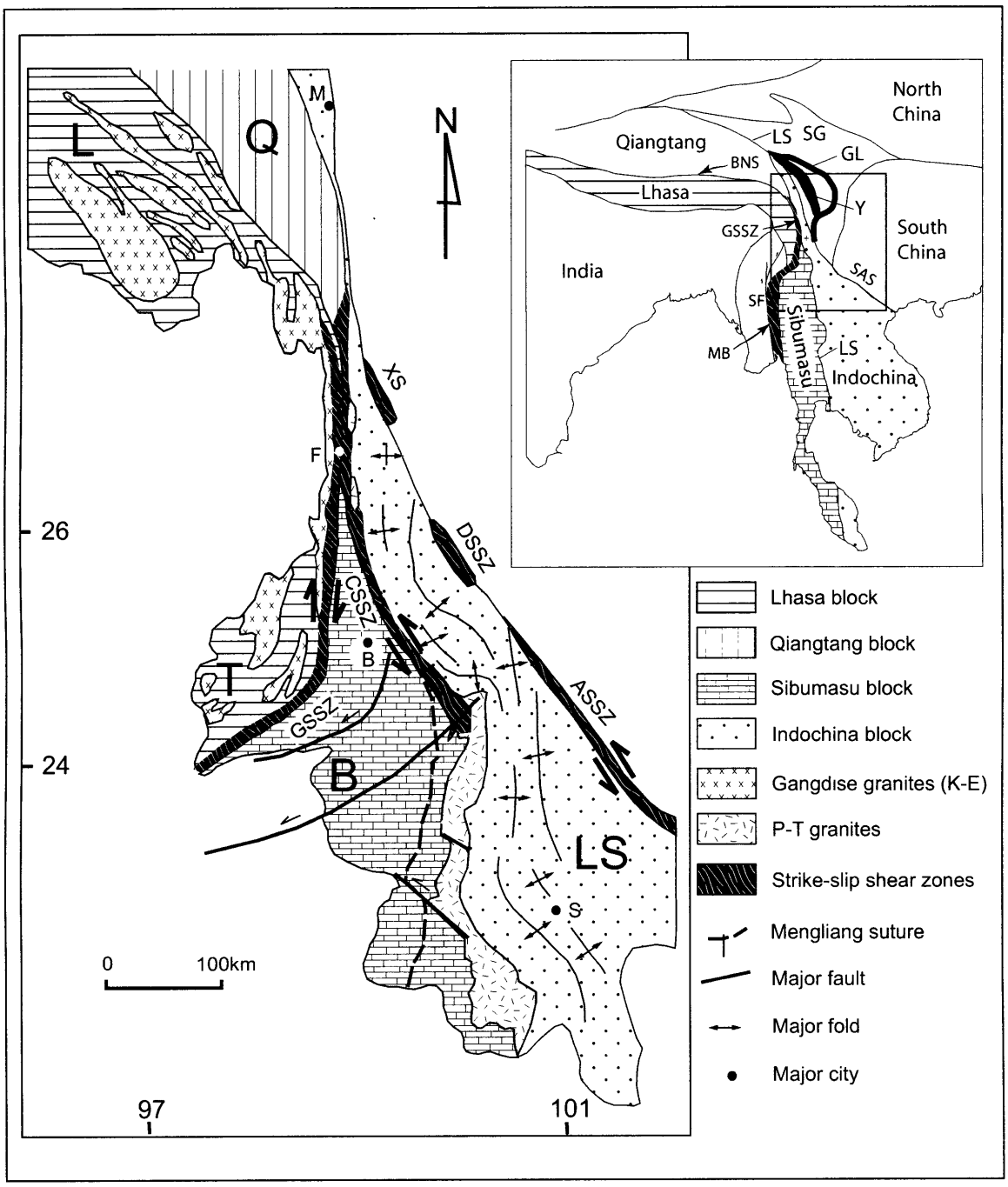
North China
Qiangtang
LS
SG
GL
BNS
Lhasa
Y
GSSZ
South China
India
SAS
SF
Sibumasu
MB
LS
Indochina
L
Q
M
N
XS
F
26
DSSZ
CSSZ
B
T
GSSZ
ASSZ
24
B
LS
S
0
100km
97
101
Lhasa block
Qiangtang block
Sibumasu block
Indochina block
Gangdise granites (K-E)
P-T granites
Strike-slip shear zones
Mengliang suture
Major fault
Major fold
Major city

FIGURE 2

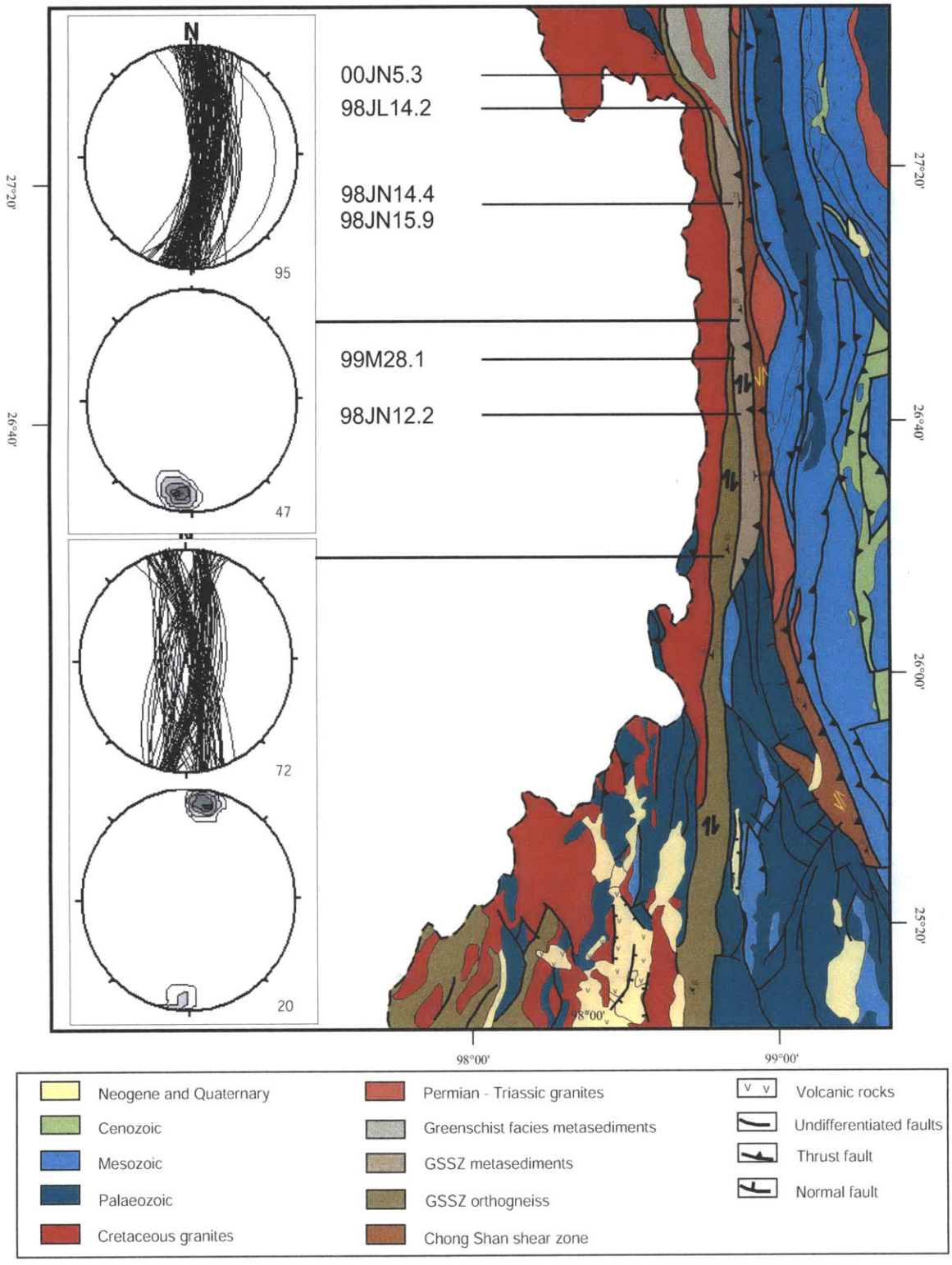
N
95
47
72
20
00JN5.3
98JL14.2
98JN14.4
98JN15.9
99M28.1
98JN12.2
27°20'
26°40'
26°00'
25°20'
98°00'
99°00'
Neogene and Quaternary
Cenozoic
Mesozoic
Palaeozoic
Cretaceous granites
Permian - Triassic granites
Greenschist facies metasediments
GSSZ metasediments
GSSZ orthogneiss
Chong Shan shear zone
Volcanic rocks
Undifferentiated faults
Thrust fault
Normal fault

FIGURE 3

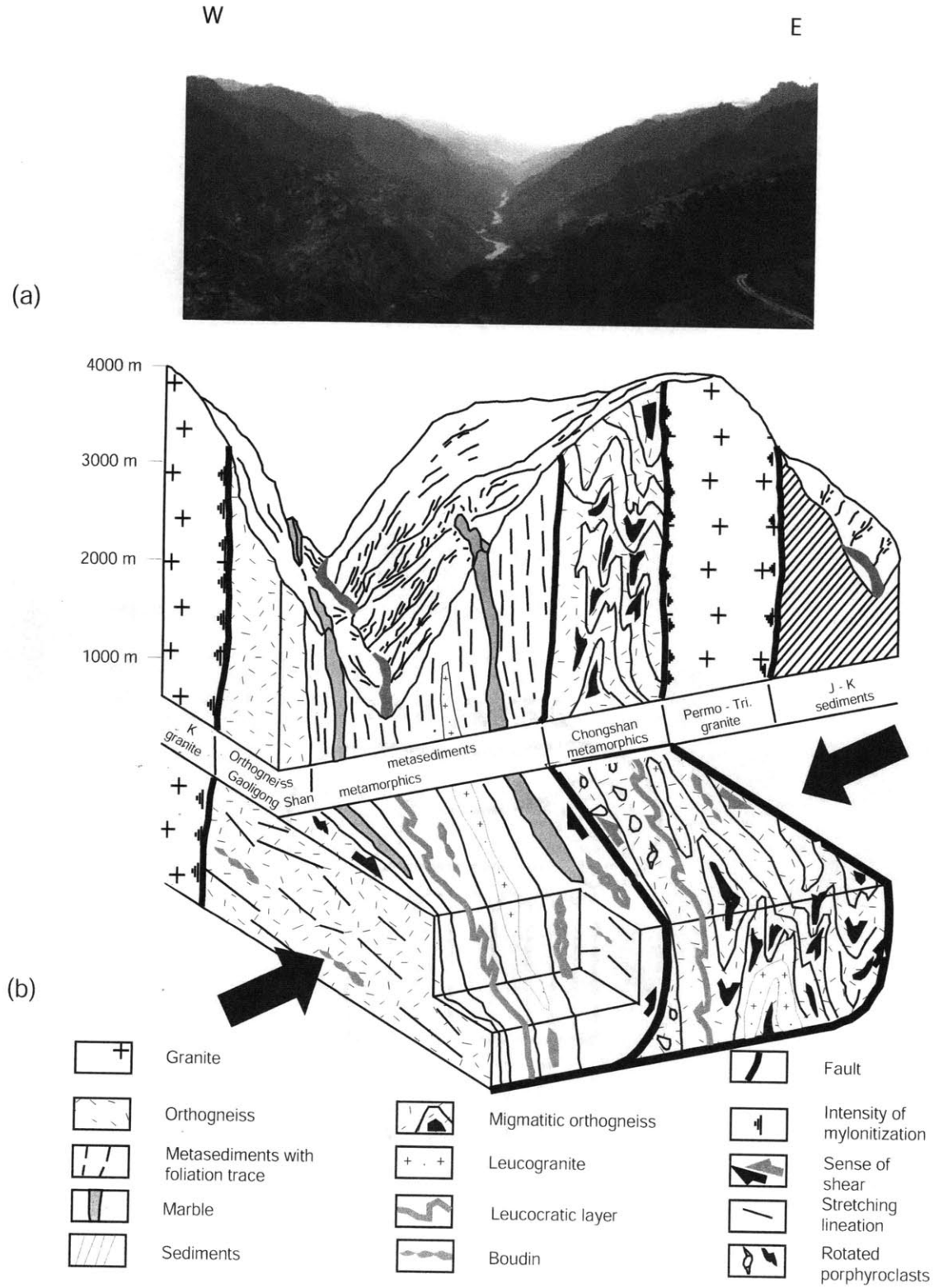
W
E
(a)
4000 m
3000 m
2000 m
1000 m
K granite
Orthogneiss
Gaoligong Shan
metasediments
metamorphics
Chongshan metamorphics
Permo - Tri. granite
J - K sediments
(b)
Granite
Orthogneiss
Metasediments with foliation trace
Marble
Sediments
Migmatitic orthogneiss
Leucogranite
Leucocratic layer
Boudin
Fault
Intensity of mylonitization
Sense of shear
Stretching lineation
Rotated porphyroclasts

FIGURE 4

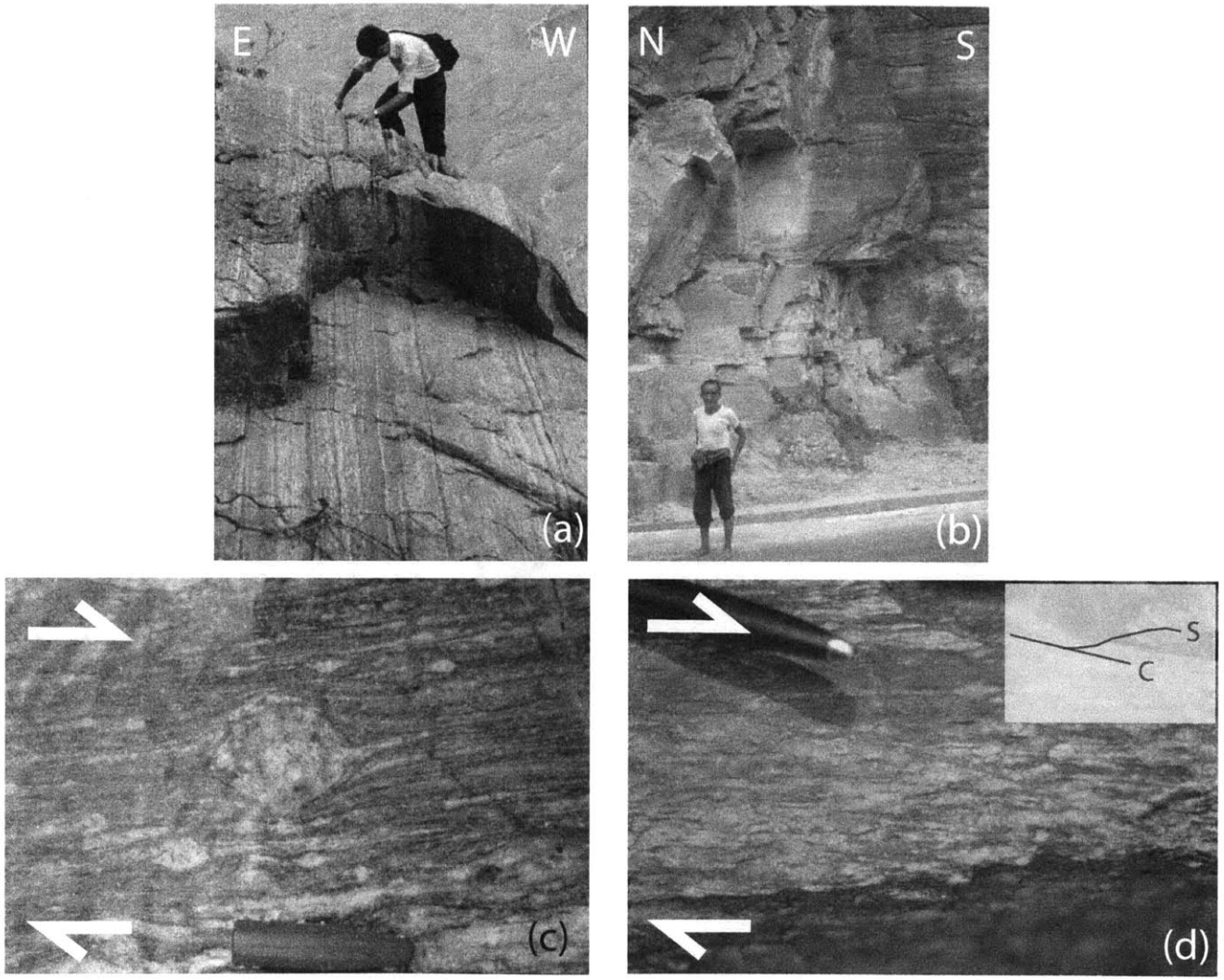

FIGURE 5

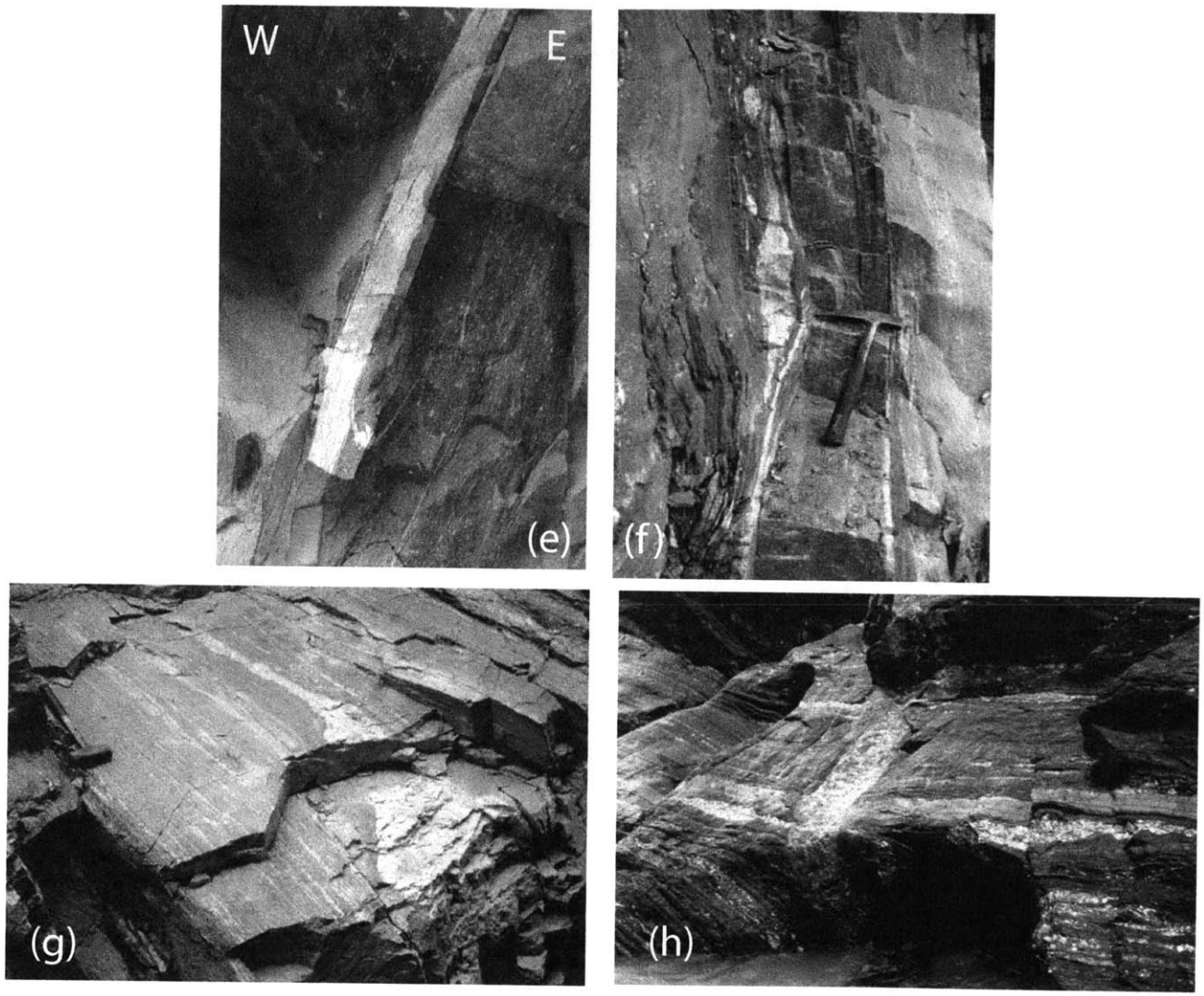

FIGURE 5 (continued)

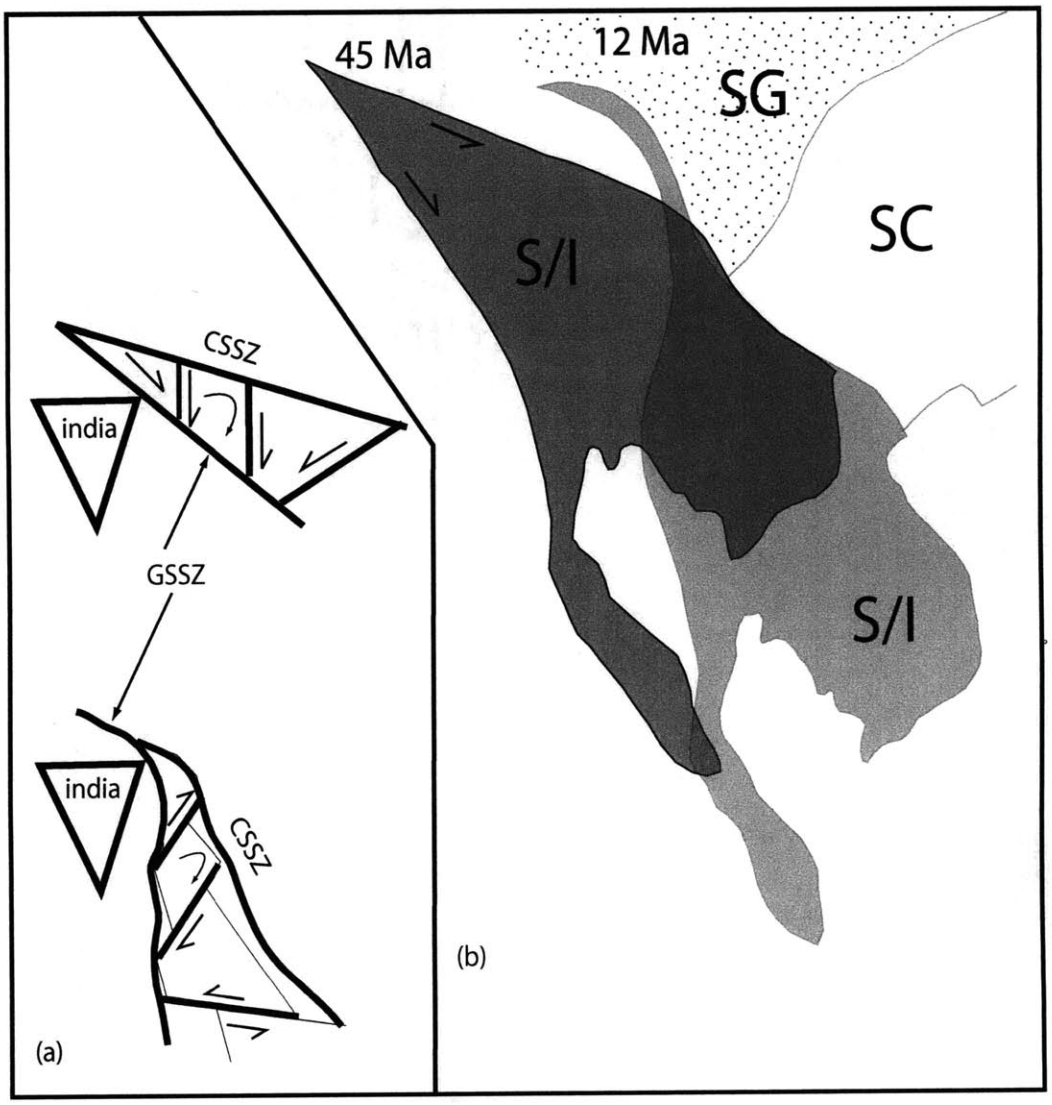

FIGURE 7

FIGURE 6

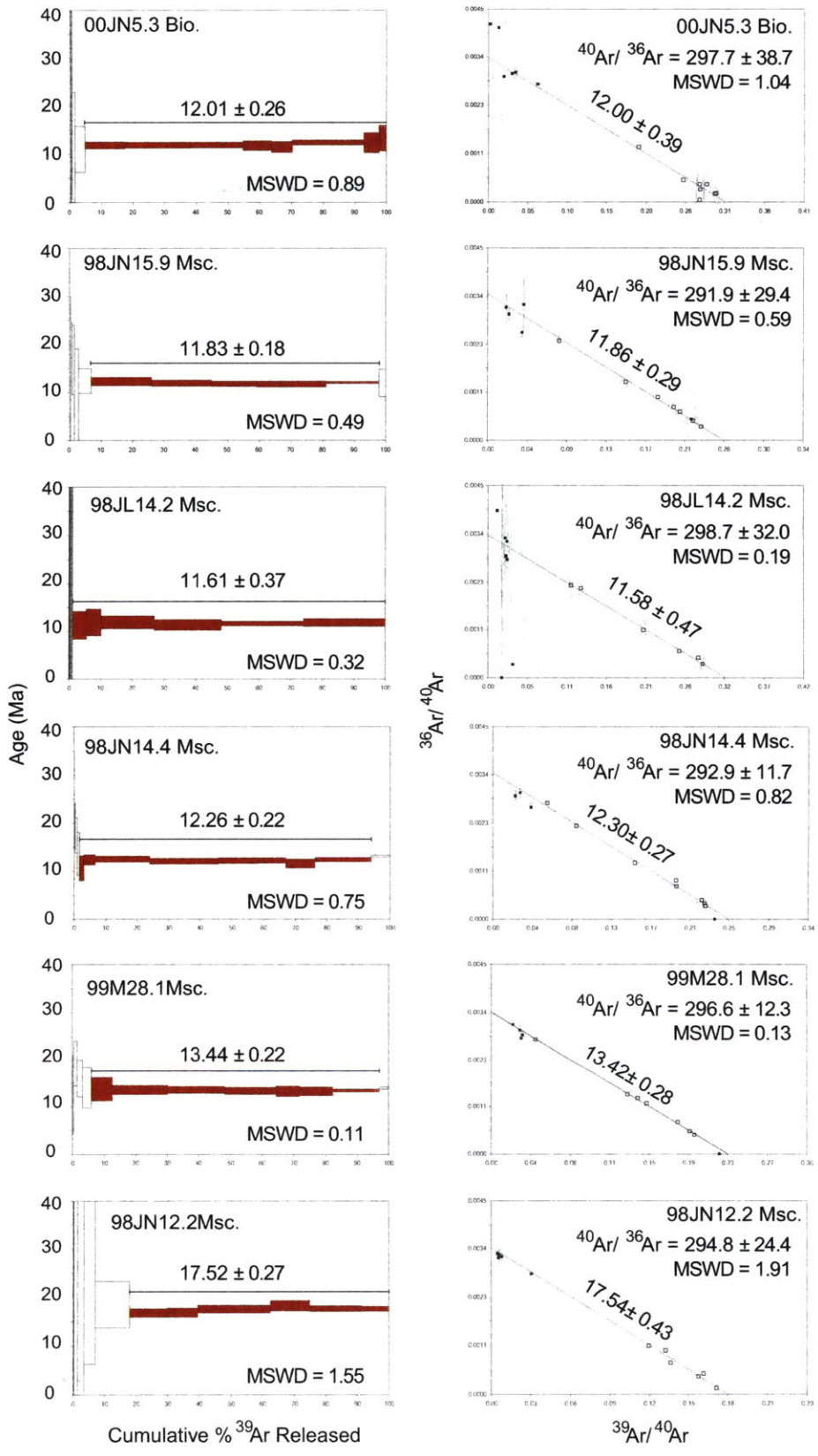
00JN5.3 Bio.
12.01 ± 0.26
MSWD = 0.89
00JN5.3 Bio.
40Ar/ 36Ar = 297.7 ± 38.7
MSWD = 1.04
12.00 ± 0.39
98JN15.9 Msc.
11.83 ± 0.18
MSWD = 0.49
98JN15.9 Msc.
40Ar/ 36Ar = 291.9 ± 29.4
MSWD = 0.59
11.86 ± 0.29
98JL14.2 Msc.
11.61 ± 0.37
MSWD = 0.32
98JL14.2 Msc.
40Ar/ 36Ar = 298.7 ± 32.0
MSWD = 0.19
11.58 ± 0.47
98JN14.4 Msc.
12.26 ± 0.22
MSWD = 0.75
98JN14.4 Msc.
40Ar/ 36Ar = 292.9 ± 11.7
MSWD = 0.82
12.30± 0.27
99M28.1Msc.
13.44 ± 0.22
MSWD = 0.11
99M28.1 Msc.
40Ar/ 36Ar = 296.6 ± 12.3
MSWD = 0.13
13.42± 0.28
98JN12.2Msc.
17.52 ± 0.27
MSWD = 1.55
98JN12.2 Msc.
40Ar/ 36Ar = 294.8 ± 24.4
MSWD = 1.91
17.54± 0.43
Age (Ma)
Cumulative % 39Ar Released
36Ar/40Ar
39Ar/40Ar

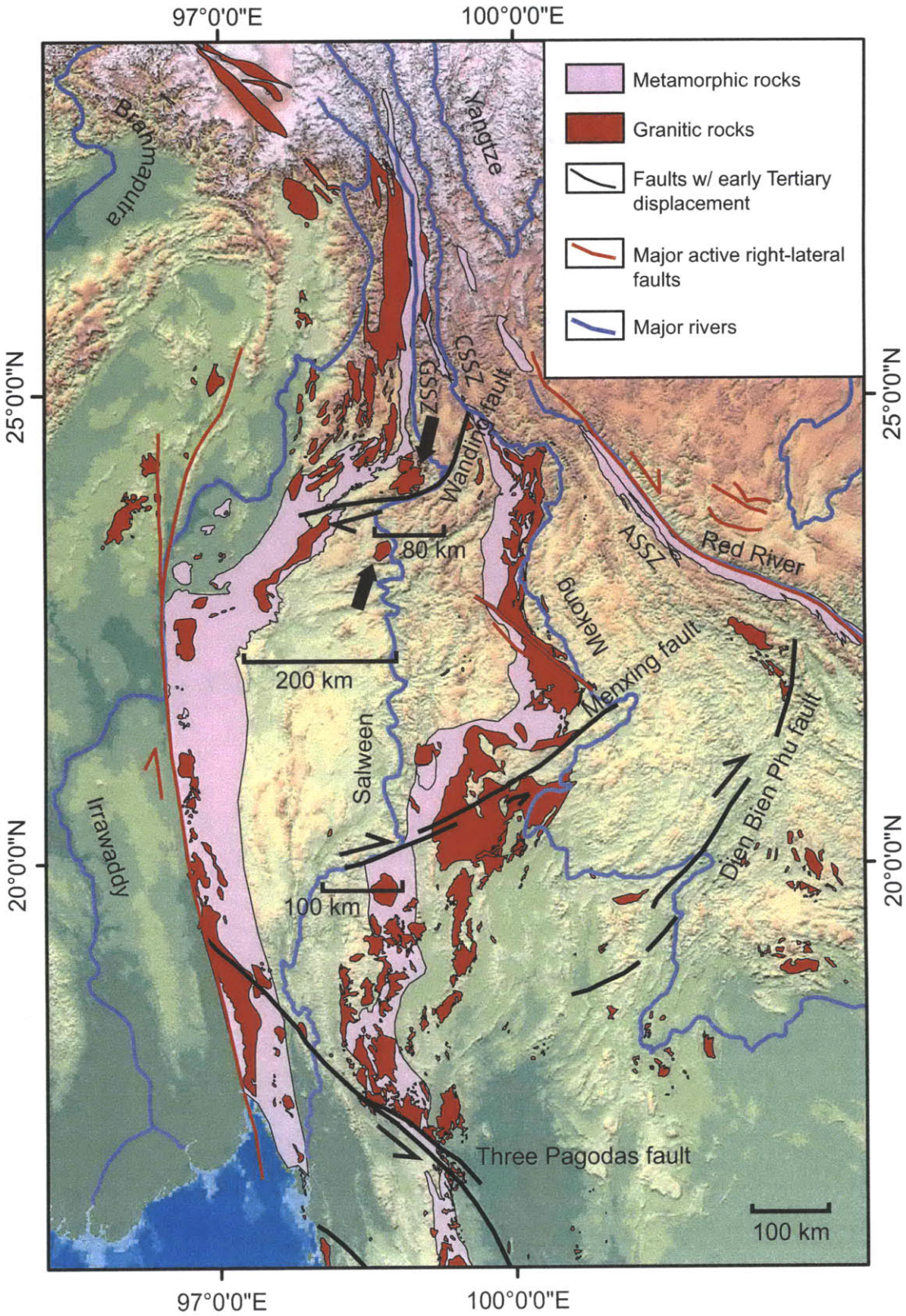
97°0'0"E
100°0'0"E
25°0'0"N
20°0'0"N
Metamorphic rocks
Granitic rocks
Faults w/ early Tertiary displacement
Major active right-lateral faults
Major rivers
Brahmaputra
Yangtze
GSSZ
Wanding fault
80 km
200 km
ASSZ
Red River
Mekong
Menxing fault
Salween
Irrawaddy
100 km
Dien Bien Phu fault
Three Pagodas fault
100 km

FIGURE 8

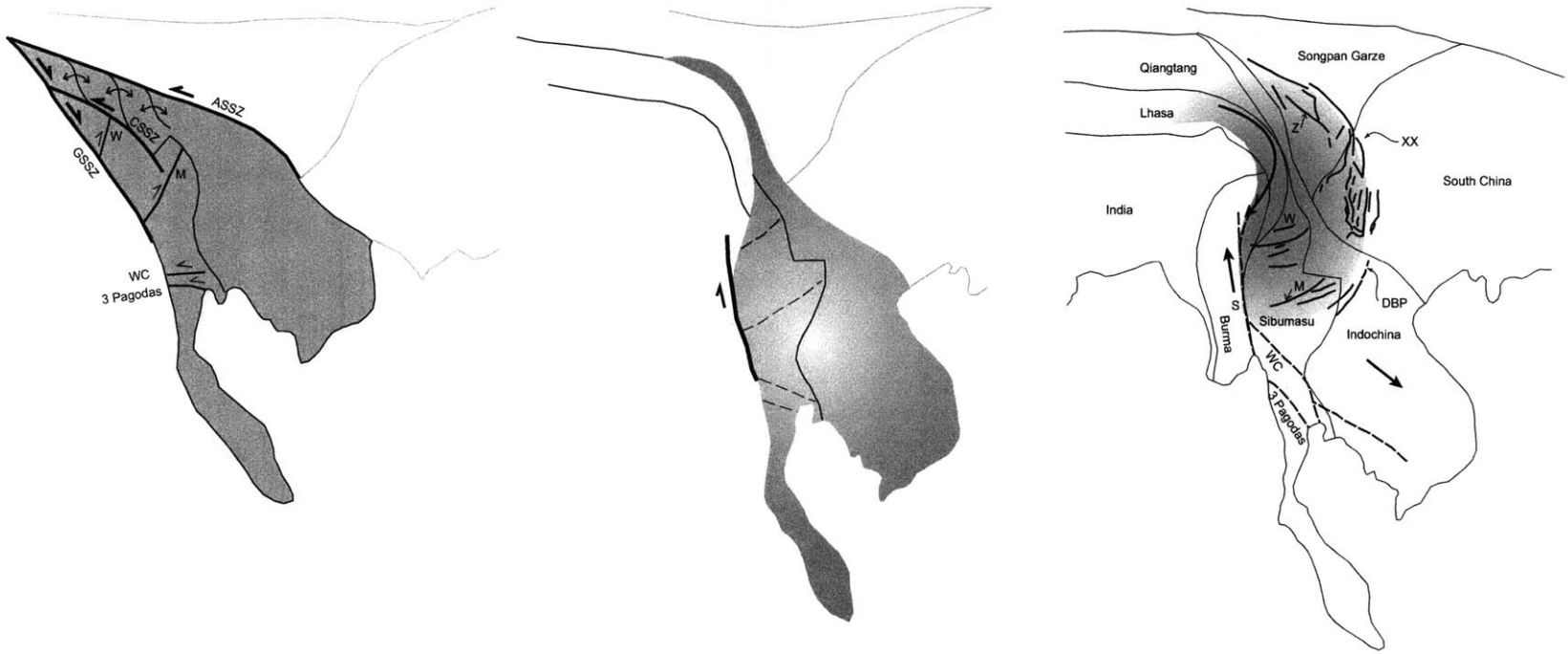

45 - 12 Ma

~12 Ma

12 Ma - Present

FIGURE 9

Sample	T (K)		$^{36}Ar(a)$	$^{39}Ar(K)$	$^{40}Ar^*$	$^{40}Ar^*$ (%)	$^{39}Ar/^{40}Ar \pm 2s$	$^{36}Ar/^{40}Ar \pm 2s$	Age ± 2s
	900		0 00058	0 00037	0 00000	0 02	0 002659 ± 0 005621	0 004147 ± 0 001438	0 00 ± 0 00
	1000		0 00031	0 00102	0 00000	0 06	0 013420 ± 0 008524	0 004061 ± 0 002418	0 00 ± 0 00
	1050		0 00038	0 00271	0 01822	0 16	0 020671 ± 0 004698	0 002914 ± 0 001308	24 74 ± 69 04
	1100		0 00057	0 00593	0 02247	0 36	0 031030 ± 0.003624	0 002986 ± 0 000734	13 99 ± 25 98
00JN5.3	1150		0 00135	0 01601	0 04901	0 97	0 035709 ± 0 001920	0.003014 ± 0 000374	11 31 ± 11 48
Biotite	1200		0 00213	0 05037	0 14974	3 04	0 064638 ± 0 002560	0 002734 ± 0 000272	10 99 ± 4 68
J= **0.002055**	1250	v	0 00137	0 20993	0 67067	12 68	0 195441 ± 0 003867	0 001271 ± 0 000114	11 81 ± 0 70
	1300	v	0 00050	0 34211	1 09591	20 67	0 274761 ± 0 004458	0 000406 ± 0 000144	11 84 ± 0 60
	1350	v	0 00017	0 27725	0 88932	16 75	0 294677 ± 0 003365	0 000185 ± 0 000150	11 85 ± 0 57
	1400	v	0 00010	0 14923	0 47387	9 02	0 296138 ± 0 003754	0 000202 ± 0 000266	11 73 ± 0 99
	1500	v	0 00016	0 10781	0 33414	6 51	0 283722 ± 0 005088	0 000408 ± 0 000271	11 45 ± 1 06
	1823	v	0 00075	0 37538	1 25855	22 68	0 253482 ± 0 005229	0.000508 ± 0 000084	12 39 ± 0 45
	1823	v	0 00008	0 07805	0 25940	4 72	0 275250 ± 0 005268	0 000288 ± 0 000498	12 28 ± 1 98
	1823	v	0 00001	0 03898	0 14015	2 35	0 274505 ± 0 005089	0 000044 ± 0 000654	13 28 ± 2 60

Sample	T (K)		$^{36}Ar(a)$	$^{39}Ar(K)$	$^{40}Ar^*$	$^{40}Ar^*$ (%)	$^{39}Ar/^{40}Ar \pm 2s$	$^{36}Ar/^{40}Ar \pm 2s$	Age ± 2s
	800		0 00036	0 00241	0 00958	0 26	0 020530 ± 0 000392	0 003108 ± 0 000403	12 13 ± 17 63
	900		0 00034	0 00504	0 03423	0 55	0 037288 ± 0 000653	0 002527 ± 0 000150	20 68 ± 3 63
	950		0 00084	0 00662	0 03610	0 72	0 023270 ± 0 000319	0 002954 ± 0 000187	16 63 ± 7 20
	1000		0 00101	0 01256	0 02028	1 37	0 039374 ± 0 000498	0 003169 ± 0 000610	4 94 ± 13 98
98JN15.9	1050		0 00104	0 03492	0 14073	3 82	0 077870 ± 0 000854	0.002322 ± 0 000217	12 30 ± 2 51
Muscovite	1100	v	0 00158	0 17470	0 69412	19 11	0 150526 ± 0 005426	0 001360 ± 0 000096	12 12 ± 0 80
J= **0.001697**	1150	v	0 00036	0 17455	0 67494	19 10	0 223553 ± 0 009264	0 000459 ± 0 000074	11 80 ± 0 60
	1200	v	0 00041	0 12944	0 49577	14 16	0 209498 ± 0 007990	0 000669 ± 0 000048	11 69 ± 0 54
	1250	v	0 00039	0 07119	0 26975	7 79	0 185315 ± 0 005089	0 001008 ± 0 000094	11 56 ± 0 59
	1350	v	0 00049	0 12945	0 49386	14 16	0 202337 ± 0 006963	0 000772 ± 0 000083	11 64 ± 0 58
	1550	v	0 00021	0 15409	0 60103	16 86	0 232463 ± 0 002882	0 000316 ± 0 000046	11 90 ± 0 23
	1823		0 00004	0 01896	0 07323	2 07	0 221806 ± 0 004450	0 000485 ± 0 000685	11 79 ± 2 79

Sample	T (K)		$^{36}Ar(a)$	$^{39}Ar(K)$	$^{40}Ar^*$	$^{40}Ar^*$ (%)	$^{39}Ar/^{40}Ar \pm 2s$	$^{36}Ar/^{40}Ar \pm 2s$	Age ± 2s
	900		0 00026	0 00083	0 00000	0 07	0 012494 ± 0 007292	0 003915 ± 0 002688	0 00 ± 0 00
	950		0 00000	0 00034	0 01842	0 03	0 018594 ± 0 022615	0 000000 ± 0 000000	189 55 ± 218 84
	1000		0 00001	0 00071	0 01935	0 06	0 033479 ± 0 015038	0 000309 ± 0 004787	98 15 ± 154 86
	1050		0 00015	0 00132	0 00856	0 11	0 024362 ± 0 006747	0 002848 ± 0 002319	24 02 ± 103 45
98JL14.2	1100		0 00032	0 00224	0 00324	0 19	0 023273 ± 0 002889	0 003270 ± 0 000812	5 36 ± 38 27
Muscovite	1150		0 00037	0 00293	0 00639	0 25	0 025534 ± 0 003977	0 003196 ± 0 000621	8 09 ± 26 90
J= **0.00206**	1200		0 00050	0 00497	0 09283	0 42	0 020785 ± 0 002809	0 002071 ± 0 000554	68 06 ± 30 61
	1250	v	0 00086	0 05102	0 15490	4 27	0 124716 ± 0 002553	0 002103 ± 0 000330	11 25 ± 2 91
	1300	v	0 00108	0 05557	0 17799	4 65	0 112004 ± 0 002089	0 002170 ± 0 000290	11 86 ± 2 85
	1350	v	0 00108	0 20158	0 64641	16 87	0 208933 ± 0 003177	0 001117 ± 0 000246	11 88 ± 1 29
	1400	v	0 00041	0 25233	0 76962	21 12	0 282812 ± 0 007046	0 000465 ± 0 000265	11 30 ± 1 06
	1500	v	0 00035	0 31096	0 97502	26 03	0 288427 ± 0 004567	0 000324 ± 0 000123	11 62 ± 0 50
	1823	v	0 00075	0 30990	0 98565	25 94	0 256822 ± 0 005112	0 000620 ± 0 000177	11 78 ± 0 79

Sample	T (K)		$^{36}Ar(a)$	$^{39}Ar(K)$	$^{40}Ar^*$	$^{40}Ar^*$ (%)	$^{39}Ar/^{40}Ar \pm 2s$	$^{36}Ar/^{40}Ar \pm 2s$	Age ± 2s
	800		0 00055	0 00464	0 02894	0 38	0 024084 ± 0 000334	0 002876 ± 0 000128	19 24 ± 4 84
	900		0 00045	0 00697	0 03920	0 56	0 040514 ± 0 000671	0 002612 ± 0 000161	17 38 ± 3 62
	950		0 00097	0 00943	0 04131	0 76	0 028768 ± 0 000324	0 002958 ± 0 000141	13 55 ± 4 46
	1000	v	0 00078	0 01664	0 05713	1 35	0 058122 ± 0 000593	0 002709 ± 0 000165	10 62 ± 2 59
98JN14.4	1050	v	0 00108	0 04395	0 17568	3 56	0 088923 ± 0 000934	0 002181 ± 0 000106	12 36 ± 1 09
Muscovite	1100	v	0 00186	0 21327	0 86148	17 27	0 151153 ± 0 004060	0 001318 ± 0 000064	12 49 ± 0 55
J= **0.00172**	1150	v	0 00054	0 27067	1 05772	21 91	0 222359 ± 0 010379	0 000444 ± 0 000035	12 09 ± 0 61
	1200	v	0 00026	0 15654	0 61807	12 67	0 225568 ± 0 008986	0 000370 ± 0 000080	12 21 ± 0 61
	1250	v	0 00042	0 10643	0 42067	8 62	0 195674 ± 0 006472	0 000767 ± 0 000067	12 22 ± 0 54
	1350	v	0 00053	0 11308	0 42418	9 16	0 194827 ± 0 010184	0 000911 ± 0 000131	11 60 ± 0 92
	1550	v	0 00030	0 22088	0 88593	17 88	0 226510 ± 0 002644	0 000310 ± 0 000091	12 40 ± 0 39
	1823		0 00000	0 07262	0 30773	5 88	0 235994 ± 0 002771	0 000000 ± 0 000000	13 10 ± 0 15

Table 1

Sample	T (K)		$^{36}Ar(a)$	$^{39}Ar(K)$	$^{40}Ar^*$	$^{40}Ar^*$ (%)	$^{39}Ar/^{40}Ar \pm 2s$	$^{36}Ar/^{40}Ar \pm 2s$	Age ± 2s
	800		0 00070	0 00481	0 02001	0 47	0 021121 ± 0 001099	0 003087 ± 0 000190	12.74 ± 8 32
	900		0 00108	0 01131	0 07105	1 11	0 029048 ± 0 000580	0 002767 ± 0 000153	19 21 ± 4 77
	950		0 00159	0 01698	0 08912	1 67	0 030429 ± 0 000489	0 002844 ± 0 000134	16 06 ± 4 01
	1000		0 00306	0 02885	0 13268	2.84	0 027812 ± 0 000462	0 002951 ± 0 000132	14 08 ± 4 31
99M28.1	1050	v	0 00434	0 06752	0 30374	6 65	0 042596 ± 0 000614	0 002736 ± 0 000115	13 78 ± 2 47
Muscovite	1100	v	0 00193	0 17835	0 79031	17 56	0 131046 ± 0.005340	0.001419 ± 0 000088	13 57 ± 0 92
J= **0.001704**	1150	v	0 00042	0 18308	0 81188	18 02	0 195534 ± 0 008012	0 000450 ± 0 000081	13 58 ± 0 70
	1200	v	0 00068	0 16305	0 70833	16 05	0 179180 ± 0 007003	0 000750 ± 0 000077	13 31 ± 0 70
	1250	v	0 00061	0 07673	0 33221	7 55	0 149585 ± 0 006798	0 001193 ± 0 000136	13 26 ± 1 11
	1350	v	0 00099	0 10614	0 46113	10 45	0 140819 ± 0 006064	0 001314 ± 0 000076	13 31 ± 0 87
	1550	v	0 00043	0 14907	0 65435	14 67	0 191001 ± 0 002445	0 000547 ± 0.000046	13.44 ± 0 28
	1823		0 00000	0 02991	0 13627	2 94	0 219481 ± 0 002732	0 000000 ± 0 000000	13 95 ± 0 17

Sample	T (K)		$^{36}Ar(a)$	$^{39}Ar(K)$	$^{40}Ar^*$	$^{40}Ar^*$ (%)	$^{39}Ar/^{40}Ar \pm 2s$	$^{36}Ar/^{40}Ar \pm 2s$	Age ± 2s
	800		0 00124	0 00209	0 02629	0 34	0 005333 ± 0 000430	0 003157 ± 0 000225	38 63 ± 38 97
	900		0 00382	0 00730	0 05931	1 17	0 006141 ± 0 000261	0 003215 ± 0 000177	25 03 ± 26 46
	950		0 00904	0 01250	0 10947	2 00	0 004498 ± 0 000121	0 003251 ± 0 000140	26 97 ± 28 36
	1000		0 00909	0 02249	0 17068	3 61	0 007870 ± 0 000164	0 003182 ± 0 000147	23 39 ± 17 06
98JN12.2	1050		0 00627	0 06716	0 40228	10 77	0 029764 ± 0 000963	0 002781 ± 0 000148	18 49 ± 4 73
Muscovite	1100	v	0 00057	0 07431	0 40381	11 92	0 129531 ± 0 003889	0 001002 ± 0 000083	16.78 ± 0 84
J= **0.001714**	1150	v	0 00018	0 05994	0 32666	9 61	0 157830 ± 0 004167	0 000473 ± 0 000141	16 83 ± 0 94
	1200	v	0 00038	0 14365	0 81892	23 04	0 154148 ± 0 006291	0 000410 ± 0 000038	17 60 ± 0 80
	1250	v	0 00041	0 07717	0 45623	12 37	0 133485 ± 0 003231	0 000713 ± 0 000133	18 25 ± 1 03
	1350	v	0 00098	0 10288	0 58797	16 50	0 117144 ± 0 002497	0 001118 ± 0 000047	17 65 ± 0 55
	1550	v	0 00005	0 05411	0 30896	8 68	0 167588 ± 0 002692	0 000146 ± 0 000061	17 63 ± 0 44

Table 1 (continued)

Chapter 3: New constraints on the structure and timing of the Gaoligong Shan Shear Zone, western Yunnan, China.

Sinan Akciz[1]*
B. Clark Burchfiel[1]
James L. Crowley[1]
Yin Jiyun[2]
Chen Liangzhong[2]

[1]Massachusetts Institute of Technology, Dept. of Earth, Atmospheric and Planeary Sciences, 77 Massachusetts Ave., Cambridge, MA 02139
[2]Yunnan Institute of Geological Sciences, 131 Baita Rd., Kunming, Yunnan, China.
*E-mail: akciz@mit.edu

ABSTRACT:

Since 45 – 50 Ma, continental India has penetrated into Eurasia approximately 3000 km at the longitude of the Eastern Himalayan Syntaxis resulting in the formation of the Himalayan range and the Tibetan Plateau. However, first order questions, such as how and where this indentation was accommodated in the region east of the India indenter are still subject to speculation due to paucity of information. The Gaoligong Shan Shear Zone (GSSZ) is the only recognized structure with the appropriate orientation in the region between the ASSZ and the Sagaing fault on which a significant amount of the northward indentation of India into Eurasia can be accommodated during early Cenozoic time. To begin to address the role of the GSSZ, and to better understand the role of extrusion tectonics in the Cenozoic evolution of SE Asia, we present new structural and U-Pb data to constrain the evolution of the GSSZ. The structural data shows that the GSSZ is a long (<400 km) and wide (<10 km) zone of mylonitic granitic gneiss in its western part and metasedimentary schist in its eastern part with consistent right-lateral kinematic indicators throughout. U-Pb data from a leucogranite dike which cross-cuts the mylonitic gneisses of the GSSZ indicates that the major fabric forming deformational episode in this part of the GSSZ ceased by ~18.5 Ma. A syn-kinematic leucogranite sill yielded U-Pb ages of ~65-79 Ma, however it is not clear how to interpret these ages. They may indicate pre-collisional shearing or post-collisional shearing. If they record post-collisional shearing it would indicate the collision was much earlier in the areas east of the syntaxis than elsewhere in the Himalaya At present the pre-18 Ma history of the shear zone is unclear. The GSSZ, and its left-lateral conjugate pair, the Ailao Shan Shear Zone (ASSZ), terminate within the Bangong Co-Nujiang suture zone and cannot be followed into the Tibetan Plateau. The implication of this observation is that the GSSZ and the ASSZ did not accommodate southeastward extrusion of Indochina from in front of India. Instead, the extrusion appears to be related to the broad dextral accommodation zone, with important clockwise rotation of crustal material, in the area of the Eastern Himalayan syntaxis by reactivating Palaeozoic and Mesozoic aged suture zones.

INTRODUCTION

One of the best natural laboratories to study intracontinental convergence is the young and active India/Eurasia collision zone that has accommodated ~2,500 km of post-collisional northward translation of the Indian subcontinent relative to Siberia (Molnar and Tapponnier, 1975; Patriat and Achache, 1984). Numerous models have been proposed for the tectonics of the India-Eurasia collision and subsequent post-collisional intracontinental deformation. Models for the tectonic evolution range from eastward extrusion of Tibetan crust beyond the boundary of the plateau (e.g. Tapponnier et al., 1982, 1986; Avouac and Tapponnier,

1993) to lateral spreading of thickened viscous lithosphere with little eastward extrusion (e.g Houseman and England, 1993), to eastward flow of middle or lower crust (Royden et al., 1997). accompanied by large-scale clockwise rotation (Shen et al., 2000, Wang and Burchfiel, 1997; Wang et al., 1998) and crustal thickening of the lower crust.

The most prominent of these models is the two-phased extrusion model of Tapponnier et al. (1982) that has been little modified since its inception (Figure 1). According to this model, the collective Ailao Shan - Diancang Shan - Xuelong Shan and Day Nui Con Voi shear zones (referred to here as the Aialo Shan Shear Zone (ASSZ)) form a continuous metamorphic belt developed along a Tertiary, intracontinental, ductile, left-lateral strike-slip shear zone. The ASSZ forms the northern boundary of the southeastward extruding Indochina tectonic element during the first phase of extrusion. However, the proposed right-lateral conjugate shear system on the southwest side of the hypothesized extruded fragment has been proposed to be the Sagaing fault zone in Burma that is only ~13 Ma old (Curray et al., 1979, Lawver et al., 1976). The documentation of an early Tertiary dextral shear zone that bounded the Indo-China crustal fragment has generally been lacking, but obvioiusly, has significant implications of how the indentation of India into Eurasia has been accommodated. The geology of the region between the eastern Himalayan syntaxis and the Ailao Shan shear zone, known as the Three Rivers Belt, holds the key to elucidating the early Teritiary tectonic evolution in the syntaxial region. There are two poorly documented and understood linear metamorphic belts in the Three Rivers Belt: the Gaoligong Shan Metamorphic Belt (hereafter the Gaoligong Shan Shear Zone (GSSZ)) and Chong Shan Metamorphic Belt (hereafter the Chong Shan Shear Zone), that are important to unraveling the tectonics of this region. In the previous chapter, I have briefly described the lithologies and structures observed along the GSSZ and presented our initial $^{40}Ar/^{39}Ar$ dates from

syn- and post-kinematic granitic intrusions which indicate that deformation within the GSSZ ended by ~ 12 Ma and the right-lateral motion between India and Sibumasu shifted to the Sagaing fault zone in Burma that accommodated at least part of the late Tertiary motion between India and Eurasia .

We present new structural and geochronological data on the GSSZ, and discuss possible regional extensions and tectonic implications of the dextral transpressional GSSZ in South Eastern Asia.

OVERVIEW OF THE GEOLOGY OF WESTERN YUNNAN

The Three Rivers region of western Yunnan lies east of the eastern Himalayan syntaxis and consists of a tectonic collage of continental fragments of Gondwana and Cathaysian origin and magmatic arcs formed by subduction within Palaeo-Tethys (e.g. Sengör, 1984; Hutchison, 1989). During intracontinental deformation following the India/Eurasia collision, the collage was modified by post-collisional Cenozoic deformation characterized by fragmentation and rotation of crustal blocks (Wang and Burchfiel, 1997) and displacement along major faults and shear zones as India moved northward relative to Indochina and South China.

The Tengchong crustal fragment (these pieces of crust are often referred to as blocks which incorrectly implies rigid behavior of the deformed crust) is here interpreted as the southeastern continuation of the Lhasa crustal fragment of southern Tibet and is bounded on the east by the GSSZ (Figure 2). Its sedimentary sequence within China lacks dated exposures of early Palaeozoic sedimentary rocks, although they probably are present in the extensively intruded metamorphic rocks in the western part of the the crustal fragment. Dated Paleozoic rocks in the Tengchong are characterized by upper Carboniferous to lower Permian marine

carbonate and clastic strata containing cold water fauna that indicate that the fragment was part of the Gondwana domain (Chenjun, 1994). All the strata were extensively intruded and metamorphosed by Mesozoic and Cenozoic(?) plutonic rocks and are partially covered by Upper Tertiary and Quaternary intermediate to basic volcanic rocks. High-grade metamorphic and igneous rocks also crop out in the eastern part of the Tengchong fragment along the Nujiang (Salween) River and form a narrow structural high that continues south into Burma as the Mogok Metamorphic Belt (Chibber, 1934). These high-grade rocks have been considered to be Middle Proterozoic in age and have been interpreted as an upthrust slice of the basement of the Tengchong crustal fragment prior to this study (Bureau of Geology and Mineral Resources of Yunnan Province, 1990). Our study, however, indicates these rocks are part of a Mesozoic batholith and their metasedimentary wall rocks that are of probable Paleozoic age. The Mesozoic plutonic rocks are the southeastward continuation of the Gangdese batholilth of southern Tibet and at least some of the high-grade metasedimentary rocks are part of the Lhasa crustal fragment. In support of this interpretation, both the less metamorphosed quartzite and limestone interbedded with fine-grained sandstone of mainly Carboniferous and Permian (?) age along with the large plutons that intrude them can be traced from the Lhasa crustal fragment into the Tengchong crustal fragment in the map area.

The Baoshan crustal fragment lies to the east of the GSSZ and forms the northernmost continuation of the more regional Sibumasu continental fragment as defined by Metcalfe (1984, 1988) (Figure 2). Upper Proterozoic to Middle Cambrian slightly metamorphosed diamictites and carbonate rocks form the basal part of the Baoshan stratigraphic sequence in the study area. The Silurian and Ordovician units consist mainly of fossiliferous shallow-water siliciclastics rocks and some argillaceous limestone and shale. From the Middle Devonian to the end of Early

Carboniferous time, various fossiliferous carbonate units were deposited. The lower part of the Upper Carboniferous strata contains diamictites, along with turbidite, conglomeratic sandstone, and siltstone (Jin, 1994). The upper part comprises black mudstones and siltstones, which are regarded as periglacial deposits. Basaltic lava flows (Woniusi basalt) with pillow lavas and tuffaceous intercalations terminate Palaeozoic sedimentation in the early Permian (Bureau of Geology and Mineral Resources of Yunnan Province, 1990). These basalts may be related to rifting and the beginning of separation of the Baoshan continental fragment from the Gondwana margin (Jin, 1994), although few data supporting this interpretation are described in the literature. Lower Permian(?) red beds lie disconformably above the Woniusi Basalts. The Mesozoic strata consist of Triassic limestone and Jurassic marine strata and red beds that are generally restricted to the margins of the Baoshan unit. Cenozoic rocks are rare and are characterized by upper Eocene-Oligocene conglomerate and sandstone that rest unconformably on deformed older rocks.

To the north of the map area between the headwaters of the Salween and Mekong rivers is the southeastern part of the Qiangtang continental fragment that is bounded by the Lancangjiang suture to the east and by the Bangong – Nujiang suture zone to the south (Figure 2). There is an ongoing debate regarding the importance of the Central Qiantang metamorphic belt of Kapp et al. (2000) which is interpreted to divide the Qiantang continental fragment into two parts: a northern section which contains warm-water faunas of Cathaysian affinity, similar to the South China block, from a southern section which includes cold water fauna and glacial deposits of Gondwana-Land affinity (Wang and Mu, 1983; Fan, 1985, 1988; Chen and Xie, 1994). Data from the the southeastern part of the Qiangtang tectonic element is very limited due

to its logistical remoteness. However, rifting of the Qiangtang continental fragment from the Lhasa continental fragment and opening of the intervening Bangong Ocean occurred during Permo-Triassic time (Sengor et al., 1988). The Bangong Ocean closed by northward subduction beneath the Qiangtang continental fragment during Middle Jurassic-Early Cretaceous time (Girardeau et al., 1984; Pearce and Deng, 1988). Geological maps of China at 1:200,000 scale covering the southeasternmost end of the Qiangtang continental fragment assign a Carboniferous age to the low-grade metasedimentary rocks that consist of quartzite, arkosic sandstone, limestone interbedded sandstone and marble without discussing whether these units belong to the Lhasa or the Qiangtang continental fragments. These Carboniferous rocks lie east of the GSSZ and the Gangdese granites, which are considered to mark the southeastern part of the Lhasa continental fragment, as well as east of the southern projection of the Bangong suture. This suggests that these Carboniferous(?) rocks do not belong to the Lhasa tectonic element. These rocks lie west of the Permo-Triassic granites and associated volcanic rocks that are considered to form the western boundary of the Simao tectonic element (Figure 2). Therefore, these Carboniferous strata are tentatively assigned to the Qiangtang tectonic element. These rocks project southward into more metamorphosed and sheared rocks of the GSSZ and indicate that the southward continuation of the Bangong suture lies as a cryptic suture within the GSSZ. Correlation of these rocks with the major tectonic elements in the region farther to the north clearly requires further examination in this poorly known part of the Eastern Himalayan Syntaxis.

THE GAOLIGONGSHAN SHEAR ZONE (GSSZ)

Chapter 3- The Gaoligong Shan Shear Zone

The GSSZ is less than 40 km wide and within the Yunnan Province of China it is at least 400 km long. The Salween River (Nujiang) flows east of the GSSZ south of LiuKu, but farther northwards, cuts through it, exposing a ~200 km-long section of the shear zone. We present here our study of the structure of the GSSZ, and the character of ductile strain along numerous cross sections as well as along its ~200 km strike-parallel length. The GSSZ consists of two distinct units (Figure 3 and Appendix A): an orthogneiss unit to the west, and a metasedimentary unit to the east. Much of the western part of the shear zone consists of rather homogeneous mylonitic granites and augen orthogneisses. These rocks lie adjacent to high-grade metasedimentary rocks that include quartz-feldspar-biotite (QFB) paragneiss, impure quartzite, calcsilicate rocks, marble, and biotite schist. There are also widespread occurrences of cm- to dm-scale leucogranite and pegmatite sills. The GSSZ is bounded to the west by undeformed granites that are here interpreted to be the southern continuation of the Gangdese granites. To the east, the GSSZ is bounded by different tectonic units. From north to south, these units are: (1) very weakly metamorphosed Carboniferous(?) sediments of the (eastern) Qiangtang tectonic element, (2) the metamorphic rocks of the CSSZ, and (3) the Baoshan segment of the Sibumasu tectonic element (Figure 2). In the following section, we describe the various different lithologies that form the GSSZ.

Granitic rocks

Granitic rocks have four modes of occurrences in the study area: 1) as an undeformed >30 km wide belt of granitic plutons , 2) a <40 km wide belt of granitic orthogneiss immediately east of the undeformed plutons, 3) a <1 km wide zone of augen gneiss pods within the metasedimentary section of the GSSZ and 4) and as a network of centimeter- to decimeter-scale

leucogranitic sills and dikes intruding the mylonitic host rocks. The undeformed granitic rocks belong to the Tengchong element and form the protolith for some of the rocks of the GSSZ to the east.

Gangdese granites:

The undeformed granites were observed at only a few isolated locations due to their proximity to the Salween River and the lack of roads or trails that cut the entire width of the GSSZ (Figure 3 and Appendix A). Their bulk composition is variable and consists of quartz diorite, biotite monzogranite, hornblende quartzdiorite, hornblende-biotite monzodiorite, and granodiorite. The western part of the granitic batholith escaped intense penetrative deformation to a very large extent, however, intense penetrative ductile shear fabric within this batholith appears at its eastern margin, where it grades into the deformed rocks of the GSSZ to the east.

Granitic orthogneiss:

The granitic orthogneiss weathers medium to dark gray and typically displays feldspar augen up to ~5 cm. in diameter. Other constituent minerals include muscovite + biotite + quartz + plagioclase ± K-feldspar ± garnet. The grain size is generally <5 mm. Biotite occurs as brownish to greenish flakes. These granitic gneisses become mylonitic and are the westernmost rocks included within the GSSZ and can be traced continusously from Tengchong to Gongshan, except for the area extending for ~ 50 km north of Fugong (Appendix A). This observation is based on field data from 2 cross-sections where the metasedimentary section of the GSSZ is found juxtaposed against undeformed granites along a steep and sharp contact, for reasons which are not known for the time being. (Fig 4). These orthogneisses along with the metasedimentary

rocks to the east that form the rest of the GSSZ have been considered to be of Precambrian age (Bureau of Geology and Mineral Resources of Yunnan Province, 1990). In contrast, we suggest in light of our structural and preliminary geochronological studies (see below) that the orthogneiss is the eastern part of the Gangdese granitic batholith and was sheared during the indentation of India into Eurasia, probably since Eocene times (Rowley, 1996, 1998).

Augen gneiss pods:

Within the metasedimentary part of the GSSZ, there are discontinuous bodies of augen gneiss that are only a few hundreds of meters in width and length (Figure 5). Their mineralogy is similar to that of the granitic gneisses described above, consisting of muscovite + biotite + quartz + plagioclase ± K-feldspar ± garnet. Even though our reconnaissance geochronological study will not report any dates from these rocks, we tentatively interpret these augen gneisses as granites that intruded the metasedimentary rocks of the GSSZ prior to collision of India with Eurasia and were deformed together with them during India's indentation into Eurasia.

Leucogranitic sills and dikes:

We have differentiated the cm- to dm-scale sills and dikes of granitic composition into three different groups in the order of increasing crystal size. They are: aplites, leucogranites and pegmatites, in the order of increasing crystal size. We will refer to them collectively as leucogranites, unless otherwise specified. Their mineralogies are almost identical, containing quartz, plagioclase feldspar, and potassium feldspar. Most of these intrusions also contain muscovite, biotite and tourmaline. They are present within both the orthgneissic and the paragneissic section of the GSSZ, but their abundance is greatest in the QFB-gneiss and biotite-

schist section of the metasedimentary rocks where they constitute no more than 20% of some outcrops by volume. The discontinuous nature of these leucogranitic stingers, their close spatial association with the pelitic gneisses, and their absence outside the GSSZ is interpreted as in situ partial melts. Shear heating, and/or localization of hot fluids along the well-developed foliation planes were probably two of the important factors that contributed to their generation. The leucogranites can be grouped by their degree of deformation as follows: (1) foliated sills, (2) foliated and boudinaged sills, (3) unfoliated sills, (4) unfoliated , but boudinaged sills, and (5) unfoliated dikes that crosscut the foliation (Figure 6). None of these sills and dikes contains a lineation, even though the host rocks they intrude display a prominent sub-horizontal mylonitic lineation associated with the strike-slip shearing along the GSSZ. We interpret the smaller degree of deformation observed in the granitic sills and dikes compared to the strongly foliated and lineated host rocks to indicate they were intruded during late stages of strike-slip shearing.

Metasedimentary rocks:

The metasedimentary rocks of the GSSZ consists of quartz-feldspar-biotite (QFB) paragneiss, impure quartzite, calcsilicate rocks, marble, and biotite schist (Figure 5 and Appendix A). The QFB gneisses are the dominant rock type in the GSSZ . They are generally dark gray due to the abundance of biotite. Some of these gneisses are garnet, biotite and muscovite rich, and the typical metamorphic mineral assemblage is quartz-plagioclase-biotite-garnet and/or silliminite ± K-feldspar ± muscovite, indicating they were metamorphosed at amphibolite grade (see discussion below). In a few samples, sillimanite is parallel to the foliation, and in others it is found as inclusions within garnets. Some garnets contain an inclusion-rich core and an inclusion-free mantle. Other QFB gneisses contain quartz-plagioclase-

biotite-chlorite and none of the minerals which would indicate metamorphism at high temperatures. Sillimanite crystals, where present, are microscopic and were never observed in the field. Therefore, it would be premature to suggest distinct zones of amphibolite grade QFB gneisses and greenschist grade QFB gneisses based on field sampling of an area that is about 400 km by 10 km.

Dark gray impure quartzites, that contain plagioclase and biotite, and narrow bands (< 20 m wide) of biotite-schists are the next most common rock types in the metasedimentary section of the GSSZ. The calcsilicate rocks are composed of alternating green and gray bands, and contain quartz, plagioclase, calcite, diopside ±wollastonite, ±muscovite, and ±biotite. White marble outcrops throughout this metasedimentary section as 50 to 100 m wide bands. These lithologies indicate that a sedimentary sequence consisting dominantly of arkosic sandstone, quartzite, with lesser amounts of shale, calcareous sandstone, and thin limestone interbeds is the protolith of these metasedimentary succession. The rarity of marble and the lack of amphibolite that would be indicative of metamorphosed basalt and support a correlation with the Baoshan sedimentary rocks of the Sibumasu tectonic element, consisting mainly of limestones and some basalts are not the protoliths for the rocks in the GSSZ. The area between the GSSZ and the CSSZ, northeast of Gongshan contain the appropriate protolith assemblage for these metasedimentary rocks . These rocks, which have been assigned a Carboniferous age on Chinese 1:200,000 geological maps, consist of slates, arkosic sandstone, quartzite, calcareous sandstone, and white marble. These Carboniferous rocks lie east of the GSSZ and the Gangdese granites, that are considered to mark the southeastern part of the Lhasa continental fragment, as well as east of the southern projection of the Bangong suture. In other words, while the protolith of the orthogneissic section of the GSSZ is the Gangdese granites of the Lhasa tectonic element, these

Carboniferous strata are tentatively assigned to the Qiangtang tectonic element are the presumed protoliths of the metasedimentary section of the GSSZ

DEFORMATION ALONG THE GNEISSIC SECTION OF THE GSSZ

Most of the foliation in the GSSZ metamorphic rocks dips steeply (≥ 60°) both to the west and east (Figure 7 and Appendix A) and shows well-developed mylonitic textures. Outcrop surfaces polished by the Nujiang River and its tributaries provide well-exposed horizontal sections, parallel to the lineation and close to the XZ plane of the finite strain ellipsoid (i.e. perpendicular to the foliation and parallel to lineation). The schistosity is marked by biotite, and quartz and/or feldspar ribbons. Locally chlorite and sillimanite also define the schistosity. This schistosity contains a prominent lineation interpreted as a stretching lineation formed by the elongation of quartz, feldspar, and biotite, although intersection lineations, formed by the intersection of foliation and compositional layering, are also present at numerous outcrops mainly within folded quartzite and calcsilicate units. All lineations are sub-horizontal and plunge both to the north and the south (Figure 8 and Appendix A). This change in the plunge direction is present both along and across the strike of the GSSZ. Sheath folds and folds with axes parallel to the lineation are present and are marked by intersection lineations that parallel the mylonitic stretching lineation. Boudinage is widespread and affects both the mylonitized leucogranitic sills that are interpreted to have formed during earlier stages of deformation as well as some of the unfoliated leucogranites and pegmatites which are interpreted to have been emplaced during later stages of deformation. Boudin axes are both horizontal and vertical and indicate both horizontal and vertical stretching even though the vertically stretched boudins are not associated with a vertical lineation. In all sections and sites studied along the ~400 km length of the GSSZ, the

steep foliation and horizontal stretching lineation appears to result from a single phase of non-coaxial, horizontal right-lateral shear. Consistent shear criteria, such as asymmetric tails on deformed feldspar porphyroclasts (Figure 9), S-C surfaces, asymmetric boudins, cm.- to dm.-scale asymmetric folds observed in horizontal sections perpendicular to the foliation and parallel to the lineation, indicate a right-lateral sense of shear.

Data from microstructural analysis of oriented thin sections confirm observations at the mesoscopic scale within the GSSZ. In thin section, the foliation is marked by metamorphic minerals (biotite, muscovite, ±chlorite, and ±sillimanite) and by quartz and feldspar ribbons, and the lineation is formed by quartz, feldspar and biotite. The most common mineral defining the lineation is quartz that forms long polycrystalline ribbons generally made of recrystallized grains. The grains have an irregular shape, sutured boundaries, often with undulatory extinction, subgrains and deformation bands. Plastic deformation combined with dynamic recrystallization thus appears to have been the dominant deformation mechanism in the quartz. None of the K-feldspar grains have plastic deformation features. Some feldspar grains, especially plagioclase, show brittle fractures. The contrast between quartz and feldspar deformation indicates temperatures were probably between 350° and ~500° C. Many feldspar grains have sigma-type tail structures that yield right-lateral sense of shear. Augens of quartz and feldspar crystals are wrapped by fine-grained quartz and feldspar. The foliation formed by various mica minerals is deflected around the augens and garnets. Few samples, which contain garnet and sillimanite that form the foliation suggest metamorphism and shearing at amphibolite facies conditions. However, their significance should be investigated further as they are by no means representative of the whole shear zone.

TIMING OF DEFORMATION WITHIN THE GSSZ

The main phase of deformation and metamorphism in the gneisses can be constrained in two ways. First by using cross-cutting relationships between deformational features (faults, folds, fabric, etc.) and other datable features (dikes, veins, metamorphic mineralogy, etc.). Second, the age of deformation can be determined directly by dating minerals related to the deformation with various well-established geochronologic methods such us U-Pb and $^{40}Ar/^{39}Ar$. In Chapter 2, preliminary $^{40}Ar/^{39}Ar$ results from leucogranite sills and dikes were presented that indicated that right-lateral shearing along the studied segment of the GSSZ ended by ~ 12 Ma. In this chapter, we provide new U/Pb and $^{40}Ar/^{39}Ar$ results from four different rock types to better constrain the time range of deformation within the GSSZ: (1) mylonitic augen gneiss, (2) foliated leucogranite sills, (3) unfoliated leucogranite sills and (4) unfoliated leucogranite dikes that cross cut the mylonitic foliation.

Sample locations and schematic block diagrams showing their structural setting are presented in Figure 4 .Table 1 lists conventional U- Pb analytical data. Figures 11-13 present the U-Pb analyses of monazite in the form of corcordia plots .

U-Pb Monazite geochronology: Sample description and results:

Mylonitic granite (Sample (98JL1.10, Fig 11):

Sample 98JL1.10 is from a mylonitic granite which contains well-developed right-lateral shear sense indicators. The mineralogy of this sample is dominated by quartz, plagioclase, K-feldspar, and biotite. The schistosity is marked by biotite, and quartz and/or feldspar ribbons. Accessory minerals include monazite and zircon. Four monazite grains (m1, m2, m3, and m5),

like all the other monazite grains and grain fragments we have analyzed, yielded reversely discordant dates (Figure X). Reverse discordance is a common feature of young monazites and is thought to indicate ^{230}Th disequilibrium (Schärer, 1984; Parrish, 1990); as a consequence, we will use the $^{207}U/^{235}Pb$ dates in our age interpretations (errors given at 2-sigma). These four grains yielded dates which range from ~67 to ~70 Ma.

Foliated leucogranite (Sample (98JL1.4, Fig 11):

Sample 98JL1.4 is from a ~ 30 cm-thick foliated leucogranite sill that intrudes mylonitic QFB gneiss of the metasedimentary rocks of the GSSZ. The QFB gneiss contains well-developed right-lateral shear sense indicators. We interpret this leucogranite sill to be syn-kinematic as it has a well-developed foliation parallel to the mylonitic foliation of its host rock, even though it lacks the sub-horizontal stretching lineation. The mineralogy of this sill is dominated by quartz, plagioclase, K-feldspar, tourmaline and muscovite. Accessory minerals include abundant monazite and zircon. Three monazite grains (m1, m5, and m6) yielded reversely discordant dates (Figure 11). These three grains yielded $^{207}U/^{235}Pb$ dates that range from ~62 to ~68 Ma.

Unfoliated pegmatite (Sample 98JN14.4, Fig 12):

Sample 98JN14.4 is from a ~ 20 cm-thick unfoliated pegmatite sill that intrudes mylonitic QFB gneiss of the metasedimentary rocks of the GSSZ. The QFB gneiss contains well-developed right-lateral shear sense indicators. The mineralogy of this sill is dominated by quartz, plagioclase, K-feldspar, tourmaline, biotite and muscovite. Accessory minerals include monazite and zircon. Unlike many of the other pegmatitic and leucogranitic sills, this pegmatite sample is from a sill which contains no foliation, no lineation and has not been stretched vertically or

horizontally. We use these observations to interpret this pegmatite sill to be post-kinematic (see discussion below). A total of 10 fragments from three monazite grains (m1a, m1b, m1c, m1d, m2a, m2b, m2c, m2d, m3a and m3c) yielded nearly concordant dates (Figure 12). These three grains were chosen based on their internal zoning as revealed by BSE imaging of polished grains. Monazite grain m1 has bright unzoned core with a weakly sector zoned mantle. M2 has sector zoning, and m3 is mostly unzoned with some weak sector zoning. Two fragments from grain m1 yielded nearly concordant dates of 75.2 and 75.8 Ma, while two other fragments yielded nearly concordant dates of 64.9 and 65.2 Ma. Four fragments from grain m2 yielded the following dates: 71.3, 73.4, 76.9, and 78.9 Ma. Two fragments from grain m3 yielded dates of 69.3 and 79.2 Ma. The biotite from this sample yielded $^{40}Ar/^{39}Ar$ date of ~12 Ma, and was presented in chapter 2.

Cross cutting dike (Sample 00M23.2, Fig 13):

Sample 00M23.2 was collected from a ~50 cm thick, undeformed, leucogranite dike that cuts across the foliation of mylonitic granites in the orthogneissic section of the GSSZ. Five fragments (m2c, m3, m4a, m5a and m5b) from 4 grains were dated. BSE images of monazite grains m3 and m4 have moderately strong oscillatory zoning that is typical of magmatic monazites, whereas grains m2 and m5 show no discernable zoning. All $^{207}U/^{235}Pb$ dates are ~18.5 Ma.

Interpretation of the monazite data:

The U-Pb data from the leucogranite dike that cross-cuts the mylonitic gneisses of the GSSZ (sample 00M23.2) indicates that the major fabric forming deformational episode in this

part of the GSSZ ceased by ~18.5 Ma. The grains and grain fragments from this sample show little spread of dates which are interpreted to be the crystallization age of this dike.

Two different types of age dispersion are observed in sample 98JN14.4 (Figure 12): (1) a spread of dates obtained from grains from the same sample, and (2) a spread of up to ~11 my between the two fragments from a single grain (sample 98JN14.4, fragments m1c and m1b). Understanding the cause of this dispersion is crucial to interpreting the age of the samples. The overall age dispersion could be produced in several ways. One possibility is that the igneous crystallization age is closely represented by the youngest monazite (64.9 Ma) and the older grains contain an inherited component. A second possibility is that each date represents a crystallization age corresponding to different metamorphic and anatectic phases over the interval constrained by the youngest and the oldest dates available. A third possibility is that the oldest dates are close to the igneous crystallization age and the other fragments have been affected by recrystallization or hydrothermal alteration at a younger time than the youngest date. BSE images of these grains, as described earlier, reveal internal zoning, which cannot be explained unequivocally with the available data.

While these end-member interpretations apply to all three of these samples, intermediate interpretations are equally viable if a combination of inheritance, and protracted mineral growth played a role in the dispersion. However, it is important to emphasize that all possible interpretations of the present data indicate an important mid- Cretaceous to Paleocene magmatic and/or metamorphic event in the GSSZ which is older than the proposed age of the India-Eurasia collision at ~45 Ma (Rowley 1996, 1998). However, it must also be pointed out there is no solid data on the time of collision in the area of the eastern Himalayan syntaxis and the data on timing of collision come from studies at least 500 km to the west . This data, therefore, can be

interpreted in two different ways: (1) The monazite grains that were analyzed from sample 98JN14.4 are all inherited, and have formed during the crystallization of the Gangdese granites from ~120 Ma until ~40 Ma. (2) The right-lateral shearing along the GSSZ has started prior to the collision of India with Eurasia, as a result of slip partitioning due to oblique convergence. Samples 98JL1.10 and 98JL1.4 show similar ranges of ages, ~67 – 70 Ma and ~62 – 67 Ma, respectively. The observed spread of dates from these samples caused us to start BSE imaging each grain, and analyzing different domains within a grain, and therefore, these are all single grain analyses and none of the grains were BSE imaged

This right-lateral shearing, however, ended by 18.5 Ma ($^{207}U/^{235}Pb$ dates from sample 00M23.2), about 6 Ma before what we have suggested in chapter 2 based on the $^{40}Ar/^{39}Ar$ biotite ages obtained from other cross-cutting dikes.

Grain fragments from sample 98JN14.4 also show a spread of dates, ranging up to ~11myr (m1). The possible interpretations for this spread are similar to the interpretations we made for the overall spread of dates. These are: (1) the igneous crystallization age is closely represented by the youngest fragment and the older fragments contain an inherited component, and (2) the oldest grain fragments represent the igneous crystallization age and the other fragments have been affected by recrystallization or hydrothermal alteration at a younger time than the youngest date. At present, we are unable to favor an explanation, as the fragments were broken along physical weaknesses of the grain, and not necessarily represent a domain corresponding to a zone determined from the BSE imaging of the grain. Future geochronological studies conducted in this area must, therefore, BSE image every grain, produce chemical maps of selective grains based on the BSE images, and date fragments corresponding to each domain in

order to not only enhance the quality of the geochronological dataset, but also to better interpret such crucial, but complicated geochronological data.

DISCUSSION:

Our preliminary geochronological results are inadequate to determine whether the dextral shearing along the GSSZ started prior to the India-Eurasia collision, in order to accommodate the oblique convergence between the two plates, or after the collision. However, we were able to document that the right-lateral shearing ended by ~18 Ma. The GSSZ is a conjugate dextral shear zone to the sinistral ASSZ. However, many questions still remain, regarding the significance of these structures, including: (1) How do the GSSZ and the ASSZ continue to the north? (2) What is the magnitude of displacement along each of these shear zones? (3) What was the significance of this extrusion in accommodating the indentation of India into Eurasia?

We can only speculate for now how these shear zones continue to the north, based on 1:200,000 Chinese geological maps. The mylonitic rocks of GSSZ can probably be followed for another 200 km north of Gongshan towards the MeiliXueShan where the shear zone strikes into the southernmost outcrops that belong to the Bangong Co-Nujiang suture, but from here rocks of the GSSZ are no longer present (Figure 2). Similarly, it can be argued based on the regional geology that the ASSZ and the northern continuation of the XueLeuShan, can also be traced into the Bangong Co-Nujiang suture. If this interpretation is correct, the eastern Tibetan portion of the Bangong Co-Nujiang suture zone is not only where the Lhasa and the Qiangtang continental fragments collided during the late Mesozoic as the Bangong Co-Nujiang ocean was consumed, but also where both the ASSZ and the GSSZ were juxtaposed during the early Cenozoic as the intervening Sibumasu/Indochina composite tectonic element extruded to the east and south east.

Field studies conducted along this segment of the Bangong Co-Nujiang suture are limited to the vicinity of a single road that connects Chengdu to Lhasa. The Eocene rocks just south of the Bangong Co-Nujiang suture suture are generally fault bounded, and locally south of the suture contain a very thick section of volcanic and volcanogenic sediments unlike any Eocene rocks present in the extruded fragments. The nature of such relations and many others in this area indicate new investigations are required to resolve the relations between the extruded crustal fragments and their original position within southeastern Tibet.

The location of this proposed sutured contact between the GSSZ, CSSZ and ASSZ is very important in determining the original location of the extruded crustal fragments and timing and magnitude of their movement. The magnitude of dextral displacement on GSSZ is difficult to constrain because displacement was predominantly parallel to the regional trends of structures. However, if we assume that the displacement along the ASSZ is 700±200 km (Leloup et al., 1995), then we can assume a similar amount of offset along the GSSZ, and also a sutured section of these bounding strike-slip shear zones that is also ~700 km long. Seven hundred kilometers along the southeastern part of the Bangong Co-Nujiang suture zone, however, would place the extruded crustal fragments east of the 96°E latitude, which is the easternmost extent of the Indian continent farther south. Thus, the extrusion of the Sibumasu/Indochina tectonic element occurred within a region which accommodated the dextral part of the indentation east of the eastern Himalayan syntaxis, and does not extend westward to lie north of the Indian indenter (e.g. Tapponnier et al., 1982; Leloup et al., 2001; Replumaz and Tapponnier, 2003).

Then what is the nature of the extrusion? A closer look at the geological maps of the region indicate that all three strike-slip shear zones are positioned within or close to pre-Cenozoic suture zones (Figure 2). The GSSZ lies along the Bangong Co-Nujiang suture zone, the

CSSZ follows the northern continuation of the Changning-Menglian suture zone (which is part of the Lancang Jiang - Changning-Menglian - Nan-Uttaradit – Sa Kaeo – Chantaburi - Bentong - Raub sutures, which will be referred to as Lanchangjiang - Raub suture for simplicity, (Figure 2)), and finally the ASSZ follows the Song Da – Anding suture zone (Sengor et al., 1988). According to our preferred interpretation, as India penetrated into Eurasia, older zones of weaknesses, the suture zones, were reactivated as strike-slip shear zones, while collectively accommodating the indentation within a broad zone of right-lateral shear and clockwise rotataion between India and the regions to the east. By at least ~18 Ma, the northern part of the GSSZ rotated until it was no longer favorably oriented to accommodate India's continued northward movement. At that time a new fault, the northern part of the Sagaing fault, was initiated immediately west of the mylonitic GSSZ, and India started to drag the small Burma crustal fragment along with it.

CONCLUSION:

The GSSZ is not a belt of Precambrian metamorphic rocks as previously suggested (Bureau of Geology and Mineral Resources of Yunnan Province, 1990), but is an important dextral Cenozoic (and possibly latest Mesozoic) shear zone that accommodated some of the post-collisional indentation of India into Eurasia at least during the late Miocene (ca. 18 – 13 Ma). Our preliminary U-Pb results are inadequate to determine whether the dextral shearing along the GSSZ started prior to the India-Eurasia collision, in order to accommodate the oblique convergence between the two plates, or after.

Two different types of age dispersion are observed in all the syn-tectonic leucogranite samples we have dated: (1) a spread of dates obtained from grains from the same sample, and (2)

a spread of up to ~11 myr between the two fragments from a single grain (sample 98JN14.4, fragments m1c and m1b). Understanding the cause of this dispersion is crucial to interpreting the age of the samples. Future geochronological studies conducted in this area must, therefore, BSE image every grain, produce chemical maps of selective grains based on the BSE images, and date fragments corresponding to each domain in order to not only enhance the quality of the geochronological dataset, but also to better interpret such crucial, but complicated geochronological data.

The deformation along the GSSZ was contemporaneous with the deformation along the ASSZ, and the CSSZ (Chapter 4), facilitating the complex extrusion of continental fragments between the two shear zones. However, neither of these faults continue far to the west into the Tibetan Plateau and thus have not facilitated the southeastward extrusion of Indochina from in front of India. In stead, the extrusion appears to be related to the broad dextral accommodation zone, with important clockwise rotation of crustal material, in the area of the Eastern Himalayan syntaxis by reactivating the Palaeozoic and Mesozoic aged suture zones.

Appendix A: The U-Pb Analytical Procedures

Separates of monazite [(Ce, La, Y, Th) PO_4] were obtained from four samples using standard magnetic and gravimetric separation techniques and hand picking under a binocular microscope. Monazites grains from samples 00JN25.1 and 00JN21.4 were mounted in epoxy and polished until the central parts of the grains were exposed. Backscattered electron (BSE) images of the polished grains were obtained using the JEOL 733 electron microprobe at the Massachusetts Institute of Technology operating at an accelerating voltage of 15 to 20 kV and a beam current of 10 to 30 nA. Brightness in the BSE images is related to average atomic mass; monazite with higher average atomic mass is brighter than that with lower average atomic mass. Therefore, BSE brightness in monazite is controlled mostly by Ce concentration, with La, Th, and Nd concentrations also being important. BSE images were made in order to characterize the internal structures of the crystals and to avoid grains with possibly inherited cores. After electron microprobe study, selected grains from samples 00JN25.1 and 00JN21.4 were removed from their mounts and broken into a number of fragments with a fine tipped tool. Some of the fragments were gently abraided (Krogh, 1982) in order to remove the anomalous rims apparent in the BSE images. Grains and fragments were then measured using a binocular microscope with calibrated reticule and video display in order to estimate their weights. Experience in our facility suggests that the estimated values have a nominal error of roughly 20%. Grains and fragments were cleaned by sonication in warm H_2O, brief immersion in warm dilute HNO_3, and rinsing in acetone and H_2O. The grains and fragments were dissolved in Teflon capsules and spiked with a mixed ^{205}Pb-^{233}U-^{235}U tracer solution. U and Pb were isolated and extracted from the samples by anion exchange chromatography. U and Pb were then loaded on Re filaments and measured by isotope-dilution, thermal ionization mass spectrometry (ID-TIMS) on a VG sector 54 mass

spectrometer at the Massachusetts Institute of Technology. Details regarding dissolution, chromatography, spectrometry, and other analytical procedures can be found in Schmitz and Bowring (2003). See Table xx for further details, including total procedural blanks, and complete isotopic data for each grain and fragment analyzed.

FIGURE CAPTIONS

Figure 1. Schematic map of Cenozoic extrusion tectonics and large faults in Eastern Asia (modified after Tapponnier et al., 1986). Heavy lines indicate major faults or plate boundaries. Small arrows show senses of finite motion on strike-slip faults. Open arrows represent the sense of motion from Eocene until mid-Miocene. Shaded areas represent the regions affected by the different extrusion phases. Large open arrows represent the major block motions with respect to Siberia since the Eocene. Boxed area refers to Figure 2.

Figure 2. Location of the four major tectonic elements within the Three Rivers area and the three ductile strike-slip shear zones: T = Tengchong (Lhasa); Q = Qiangtang; LS = Lanping/Simao; B = Baoshan (Sibumasu) Dashed line within the Baoshan element is the Late Palaeozoic Changling-Mengliang suture. Strike-slip shear zones are shown in black with white stripes. The stripes orientation does not refer to the orientation of the fabrics observed within all three of these shear zones. Abbreviations: ASSZ = Ailao Shan Shear Zone; CSSZ = Chong Shan Shear Zone; DSSZ = Dianchang Shan Shear Zone; GSSZ = Gaoligong Shan Shear Zone; XS = Xuelong Shan; M = Mangkang; S = Simao. Inset map shows location of Figure 2, in relation to the India/Eurasia collision zone and the major tectonic blocks that form Eurasia. Abbreviations: SG = Songpan – Garze flysch belt, BNS = Bangong Co-Nujiang suture zone, LS = Lanchangjiang suture zone, SAS = Song Da – Anning suture zone; Y = Yidun volcanic arc; GL = Garze-Litang suture zone.

Figure 3. The section of the Nujiang (Salween) valley where the GSSZ and CSSZ juxtapose against each other. (a) Nujiang morphology. View to the north. (b) A cenceptial model for the style of deformation observed in the field. The GSSZ, a ductily deforming dextral shear zone, is located to the west of another ductily deformed, sinistral shear zone, the CSSZ. Horizontal shortening perpendicular to the shear zone boundaries (indicated by full arrows) results in vertical stretching of the rocks within the shear zones. The stretching lineations of the GSSZ, plunging <20° both to the north and south, and the various shear sense indicators, observed on surfaces perpendicular to the foliation and parallel to these lineations, including folded porphyroclast tails, asymmetric folding of syntectonic dikes and S-C fabrics, however, indicate a very strong dextral strike-slip shearing along this mylonitic zone. The CSSZ has similar shear sense indicator types, which are dominantly left-lateral, with a right-lateral

overprint along the section where it is in contact with the GSSZ. The lower section of the block diagram is not drawn to scale.

Figure 4. Generalized geological map of the Three Rivers area showing the sample locations, U-Pb dates, previously reported Ar/Ar dates. Geochronological results which are grouped inside a box, refer to dates obtained from the same sample. Block diagrams schematically represent the samples that were dated. (a) a cross-cutting dike, (b) unfoliated, foliation parallel sill, (c) foliated, foliation parallel sill, and (d) well-foliated, sub-vertically stretched host-rock.

Figure 5. Outcrop pictures of the different lithologies that constitute the GSSZ. (a) Green-gray colored, well foliated calc-silicate rocks, (b) narrow (<100 m) and discontinuous bands of white marble, (c) QFB gneiss, and (d) mylonitic augen gneiss.

Figure 6. (a) Leucogranite dikes are mostly foliation parallel and undeformed. (b) Leucogranite sills are both vertically, and (c) horizontally stretched. (d) Foliation cross-cutting dikes help determine the age of the termination of shearing.

Figure 7. All the rock assemblages that form the GSSZ are sub-vertically foliated.

Figure 8. Nearly horizontal stretching lineations on steep foliation planes.

Figure 9. Rotated feldspar porphyroblasts indicate dextral shearing.

Figure 10. S-C fabrics indicate dextral shearing.

Figure 11 U-Pb Concordia diagrams for samples (a) 98JL1.10 and (b) 98JL1.4

Figure 12 (a) BSE images of the monazite grains from sample 98JN14.4 that were dated. (b)U-Pb Concordia diagram for the same sample.

Figure 13 (a) BSE images of the monazite grains from sample 00M23.2 that were dated. (b)U-Pb Concordia diagram for the same sample.

Figure 14. The motion of India with respect to Eurasia since about 45 Ma (modified after Klootwijk et al., 1992) and the present location of the three ductile strike-slip shear zones that accommodated part of the indentation of India into Eurasia until ~17 Ma. The GSSZ and the ASSZ merge together at around 30° latitude and disappear within the Bangong Co-Nujiang suture. 96°E latitude, the easternmost extent of India, is also drawn for reference, which shows that the extrusion of Indochina and Sibumasu occurred in the region east of the indenter.

REFERENCES:

Bureau of Geology and Mineral Resources of Yunnan Province, 1990, Regional Geology of Yunnan Province: Beijing, Geological Publishing House, 728 p.

Chenjun, F., Zhang, Y., 1994, The structure and tectonics of Western Yunnan.: Journal of southeast Asian earth sciences, v. 9, p. 355-361.

Chhibber, H.L., 1934, The Geology of Burma: London, Macmillan & Co., 590 p.

Curray, J.R., Moore, D.G., Lawver, L.A., Emmel, F.J., Raitt, R.W., Henry, M., Kieckhefer, R., 1979, Tectonics of the Andaman sea and Burma, *in* Watkins, T.S. et al., eds., Geological and geophysical investigations of continental margins: AAPG Memoir no. 29, p.189-198.

Girardeau, J., Marcoux, J., Allegre, C. J., Bassoullet, J. P., Tang Youking, Xiao Xuchang, Zao Yougong, Wang Xibin, 1984, Tectonic environment and geodynamic significance of the Neo-Cimmerian Donqiao Ophiolite, Bangong Co-Nujiang suture zone, Tibet: Nature (London), v. 307 , p. 27-31.

Houseman, G., and England, P., 1993, Crustal thickening versus lateral expulsion in the Indian-Asian continental collision: JGR, v. 98, p. 12,233-12,249.

Hutchison, C.S., 1989, Geological evolution of South-east Asia: Oxford Monographs on Geology and Geophysics, Clarendon Press, Oxford, pp. 368.

Jin Xiaochi, 1994, Sedimentary and paleogeographic significance of Permo-Carboniferous sequences in western Yunnan, China. Geologisches Institut der Universitat zu Koln, Sonderveroefentlichungen, 136 p.

Klootwijk, C.T., Gee, J.S., Peirce, J.W., Smith, G.M., McFadden, P.L., 1992, An early India-Asia contact: Paleomagnetic constraints from Ninetyeast Ridge, ODP Leg 121: Geology v. 20, p. 395-398.

Lawver, L.A., Curray J.R., Moore, D.G., 1976, Tectonic evolution of the Andaman Sea: EOS, v. 57, p. 333-334.

Leloup, P. H., Lacassin, R., Tapponnier, P., Zhong Dalai, Liu Xiaohan, Zhang Lianshang, Ji Shaocheng, Phan Trong Trinh, 1995, The Ailao Shan-Red River shear zone (Yunnan, China), Tertiary transform boundary of Indochina: Tectonophysics, v. 251, p. 3-84.

Leloup P.H., Arnaud N., Lacassin R., Kienast J.R., Harrison T.M., Phan Trong Trinh, Replumaz A., Tapponnier P, 2001, New constraints on the structure, thermochronology and timing of the Ailao Shan - Red River shear zone, SE Asia: Journal of Geophysical Research, v. 106, p. 6,657-6,671.

Metcalfe, I., 1988, Origin and assembly of South-East Asian continental terranes, in Audley-Charles, M.G., and Hallam, A., eds., Gondwana & Tethys, Geological Society of London Special Publication No. 37, p. 101-118. Oxford University Press.

Molnar, P., Tapponnier, P., 1975, Cenozoic tectonics of Asia; effects of a continental collision: Science, v. 189, p. 419-426.

Patriat, P., Achache, J., 1984, India-Eurasia collision chronology has implications for crustal shortening and driving mechanism of plates: Nature, v. 311, p. 615-621.

Replumaz, A., and P. Tapponnier, 2003, Reconstruction of the deformed collision zone Between India and Asia by backward motion of lithospheric blocks: Journal of Geophysical Research., v. 108, p. 2285, doi:10.1029/2001JB000661.

Rowley, D.B., 1996, Age of initiation of collision between India and Asia: A Review of stratigraphic data: Earth and Planetary Science Letters, v. 145, p. 1-13.

Rowley, D.B., 1998, Minimum age of initiation of collision between India and Asia north of Everest based on the subsidence history of the Zhepure Mountain section: Journal of Geology, v. 106, p. 229-235.

Royden, L.H., Burchfiel, B. C., King, R. W., Wang, E., Chen Zhiliang, Shen Feng, Liu Yuping, 1997, Surface deformation and lower crustal flow in eastern Tibet: Science, v. 276, p. 788-790.

Şengör, A.M.C., 1984, The Cimmeride orogenic system and the tectonics of Eurasia: Geological Society of America, Special paper 195, xi+82 pp.

Şengör, A.M.C., Altiner, D., Cin, A., Ustaomer, T., and Hsu, K.J., 1988, Origin and assembly of the Tethyside orogenic collage at the expense of Gondwanaland, in Audley-Charles, M.G., and Hallam, A., eds, Gondwana and Tethys: Geological Society Special Publications, no. 37, p. 119-181.

Tapponnier, P., Peltzer, G., Le Dain, A.Y., Armijo, R., Cobbold, P., 1982, Propagating extrusion tectonics in Asia: new insights from simple experiments with plasticine: Geology, v. 10, p. 611-616.

Tapponnier, P., Peltzer, G., Armijo, R., 1986, On the mechanics of the collision between India and Asia: Coward, M.P., and Ries, A.C., eds., Collision Tectonics: London, Geological Society, Geological Society Special Publication, no. 19, p. 115-157.

Wang, E., Burchfiel, B.C., 1997, Interpretation of Cenozoic tectonics in the right-lateral accommodation zone between the Ailao Shan shear zone and the Eastern Himalayan Syntaxis: International Geology Review, v. 39, p. 191-219.

Wang, E., Burchfiel, B. C., Royden, L. H., Chen Liangzhong, Chen Jishen, Li Wenxin, Chen Zhiliang, 1998, Late Cenozoic Xianshuihe-Xiaojiang, Red River, and Dali fault systems of southwestern Sichuan and central Yunnan, China: Geological Society of America Special Paper, no. 327, 108 p.

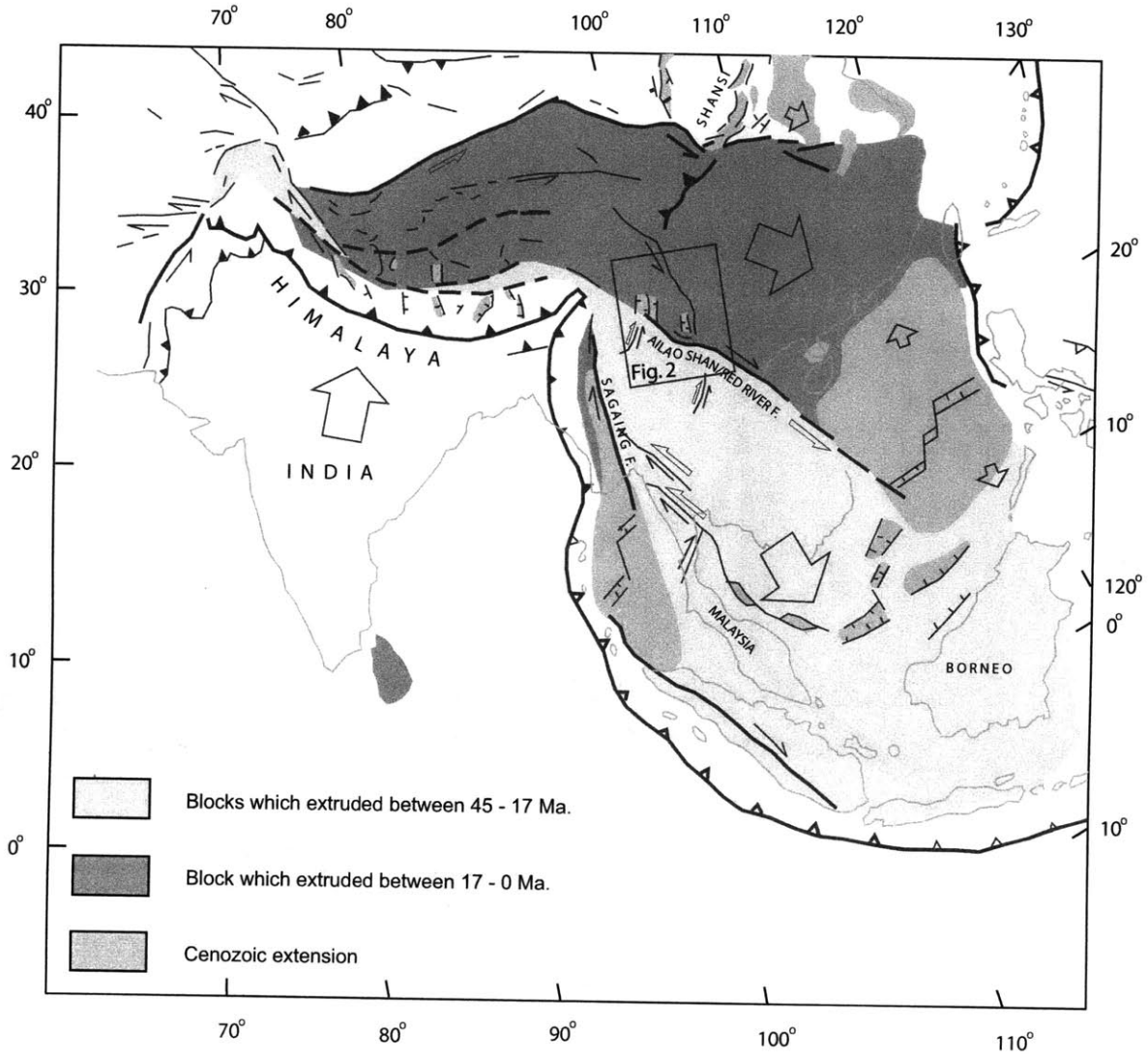
70°
80°
100°
110°
120°
130°
40°
30°
20°
10°
0°
20°
10°
120°
0°
10°
SHANSI
HIMALAYA
INDIA
Fig. 2
AILAO SHAN/RED RIVER F.
SAGAING F.
MALAYSIA
BORNEO
Blocks which extruded between 45 - 17 Ma.
Block which extruded between 17 - 0 Ma.
Cenozoic extension
70°
80°
90°
100°
110°

FIGURE 1

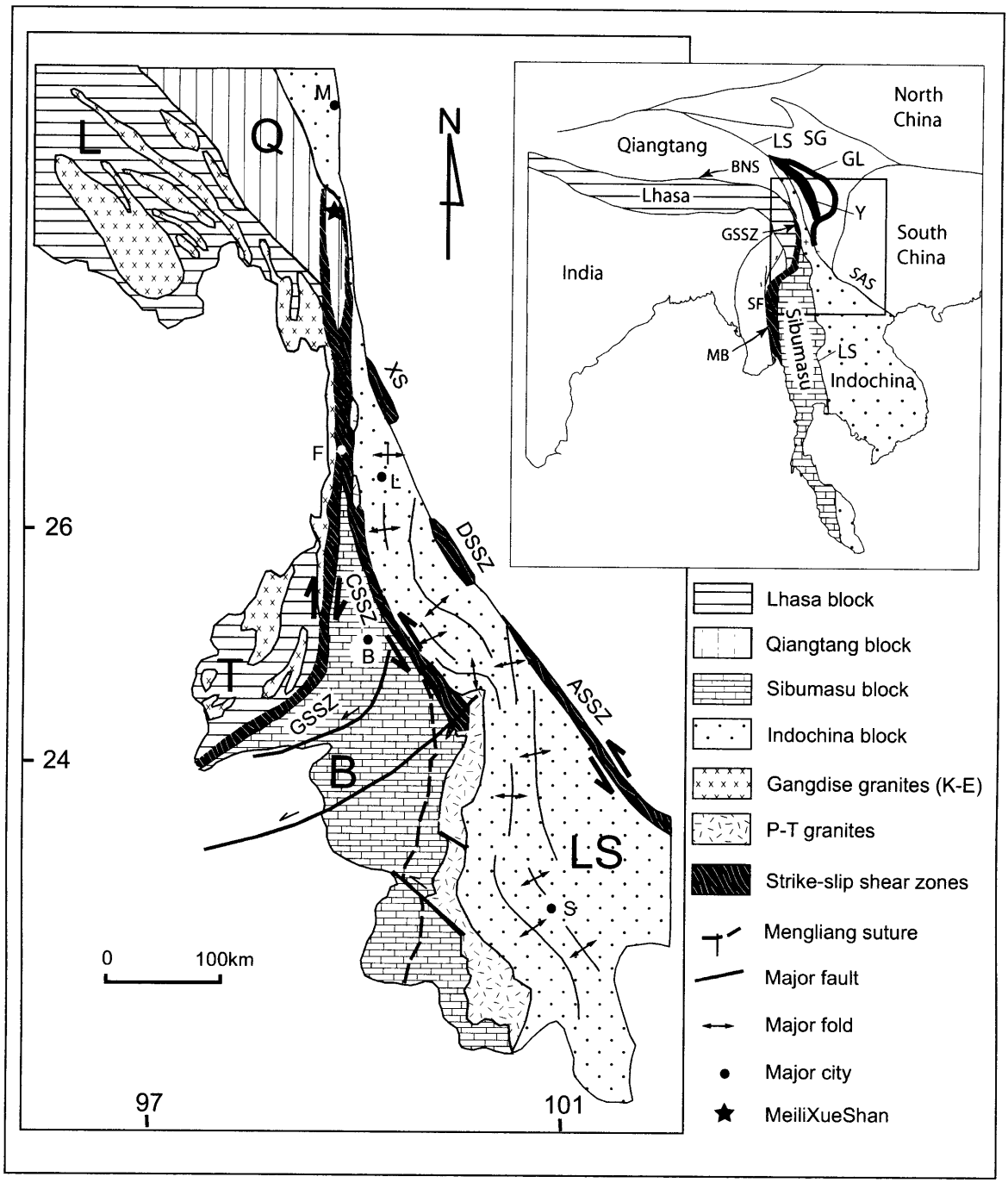
L
Q
M
N
XS
F
L
DSSZ
CSSZ
B
T
GSSZ
B
ASSZ
LS
S
26
24
0
100km
97
101
North China
Qiangtang
LS SG
GL
BNS
Lhasa
Y
GSSZ
South China
India
SAS
SF
Sibumasu
MB
LS
Indochina
Lhasa block
Qiangtang block
Sibumasu block
Indochina block
Gangdise granites (K-E)
P-T granites
Strike-slip shear zones
Mengliang suture
Major fault
Major fold
Major city
MeiliXueShan

FIGURE 2

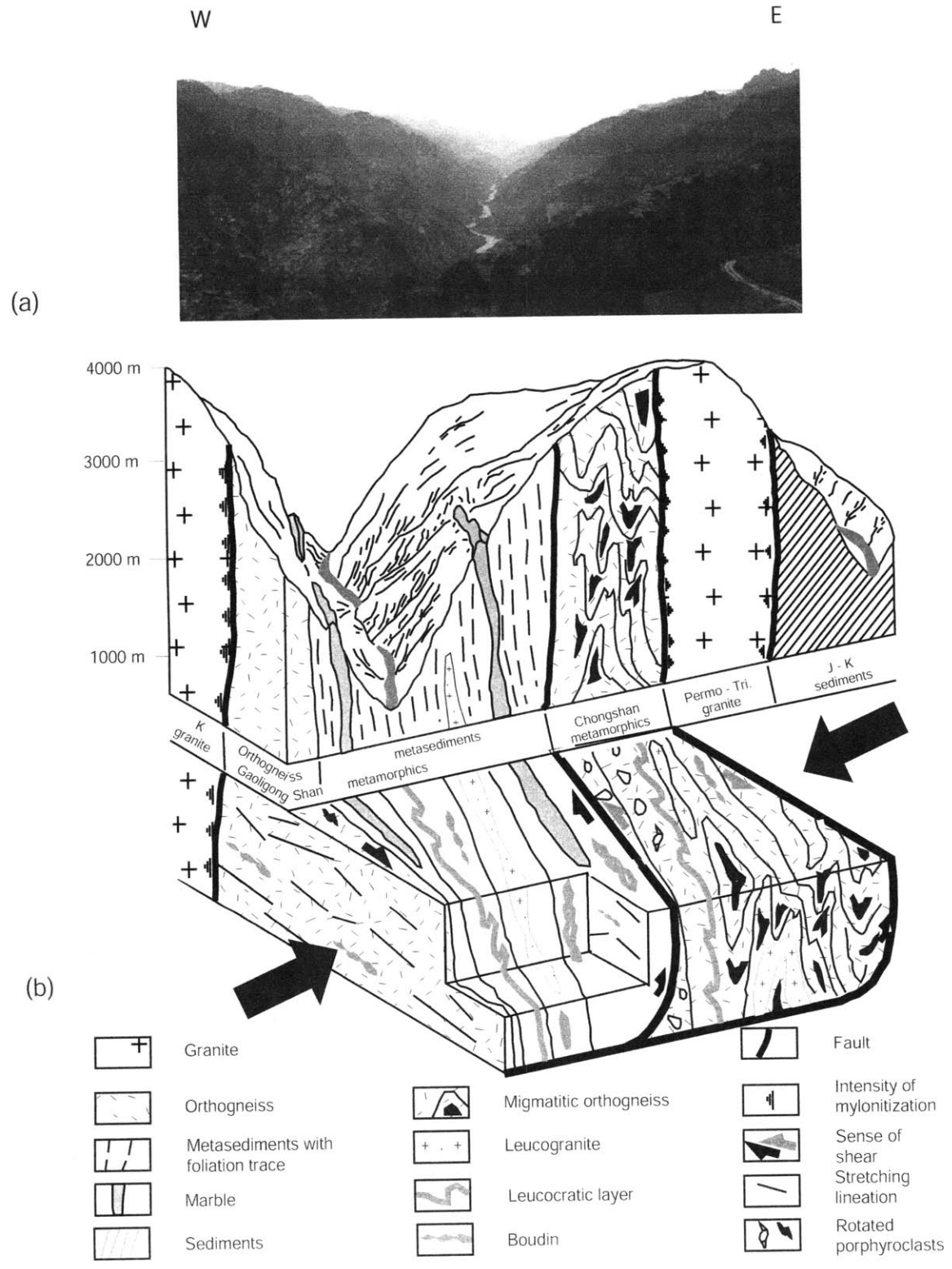
W
E
(a)
4000 m
3000 m
2000 m
1000 m
K granite
Orthogneiss
Gaoligong Shan
metasediments
metamorphics
Chongshan metamorphics
Permo - Tri. granite
J - K sediments
(b)
Granite
Orthogneiss
Metasediments with foliation trace
Marble
Sediments
Migmatitic orthogneiss
Leucogranite
Leucocratic layer
Boudin
Fault
Intensity of mylonitization
Sense of shear
Stretching lineation
Rotated porphyroclasts

FIGURE 3

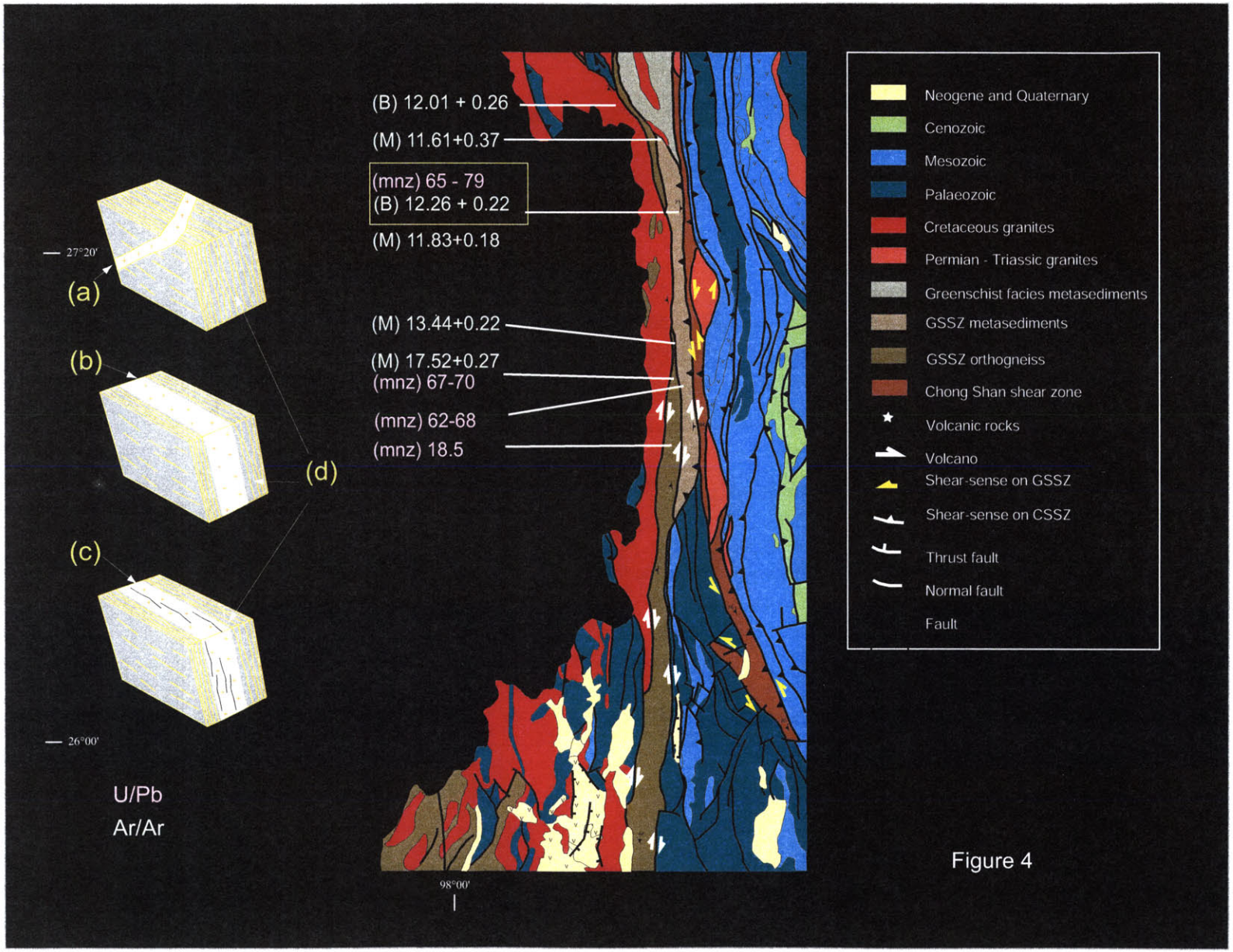
(B) 12.01 + 0.26
(M) 11.61+0.37
(mnz) 65 - 79
(B) 12.26 + 0.22
(M) 11.83+0.18
(M) 13.44+0.22
(M) 17.52+0.27
(mnz) 67-70
(mnz) 62-68
(mnz) 18.5
27°20'
26°00'
98°00'
(a)
(b)
(c)
(d)
U/Pb
Ar/Ar
Neogene and Quaternary
Cenozoic
Mesozoic
Palaeozoic
Cretaceous granites
Permian - Triassic granites
Greenschist facies metasediments
GSSZ metasediments
GSSZ orthogneiss
Chong Shan shear zone
Volcanic rocks
Volcano
Shear-sense on GSSZ
Shear-sense on CSSZ
Thrust fault
Normal fault
Fault

Figure 4

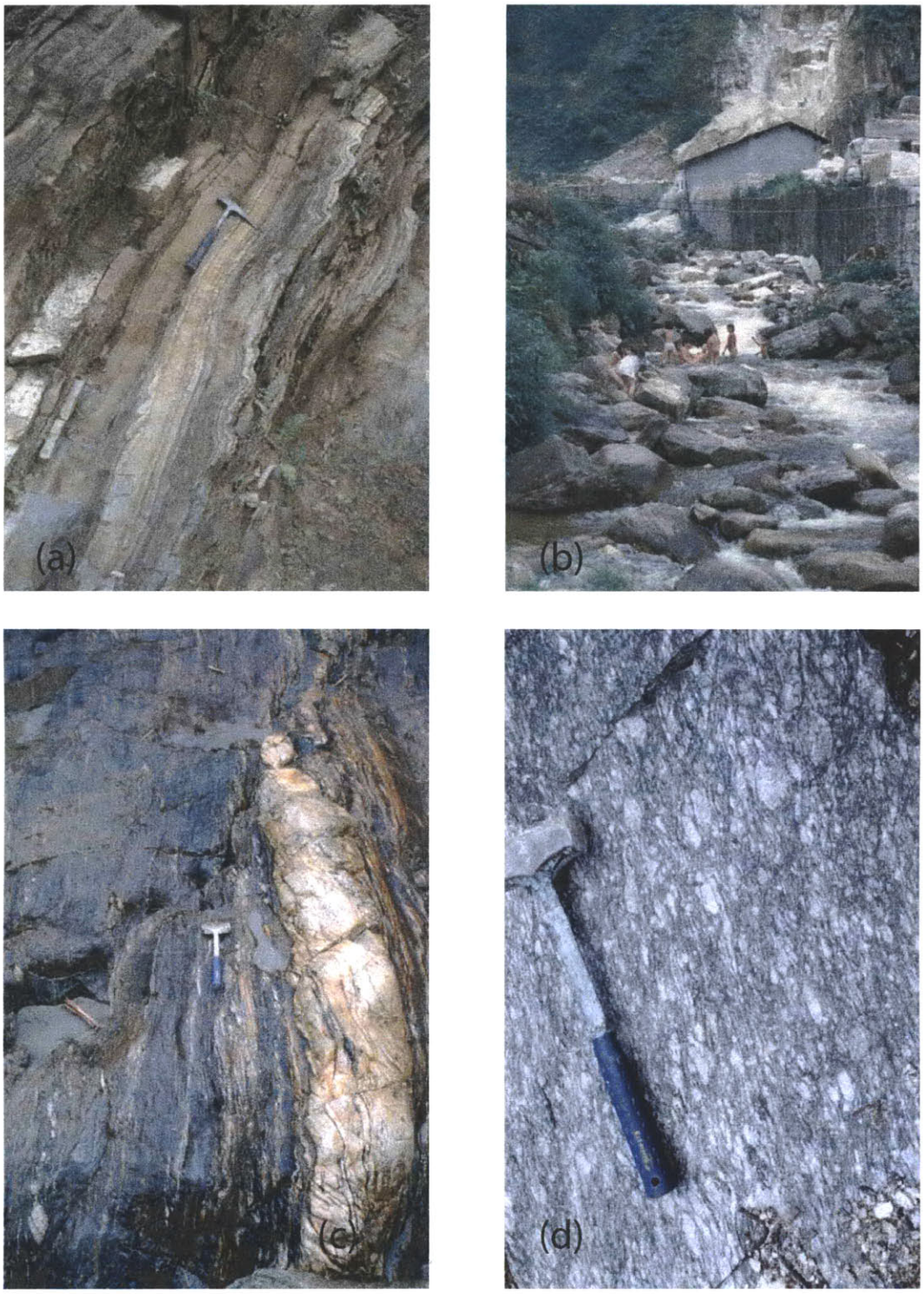

FIGURE 5

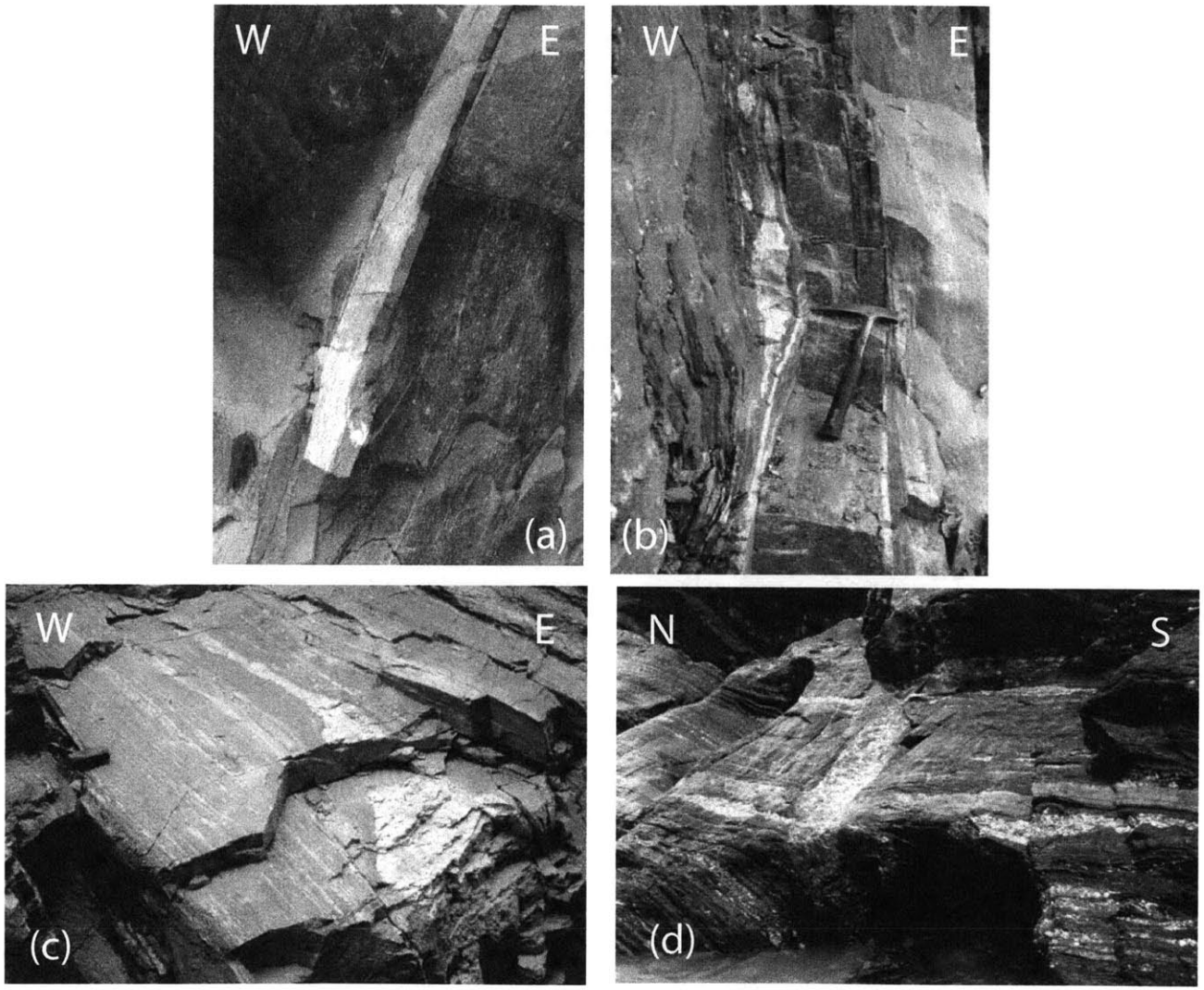

FIGURE 6

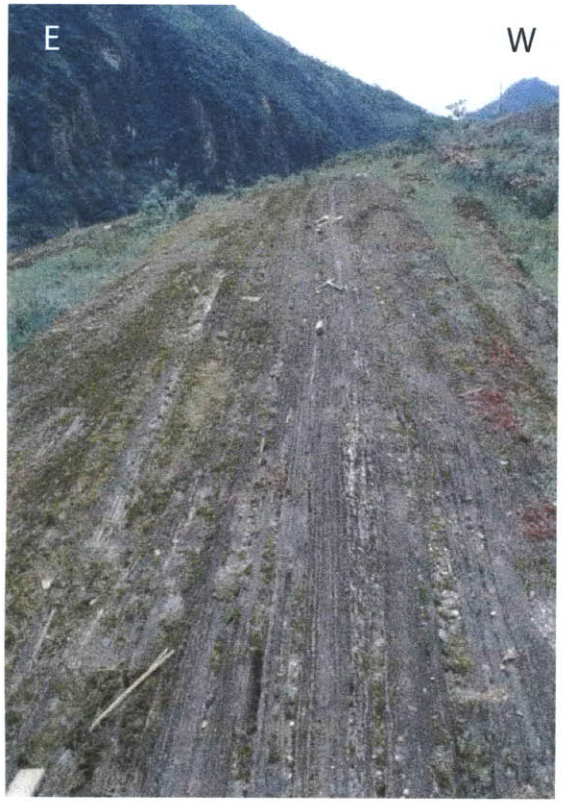

(a)

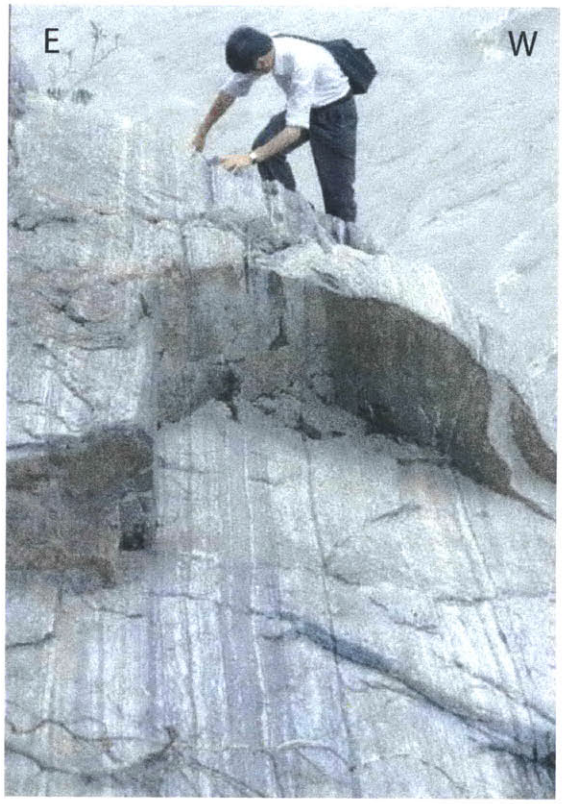

(b)

(c)

FIGURE 7

(a)

(b)

(c)

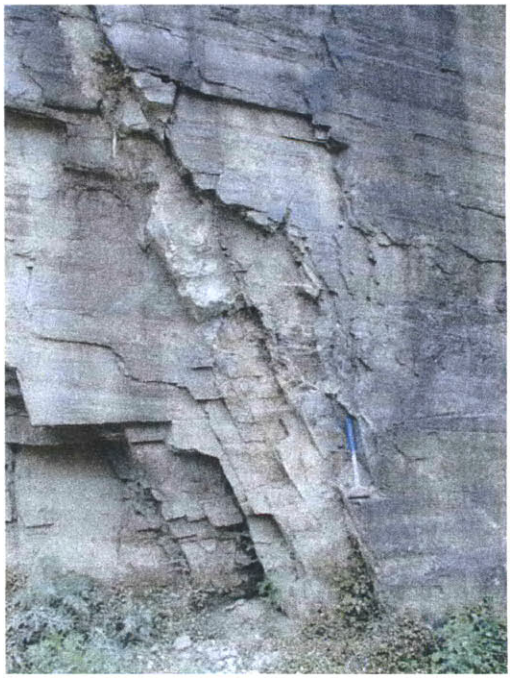

(d)

FIGURE 8

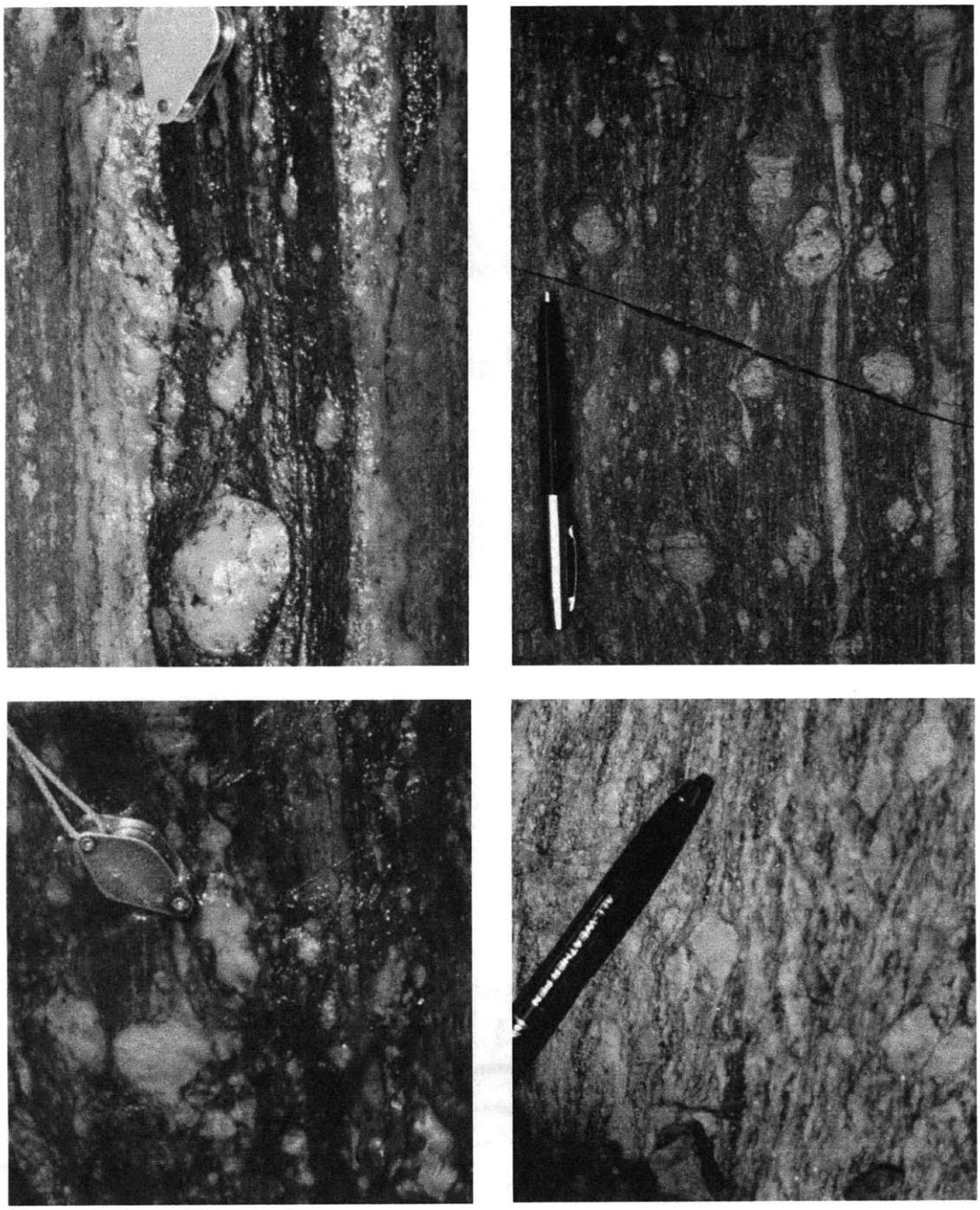

FIGURE 9

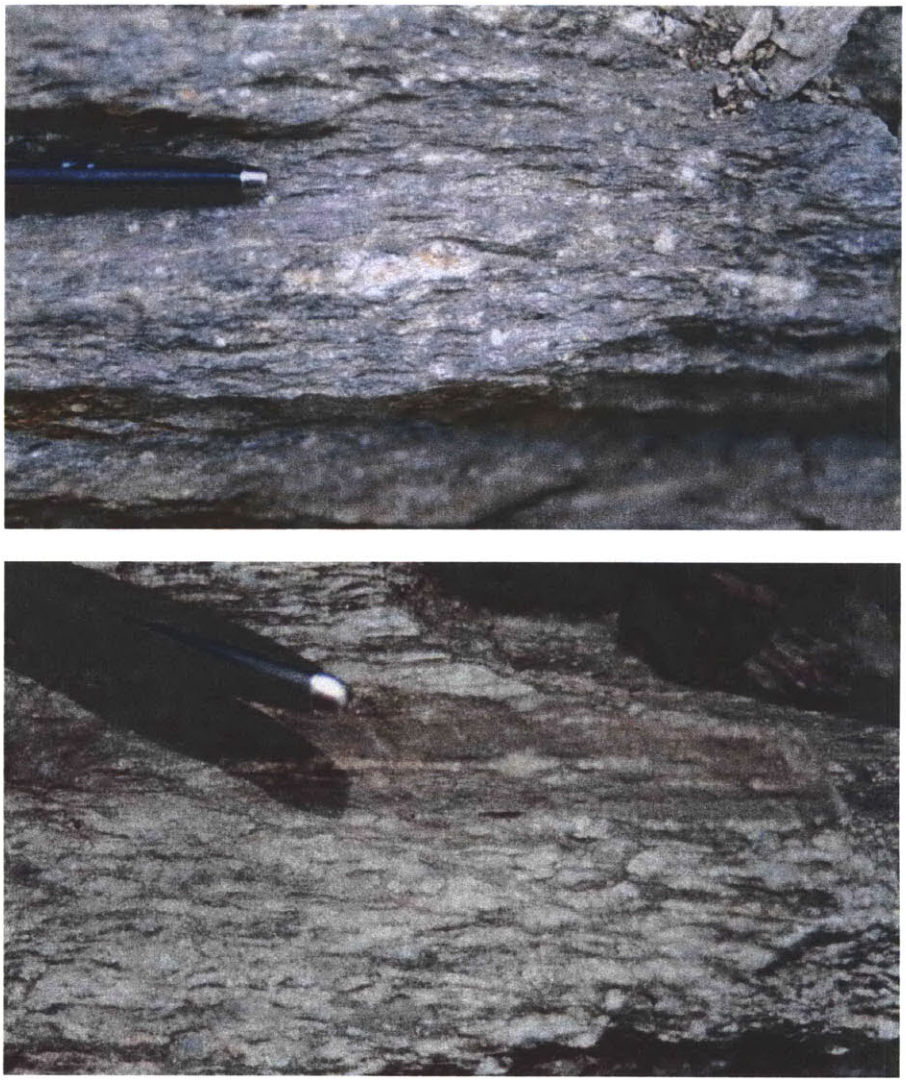

FIGURE 10

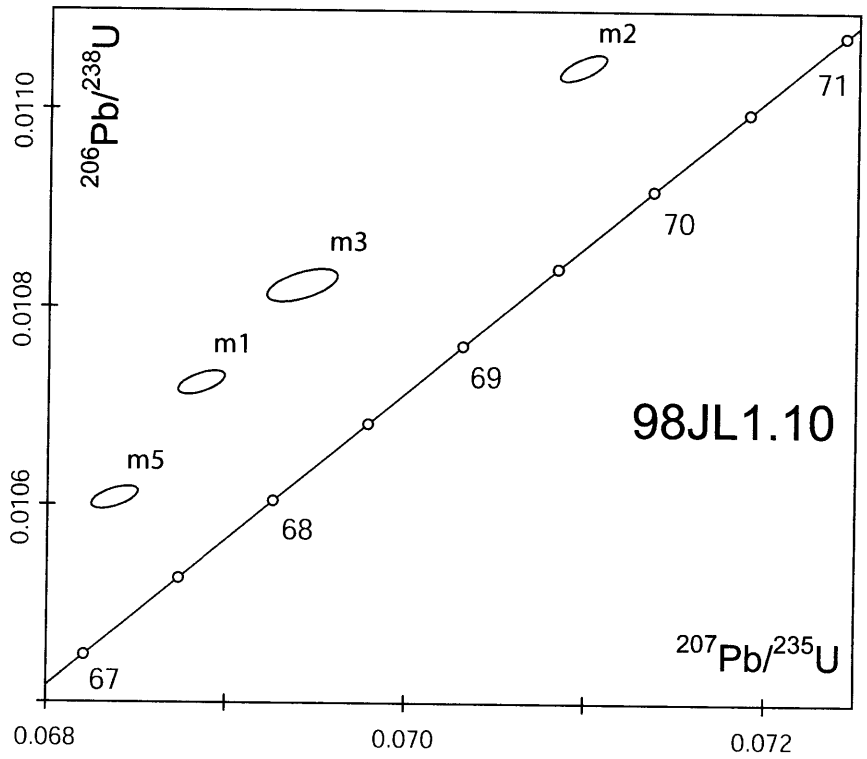
m2
71
70
m3
m1
69
98JL1.10
m5
68
67
$^{206}Pb/^{238}U$
$^{207}Pb/^{235}U$
0.0110
0.0108
0.0106
0.068
0.070
0.072

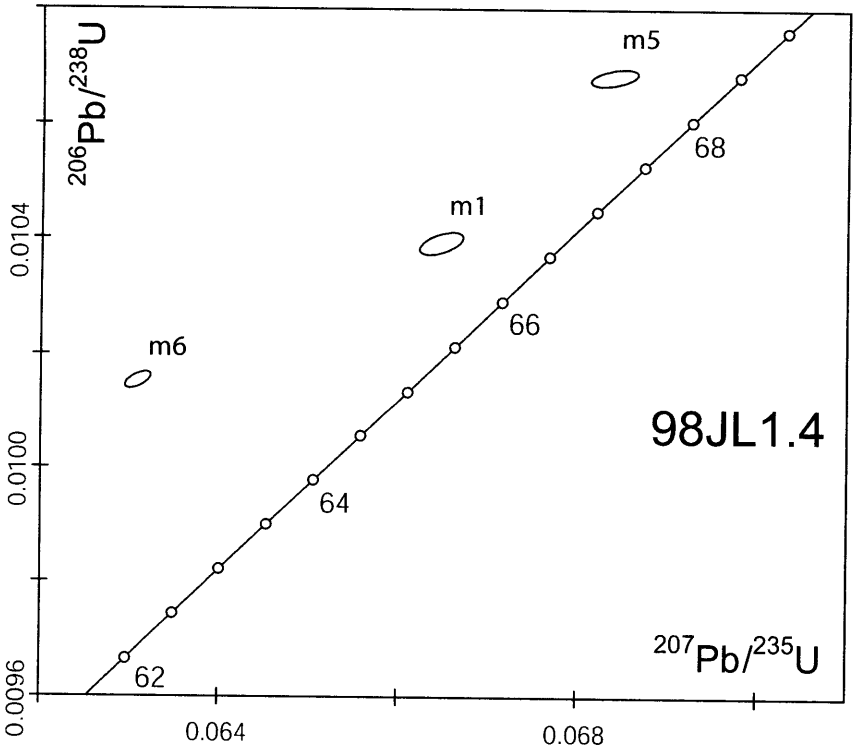
m5
68
m1
66
m6
98JL1.4
64
62
$^{206}Pb/^{238}U$
$^{207}Pb/^{235}U$
0.0104
0.0100
0.0096
0.064
0.068

FIGURE 11

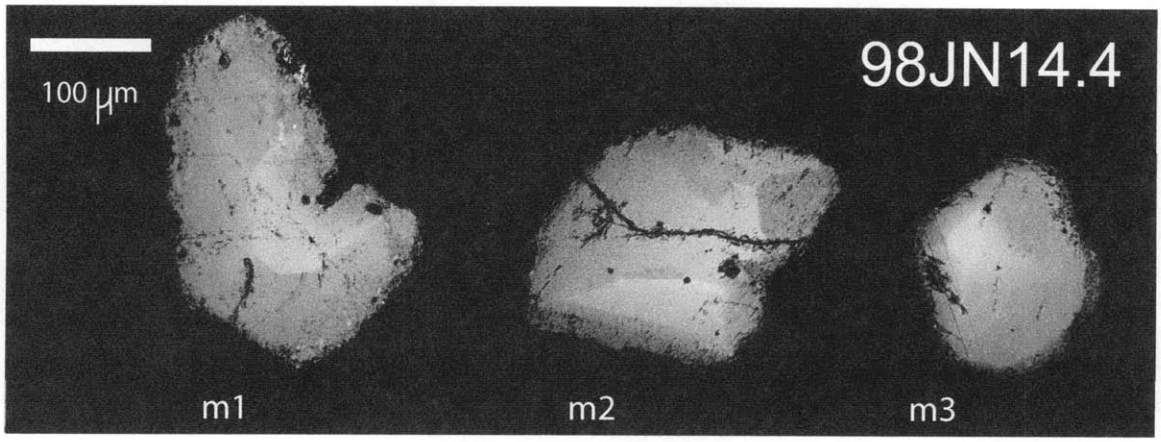
100 µm
98JN14.4
m1
m2
m3

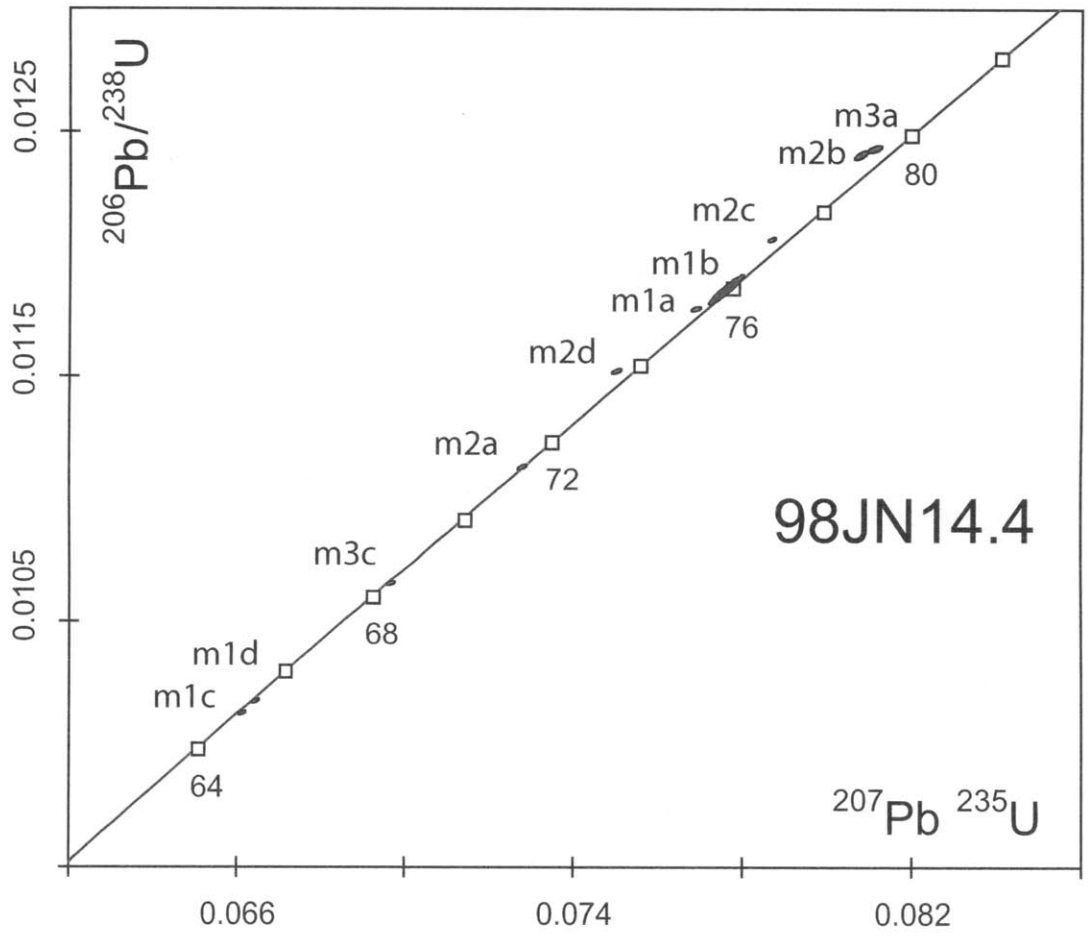
0.0125
0.0115
0.0105
$^{206}Pb/^{238}U$
m3a
m2b
80
m2c
m1b
m1a
76
m2d
m2a
72
98JN14.4
m3c
68
m1d
m1c
64
^{207}Pb ^{235}U
0.066
0.074
0.082

FIGURE 12

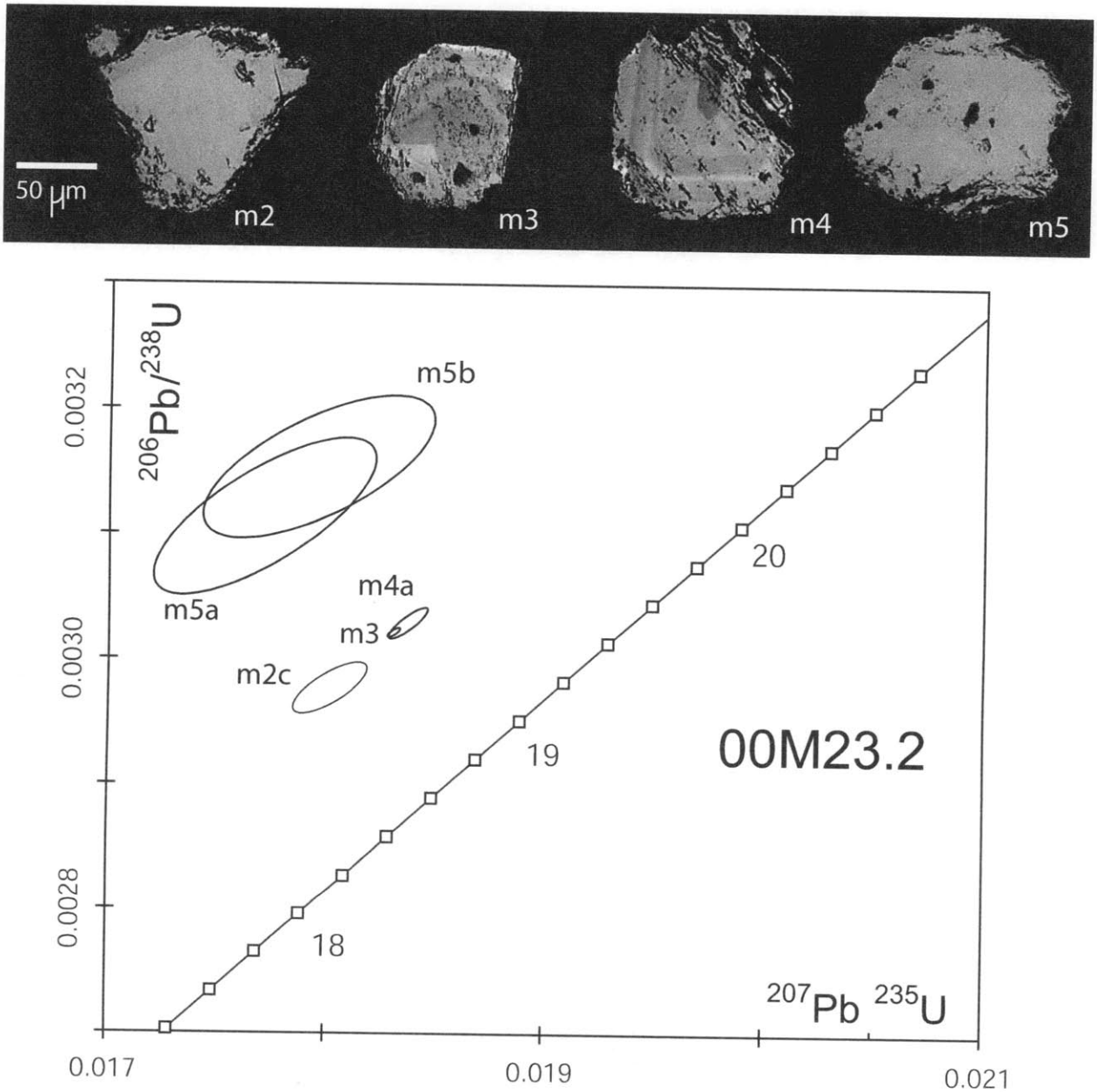
50 μm
m2
m3
m4
m5
$^{206}Pb/^{238}U$
0.0032
0.0030
0.0028
m5b
m5a
m4a
m3
m2c
20
19
18
00M23.2
^{207}Pb ^{235}U
0.017
0.019
0.021

FIGURE 13

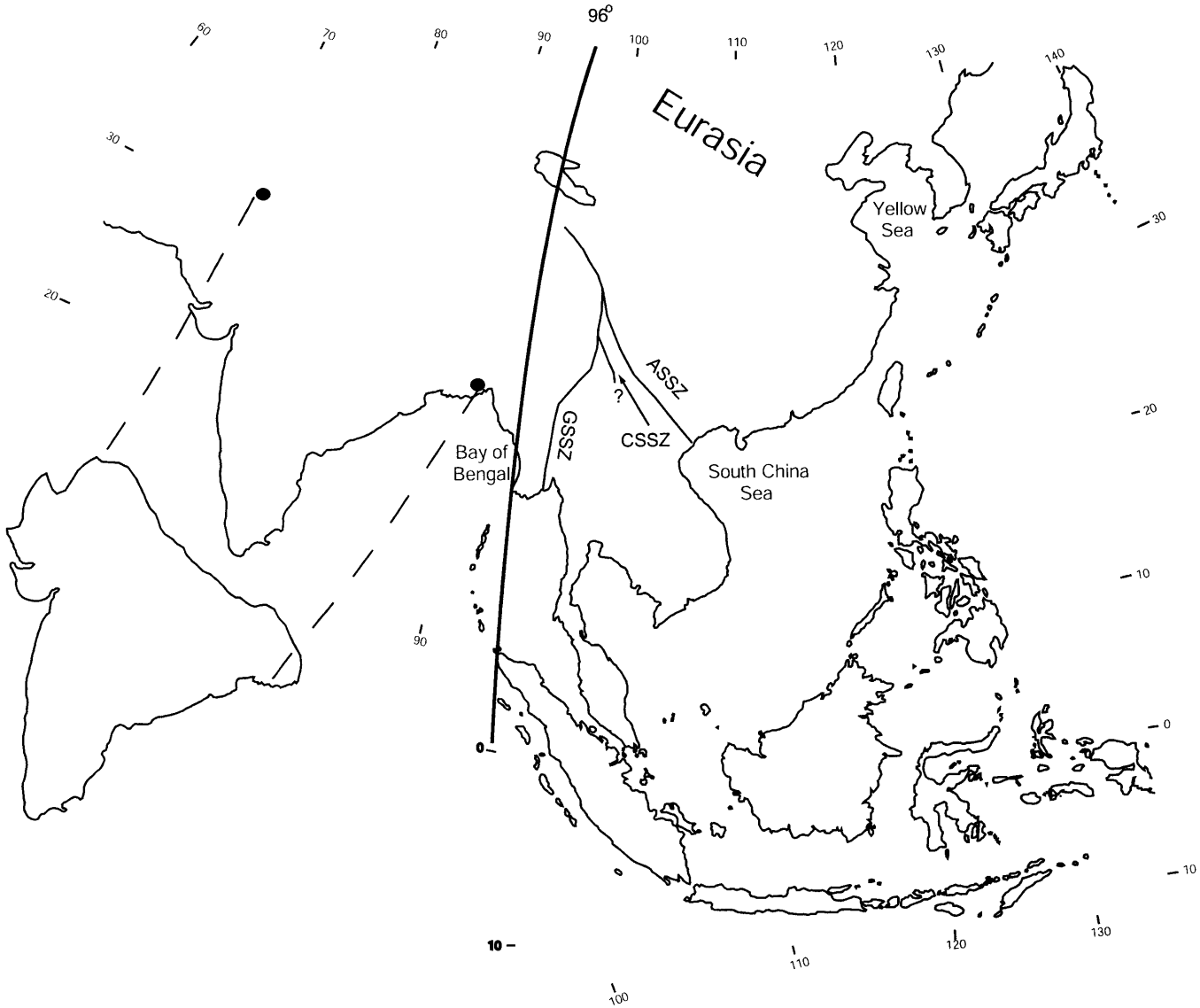
96°
Eurasia
Yellow Sea
South China Sea
Bay of Bengal
ASSZ
CSSZ
GSSZ
?
60
70
80
90
100
110
120
130
140
30
20
10
0
10
90
100
110
120
130

FIGURE 14

Chapter 4: Geometry, Kinematics and Regional Significance of the Chong Shan Shear Zone, Yunnan, China

Sinan Akciz[1]*
B. Clark Burchfiel[1]
James L. Crowley[1]
Yin Jiyun[2]
Chen Liangzhong[2]

[1]Massachusetts Institute of Technology, Dept. of Earth, Atmospheric and Planeary Sciences, 77 Massachusetts Ave., Cambridge, MA 02139

[2]Yunnan Institute of Geological Sciences, 131 Baita Rd., Kunming, Yunnan, China.

*E-mail: akciz@mit.edu

ABSTRACT:

The geology of the area east of the Eastern Himalayan Syntaxis is poorly known, although it figures prominently in many models for the Cenozoic tectonics of the India-Eurasia collision and subsequent intracontinental deformation. Our detailed field mapping and laboratory studies of an area in western Yunnan, China between the active right-lateral Sagaing Fault in Burma and the active Red River Fault of Yunnan, reveals the presence of two major linear metamorphic belts, the Gaoligong Shan and Chong Shan belts, both of which are mylonitic shear zones that accommodated much of the penetration if India into Eurasia during early and middle Cenozoic time. Here we focus on the little known Chong Shan shear zone, a long (>300 km) and wide (10-20 km) metamorphic belt of low- to high-grade rocks whose presence has often been neglected in models of Eurasian deformation. The CSSZ is composed mainly of mylonitic augen gneisses and migmatites, and the rocks appear to have been derived from more than one tectonic unit. Foliation within the shear zone is moderately to steeply west-dipping. Stretching lineations defined by the alignment of elongate mineral grains are sub-horizontal, consistent with dominantly strike-slip transport. Kinematic indicators including rotated porphyroclasts, S-C fabrics, and asymmetric folds are common at microscopic and outcrop scale and provide evidence for both dextral and sinistral movements. Our preliminary geochronological studies indicate that the CSSZ has been active since at least ~34 Ma, and perhaps as early as 41 Ma. Strike-slip shearing continued at least until ~29 Ma, and perhaps as late as ~24 Ma, and terminated by ~17 Ma. The CSSZ, therefore, is not a belt of Precambrian metamorphic rocks as previously thought, but a Cenozoic shear zone of great significance, which was contemporaneous with movement on the left-lateral Ailao Shan and the right-lateral Gaoligong Shan shear zones. These new data from the CSSZ along with the data from the GSSZ indicate that while the region between the GSSZ and ASSZ extruded to the southeast, it did not extrude as a single rigid block, but rather it was dismembered into at least two major fragments.

INTRODUCTION:

The mechanism by which the Cenozoic post-collisional northward motion of India relative to Eurasia and South China was accommodated along its eastern boundary is still a poorly understood aspect of the tectonic evolution of SE Asia. Models for the tectonic evolution range from southeastward extrusion of the region between the right-lateral Sagaing Fault in Burma and the left-lateral Ailao Shan Shear Zone (ASSZ) in Yunnan (Figure 1), China, as a single lithospheric block with minimal internal deformation and minor rotation (e.g. Tapponnier et al., 1982, 1986), to lateral spreading of thickened viscous lithosphere with little eastward extrusion

(Houseman and England, 1993). Alternate models argue for eastward flow of lower crust accompanied by large-scale clockwise rotation and crustal thickening (Royden et al., 1997) and extrusion of crustal material accompanied by significant internal deformation and large-scale rotation of smaller crustal fragments (Wang and Burchfiel, 1997).

In particular, the concept of lateral extrusion in Cenozoic time, has played an important role in tectonic interpretations of Asia, especially since the publication of numerous detailed studies conducted along the ASSZ (e.g. Tapponnier et al., 1982, 1986; Harrison et al., 1992; Leloup et al., 1993, 1995; Schärer et al., 1990, 1994; Harrison et al., 1996; Gilley et al., 2003). The ASSZ is interpreted to have accommodated 700±200 km of displacement of Indochina to the southeast relative to South China (Leloup et al., 1995) since at least 34 Ma, based on dating of monazite inclusions in syn-kinematic garnet (Gilley et al., 2003). U-Pb ages of accessory minerals from late syntectonic leucogranites parallel to the foliation and affected by left-lateral shearing cluster around 24 Ma (Leloup et al., 1995), indicating that the left-lateral shearing continued at least until this time and possibly as late as 17 Ma (Briais et al., 1993). However, numerous important questions still remain unanswered regarding the nature and the style of deformation induced by the indentation of India into Asia: (1) Where is the right-lateral conjugate shear system to the left-lateral ASSZ, since the proposed Sagaing fault is only ~13 Ma old (Curray et al., 1979, Lawver et al., 1976) ? (2) Has extrusion tectonics been largely accomplished by rigid block motion (Leloup et al., 1995), or by a series of internally deformed crustal fragments that translated and rotated differentially (Wang and Burchfiel, 1997) (Figure 2)?

The bedrock geology of the region around the eastern Himalayan syntaxis has been insufficiently known to evaluate these outstanding questions, particularly for the early Cenozoic part of the deformation history, since seismological, neotectonic, and geodetic studies cannot be

used. We have, therefore, conducted detailed field mapping and structural and geochronological studies of several transects across two poorly documented linear metamorphic belts located between the Sagaing fault and the ASSZ: the Gaoligong Shan Metamorphic Belt (hereafter the Gaoligong Shan Shear Zone, or GSSZ) and Chong Shan Metamorphic Belt (hereafter the Chong Shan Shear Zone, or CSSZ) in Yunnan, China (Figure 3). In chapters 2 and 3, we addressed the first question and showed that the presently inactive Gaoligong Shan Shear Zone is the only right-lateral ductile shear zone that could have accommodated a significant portion of the motion between India and Eurasia prior to the initiation of the presently active Sagaing fault in Burma. In this chapter, we address the second question by focusing on the Chong Shan Shear Zone, a long (~250 km), narrow (<10 km) belt of metamorphic rocks which divides the proposed rigid Indochina block of the extrusion model into two different tectonic fragments. The CSSZ is rarely considered in syntheses of the Cenozoic tectonics of the area because regional studies, in general, have considered the metamorphic rocks that form the CSSZ to be Precambrian basement of the Baoshan tectonic element. In this chapter, the CSSZ is described in detail for the first time, with emphasis on its lithologies, structural style, and deformational history based on our field observations along seven transects across the belt. Preliminary $^{40}Ar/^{39}Ar$ and U/Pb results are also presented followed by the tectonic implications of our field observations and geochronological results. These data show that the CSSZ is a zone of early Cenozoic shearing, both left- and right-lateral and was active coevally with the GSSZ and the ASSZ.

OVERVIEW OF THE GEOLOGY OF WESTERN YUNNAN

The CSSZ (Figure 3) separates the Baoshan segment that forms the northern part of the of the Sibumasu continental fragment (hereafter the Baoshan tectonic element (B)) from the

Lanping-Simao part of the Indochina continental fragment (hereafter the Simao tectonic element (S)). The Simao tectonic element lies east of the Baoshan tectonic element, and west of the South China continental fragment. It is bounded to the west by Lancangjiang suture, the CSSZ and the Linchang granites and to the east by the discontinuous belt of mylonitic rocks in the Ailao Shan, Diancang Shan, and Xuelong Shan, which will be collectively referred to as the Ailao Shan shear zone (ASSZ). The ASSZ is the most thoroughly studied of all the shear zone rocks in this region. It has been interpreted to be a major left-lateral shear zone of middle Cenozoic age (e.g. Harrison et al., 1992; Leloup et al., 1993, 1995; Schärer et al., 1994, 1996; Harrison et al., 1996; Gilley et al., 2003). Most of the Simao tectonic element consists of a thick (structural thicknesses up to 7.5 km) succession of mostly nonmarine redbeds of Jurassic to early Cenozoic age (Bureau of Geology and Mineral Resources of Yunnan Province, 1990), which extends into Laos, Cambodia and Thailand. Triassic rocks are present as are Palaeozoic strata; the latter are less extensively exposed and lie unconformably below the Mesozoic strata in limited areas mostly on the eastern and western margins of the Simao element. The only palaeontologically well-dated lower Palaeozoic strata are Silurian turbidites consisting of black shales with graptolites, siltstones and siliceous deposits, which crop out along the eastern margin of the Simao tectonic element (Bureau of Geology and Mineral Resources of Yunnan Province, 1990). Devonian strata are represented by siliciclastic deposits and limestones of a relatively stable littoral and shallow water environment. Carboniferous and Permian strata in this area contain carbonate rocks and interbedded sandstone and shale. An extensive mafic to felsic volcanic sequence (of Carboniferous and Permian age?) is widely distributed along the Lancang River on the western margin of the Simao tectonic element. Lower Triassic deposits are rare but often contain volcanic rocks. Middle Triassic strata in the western part of the Simao element contain abundant acid, intermediate, and locally mafic volcanic

and associated sedimentary rocks. Rocks of similar age are non volcanic further to the east. The Upper Triassic sequence consists of non-marine conglomerates and sandstones in the lower part, shallow-marine clastic deposits with carbonates in the middle part, and littoral coal-bearing clastic deposits in the upper part. Some acid and intermediate volcanic rocks are present in the lower part of the Upper Triassic succession, but only on the eastern and western margins of the Simao tectonic unit (Bureau of Geology and Mineral Resources of Yunnan Province, 1990).

The Baoshan tectonic element (Figure 3) lies to the west of the Simao tectonic element and forms the northernmost continuation of the more regional Sibumasu continental fragment as defined by Metcalfe (1984, 1988). A thick section of about 10 km (probably a structural thickness and not a true statigraphic thickness) of Upper Proterozoic to Middle Cambrian slightly metamorphosed siliceous clastic and carbonate rocks form the basal part of the Baoshan stratigraphic sequence in the study area (Bureau of Geology and Mineral Resources of Yunnan Province, 1990; Jin, 1994). Ordovician and Silurian units consist mainly of fossiliferous shallow water siliciclastics and some argillaceous limestone and shale. From the Middle Devonian to the end of the Early Carboniferous time, various fossiliferous carbonate units were deposited. The lower part of the Upper Carboniferous strata contains diamictite, along with turbidite, conglomeratic sandstone, and siltstone (Jin, 1994). The upper part contains black mudstone and siltstone, which are regarded as glacial deposits. The Woniusi basaltic lava flows, with pillow lavas and tuffaceous intercalations, terminate deposition in early Permian time (Bureau of Geology and Mineral Resources of Yunnan Province, 1990). These basalts probably are related to rifting and the beginning of separation of the Baoshan continental fragment from the Gondwana margin (Jin, 1994), although data supporting this interpretation is poorly documented. Lower Permian (?) red beds lie disconformably above the Woniusi Basalts. The Mesozoic strata consist of

Triassic limestone and Jurassic marine strata and red beds and are generally restricted to the margins of the Baoshan tectonic element. Cenozoic rocks are rare and are characterized by upper Eocene-Oligocene conglomerate and sandstone that rest unconformably on deformed older rocks.

The Baoshan tectonic element contains a very characteristic and distinct Palaeozoic sedimentary and volcanic sequence that is different from the Simao tectonic element of the Indochina continental fragment. Within the map area, rocks that would establish the existence and location of the suture bounding the Baoshan tectonic element on the east side are missing because of intense Cenozoic shearing and dislocation along the Lancangjiang section of the Lancangjiang – Changning – Menglian – Nan – Uttaradit – Bentong - Raub suture zone (Figure 3) hereafter called the Lancangjiang suture zone (LS). The Lancangjiang suture in the study area is cryptic, but its existence is proposed along the northern part of the Lancang River and is based only on the regional analysis of suture zones to the north in Tibet and to the south in southern Yunnan and Thailand.

The Baoshan tectonic element is bounded by the GSSZ to the west that will be discussed only briefly here since it was discussed earlier (Chapter 2 and 3). The GSSZ comprises an orthogneissic section to the west, and a paragneissic section the east, both of which consist of amphibolite-grade metamorphic rocks. Most of the foliation in the GSSZ metamorphic rocks dip steeply ($\geq 60°$) both to the west and east and shows well-developed mylonitic textures. The mylonitic foliation contains a prominent lineation, interpreted as a stretching lineation, formed by the elongation of quartz, feldspar, and biotite. Consistent shear criteria, such as asymmetric tails on deformed feldspar porphyroclasts, S-C surfaces, asymmetric boudins, and cm- to dm-scale asymmetric folds observed in horizontal sections perpendicular to the foliation and parallel to the lineation, indicate a right-lateral sense of shear (Chapter 2). Syn-tectonic pegmatite dikes and

leucogranite bodies generally form concordant veins, layers and lens-shaped bodies and contain a foliation formed by micas indicating they have been affected by same ductile deformation as their host mylonitic metamorphic rocks.

To the north of the map area between the headwaters of the Salween and Mekong rivers is the southeastern part of the Qiangtang continental fragment that is bounded by the Lancangjiang suture to the east and by the Bangong – Nujiang suture zone to the southwest (Figure 3). There is an ongoing debate regarding the importance of the Central Qiantang metamorphic belt of Kapp et al. (2000) which is interpreted to divide the Qiantang continental fragment into two parts: a northern section which contains warm-water faunas (Cathaysian affinity; similar to the South China block) from a southern section which includes cold water fauna and glacial deposits (Gondwana-Land affinity) (Wang and Mu, 1983; Fan, 1985, 1988; Chen and Xie, 1994). Information regarding the southeastern part of the Qiangtang tectonic element is very limited due to its logistical remoteness. However, rifting of the Qiangtang continental fragment from the Lhasa continental fragment and opening of the intervening Bangong Ocean occurred during Permo-Triassic time (Sengor et al., 1988). The Bangong Ocean was subsequently closed by northward subduction beneath the Qiangtang continental fragment during Middle Jurassic-Early Cretaceous time (Girardeau et al., 1984; Pearce and Mei, 1988). 1:200,000 scale geological maps of China of this area assign a Carboniferous age to the low-grade metasedimentary rocks that consist of light-colored quartzite, sandstone, interbedded limestone and marble, but do not assign them to the Lhasa or the Qiangtang continental fragments. These Carboniferous rocks lie east of the GSSZ and the Gangdese granites, which are considered to mark the southeastern part of the Lhasa continental fragment, as well as east of the southern projection of the Bangong suture, suggesting that these rocks do not belong to the Lhasa tectonic element. These Carboniferous

rocks lie west of the Permo-Triassic granites and associated volcanic rocks which are considered to form the western boundary of the Simao tectonic element (Figure 3) Therefore, these Carboniferous strata are tentatively assigned to the Qiangtang tectonic element. Correlation of these rocks with the major tectonic elements in the region clearly requires further examination in this poorly known part of the Eastern Himalayan Syntaxis.

THE CHONG SHAN SHEAR ZONE (CSSZ)

The CSSZ collectively consists of migmatite, quartz-feldspar-biotite-bearing paragneiss (hereafter the QFB gneiss), mica-schist, impure quartzite, calc-silicate rocks, marble, augen gneiss and mylonitic granite. Seven structural sections across the CSSZ were studied that had varying exposure quality (See Figure 4 for locations of the 6 geological cross-sections illustrated in Figure 5. The Wayao (Figure 5, a) and Chaojian (Figure 5, b) sections cross the entire shear zone, whereas the Shidu (Figure 5, g) section, with nearly continuous outcrop, crosses all but the easternmost part of the CSSZ. Unlike the better documented ASSZ (e.g. Leloup et al., 1995) and the GSSZ (Chapters 2 and 3), the rock units that form the CSSZ change from south to north and cannot be easily connected between cross-sections, probably due to different protoliths in different sections of the shear zone. The rock assemblage in the CSSZ is distinct and separated from the rocks of the GSSZ by the Baoshan sequence in the south. Where the Baoshan rocks pinch out to the north, the same assemblage can be separated from the GSSZ based on lithologic determinations. The GSSZ, which consist of metasedimentary rocks along its eastern section, lacks any migmatite and augen gneiss, that form the CSSZ. Most of these units contain a prominent sub-vertical foliation and a sub-horizontal stretching lineation (Figure 6). The main trace of the CSSZ was studied along seven

road sections on the route from the cities of Baoshan to Gongshan (Figure 4). The rock types and structures in these sections are discussed below from the south to the north.

a) Wayao section (Figure 5, a):

This is the most accessible section across the CSSZ, but it is not very representative of the CSSZ as a whole. At this section the Lancang River makes a sharp bend and exposes a narrow, nearly complete section of the southern CSSZ. Here, the lower Palaeozoic sedimentary section of the Baoshan tectonic element can be traced progressively from west to east into the high-grade metamorphic core. The high-grade rocks of the CSSZ consist of the following from west to east: quartz-feldspar-biotite (QFB) paragneiss intruded by weakly foliated to unfoliated leucogranitic sills; muscovite and biotite schists with impure quartzite that forms thick units; calcsilicate rocks, marble, and an intensely folded impure quartzite interlayered with pure quartzite; and finally QFB gneiss and biotite schist (Figure 6). Observations of large outcrops with fresh surfaces suggest that some of the QFB gneisses may in fact be the melanosome and the leucogranites be the leucosomes of local migmatitic sections. Unlike the rest of the CSSZ, most of the foliation along this transect dips moderately (40° - 60°) west (Figure 7). A subhorizontal stretching lineation associated with the mylonitic fabric is only seen within the QFB gneisses and the micaceous schists. The schistosity is marked by biotite, ± chlorite, ± actinolite and quartz ± feldspar ribbons. No minerals were present which would indicate metamorphism at high temperatures, such as garnet or aluminosilicate minerals. Quartz usually defines the lineation, forming long polycrystalline ribbons generally made of recrystallized grains. The grains have an irregular shape, sutured boundaries, often with undulatory extinction, subgrains and deformation bands.

The dominant east-vergent folds, west-dipping thrust faults, and the increasing metamorphic grade from the unmetamorphosed to weakly-metamorphosed sedimentary rocks of

the Baoshan sedimentary sequence in the west to the higher-grade metamorphic rocks that form the CSSZ to the east, suggest the protoliths of the CSSZ were Baoshan sediments and their metamorphic basement. The CSSZ was thrust east over the Jurassic and Cretaceous aged sedimentary rocks of the Simao tectonic element. The contact between the CSSZ and the Simao tectonic element is seen only here and along the Chaojian road section, is foliation parallel, and is referred to as the Lancangjiang fault below. The contact between the CSSZ and the Baoshan tectonic element is not exposed along this road section, as it is obscured by thick vegetation. We interpret this sharp contact between high-grade rocks of the CSSZ and the unmetamorphosed Palaeozoic rocks of the Baoshan tectonic element as a steeply west-dipping normal fault based on the interpretations of remotely sensed data including Landsat 7 and CORONA images (Figure 8). The age of this fault, which will be referred to as the Chaojian fault, as well as its sense of displacement and continuation to the north, remain to be resolved.

b) Chaojian road (Figure 5, b):

The Chaojian section offers a nearly continuous exposure of the CSSZ. Here, the CSSZ consists mainly of migmatites, mylonitic granites, augen gneisses, quartzofeldspathic gneisses, and QFB gneisses as well as strongly foliated impure quartzite. All foliations dip steeply ($\geq 60°$) to the west. The schistosity is marked by biotite, and quartz and/or feldspar ribbons. This schistosity contains a prominent lineation interpreted as a stretching lineation formed by the elongation of quartz, feldspar, and biotite. Unlike the Waoyao section, the metamorphic rocks of the Chaojian section contain garnet, staurolite and rutile, indicating metamorphism at higher temperatures (Figure 8). All shear sense indicators, including S-C fabrics (Figure 9) and rotated plagioclase porphyroclasts indicate left-lateral shear. Weakly to strongly foliated pegmatite and

tourmaline-bearing micaceous leucogranite dikes, which are interpreted to be syn-deformational, intrude all the other units within the shear zone. The contact between the CSSZ and the Langping-Simao belt, the Lanchangjiang fault is foliation parallel, but can be located to within a few meters.

c) Tuer section (Figure 5, c):

The Tuer section (c) consists only of limited exposures of the easternmost part of the CSSZ. The rocks consist of grayish green actinolite schists and ultramylonites (Figure 11), and highly weathered leucogranite sills sheared at the decimeter scale, all of which contain S-C fabrics and rotated plagioclase porphyroclasts that indicate left-lateral strike-slip shearing. To the east, the contact between the CSSZ metamorphic rocks and the very weakly metamorphosed fine-grained Jurassic-Cretaceous sedimentary rocks of the Lanping-Simao belt can be located within a few meters, though the contact is never exposed. All foliations dip steeply ($\geq 70°$) to the west. The actinolite schists consist mostly of alternating bands of medium to coarse-grained actinolite with quartz and trace amounts of titanite and epidote. The ultramylonite matrix is fine-grained and composed of quartz, mica and plagioclase. Feldspar and quartz porphyroclasts mostly have symmetric tails of recrystalized grains.

d) Bijiang road (Figure 5, d and also Appendix A):

The Bijiang section is along a dirt road constructed for timber trucks which goes up from the Nujiang River to the small village of Bijiang and continues further east. The Bijiang section passes through the metasedimentary rocks of the Gaoligong Shan shear zone (GSSZ) that consist

mainly of isoclinally folded, narrow (50 – 100 m) bands of marble and calc-silicate rocks as well as impure quartzite, none of which contain good shear sense indicators, even though they are well-foliated. These metasedimentary rocks are juxtaposed against mylonitic granites that contain a subhorizontal stretching lineation. Both left- and right-lateral shear sense indicators are present and include S-C fabrics and rotated plagioclase porphyroclasts (Figure 11). In the eastern part of the section, the CSSZ metamorphic rocks consist mainly of foliated mylonitic granites and QFB gneisses that dip $\geq 60°$ both to the east and west. No right-lateral shear sense indicators were observed beyond 5 km east of the town of Bijiang, although the left-lateral shear sense indicators are present. Foliation parallel leucogranite and pegmatite dikes are abundant and are either weakly foliated or undeformed, compared to their strongly foliated host rocks. No mineral lineations were observed in these leucogranitic sills.

e) Fugong granite (Figure 4, section e):

The section north of the town of Fugong has limited exposures, which makes the location of the boundary between the GSSZ metasedimentary rocks and the CSSZ rocks difficult to locate accurately. We have located the contact based on the first occurrence of dominantly migmatitc / orthogneissic rocks with both right- and left-lateral shear sense indicators, because the metasedimentary section of the GSSZ contains neither orthogneisses nor any left-lateral shear sense indicators. QFB gneisses along with impure quartzite occur only locally within the dominantly mylonitic granites and orthogneisses. Near the mountain summit, remnants of an undeformed granitic body are present (Figure 13). The contact between the granite and the orthogneisses is a zone of mylonitic granites (Figure 13) with vertical foliations and sub-horizontal lineations with left-lateral shear sense indicators.

f) LiShiNerHe section (Figure 5, f and also Appendix A):

The LiShiNerHe valley is a tributary of the Nujiang valley and offers excellent exposures of the western part of the CSSZ, but it never crosses the entire shear zone. This section consists mainly of migmatites and augen gneisses as well as mylonitic granites, all of which contain subvertical foliation and subhorizontal stretching lineation which is marked by biotite, muscovite, sillimanite, and ribbons of recrystallized quartz and feldspar. Kinematic shear criteria include asymmetric folds, pervasive S-C fabrics, mica fish, and feldspar porphyroclasts with asymmetric tails made of small, recrystallized quartz and feldspar grains (Figure 14). These rocks contain dominantly left-lateral shear indicataor although some right-lateral shear sense indicators, such as S-C fabrics and rotated porphyroclasts are also present near the contact with the GSSZ. The migmatitic core of the CSSZ is characterized by an abundance of variably deformed leucogranite dikes and sills (Figure 15), whereas the remainder of the orthogneissic rocks is intruded by leucogranitic sills which are either weakly foliated or completely undeformed.

g) ShiDu section (Figure 5, g and also Appendix A):

The ShiDu section is along a trail east from the Nujiang River and contains an almost complete section of the CSSZ. There is a progressive increase in metamorphic grade from west to east along this section. The village of ShiDu is located on top of a thick section of brown-beige colored impure- to pure quartzite. Further east, the quartzite are interlayered with QFB gneiss. East of a thin marble unit, the dominant rock type is QFB gneiss with leucogranite sills and local occurrences of biotite schists and fine-grained impure quartzites. No aluminosilicate minerals or

garnets were observed to this part of the cross section A higher grade migmatite-rich section occurs east of these low-grade metasedimentary units and then contains abundant garnet, K-feldspar, and sillimanite, as well as muscovite and biotite, along with quartz and plagioclase. The rest of the section to the east consists of garnet, and silliminite-bearing QFB-gneiss interlayered with cm-scale leucogranite sills as well as augen gneiss, mylonitic granite and migmatite (Figure 16). The increased metamorphic grade is also well-expressed by the progressive transformation of the eastern Qiangtang arkosic sediments, quartzites and slates into the CSSZ schists, gneisses and migmatites. All of these rock units have well-developed foliations, however, lineations and mylonitic fabrics are more abundant in the eastern part of the section. Similar to some of the southern sections, both the dextral and sinistral shear sense indicators are abundant in the high-grade section. Sample 00JN6.2, for which U/Pb dates are presented below is an unfoliated leucogranite that cross-cuts the foliated and mylonitized QFB gneiss.

DEFORMATION ALONG THE GNEISSIC SECTION OF THE CSSZ

A major, penetrative ductile deformation with steep foliations and nearly horizontal lineations affects almost all the rock types of the CSSZ, and is particularly well-developed in the pelitic gneiss, mylonitic granite and augen gneiss. The foliation generally dips moderately to steeply to the west. A stretching lineation defined by the alignment of elongate mineral grains is consistently sub-horizontal with a dominantly left-lateral strike-slip shear sense. Boudinage is widespread and affects both compositional bands in mylonitic rocks formed during earlier stages of deformation and leucocratic (leucogranite and pegmatite) veins emplaced during later stages of deformation. Most of the paragneiss, micaschist, and orthogneiss are mylonitic and kinematic

indicators such as rotated porphyroclasts of K-feldspar and plagioclase, S-C fabrics, and asymmetric folds are common at mesoscopic scales, indicating dominantly sinistral shear, as was suggested in a previous study by Wang and Burchfiel (1997). However, at and north of Bijiang, the cross sections of the CSSZ contain asymmetric porphyroclasts and S-C fabrics that indicate both a dextral and a sinistral sense of motion. From Bijiang to Shidu, the dextral shear sense indicators are generally, but not always, present near the GSSZ and the sinistral indicators are observed farther east.

Microstructures in CSSZ rocks were analyzed using oriented thin sections cut perpendicular to the foliation and parallel to the lineation. The study of these rocks confirms outcrop observations. In thin section, the foliation and the lineation are marked by metamorphic minerals (chlorite, actinolite, biotite, muscovite, and sillimanite) and by quartz and feldspar ribbons. The quartz forms long polycrystalline ribbons generally composed of recrystallized grains. The grains have an irregular shape, sutured boundaries, often with undulose extinction, subgrains and deformation bands, attesting to strong internal deformation. Plastic deformation combined with dynamic recrystallization thus appears to have been the dominant deformation mechanism in the quartz. The dominant stretching lineation is penetrative, regionally pervasive and interpreted to represent the principal relative transport vector. The stretching lineation orientation consistently plunges shallowly (<30°) both to the N and S, parallel to the strike of the CSSZ. Interpretation of the shear sense in both outcrop and thin section are considered reliable because two or more independent criteria were employed at each locality. Just as with our outcrop interpretations, this section data indicates that the shear sense within the CCSZ is dominantly sinistral, but with dextral shear sense documented along the west side of the CSSZ where it is juxtaposed with the GSSZ, and also along the Shidu section at the very north.

Boudinage of early veins and compositional layering is common in the gneissic section of the CSSZ and it is interpreted to have formed during layer-parallel shear, with some flattening, associated with formation of the dominant L-S fabric. Boudins are enveloped by the dominant foliation and the extension axis of these boudins is sub-parallel to the mylonitic lineation in the host.

Strike-slip deformation occurred in the ductile field above 300°C as indicated by the recrystallization of quartz and formation of biotite, but probably not much above 500°C, as K-feldspar porphyroclasts are generally preserved and do not show evidence for recrystallization, and muscovite, where present, forms the mylonitic foliation (Gapais, 1989; LeGoff and Ballevre, 1990). The presence of both deformed and undeformed cm- to dm-scale aplitic, leucogranitic and pegmatitic sills and a leucogranite dike that cross-cuts the mylonitic foliation suggest that magmatism was contemporaneous with strike-slip deformation. Outside of the CSSZ, neither the Baoshan tectonic element (with the exception of the Luxi granite of unknown age), nor the Jurassic-Cretaceous redbeds of the Simao tectonic element contain any intrusive rocks of granitic composition.

Even though the lithology of the shear zone changes from the south to the north, and cannot be easily correlated from one cross-section to the next (see the discussion below), there is no evidence for a change of attitude in the fabrics along the gneiss belt, which indicates that our observations along this shear zone are characteristic for the overall structure and deformation of the belt.

TIMING OF DEFORMATION WITHIN THE CHONG SHAN METAMORPHIC BELT

All of the rocks forming the CSSZ, except for the discontinuous bands of marble, regardless of their degree of metamorphism, have been intruded by cm- to dm-scale pegmatitic, leucogranitic and aplitic sills of granitic composition. The mineralogy of the sills is dominated by quartz, plagioclase, ±microcline, ±garnet, ±tourmaline ±biotite ±muscovite. While some of the granitic intrusions within the migmatitic section of the CSSZ contain a folded foliation, the intrusions in the ortho- and pelitic gneisses show evidence for only one deformational event and can be grouped by their degree of deformation as follows: (1) foliated sills, (2) foliated and boudinaged sills, (3) unfoliated sills, (4) unfoliated , but boudinaged sills, and (5) unfoliated dikes that crosscut the foliation. None of these sills and dikes contains a lineation, even though the host rocks they intrude display a prominent sub-horizontal mylonitic lineation associated with the strike-slip shearing along the CSSZ. We interpret the smaller degree of deformation observed in the granitic sills and dikes compared to the strongly foliated and lineated host rocks to indicate they were intruded during the later stages of the strike-slip shearing.

Developing an understanding of the mechanism by which the Cenozoic post-collisional northward motion of India relative to Eurasia and South China was accommodated along its eastern boundary depends on building a framework of geochronological data on the appropriate rocks to delineate the temporal deformational evolution of the tectonic system through time. We have, therefore, conducted a preliminary U/Pb and $^{40}Ar/^{39}Ar$ geochronological study on four different rock types to constrain the age of the large-scale strike-slip deformation along the CSSZ: (1) mylonitic orthogneisses, (2) foliated leucogranite sills, (3) unfoliated leucogranite sills and (4) unfoliated leucogranite dikes that cross cut the mylonitic foliation.

Sample locations and schematic block diagrams showing their structural setting are shown in Figure 5 .Table 1 lists conventional U- Pb, and Table 2 $^{40}Ar/^{39}Ar$ analytical data. Figures 17-19 present the U-Pb analyses of monazite in the form of corcordia plots. The main findings of this reconnaissance geochronological study of the crystalline core of the CSSZ are summarized in a chart of U-Pb and $^{40}Ar/^{39}Ar$ age results in Figure 20.

U-Pb Monazite geochronology: Sample description and results:

Foliated leucogranite (Sample 00JN25.1, Fig 17):

Sample OOJN25.1 is from a ~ 50 cm-thick foliated leucogranite sill within the Wayao section, which intruded the mylonitic QFB gneiss that contains well-developed left-lateral shear sense indicators. We interpret this leucogranite sill to be syn-tectonic as it has a well-developed foliation parallel to the mylonitic foliation of its host rock, even though it lacks the sub-horizontal stretching lineation. The mineralogy of this sill is dominated by quartz, plagioclase, K-feldspar, tourmaline and muscovite. Accessory minerals include abundant monazite and zircon. Seven fragments from four monazite grains (m1a, m1b, m2a, m2b, m3a, m3b and m4a) yielded reversely discordant dates (Figure 17). Reverse discordance is a common feature of young monazites and is thought to indicate ^{230}Th disequilibrium (Schärer, 1984; Parrish, 1990); as a consequence, we will use the $^{207}U/^{235}Pb$ dates in our age interpretations (errors given at 2σ). Backscatted electron images (BSE) images of monazite grains m1, m2 and m3 shows moderately strong oscillatory zoning that is typical of magmatic monazites, whereas grain m4 show no discernable zoning. Fragments from grain m2 yielded the youngest dates of 33.60 ± 0.04 Ma and 34.38 ± 0.03 Ma. The two fragments from grain m1 yielded the next youngest dates of 36.55 ± 0.05 Ma and 37.78 ± 0.10 Ma. Three fragments from grain m3 yielded older dates of 38.49 ± 0.06 Ma, 40.63 ± 0.07 Ma, and 41.00 ±

0.07 Ma with a larger spread, spanning ~ 2.5 my relative to the dates of the fragments from grains m1 and m2 which span only ~1 myr. One fragment from grain m4 yielded the oldest date of, 41.25 ± 0.07 Ma.

Unfoliated leucogranite (Samples 98JL18.4 and 99JU27.1, Figure 18):

Samples 98JL18.4 and 99JU27.1 are from ~20 cm thick undeformed leucogranite sills which intrude the QFB gneiss portions of the CSSZ and crop out along the Bijiang and Chaojian sections, respectively. We interpret the lack of foliation, lineation and boudinage to indicate that these sills intruded the mylonitic QFB gneisses of the CSSZ either at a time when the shearing ceased, was located in a different part of the shear zone, or was coming to an end. The mineralogy of these sills is dominated by quartz, plagioclase, K-feldspar, garnet, tourmaline, biotite and muscovite. Three monazite grains from sample 98JL18.4 (m1, m3, and m4(m2 has not been analyzed, yet)) and four monazite grains from sample 99JU27.1 (m1, m2, m3, m4), none of which were BSE imaged, yielded reversely discordant dates (Figure 18). As with sample 00JN25.1, we will use the $^{207}U/^{235}Pb$ dates that range from 24.3 ± 0.06 to 29.4 ± 0.05 Ma and 24.4 ± 0.08 to 26.0 ± 0.14 Ma for samples 98JL18.4 and 99JU27.1, respectively, in our age interpretations. We have also obtained $^{40}Ar/^{39}Ar$ ages from the biotite and muscovite crystals of sample 98JL18.4 (See $^{40}Ar/^{39}Ar$ section for results).

Cross cutting dike (Sample 00JN21.4, Fig 19):

Sample OOJN21.4 was collected from a ~50 cm thick, undeformed, leucogranite dike along the Shidu section that cuts across the foliation of the QFB gneiss very near the eastern

boundary of the CSSZ. The mineralogy of this dike is dominated by quartz, plagioclase, and tourmaline. Accessory minerals include monazite and zircon, however, they are less abundant and smaller in size compared to those in the other granitic rocks we sampled. One monazite grain with little or no discernable zoning (m2b) in the BSE image yielded a reversely discordant $^{207}U/^{235}Pb$ date of 17.1 ± 0.4 Ma.

Interpretation of the monazite data:

Two different types of age dispersions are observed in the leucogranite sample 00JN25.1 (foliated leucogranite): (1) an overall spread of dates from ~33.7 to ~41.3 Ma, and (2) a spread of up to ~2.5 my between the 2-3 fragments from a single grain. Understanding the cause of this dispersion is crucial to interpreting the age of the samples. The overall age dispersion could be produced in several ways. One possibility is that the igneous crystallization age is closely represented by the youngest monazite and the older grains contain inherited component that are probably not more than several tens of millions of years older than the oldest date. A second possibility is that each date represents a crystallization age corresponding to different metamorphic and anatectic phases over the ~33.7 to ~41.3 Ma interval. A third possibility is that the oldest dates obtained from grains m3 (41.00 ± 0.07 Ma) and m4 (41.25 ± 0.07 Ma) are close to the igneous crystallization age and the other fragments have been affected by recrystallization at a younger time than the youngest date (~33.7 Ma). However, there is little indication of such recrystallization in the BSE images of the grains we have analyzed. However, because BSE images are controlled by Ce, La, Th, and Nd, it is possible that minor recrystallization did occur, but the Ce, La, Th, and Nd concentrations remained similar to the original magmatic monazite. Chemical mapping of several elements (e.g. Y, Ca, Si, REE) in the grains before TIMS dating

would indicate whether all parts are chemically homogeneous or not, but such analyses were not made.

While these end-member interpretations imply that sample 00JN25.1 crystallized at either ~34 Ma, episodically from ~34 to ~41 Ma, or at ~41 Ma, intermediate interpretations are equally viable if a combination of inheritance, and protracted mineral growth played a role in the dispersion. Regardless, all possible interpretations of the present data indicate an important mid- to late Eocene to Oligocene magmatic and/or metamorphic event in the CSSZ which is younger than the proposed age of the India-Eurasia collision at ~45 Ma (Rowley 1996, 1998).

Fragments from single grains of sample 00JN25.1 also show a spread of dates, ranging from ~0.8 Ma for grain m2 to ~2.5 Ma for grain m3. BSE images of the monazite grains m1 and m2 show moderately strong oscillatory zoning that is typical of magmatic monazites, though the nature of the zoning geometry is very different. The oscillatory zones of m1 are narrower and more diffuse compared to the wider and more discrete zones of m2. The morphology of the grains is also different: m2 is larger and its crystal edges make an obtuse angle with each other, whereas m1 is smaller and has pointed edges with acute angles in between. The contrasting morphologies and the apparent lack of any core-rim zoning structures can be used to argue that these two grains crystallized during two different anatectic phases, at ~34 Ma and at ~37 Ma. However a detailed systematic study with more grains categorized based on BSE imaging and chemical composition of the various domains is clearly needed to test preliminary hypothesis regarding the significance of the dates from these two grains.

The spread of dates of the three fragments obtained from grain m3 is ~2.5 Ma, significantly more than the ~0.9 Ma spread observed in grains m1 and m2. A closer examination of the BSE image reveals that m3 has a core with a patch zoning, and a mantle with good oscillatory zoning.

Therefore, these monazites dates may represent a mixture of an older inherited core and a younger magmatic mantle.

Note that the constraint provided by the age of the foliated leucogranite sill does not address the timing of the initiation of strike-slip shearing, but rather the time during which strike-slip shearing was occurring, even though none of these sills are lineated. It is premature to say that because the deformed sills are older than the undeformed ones they date all the shearing within the CSSZ. Shearing may have been temporally and spatially partitioned across the width of this broad shear zone; some of the leucogranites might have escaped the deformation at the same time as others were being sheared. While this is an important issue to be addressed, our preliminary geochronological dataset is too limited to test all the possibilities.

$^{207}U/^{235}Pb$ data from the unfoliated leucogranite sill sample 98JL18.4 suggest that the strike-slip shearing ended before ~29 Ma, and perhaps as late as ~24 Ma if the lack of any deformation is interpreted to indicate that the intrusion post-dates the strike-slip shearing. While the spread of $^{207}U/^{235}Pb$ ages is less than that reported for sample 00JN25.1, these single grain analyses, which were obtained before the need for BSE imaging was recognized, should be interpreted with caution considering the possible internal complexity of these monazite grains.

The U-Pb data from sample 00JN21.4 from the leucogranite dike which cross-cuts mylonitic gneisses of the CSSZ indicates that the major fabric forming deformational episode in this part of the CSSZ ceased by ~17 Ma. Even though this particular sill has intruded QFB gneisses which contain macroscopic left-lateral shear sense criteria, it is not clear whether the U-Pb data constrain the termination of the hypothesized earlier left-lateral or subsequent right-lateral shearing. Nevertheless, this is our best temporal constraint on the termination of the strike-slip shearing along the CSSZ with present data .

$^{40}Ar/^{39}Ar$ geochronology: Sample description and results:

Orthogneisses (Sample 99M18.6 and 99JU4.2):

The two orthogneisses we sampled for $^{40}Ar/^{39}Ar$ dating were both sinistrally deformed and contain well-preserved micas (See Figure 5 for locations). Like most of the deformed rocks along the CSSZ, the samples contain a vertical foliation and a subhorizontal stretching lineation and sinistral shear criteria, such as shear bands with biotite and sigmoid feldspathic clasts with asymmetric tails. Recrystallized quartz, plagioclase, and micas form the foliation. None of the infrequent K-feldspar grains display plastic deformation features. Some feldspar grains, especially plagioclase, show brittle fractures. The contrast between quartz and feldspar deformation indicates temperatures were probably between 350° and ~500° C. Muscovite from 99JU4.2 yielded an age of ca. 23.0 Ma and biotite from sample 99M18.6 yielded an age of ca. 21.7 Ma.

While the $^{40}Ar/^{39}Ar$ ages on micas are interpreted as cooling ages, the ~ 22 Ma age from the greenschist facies orthogneiss sample (99M18.6) can also potentially be interpreted as the time of mica growth during the shearing, and thus date the shearing event.

DISCUSSION

Although sinistral strike-slip shear has been recognized in the structural development of the region (Wang and Burchfiel, 1997), the role and importance of dextral shearing, which is observed only in the CSSZ near the GSSZ contact zone, has not been extensively explored. According to our preferred explanation, left-lateral strike slip shearing, which decoupled the Baoshan tectonic element from Simao tectonic element, was active during the earlier stages of the

extrusion (Figure 21). This left-lateral motion along the CSSZ came to end, for an unknown reason before ~ 17 Ma. However, the motion along the GSSZ and ASSZ continued beyond at least 17 Ma, causing the now coupled Baoshan/Simao tectonic elements to continue to extrude to the south (Figure 21). This continued right-lateral motion along the GSSZ overprinted the earlier left-lateral structures of the CSSZ.

Unlike the GSSZ and ASSZ, the protolith of the CSSZ metamorphic rocks is not easy to characterize, as the rock types are not continuous throughout the extent of the shear zone. This, we believe, is due to the location of the CSSZ, which coincides with the Lancangjiang suture that juxtaposed the Qiangtang, Sibumasu and Indochina continental fragments during Mesozoic time (Figure 3). We propose that there are at least three different protoliths for the CSSZ metamorphic rocks. In the south, basement rocks of the Baoshan tectonic element and its lower Palaeozoic sedimentary cover rocks are the protoliths of the metasedimentary and metaigneous core of the CSSZ in the south. Further north, from Tuer to Lishinerhe, mylonitic and ultramylonitic rocks of the CSSZ are equivalent to the basement rocks of the Baoshan tectonic element, its lower Palaeozoic sedimentary cover, and Permo-Triassic granites likely from the Lingchang unit. The basement rocks of the Qiangtang block and its upper Palaeozoic sedimentary cover rocks (Carboniferous?) are the probable protoliths of the northern most section of the CSSZ.

Suture zones in Tibet and SE-Asia are reasonably well documented (Figure 22). Readers are referred to Metcalfe (1998) for the most recent, most detailed review of these suture zones. The three main suture zones in central and southern Tibet, namely the Indus-Zangbo, Bangong-Co and Jingshajiang sutures, along with a forth possible major suture zone, the Lancangjiang suture zone, trend more or less east-west, and the four in continental SE-Asia, namely the Indo-Burman, Nujiang, Changning-Raub (Changning – Menglian – Nan – Uttaradit – Bentong - Raub suture

zone) and Song Da – Anding sutures, trend roughly north-south (Figure 22). This change in trend is generally accepted to be due to the deformation around the eastern Himalayan syntaxis in order to accommodate the continuing indentation of India into Eurasia. There is no consensus, however, on how the four southern suture zones to the south connect with the three suture zones to the north. Our detailed field work along the GSSZ and the CSSZ and the intervening Baoshan tectonic element, as well as regional reconnaissance field work conducted along all accessible roads around the eastern Himalayan syntaxis, indicate that the sedimentary rocks of the Baoshan tectonic element pinch out just south of Bijiang, between the GSSZ and CSSZ and do not reappear to the north. Likewise, the region north and east of the GSSZ and Bangong-Nujiang suture zone and west of the Permo-Triassic granites and related volcanics which mark the western edge of the Indo-China continental fragment, considered to be the eastern Qiangtang continental fragment, also pinch out in between the GSSZ and the CSSZ, just south of Gongshan and do not crop out again to the south. The region west of the GSSZ, which is generally referred to as the Tengchong "block" is the southern continuation of the Lhasa continental fragment, and is bounded by the Sagaing fault to the west, and the GSSZ to the east and south. These observations, schematically shown in figures 22 and 23, provide an explanation to the suture zone problem encountered in the Three Rivers area of China.

Because the CSSZ is a reactivated suture zone, piercing points to determine the amount of strike-slip offset cannot be identified. However, geological relationships indicated at least 140 km displacement for the following reason. It is quite likely that the CSSZ and GSSZ were not active as strike-slip shear zones while they were juxtaposed but rather were separated by at least several tens of kilometers. Field observations in the northern part of the field area show that the Baoshan tectonic element does not continue to the north, but rather pinches out just south of Bijiang

(Figures 3, 5, 22 and 23). If the region between the CSSZ and the GSSZ is assumed to have extruded to the south, the space it created behind was closed as the two bounding shear zones "sutured" like a zipper (Figure 21). The juxtaposed section is about 140 km long, and therefore is a minimum estimate for the amount of displacement along the CSSZ.

The CSSZ can be followed for a very short distance (~ 50 km) north of the town of Gongshan, after which accessibility is extremely limited. Chinese geological maps (reference) at a 1:200,000 scale, however, indicate the rock assemblages of the CSSZ do not continue beyond this point. The southern most locality where CSSZ mylonitic rocks are observed is found near the major bend in the Lancang river. Here, intensely folded sedimentary rocks of possible Devonian age lie just south of the CSSZ. The contact between the CSSZ and the Devonian rocks is unfortunately obscured by heavy vegetation and was not observed by us in the field. We infer, however, that the mylonitic rocks plunge to the south below the Paleozoic rocks. Further south, the western part of the Linchang granite is associated with gneissic and mylonitic rocks, but because of limited exposure we are unable to make a direct correlation with the CSSZ.

A striking feature of the geology in this region is that all of the ductile shear zones composed of mylonitized mid-crustal rocks are structurally high relative to adjacent, low-grade to unmetamorphosed rocks which implies significant uplift of shear zone rocks (Figure 24). Our field observations indicate that the mid-crustal material along the CSSZ moved vertically by both thrusting and upward extrusion during transpressive shortening following India-Eurasia collision (Figure 25). The CSSZ is also bounded by the steeply west-dipping Chaojian normal fault to the west, and a subvertical to west-dipping thrust fault on the east. One of the four major rivers that drain the eastern Tibetan Plateau, the Lancang River, follows the eastern boundary fault and may have also contributed to more recent exhumation of the CSSZ (Figure 25). In an effort to establish

a basis to explore the cooling history of the CSSZ, we analyzed biotite and muscovite separated from two of the granitic intrusions (98JL18.4 and 00JN25.1), for which we have reported U-Pb ages in the previous section, and three other samples (99JU4.3, 99JU4.6, and 99JU18.4) of leucogranitic sills. We interpret these preliminary $^{40}Ar/^{39}Ar$ results as cooling ages.

Sample description and results

Foliated leucogranites:

The locations of the two selected samples from foliated leucogranite sills, sample 00JN25.1 and sample 99JU4.6 are shown in figure 5. The mineralogy and the texture of sample 99JU4.6 is similar to that of sample 00JN25.1, which was described in the U-Pb sample description and results section above, other than the presence of muscovite instead of biotite. We have analyzed two foliated leucogranite sills with the $^{40}Ar/^{39}Ar$ method. Biotite from sample 00JN25.1 and muscovite from sample 99JU4.6 yielded cooling ages ca. 19 Ma, and ca. 27 Ma, respectively.

Unfoliated leucogranites:

The locations of the two selected samples from unfoliated leucogranite sills, sample 99JU18.4 and sample 99JU4.3 are shown in figure 5. Both of these samples are from ~30 cm thick undeformed leucogranite sills which intruded the QFB gneisses of the CSSZ. We interpret the lack of foliations, lineations and boudins as an indication that this sill intruded the mylonitic QFB gneisses of the CSSZ either at a time when shearing had ceased or when strike-slip shearing was coming to an end. The mineralogy of this sill is dominated by quartz, plagioclase, garnet,

tourmaline, biotite and muscovite. Samples from the undeformed leucogranitic sills consistently yielded younger cooling ages: Biotite from sample 99JU18.4, muscovite from 99JU4.3 and biotite and muscovite from sample 98JL18.4 yielded ca. 23.4 Ma, 19.6, 13.6 and 14 Ma, respectively.

Interpretation of the $^{40}Ar/^{39}Ar$ data:

In general, the cooling ages of the unfoliated leucogranites are younger than the cooling ages of the foliated leucogranites, but sample 00JN25.1 is an exception. Even though the leucogranite crystallized at least at 34 Ma, it did not cool to ~350 C until after most of the unfoliated leucogranite samples had already cooled to the same temperature. This can be explained in a number of ways, but considering the length (> 250 km) and width (<10 km) of the CSSZ, our preferred interpretation is that the strike-slip shearing, as well as exhumation, was probably not uniform, and may have been partitioned into numerous zones across and along the shear zone. As a result, different generations of leucogranites probably experienced deformation at different times, regardless of the time of their initial intrusion and crystallization.

Cooling Rate Determination

If we assume that (1) the U/Pb monazite dates we have obtained reflect the final crystallization ages of the respective leucogranites, and (2) the $^{40}Ar/^{39}Ar$ dates from the same samples reflect cooling to the nominal closure temperatures of minerals that were dated (muscovite, ca. 400 °C and biotite , ca. 350 °C) then the foliated leucogranite sample 00JN25.1 cooled at a rate of ca. 23 to 17 °C/Myr during the time interval ~41 - ~19 Ma and the unfoliated leucogranite sample 98JL18.4 cooled at a rate of ca. 32 °C/Myr during the interval ~26 - ~13 Ma.

Our preliminary geochronological study is not adequate for an unequivocal interpretation regarding the cooling history of the CSSZ, as the effect of the bounding structures of the CSSZ is not known. Furthermore, exhumation of the CSSZ, as well as the strike-slip shearing along it, was likely temporally and spatially partitioned across the width of this broad shear zone. Some of the leucogranites might have escaped the deformation at the same time as others were being sheared. Likewise, different parts of the CSSZ were probably exhumed at different times and even perhaps at different rates. While these are all important issues to be addressed, our preliminary geochronological dataset is too limited to test all the possibilities, but should set an important basis for future geochronological studies carried along this structurally complicated strike-slip shear zone.

CONCLUSIONS AND IMPLICATIONS FOR ASIAN TECTONICS:

Our preliminary geochronological studies indicate that the CSSZ has been active since at least ~34 Ma, and perhaps as early as 41 Ma. Strike-slip shearing continued until at least until ~29 Ma, and perhaps as late as ~24 Ma, and terminated by ~17 Ma. These age constraints are comparable to the published ages for the ASSZ (Harrison et al., 1992; Leloup et al., 1993, 1995; Schärer et al., 1994, 1996; Harrison et al., 1996; Gilley et al., 2003) which show that left-lateral shearing along the ASSZ started at least 34 Ma and continued to at least until 17 Ma. This new data from the CSSZ along with the data from the GSSZ (chapters 2 and 3) indicate that while the region between the GSSZ and ASSZ extruded to the southeast, it did not extrude as a single rigid block (Tapponnier et al., 1982, 1986), but rather it was dismembered into at least two major fragments with different styles of internal deformation, the Sibumasu and the Indochina continental fragments.

Folds and thrust faults within the Simao tectonic element trend ~NW-SE, but have arcuate trends because of left-lateral shear along the CSSZ and the ASSZ, and clockwise rotation up to 90° throughout the Simao tectonic unit (e.g. Huang and Opdike, 1993; Funahara et al., 1992, 1993; Chen et al., 1995; Geissman 1999, 2001). The structures have a foreland-fold thrust belt style and are interpreted to be detached within the middle to upper crust (Wang and Burchfiel, 1997). The youngest units affected by this deformational event are Paleocene to Oligocene age (Wang and Burchfiel, 1997) and indicate that it was contemporaneous with motion along the ASSZ (e.g. Harrison et al., 1992; Leloup et al., 1993; Schärer et al., 1994; Leloup et al., 1995; Harrison et al., 1996; Gilley et al., 2003) and along the CSSZ as shown in this study.

The internal structure of the Baoshan tectonic element, bounded by the right-lateral GSSZ and the left-lateral CSSZ, is complex and the ages of the major folds and thrusts are poorly determined, but are bracketed between middle Jurassic and early Eocene time. The vergence of the folds and thrust faults both to the east and west, are truncated by the CSSZ and by NE-trending strike-slip faults to the north (Chapter 2). We follow the suggestion of Wang and Burchfiel (1997) and consider this fold and thrust belt structure to have formed in at least two events, one following deposition of middle Jurassic rocks but before deposition of Upper Eocene strata, and a second, less intense folding following deposition of the Upper Eocene and Oligocene strata in the central and southeastern part of the Baoshan tectonic element. Folding was followed by strike-slip faulting of early and late Cenozoic age and many of the faults are presently active.

Appendix A: The U-Pb Analytical Procedures

Separates of monazite [(Ce, La, Y, Th) PO_4] were obtained from four samples using standard magnetic and gravimetric separation techniques and hand picking under a binocular

microscope. Monazites grains from samples 00JN25.1 and 00JN21.4 were mounted in epoxy and polished until the central parts of the grains were exposed. Backscattered electron (BSE) images of the polished grains were obtained using the JEOL 733 electron microprobe at the Massachusetts Institute of Technology operating at an accelerating voltage of 15 to 20 kV and a beam current of 10 to 30 nA. Brightness in the BSE images is related to average atomic mass; monazite with higher average atomic mass is brighter than that with lower average atomic mass. Therefore, BSE brightness in monazite is controlled mostly by Ce concentration, with La, Th, and Nd concentrations also being important. BSE images were made in order to characterize the internal structures of the crystals and to avoid grains with possibly inherited cores. After electron microprobe study, selected grains from samples 00JN25.1 and 00JN21.4 were removed from their mounts and broken into a number of fragments with a fine tipped tool. Some of the fragments were gently abraided (Krogh, 1982) in order to remove the anomalous rims apparent in the BSE images. Grains and fragments were then measured using a binocular microscope with calibrated reticule and video display in order to estimate their weights. Experience in our facility suggests that the estimated values have a nominal error of roughly 20%. Grains and fragments were cleaned by sonication in warm H_2O, brief immersion in warm dilute HNO_3, and rinsing in acetone and H_2O. The grains and fragments were dissolved in Teflon capsules and spiked with a mixed ^{205}Pb-^{233}U-^{235}U tracer solution. U and Pb were isolated and extracted from the samples by anion exchange chromatography. U and Pb were then loaded on Re filaments and measured by isotope-dilution, thermal ionization mass spectrometry (ID-TIMS) on a VG sector 54 mass spectrometer at the Massachusetts Institute of Technology. Details regarding dissolution, chromatography, spectrometry, and other analytical procedures can be found in Schmitz and

Bowring (2003). See Table xx for further details, including total procedural blanks, and complete isotopic data for each grain and fragment analyzed.

Appendix B: The $^{40}Ar/^{39}Ar$ Analytical Procedures

Analytical work was performed at the Massachusetts Institute of Technology CLAIR (Cambridge Laboratory for Argon Isotopic Research) facility (Hodges, et al., 1994). Samples were crushed and sieved to 500 μm, defiled to remove metal residue from the crushing procedures, and washed in distilled water to remove the finest silt and dust fractions.

Minerals were hand-picked to increase purity of the separates and to ensure sample homogeneity. Final mineral separates varied in grain size from ca. 100 μm to several millimeters in diameter. Prior to packaging for irradiation, all mineral separates were cleaned in an ultrasonic bath with acetone, distilled water, and ethanol. 50 to 100 mg of material were sealed in ca. 1 cm^2 Al foil envelopes for irradiation. Two to four individual sample packets were placed in Al disks, and up to nine disks were stacked for irradiation. The Al disks were then shielded with Cd foil, and sent to the research nuclear reactor at McMaster University, Ontario, Canada.

K, Ca, and Cl production factors during irradiation were determined by including packets of synthetic, reagent grade K_2SO_4, CaF_2, and KCl salts with the samples. Taylor Creek Rhyolite sanidine (TCR-2; 27.87 Ma, Duffield & Dalrymple, 1990) for package clair-131 and Fish Canyon sanidine (28.02 Ma, Renne et al., 1998) for package clair-104 were used for the calculation of the fast neutron flux and the irradiation parameter, J, (e.g. McDougall and Harrison, 1999). The mean J calculated for a disk was assigned to all samples in that disk. A conservative 2% uncertainty in J (at 2σ) was assumed for all samples in order to account for potential heterogeneities in the monitor materials and neutron flux.

Gas extraction was accomplished by incremental heating in a double-vacuum resistance furnace. Additional details of the extraction line and gas purification are given by Hodges et al. (1994). The furnace contributes the dominant component of the operational blank which is therefore strongly temperature dependent. Furnace system blanks were measured as a function of temperature prior to each sample analysis.

$^{40}Ar/^{39}Ar$ model ages for each gas extraction step were calculated assuming an initial $^{40}Ar/^{39}Ar$ value of 295.5 and are assigned a 2σ uncertainty that reflects propagated errors in all correction factors and J. Release spectra illustrate model ages for incremental heating analyses as a function of the amount of $^{39}Ar_K$ in each step. Plateau ages determined from the release spectra are defined as the error-weighted mean age of at least three consequent increments that define 50% or more of the total ^{39}Ar released and have model ages that overlap the 2σ confidence level when the error in J is ignored. Age estimates also were derived from linear fits of the data on $^{36}Ar/^{40}Ar$ versus $^{39}Ar/^{40}Ar$ isotope correlation diagrams. For all samples, the two methods of data analysis yield dates that are indistinguishable at the 2σ confidence level. We have, therefore, chosen to use the plateau ages as the best estimate of the closure age of the sample since the errors associated with the plateau age are slightly smaller.

Figure Captions

Figure 1. Schematic map of Cenozoic extrusion tectonics and large faults in Eastern Asia (modified after Tapponnier et al., 1986). Heavy lines indicate major faults or plate boundaries. Small arrows show senses of finite motion on strike-slip faults. Open arrows represent the sense of motion from Eocene until mid-Miocene. Shaded areas represent the regions affected by the different extrusion phases. Large open arrows represent the major block motions with respect to Siberia since the Eocene. Boxed area refers to Figure 3.

Figure 2. A schematic diagram which demonstrates two possible extrusion styles. (a) Undeformed Eurasia continent prior to the collision of India. (b) Extrusion of a single rigid block, with minor clockwise rotation. (c) Extrusion of dismembered crustal blocks which also rotate clockwise.

Figure 3. Location of the four major tectonic elements within the Three Rivers area and the three ductile strike-slip shear zones: T = Tengchong (Lhasa); Q = Qiangtang; LS = Lanping/Simao; B = Baoshan (Sibumasu) Dashed line within the Baoshan element is the Late Palaeozoic Changling-Mengliang suture. Strike-slip shear zones are shown in black with white stripes. The stripes orientation does not refer to the orientation of the fabrics observed within all three of these shear zones. Abbreviations: ASSZ = Ailao Shan Shear Zone; CSSZ = Chong Shan Shear Zone; DSSZ = Dianchang Shan Shear Zone; GSSZ = Gaoligong Shan Shear Zone; XS = Xuelong Shan; M = Mangkang; S = Simao. Inset map shows location of Figure 2, in relation to the India/Eurasia collision zone and the major tectonic blocks that form Eurasia. Abbreviations: SG = Songpan – Garze flysch belt, BNS = Bangong-Nujiang suture zone, LS = Lanchangjiang suture zone, SAS = Song Da – Anning suture zone; Y = Yidun volcanic arc; GL = Garze-Litang suture zone.

Figure 4. Generalized geological map of the GSSZ and the CSSZ and the tectonic elements they separate and the geological cross-sections. Cross section location and sample locations are also shown. Geochronological results which are grouped inside a box, refer to dates obtained from the same sample. Block diagrams schematically represent the samples that were dated. (a) a cross-cutting dike, (b) unfoliated, foliation parallel sill, (c) foliated, foliation parallel sill, and (d) well-foliated, sub-vertically stretched host-rock.

Figure 5. Geologic cross sections. No vertical exaggeration. Location of section lines indicated on map in Figure 4.

Figure 6. Deformation along the Chong Shan shear zone. Nearly vertical foliations striking roughly N-S are particularly well observed along the (a) Wayao, (b) Chaojian and (c) LiShiNerHe sections (See Figure 4 for locations of these sections). (d) subhorizontal stretching lineation is also commonly observed.

Figure 7. Field pictures from the Wayao section. (a) QFB gneiss section of the CSSZ strike NNW-SSE, and dip to the W. (b) A horizontally stretched leucogranite sill within the QFB gneiss section of the CSSZ.

Figure 8. (a) Landsat 7 image of the GSSZ and the CSSZ, and the Salween river flowing in between the two. Labels correspond to the field pictures of the sharp lineament that bounds the CSSZ to the east. Arrows point to the viewing direction. (b) Wayao section boundary. (c) Northern Chaojian section boundary. (d) Southern Chaojian section boundary

Figure 9. Photomicrograph of two gneiss samples from the Chaojian section. (a) garnet in a groundmass of very fine grained quartz and feldspar. Thin seams of muscovite and biotite define the foliation. (b) a weakly foliated section of an otherwise well-foliated gneiss sample with biotite, quartz, plagioclase and trace amounts of muscovite. A remnant of a sturolite crystal is also seen. Quartz and plagioclase have mostly recrystallized, but relict large grains can still be picked.

Figure 10. Left-lateral C-S mylonitic fabrics in the Chaojian section of the CSSZ.

Figure 11. Thin sections of the dominant rock types observed along the Tuer section: (a) biotite-chlorite schist, (b) actinolite schist, (c) and (d) ultramylonites.

Figure 12. Asymmetric deformation of feldspar porphyroclasts observed in samples collected along the Bijiang section imply left-lateral shearing. Near the GSSZ contact, however, right-lateral shear sense indicators, including S-C fabrics are just abundant.

Figure 13. (a) Undeformed Fugong granite of Permo-Triassic? age. (b) The same granite gets progressively more mylonitic to the west.

Figure 14. (a) Microfish and (b) asymmetric folding along the Lishinerhe section indicate left-lateral shearing.

Figure 15. Outcrop pictures of the complicated migmatitic sections of the CSSZ observed along the Lishinerhe section.

Figure 16. Outcrop pictures of both horizontally and vertically stretched leucogranite sills.

Figure 17 (a) BSE images of the monazite grains from sample 00JN25.1 that were dated. (b)U-Pb Concordia diagram for the same sample.

Figure 18 U-Pb Concordia diagrams for samples (a) 98JL18.4 and (b) 98JU27.1

Figure 19 (a) BSE images of the monazite grains from sample 00JN21.4 that were dated. (b)U-Pb Concordia diagram for the same sample.

Figure 20. A summary of all of the U-Pb and $^{40}Ar/^{39}Ar$ age results, sample numbers and rocks types presented in a chart form.

Figure 21. A schematic diagram that shows the possible two stage evolution of the region between the ASSZ and the GSSZ. (a)Sibumasu and Indochina tectonic elements extrude to the south east as independent tectonic elements, split by the CSSZ. The dominant left-lateral shear sense indicators along the CSSZ indicate that the differential motion between the Sibumasu and the Indochina tectonic elements was left-lateral. (2) During the second stage, the Sibumasu and the Indochina tectonic elements are coupled, and they extrude to the southeast together. As the Sibumasu tectonic element extrudes, the structures that bound it, the GSSZ and the CSSZ progressively sutures. The section of the GSSZ the CSSZ that is sutured is ~140 km, and this is the minimum amount of displacement along both of these shear zones. (c) A cartoon drawing of a zipper depicts our conceptual idea of the "zipper effect".

Figure 22. (a) Traces of the major sutures in Tibet and western Yunnan (modified after Jin, 1994). 1- Indus-Tsangbo, (2) Bangong, (3) Lancangjiang, (4) Jinshajiang, (5) Indo-Burma, (6) Nujiang, (7) Changning-Menglian, 8) Song Da – Anding..(b) Our favored interpretation of these suture zones should be connected. Note the pinching-out nature of almost all of the tectonic elements, especially the Sibumasu, Qiangtang, Lhasa and Indochina.

Figure 23 (a) A schematic map view diagram that shows the locations of the various tectonic elements that formed southeastern Eurasia prior to intense Cenozoic deformations. The segment of the main Paleo-Tethys ocean from Changning to Raub is the name of the ocean that separated Sibumasu from Indochina. Jinshajiang and Lancangjiang oceans likely refer to the same, westernmost part of the same ocean separating mainland Eurasia from the Qiangtang block. Island arcs (e.g. the Yidun arc) and small continental fragments existed between the two. Nujiang suture is the suture between the Sibumasu and the Qiangtang blocks, and not a direct continuation of the Bangong suture. (b) Traces of the major sutures in Tibet and western Yunnan (modified after Jin,

1994). 1- Indus-Tsangbo, (2) Bangong, (3) Lancangjiang, (4) Jinshajiang, (5) Indo-Burma, (6) Nujiang, (7) Changning-Menglian, 8) Song Da - Anding.

Figure 24. Maximum elevations from a 20-km wide SWATH profile based on GTOPO30 data. Major rivers and tectonic features are also labled. Nset shows the location of the profile.

Figure 25. Schematic structural interpretation of relations between the GSSZ, Sibumasu, CSSZ and the Lanping-Simao structural units, also shows the structures and the morphological features that bound the CSSZ and have played an important role in its exhumational history. As this diagram shows, the CSSZ is bounded to the west by a normal fault, and to the east, by a thrust fault and a major river, the Lancangjiang, that follow this boundary very closely. Contractional structures observed on either side of the shear zone indicate that pure shear and simple shear likely have effected the CSSZ rocks at the same time. Thus vertical stretching was also one of the agents that contributed to the exhumation of the CSSZ.

REFERENCES:

Bureau of Geology and Mineral Resources of Yunnan Province, 1990, Regional Geology of Yunnan Province: Beijing, Geological Publishing House, 728 p.

Chen Bingwei and Xie Guanglian, 1994, Evolution of the Tethys in Yunnan and Tibet: Journal of Southeast Asian Earth sciences, v. 9, p. 349-354.

Chen, H., Dobson, J., Heller, F., Jie Hao, 1995, Paleomagnetic evidence for clockwise rotation of the Simao region since the Cretaceous: A consequence of India-Asia collision: Earth and Planetary Science Letters, v. 134, p. 203-217.

Curray, J.R., Moore, D.G., Lawver, L.A., Emmel, F.J., Raitt, R.W., Henry, M., Kieckhefer, R., 1979, Tectonics of the Andaman sea and Burma, *in* Watkins, T.S. et al., eds., Geological and geophysical investigations of continental margins: AAPG Memoir no. 29, p.189-198.

Duffield, W.A., Dalrymple, G.B., 1990, The Taylor Creek Rhyolite of New Mexico: a rapidly emplaced field of lava domes and flows: Bulletin of Volcanology, v. 52, p. 475-487.

Funahara, S., Nishiwaki, N., Miki, M., Murata, F., Yo-ichiro Otofuji, Yi Zhao Wang, 1992, Paleomagnetic study of Cretaceous rocks from the Yangtze block, central Yunnan, China: implications for the India-Asia collision: Earth and Planetary Science Letters, v. 113, p. 77-91.

Funahara, S., Nishiwaki, N., Murata, F., Yo-ichiro Otofuji, Yi Zhao Wang, 1993, Clockwise rotation of the Red River fault inferred from paleomagnetic study of Cretaceous rocks in the Shan-Thai-Malay block of Western Yunnan, China: Earth and Planetary Science Letters, v. 117, p. 29-42.

Gapais, D., 1989, Shear structures within deformed granites; mechanical and thermal indicators: Geology, v. 17, p. 1,144-1,147.

Geissman, J.W., Burchfiel, B. C., Lianzhong, C., Harlan, S. S., Wawrzyniec, T. F., 1999, Paleomagnetic data from Upper Jurassic to lower Tertiary redbeds, western Yunnan, PRC; testing spatial variability in large-magnitude intracontinental deformation: Geological Society of America Abstracts with Programs, v. 7, p. 371.

Geissman, J.W., Burchfiel, B.C., Wang, E., Chen, L., Yin, J., 2001, Paleomagnetic data and Cenozoic tectonic rotations in northern Indochina, with implications for middle Cenozoic extrusion of crust south of the Ailao Shan shear zone: Geological Society of America Abstracts with Programs, Cordilleran Section, 97th annual meeting, v. 33, no. 3, p. 43.

Gilley, L.D., Harrison, T.M., Leloup, P. H., Ryerson, F. J., Lovera, O. M., Wang, J.-H., 2003, Direct dating of left-lateral deformation along the Red River shear zone, China and Vietnam: Journal of Geophysical Research, v. 108, no. B2, p ECV 14-1 to 14-21.

Girardeau, J., Marcoux, J., Allegre, C. J., Bassoullet, J. P., Tang Youking, Xiao Xuchang, Zao Yougong, Wang Xibin, 1984, Tectonic environment and geodynamic significance of the Neo-Cimmerian Donqiao Ophiolite, Bangong-Nujiang suture zone, Tibet: Nature (London), v. 307 , p. 27-31.

Harrison, T. M., Chen Wenji, Leloup, P.H., Ryerson, F.J., Tapponnier, P., 1992, An early Miocene transition in deformation regime within the Red River fault zone, Yunnan, and its significance for Indo-Asian tectonics: Journal of Geophysical Research, v. 97, p. 7,159-7,182.

Harrison T.M., Leloup, P.H., Ryerson, F.J., Tapponnier, P., Lacassin, R., Chen Wenji, 1996, Diachronous initiation of Transtension along the Ailao Shan-Red River Shear zone, Yunnan and Vietnam, in Yin, A. and Harrison, T.M., eds., The Tectonics of Asia: New York, Cambridge University Press, p. 208-226.

Hodges, K.V., Hames, W.E., Olszewski, W.J., Burchfiel, B.C., Royden L.H., Chen, Z., 1994, Thermobarometric and $^{40}Ar/^{39}Ar$ geochronologic constraints on Eohimalayan metamorphism in the Dinggye area, southern Tibet:: Contributions to Mineralogy and Petrography, v. 117, p. 151-163.

Houseman, G., and England, P., 1993, Crustal thickening versus lateral expulsion in the Indian-Asian continental collision: JGR, v. 98, p. 12,233-12,249.

Huang, K., Opdike, N., 1993, Paleomagnetic results from Cretaceous and Jurassic rocks of South and Southwest Yunnan: evidence for large clockwise rotation in the Indochina and Shan-Tai-Malay terranes: Earth and Planetary Science Letters, v. 117, p. 507-524.

Jin Xiaochi, 1994, Sedimentary and paleogeographic significance of Permo-Carboniferous sequences in western Yunnan, China. Geologisches Institut der Universitat zu Koln, Sonderveroefentlichungen, 136 p.

Kapp, P., Yin, A., Manning, C.E., Murphy, M., Harrison, T. M., Spurlin, M., Ding Lin, Deng Xi-Guang, Wu Cun-Ming, 2000. Blueschist-bearing metamorphic core complexes in the Qiangtang Block reveal deep crustal structure of northern Tibet: Geology, v. 28, p. 19-22.

Krogh, T.E., 1982, Improved accuracy of U-Pb ages by the creation of more concordant systems using an air abrasion technique: Geochim Cosmoshim Acta, v. 46, p. 831-834.

Lawver, L.A., Curray J.R., Moore, D.G., 1976, Tectonic evolution of the Andaman Sea: EOS, v. 57, p. 333-334.

Le Goff, E., Ballevre, M., 1990. Geothermobarometry in albite-garnet orthogneiss; a case study from the Gran Paradiso Nappe (Western Alps): Lithos, v. 25, p. 261-280.

Leloup, P. H., Kienast, J.R., 1993, High-temperature metamorphism in a major strike-slip shear zone: the Ailao Shan-Red River, People's Republic of China: Earth and Planetary Science Letters, v. 118, p. 213-234.

Leloup, P. H., Lacassin, R., Tapponnier, P., Zhong Dalai, Liu Xiaohan, Zhang Lianshang, Ji Shaocheng, Phan Trong Trinh, 1995, The Ailao Shan-Red River shear zone (Yunnan, China), Tertiary transform boundary of Indochina: Tectonophysics, v. 251, p. 3-84.

Leloup P.H., Arnaud N., Lacassin R., Kienast J.R., Harrison T.M., Phan Trong Trinh, Replumaz A., Tapponnier P, 2001, New constraints on the structure, thermochronology and timing of the Ailao Shan - Red River shear zone, SE Asia: Journal of Geophysical Research, v. 106, p. 6,657-6,671.

McDougall, I., Harrison, T.M., 1999, Geochronology and Thermochronology by the $^{40}Ar/^{39}Ar$ Method (2^{nd} Ed.): New York, Oxford University Press, 269 p.

Molnar, P., Tapponnier, P., 1975, Cenozoic tectonics of Asia; effects of a continental collision: Science, v. 189, p. 419-426.

Parrish, P.P., 1990, U-Pb dating of monazite and its application to geological problems. Canadian Journal of Earth Sciences, v. 27, p. 1,431-1,450.

Pearce, J.A., Mei, H., 1988, Volcanic rocks of the 1985 Tibet Geotraverse; Lhasa to Golmud. In: The geological evolution of Tibet; report of the 1985 Royal Society - Academia Sinica geotraverse of the Qinghai-Xizang Plateau: Philosophical Transactions of the Royal Society of London, Series A: Mathematical and Physical Sciences, v. 327, p. 169-201.

Royden, L.H., Burchfiel, B. C., King, R. W., Wang, E., Chen Zhiliang, Shen Feng, Liu Yuping, 1997, Surface deformation and lower crustal flow in eastern Tibet: Science, v. 276, p. 788-790.

Schärer, U., 1984, The effect of initial 230 Th disequilibrium on young U-Pb ages: the Makalu case, Himalaya. Contributions to Mineralogy and Petrology, v. 67, p. 191-204.

Schärer, U., Tapponnier, P., Lacassin, R., Leloup, P.H., Zhong Dalai, Ji Shaocheng, 1990, Intraplate tectonics in Asia: a precise age for large-scale Miocene movement along the Ailao Shan-Red River shear zone, China: Earth and Planetary Science Letters, v. *97*, p. 65-77.

Schärer, U., Zhang Lian-Sheng, Tapponnier, P., 1994, Duration of strike-slip movements in large shear zones: The Red River belt, China : Earth and Planetary Science Letters, v. 126, p. 379-397.

Schmitz, M.D., Bowring, Samuel A., 2003, Constraints on the thermal evolution of continental lithosphere from U-Pb accessory mineral thermochronometry of lower crustal xenoliths, Southern Africa: Contributions to Mineralogy and Petrology, v. 144, p. 592-618.

Şengör, A.M.C., Altiner, D., Cin, A., Ustaomer, T., and Hsu, K.J., 1988, Origin and assembly of the Tethyside orogenic collage at the expense of Gondwanaland, in Audley-Charles, M.G., and Hallam, A., eds, Gondwana and Tethys: Geological Society Special Publications, no. 37, p. 119-181.

Tapponnier, P., Peltzer, G., Le Dain, A.Y., Armijo, R., Cobbold, P., 1982, Propagating extrusion tectonics in Asia: new insights from simple experiments with plasticine: Geology, v. 10, p. 611-616.

Tapponnier, P., Peltzer, G., Armijo, R., 1986, On the mechanics of the collision between India and Asia: Coward, M.P., and Ries, A.C., eds., Collision Tectonics: London, Geological Society, Geological Society Special Publication, no. 19, p. 115-157.

Wang, E., Burchfiel, B.C., 1997, Interpretation of Cenozoic tectonics in the right-lateral accommodation zone between the Ailao Shan shear zone and the Eastern Himalayan Syntaxis: International Geology Review, v. 39, p. 191-219.

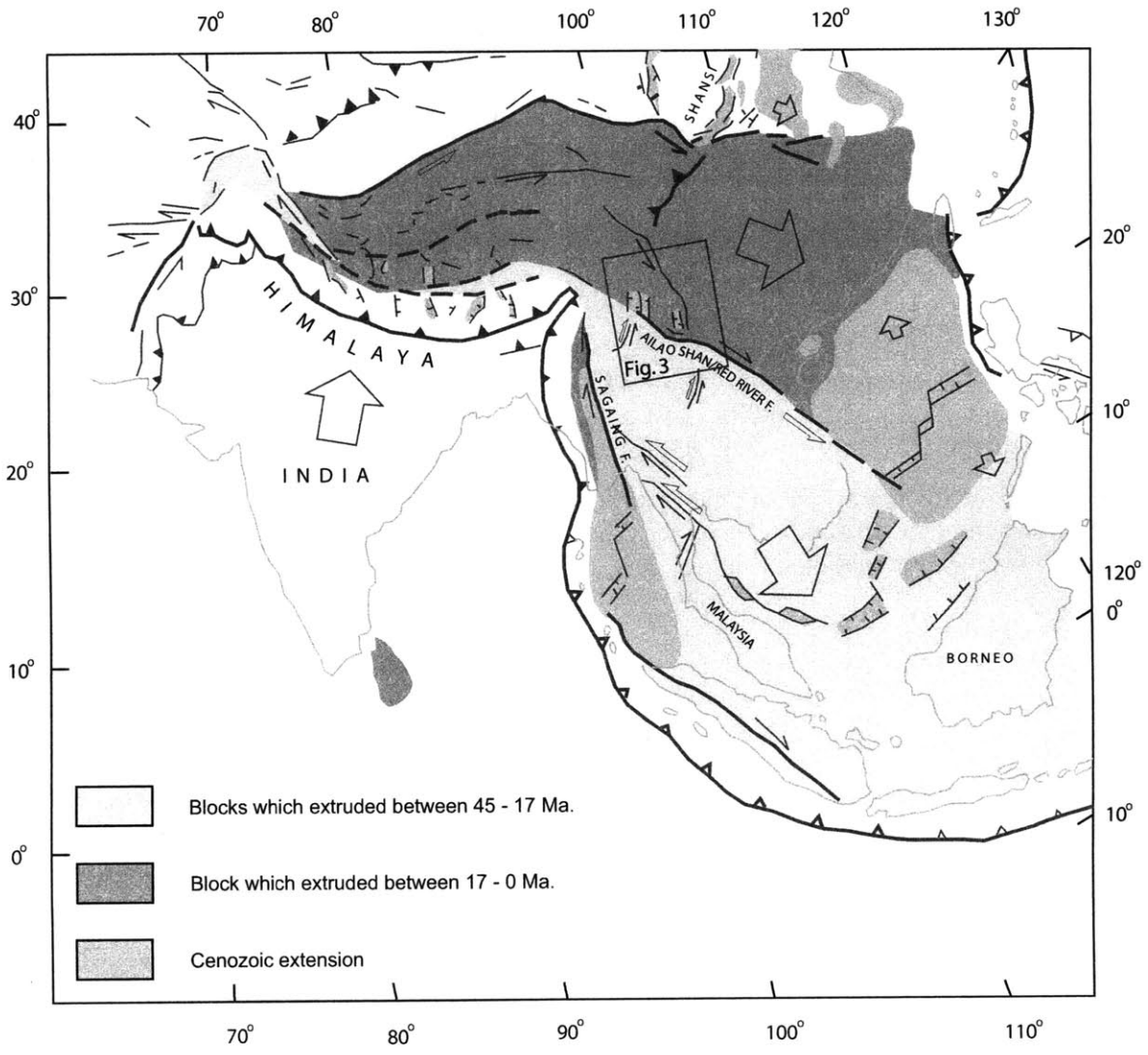
70°
80°
100°
110°
120°
130°
40°
30°
20°
10°
0°
HIMALAYA
INDIA
SHANSH
AILAO SHAN
RED RIVER F.
Fig.3
SAGAING F.
MALAYSIA
BORNEO
Blocks which extruded between 45 - 17 Ma.
Block which extruded between 17 - 0 Ma.
Cenozoic extension
70°
80°
90°
100°
110°
20°
10°
120°
0°
10°

FIGURE 1

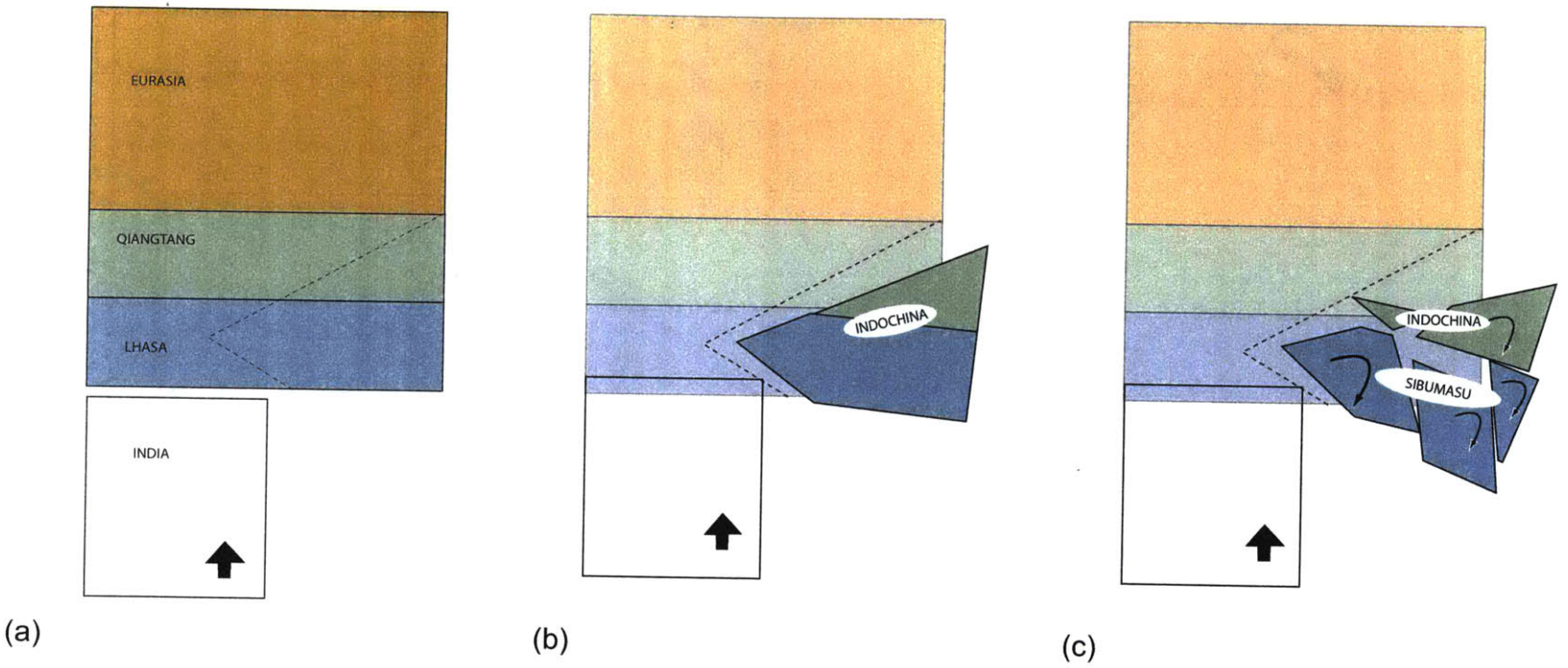
EURASIA
QIANGTANG
LHASA
INDIA
INDOCHINA
INDOCHINA
SIBUMASU
(a)
(b)
(c)

FIGURE 2

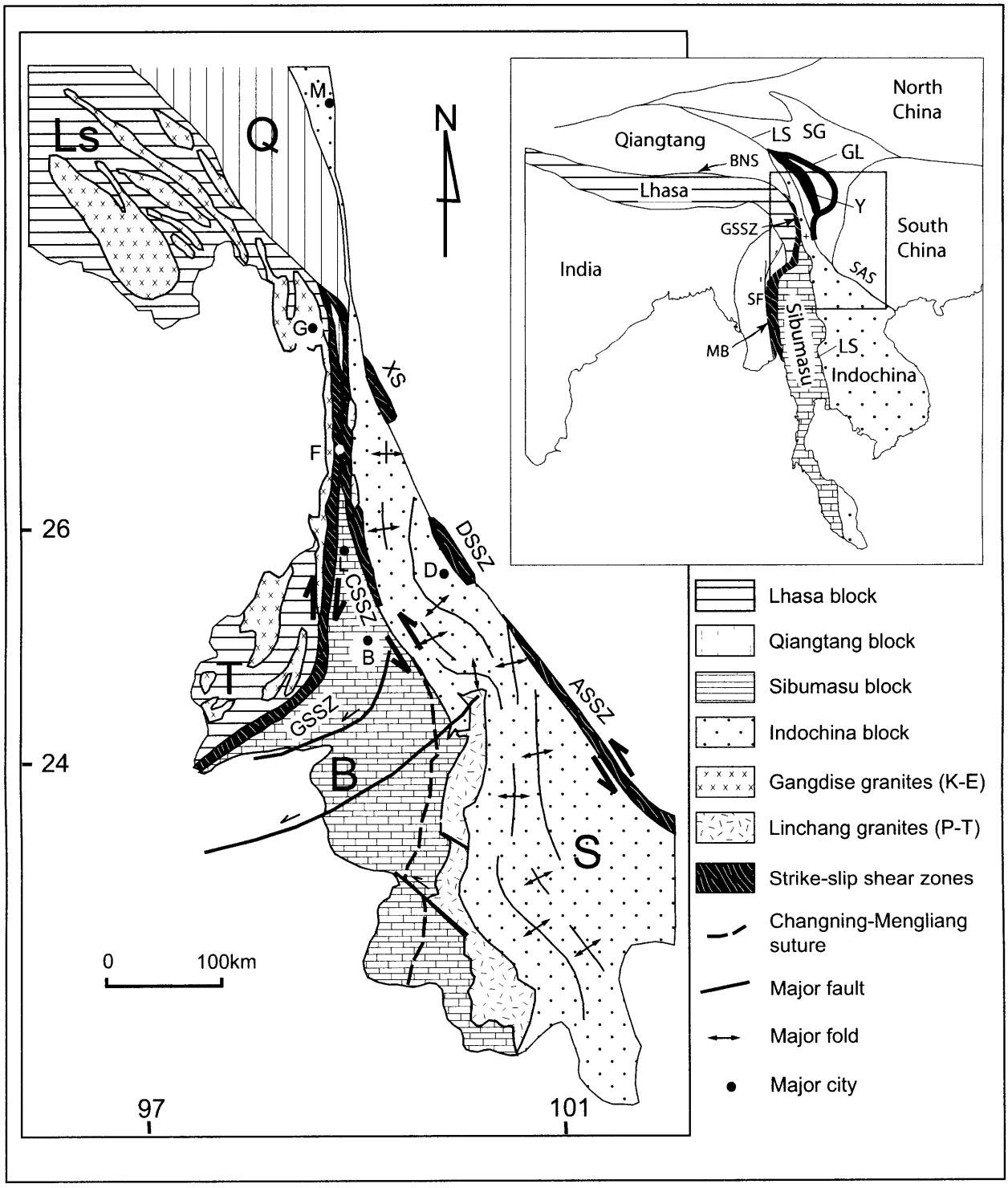
Ls
Q
M
N
G
XS
F
DSSZ
D
CSSZ
B
GSSZ
ASSZ
T
B
S
26
24
0
100km
97
101
North China
Qiangtang
LS SG
GL
BNS
Lhasa
Y
GSSZ
South China
India
SAS
SF
Sibumasu
MB
LS
Indochina
Lhasa block
Qiangtang block
Sibumasu block
Indochina block
Gangdise granites (K-E)
Linchang granites (P-T)
Strike-slip shear zones
Changning-Mengliang suture
Major fault
Major fold
Major city

FIGURE 3

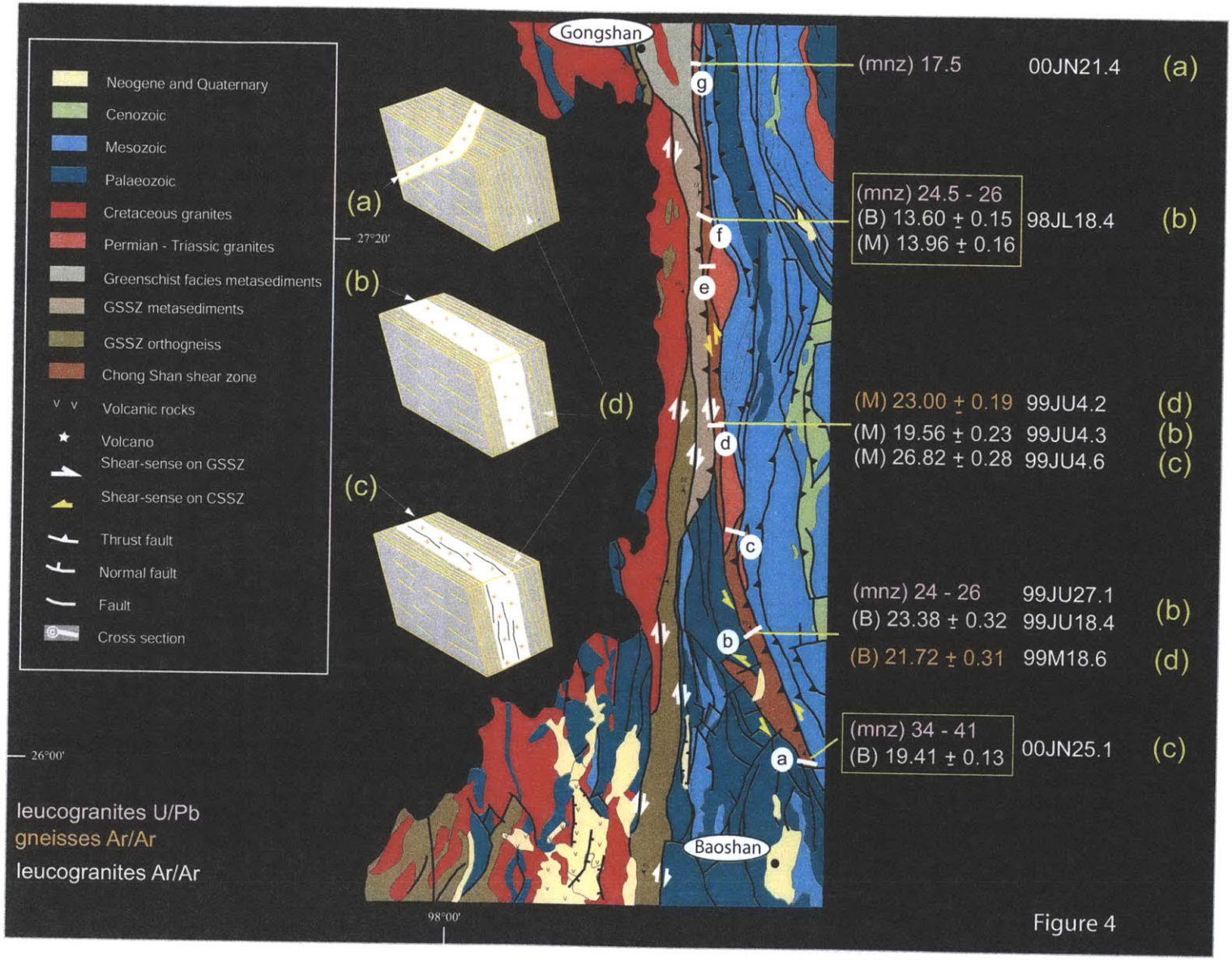
Neogene and Quaternary
Cenozoic
Mesozoic
Palaeozoic
Cretaceous granites
Permian - Triassic granites
Greenschist facies metasediments
GSSZ metasediments
GSSZ orthogneiss
Chong Shan shear zone
Volcanic rocks
Volcano
Shear-sense on GSSZ
Shear-sense on CSSZ
Thrust fault
Normal fault
Fault
Cross section
(a)
(b)
(c)
(d)
27°20'
26°00'
98°00'
Gongshan
Baoshan
(mnz) 17.5 00JN21.4 (a)
(mnz) 24.5 - 26
(B) 13.60 ± 0.15 98JL18.4 (b)
(M) 13.96 ± 0.16
(M) 23.00 ± 0.19 99JU4.2 (d)
(M) 19.56 ± 0.23 99JU4.3 (b)
(M) 26.82 ± 0.28 99JU4.6 (c)
(mnz) 24 - 26 99JU27.1
(B) 23.38 ± 0.32 99JU18.4 (b)
(B) 21.72 ± 0.31 99M18.6 (d)
(mnz) 34 - 41
(B) 19.41 ± 0.13 00JN25.1 (c)
leucogranites U/Pb
gneisses Ar/Ar
leucogranites Ar/Ar

Figure 4

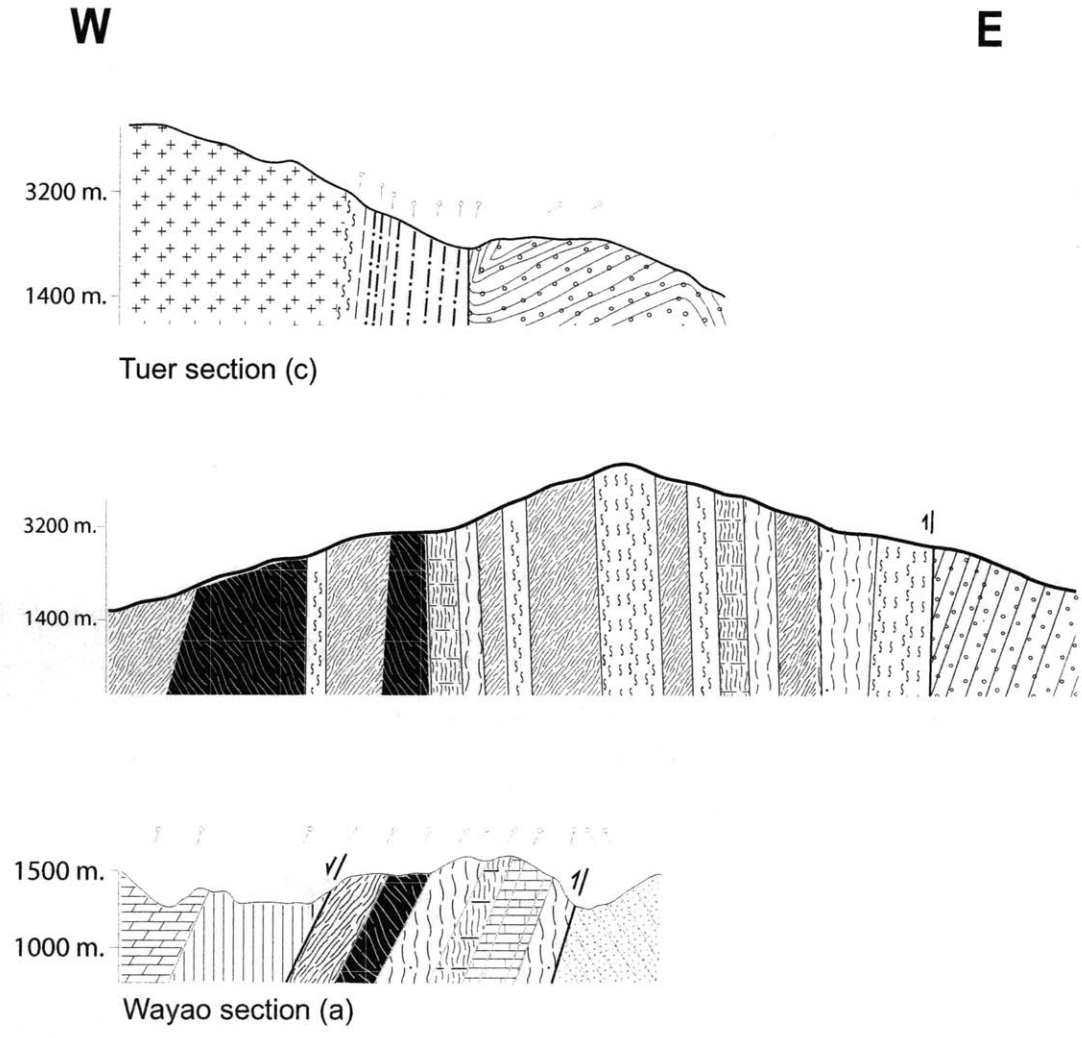
W
E
3200 m.
1400 m.
Tuer section (c)
3200 m.
1400 m.
1500 m.
1000 m.
Wayao section (a)
granite
mylonitic granite
orthogneiss
QFB-gneiss
ultramylonite
calc-silicate
marble
slate
limestone
Lanping-Simao redbeds
albite schist
impure quartzite
mica schist

FIGURE 5

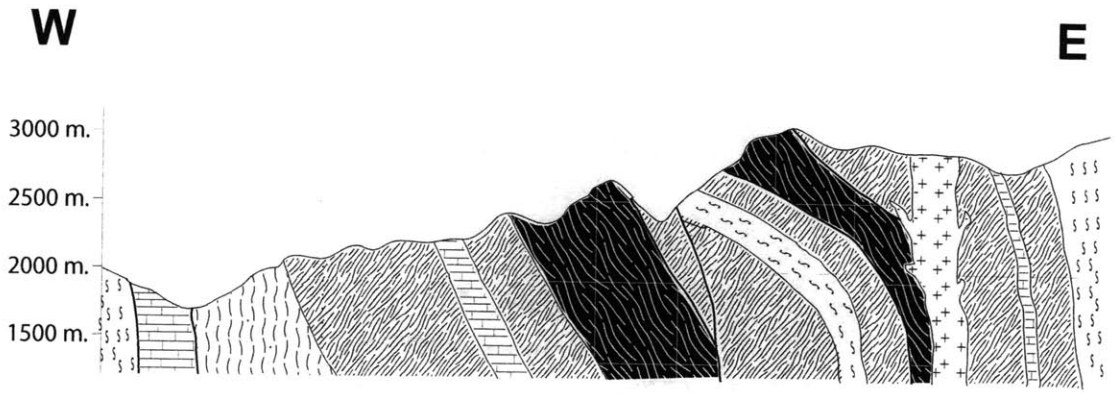

Shidu section (g)

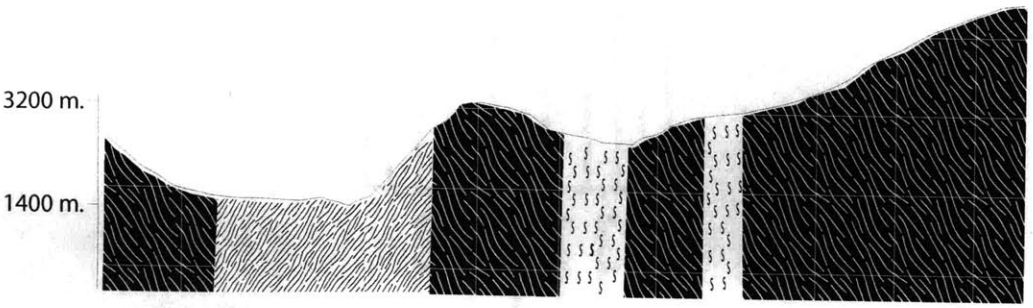

Lishinerhe section (f)

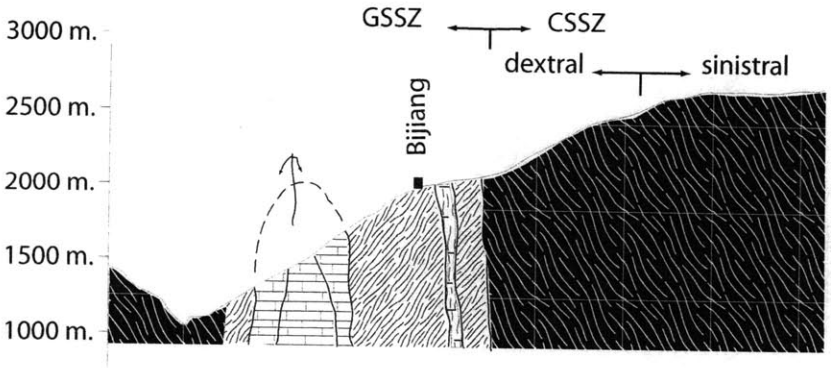

Bijiang section (d)

FIGURE 5 continued

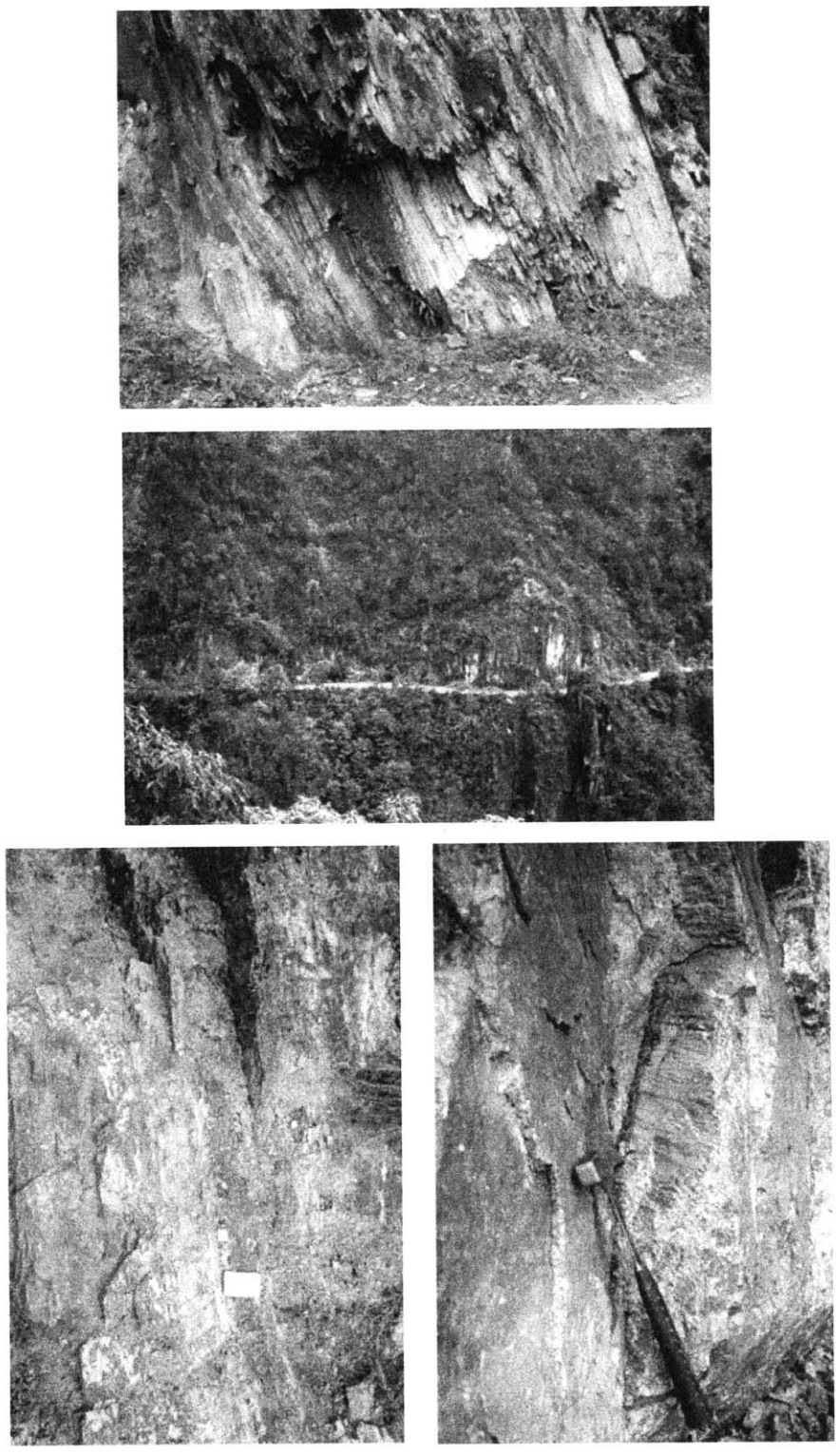

FIGURE 6

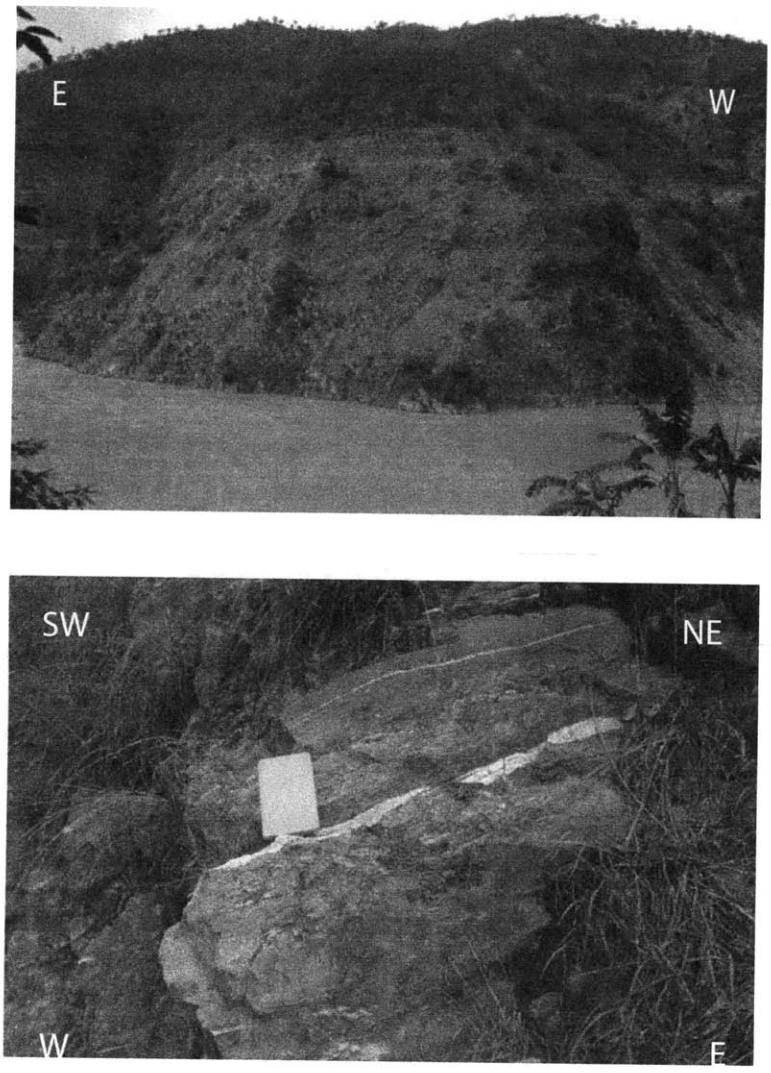

FIGURE 7

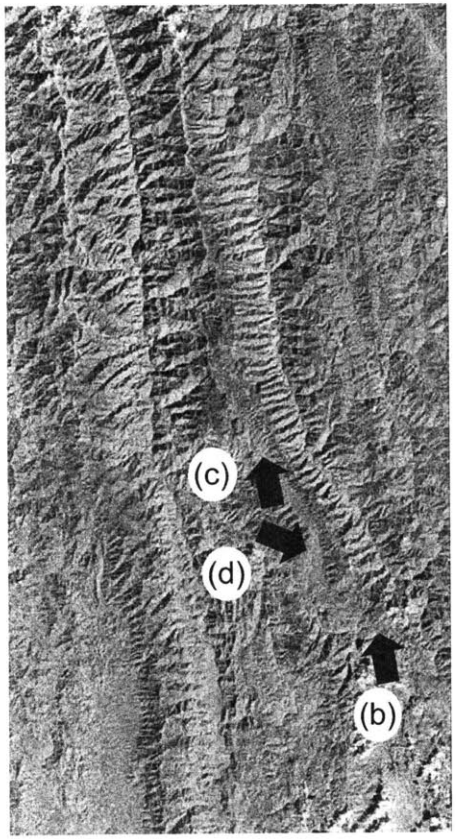

(a)

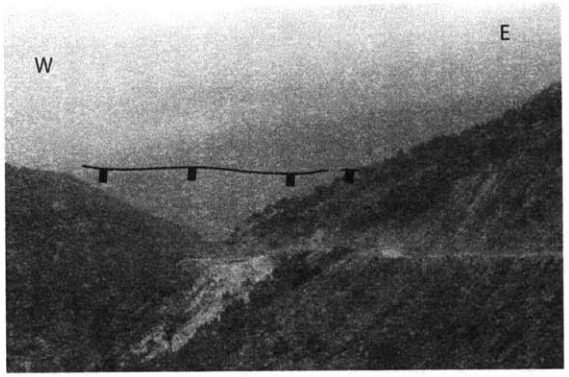

(b)

(c)

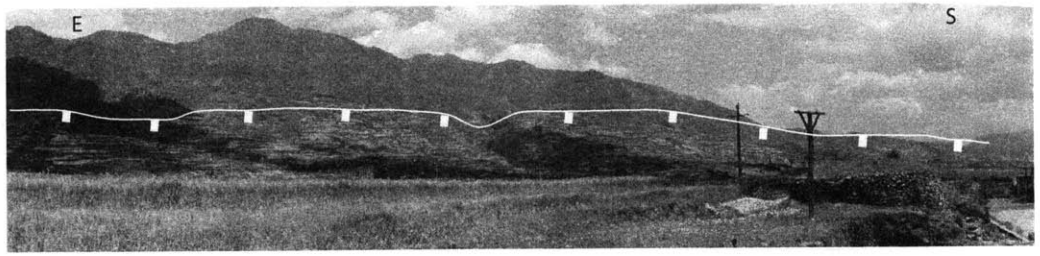

(d)

FIGURE 8

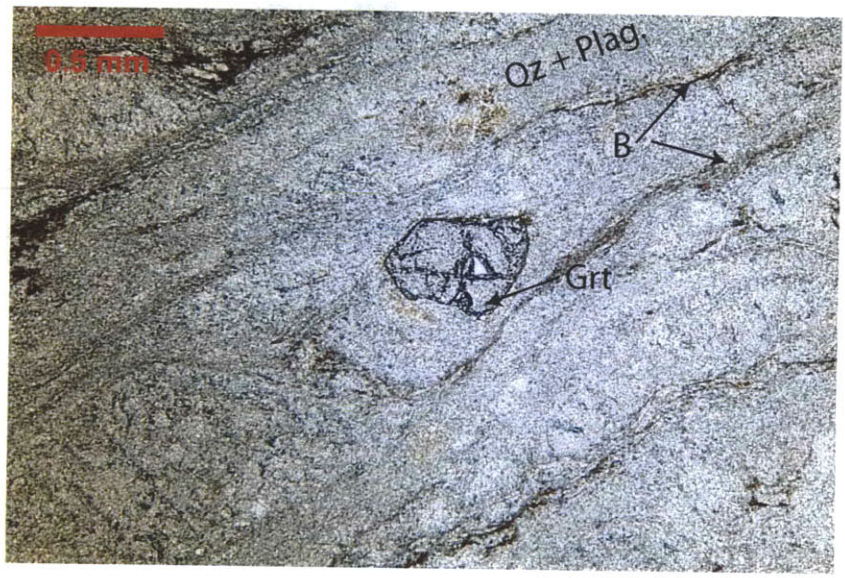

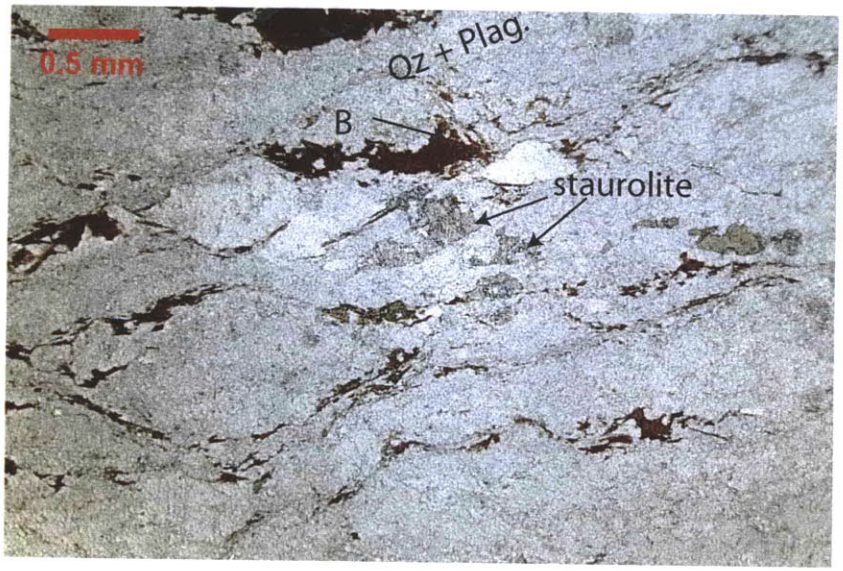

FIGURE 9

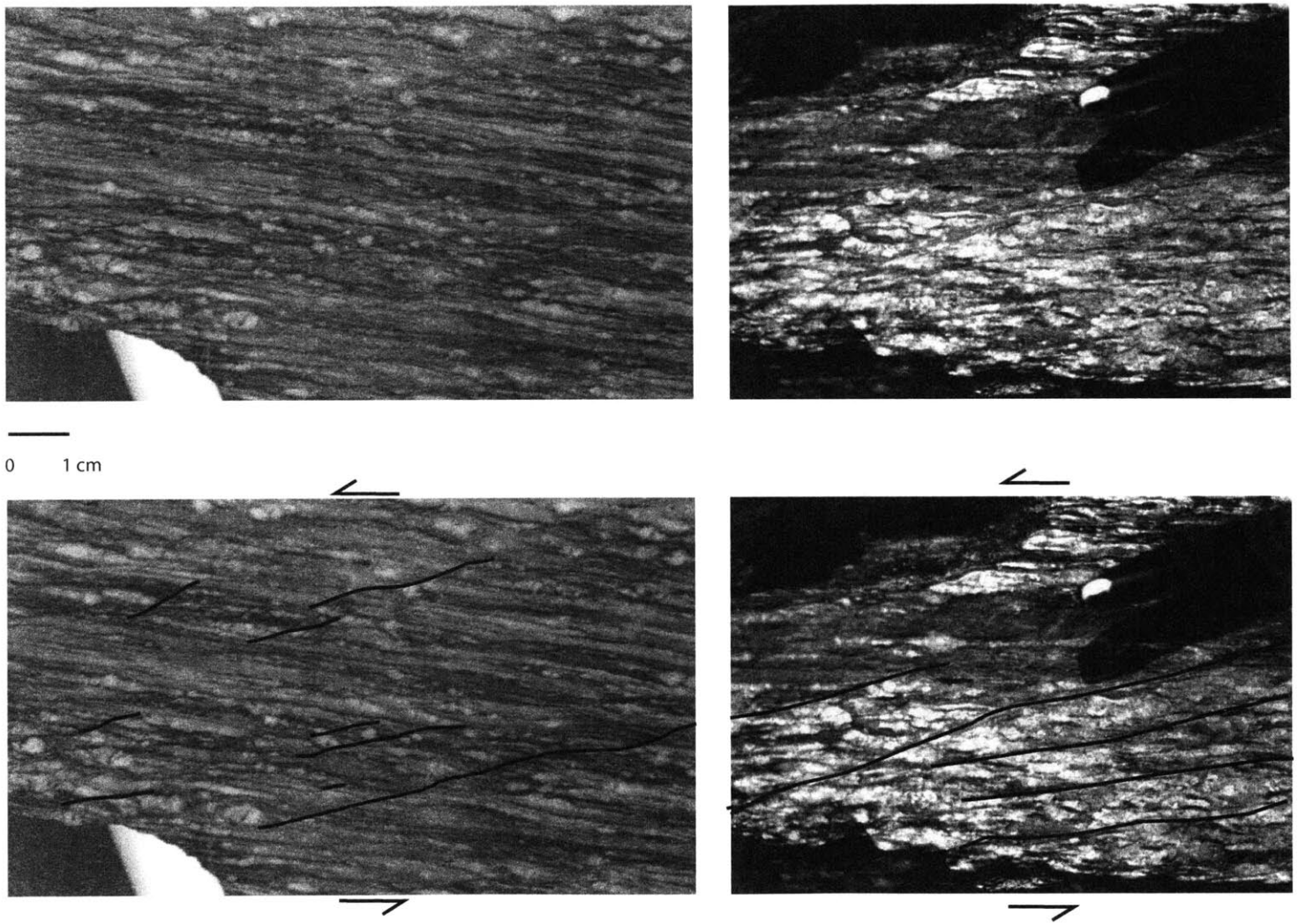

FIGURE 10

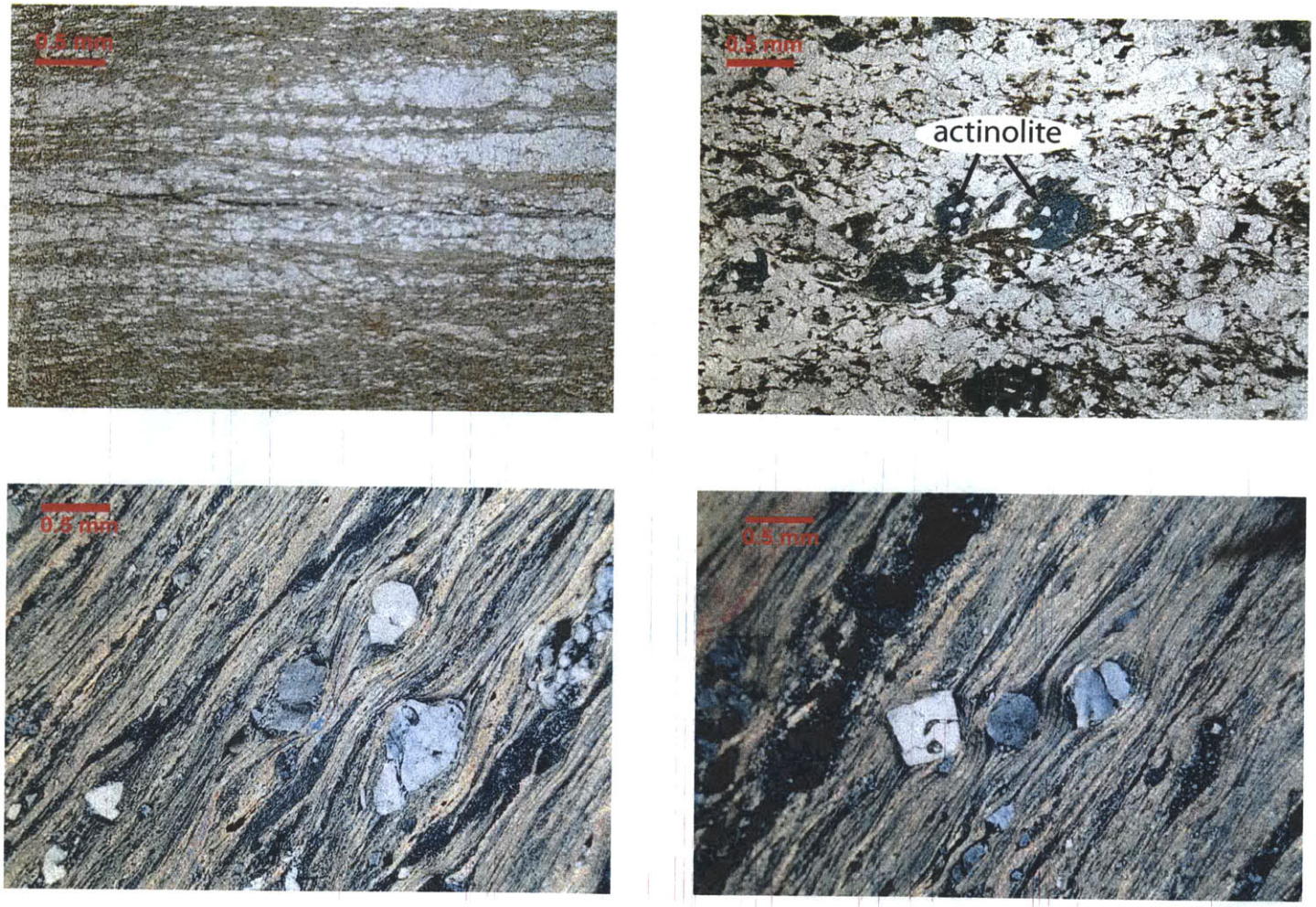

FIGURE 11

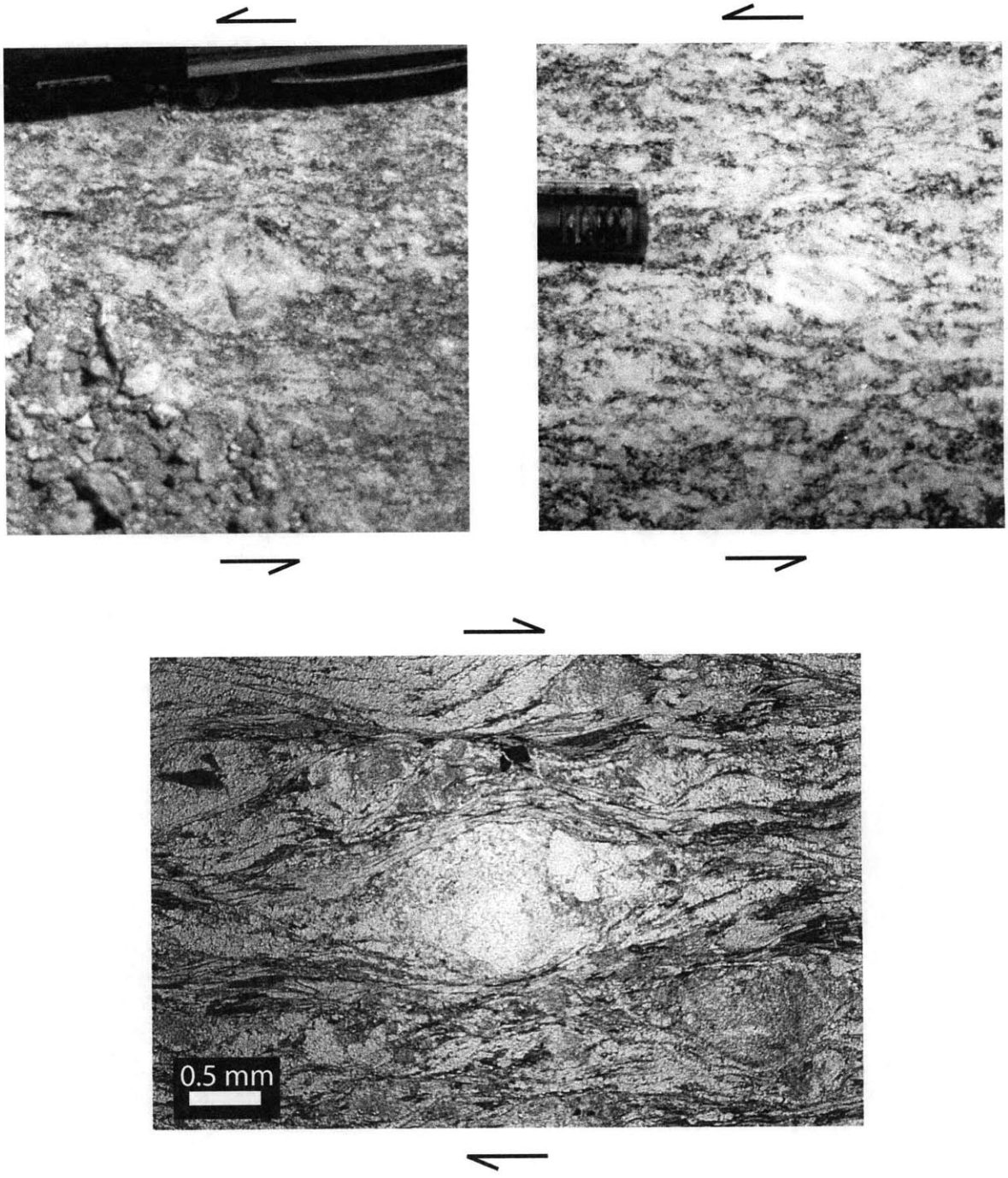

FIGURE 12

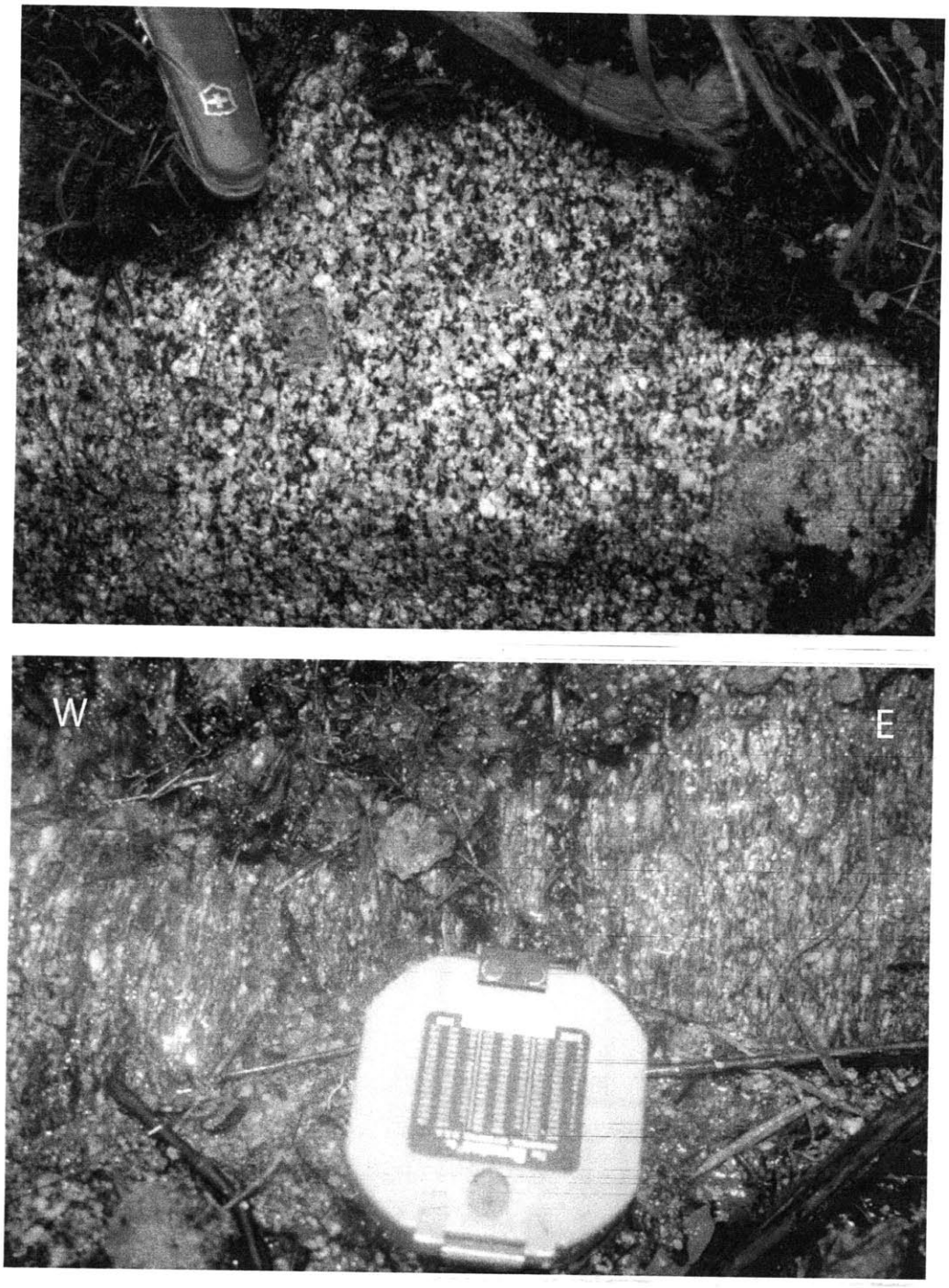

FIGURE 13

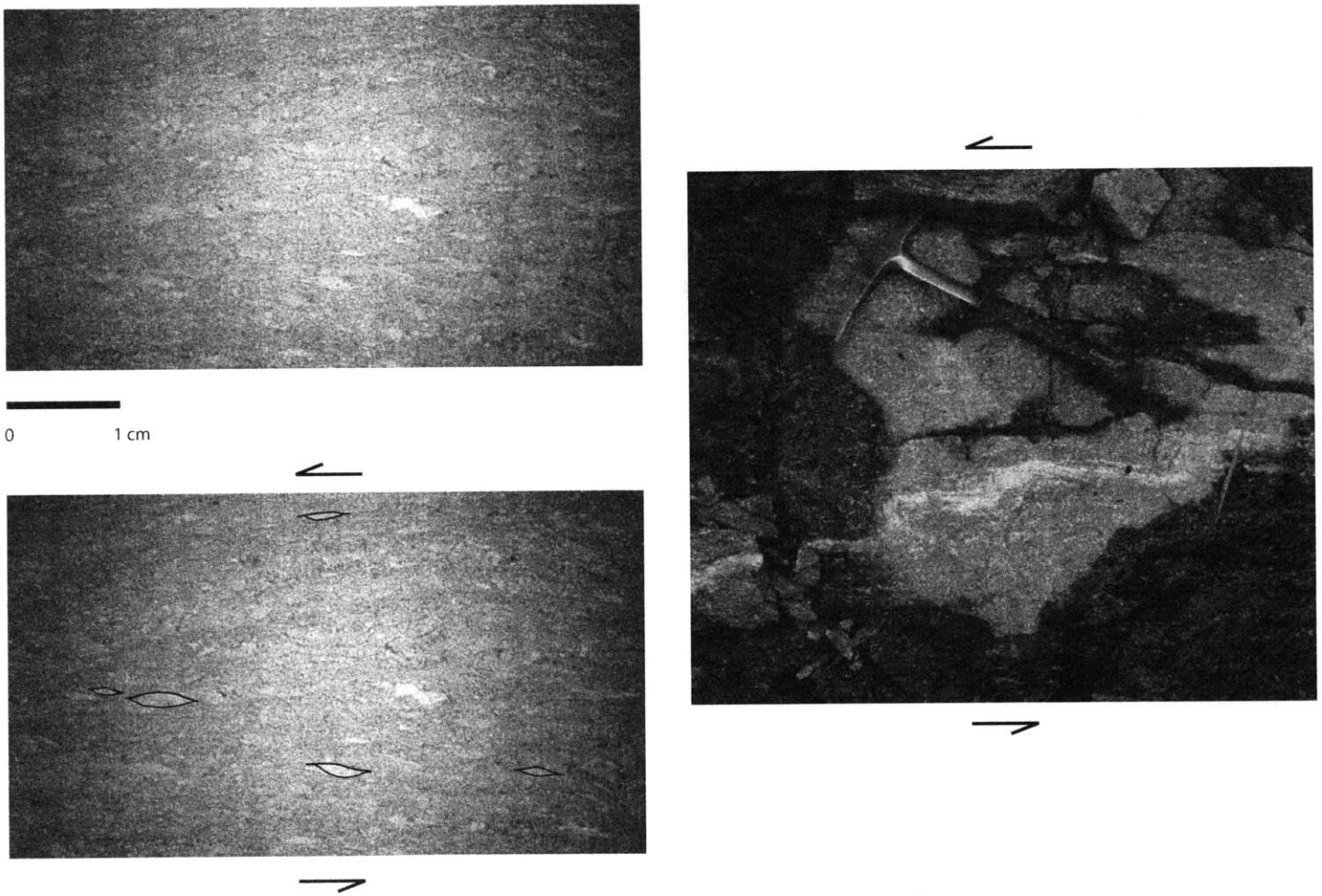

FIGURE 14

FIGURE 15

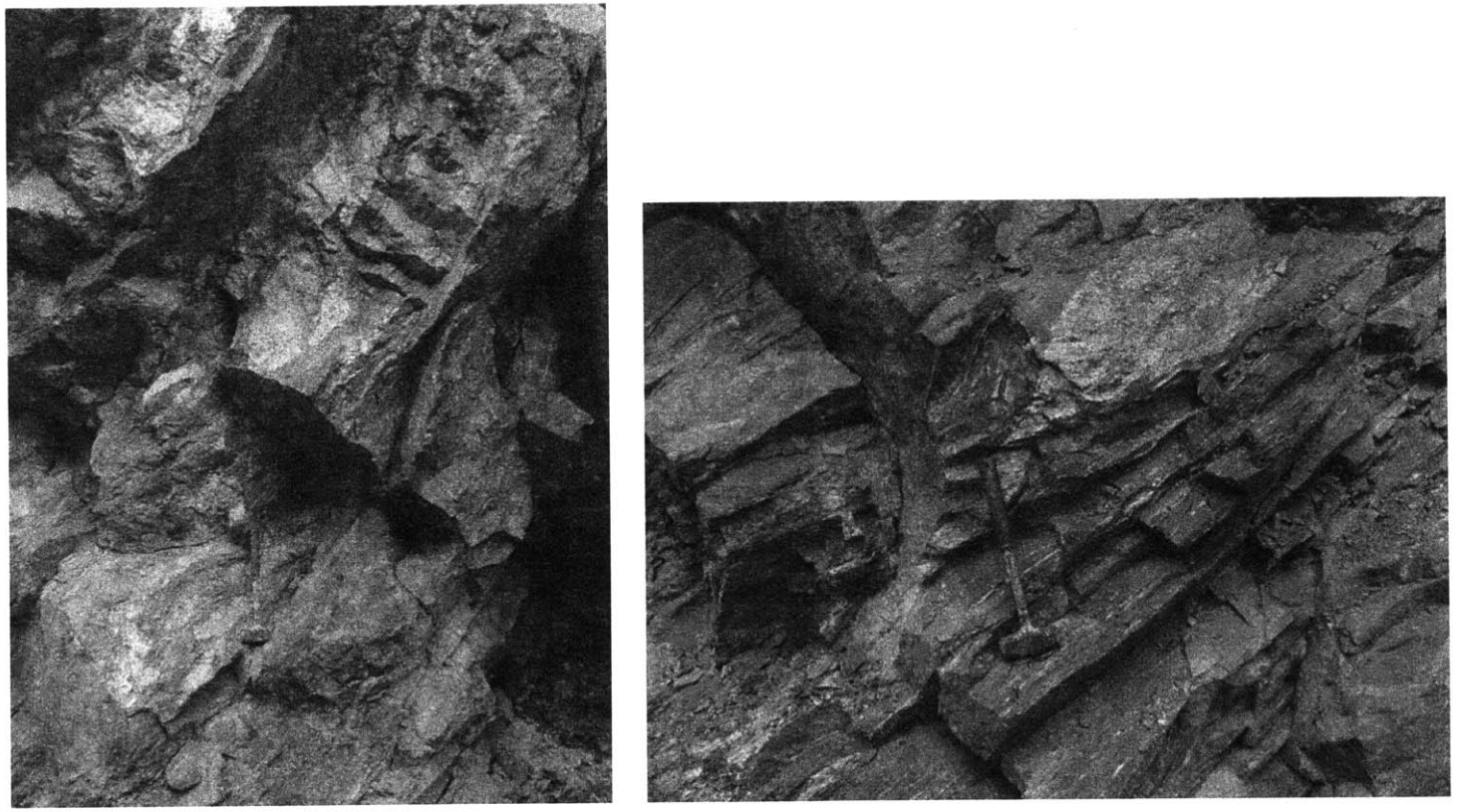

(a) (b)

FIGURE 16

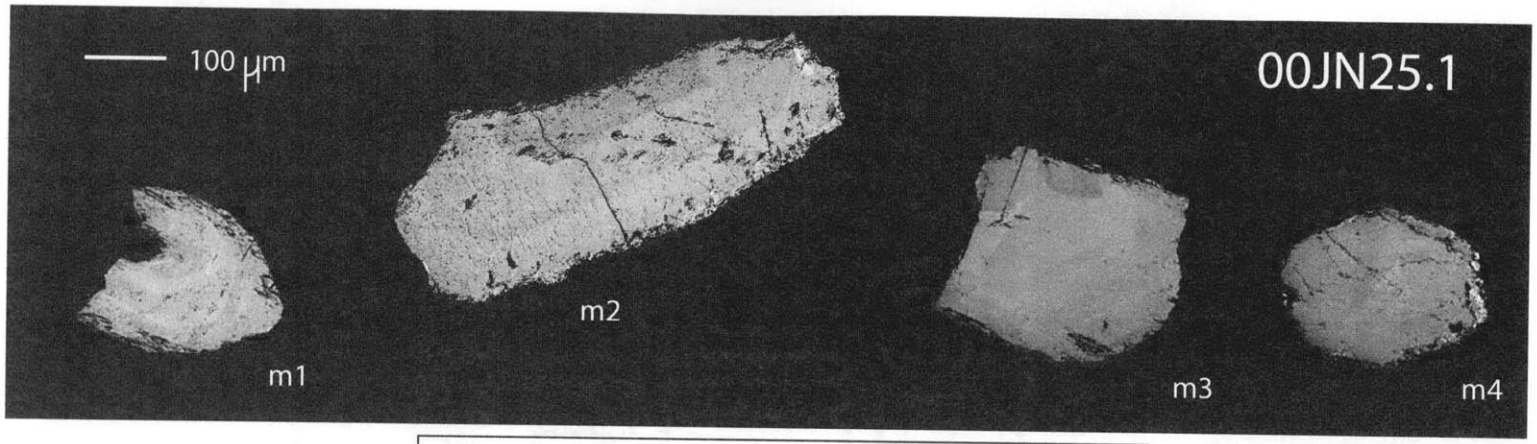
100 μm
00JN25.1
m1
m2
m3
m4

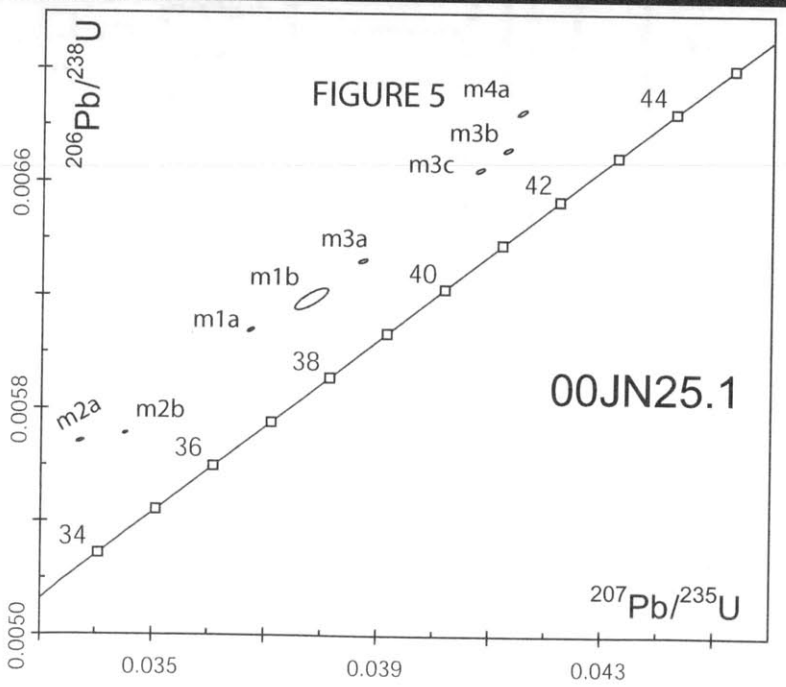
FIGURE 5
$^{206}Pb/^{238}U$
$^{207}Pb/^{235}U$
00JN25.1
m4a
m3b
m3c
m3a
m1b
m1a
m2a
m2b
34
36
38
40
42
44
0.0050
0.0058
0.0066
0.035
0.039
0.043

FIGURE 17

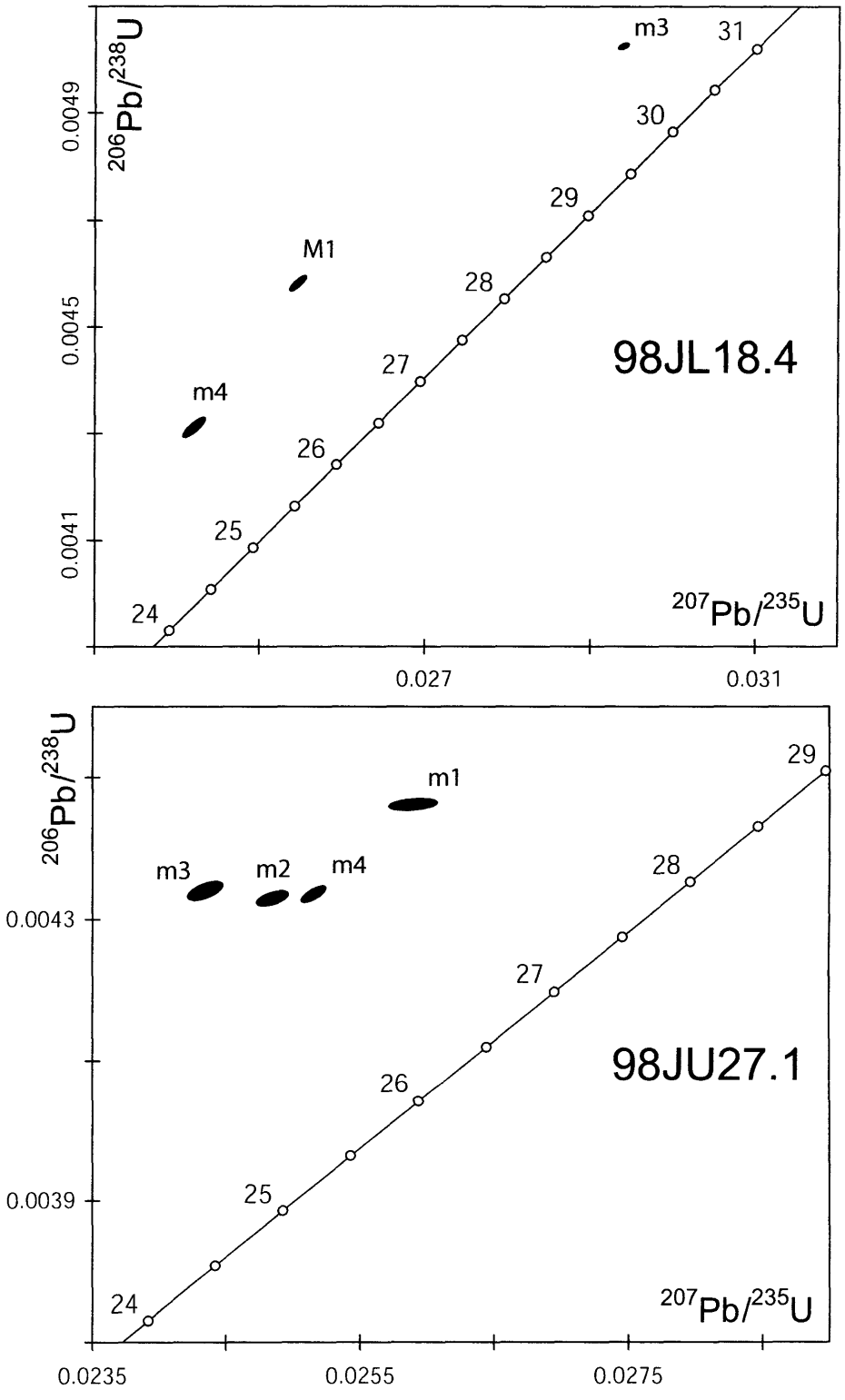
m3
31
30
29
M1
28
27
m4
26
25
24
0.0049
0.0045
0.0041
206Pb/238U
207Pb/235U
98JL18.4
0.027
0.031
m1
29
m3
m2
m4
28
0.0043
27
98JU27.1
26
25
0.0039
24
207Pb/235U
0.0235
0.0255
0.0275

FIGURE 18

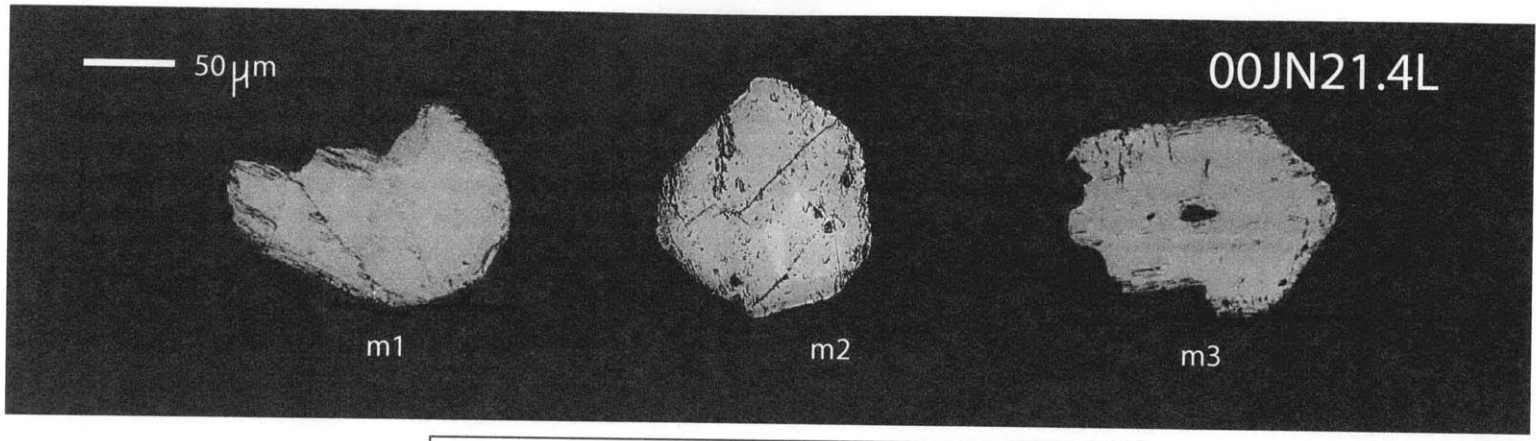
50 μm
00JN21.4L
m1
m2
m3

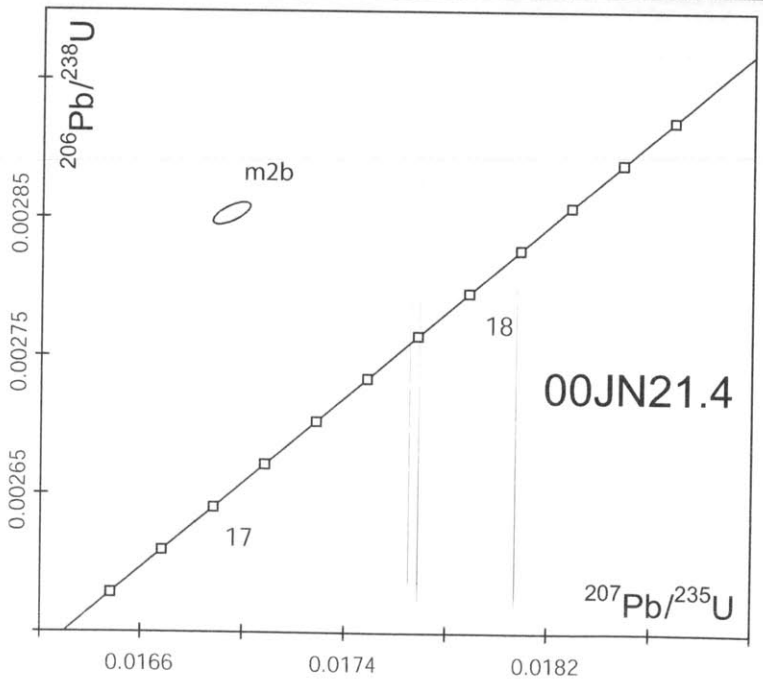
$^{206}Pb/^{238}U$
m2b
0.00285
0.00275
0.00265
18
17
00JN21.4
$^{207}Pb/^{235}U$
0.0166
0.0174
0.0182

FIGURE 19

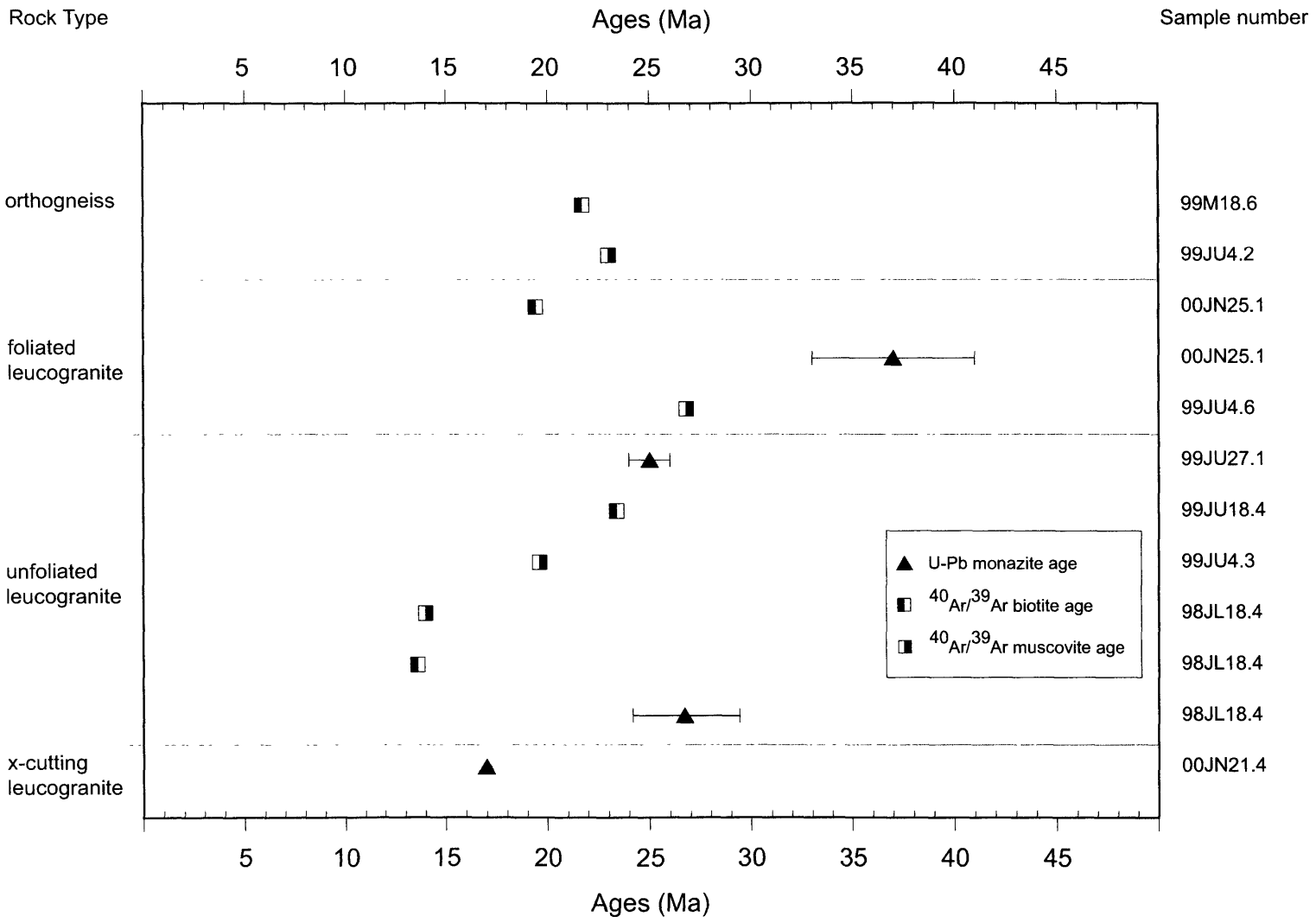
Rock Type
Ages (Ma)
Sample number
5
10
15
20
25
30
35
40
45
orthogneiss
foliated leucogranite
unfoliated leucogranite
x-cutting leucogranite
99M18.6
99JU4.2
00JN25.1
00JN25.1
99JU4.6
99JU27.1
99JU18.4
99JU4.3
98JL18.4
98JL18.4
98JL18.4
00JN21.4
U-Pb monazite age
40Ar/39Ar biotite age
40Ar/39Ar muscovite age
Ages (Ma)

FIGURE 20

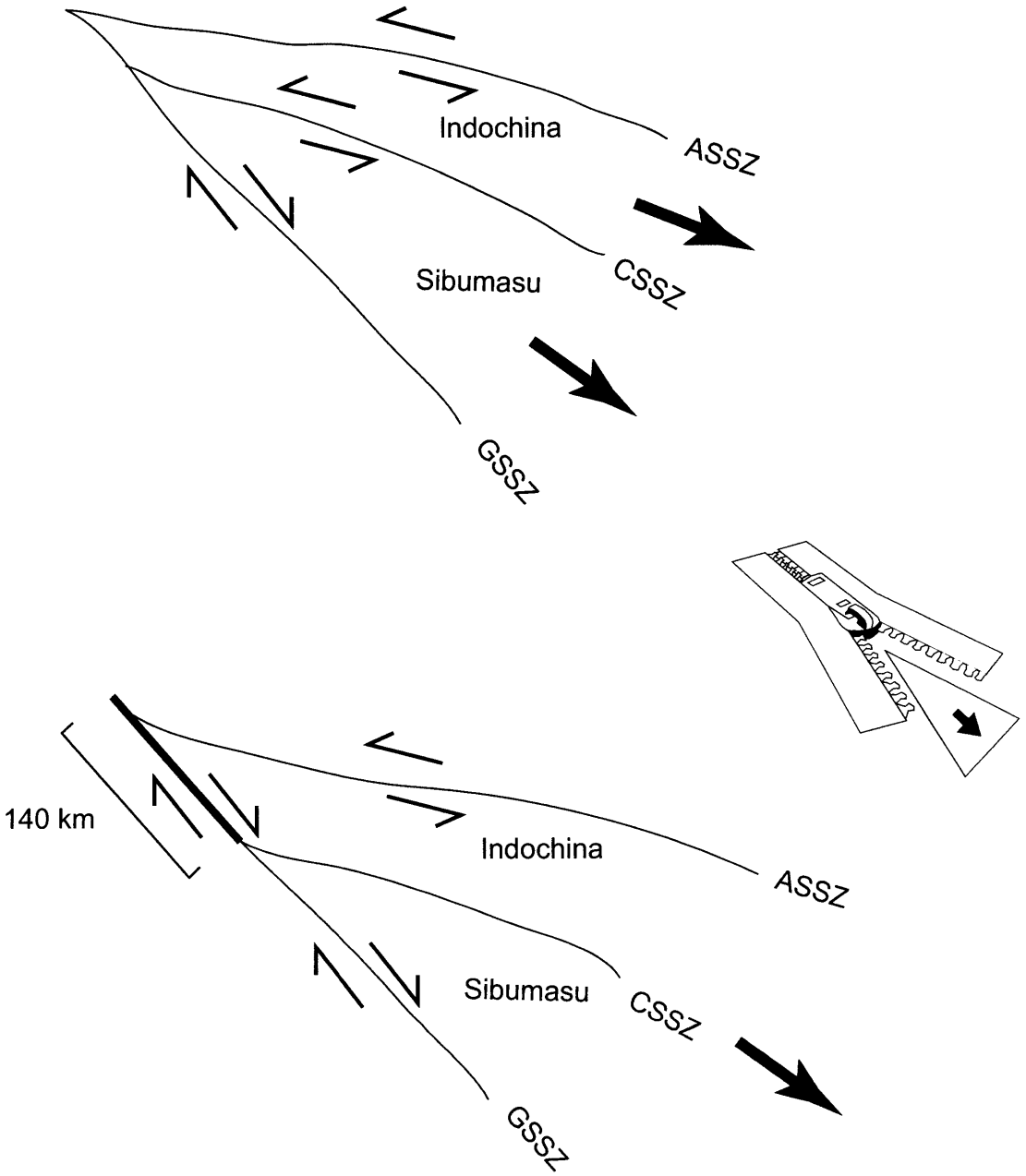
Indochina
ASSZ
Sibumasu
CSSZ
GSSZ
140 km
Indochina
ASSZ
Sibumasu
CSSZ
GSSZ

FIGURE 21

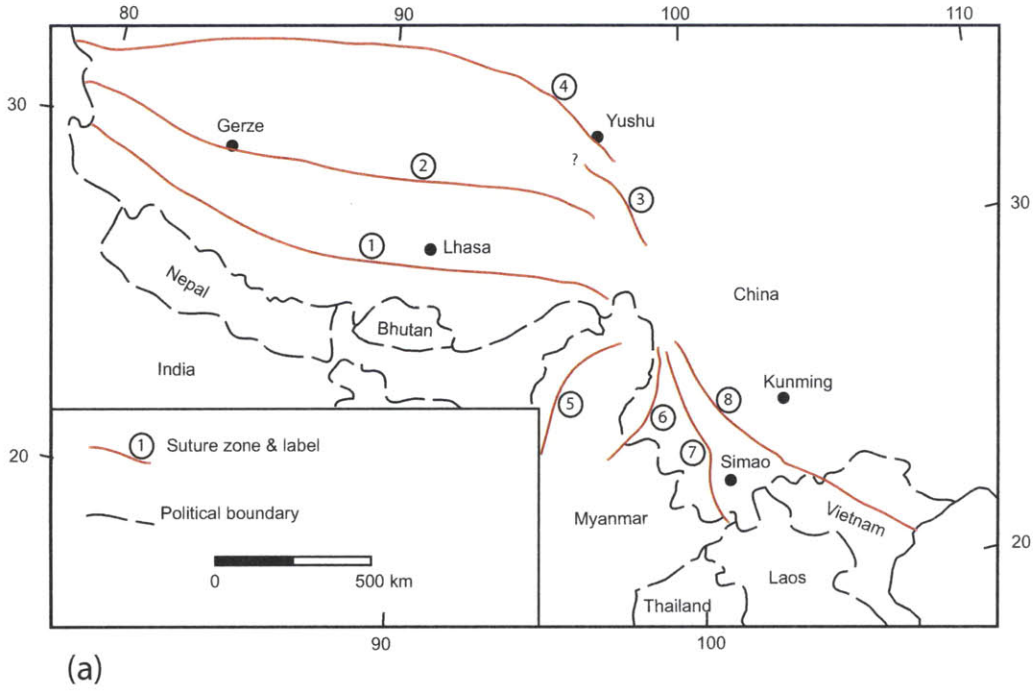
80
90
100
110
30
20
Gerze
Yushu
Lhasa
Nepal
Bhutan
India
China
Kunming
Simao
Myanmar
Vietnam
Laos
Thailand
1 Suture zone & label
Political boundary
0
500 km
(a)

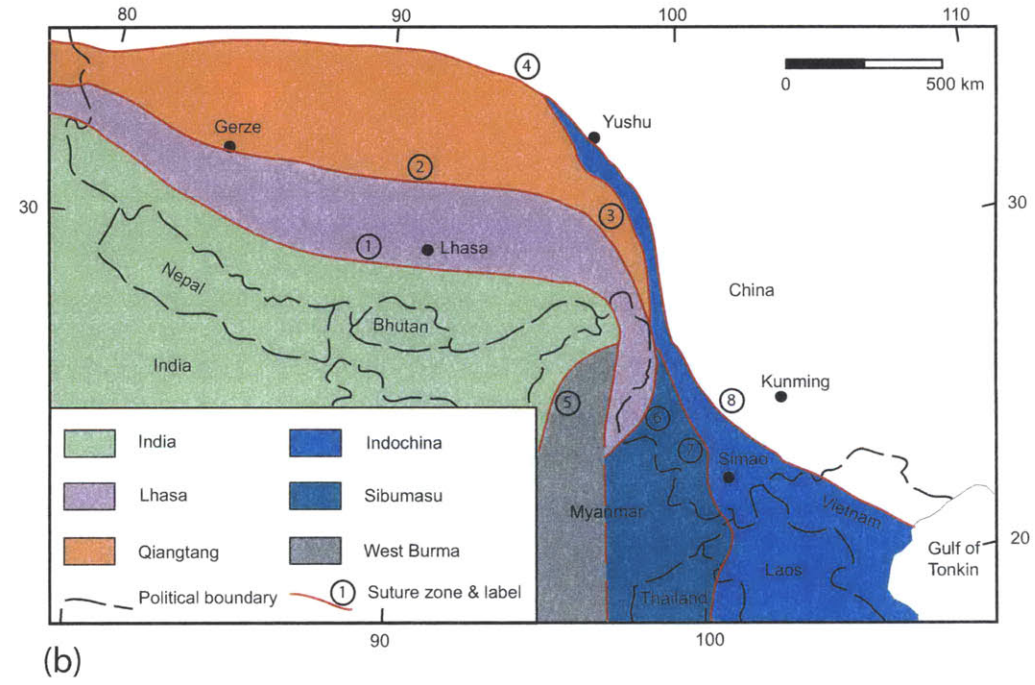
80
90
100
110
30
20
0
500 km
Gerze
Yushu
Lhasa
Nepal
Bhutan
India
China
Kunming
Simao
Myanmar
Vietnam
Laos
Thailand
Gulf of Tonkin
India
Indochina
Lhasa
Sibumasu
Qiangtang
West Burma
Political boundary
1 Suture zone & label
(b)

FIGURE 22

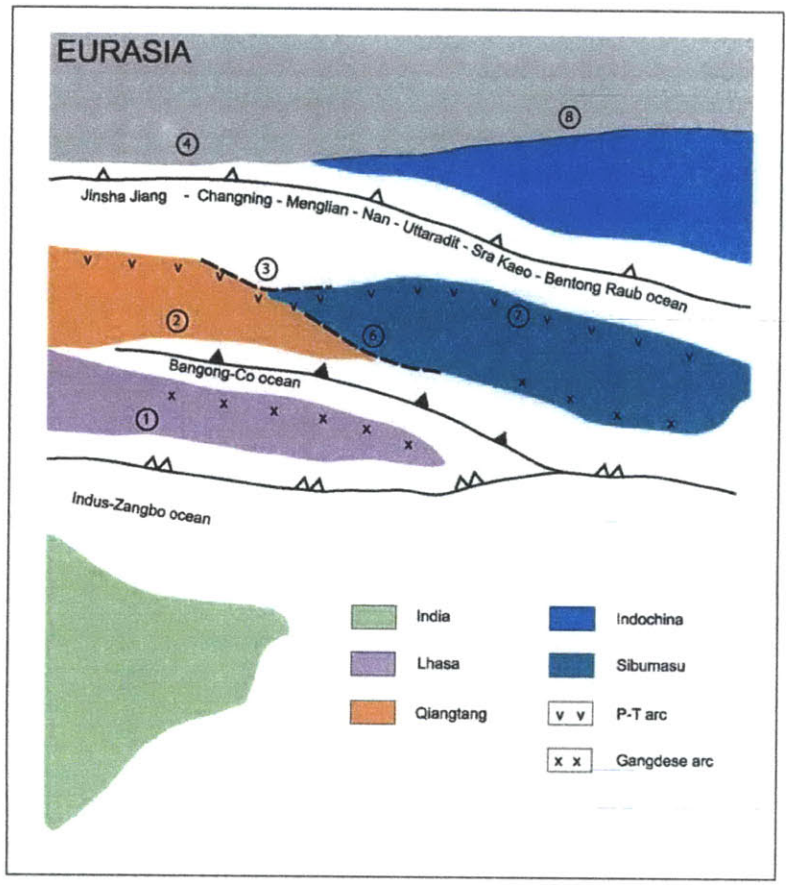
EURASIA
Jinsha Jiang - Changning - Menglian - Nan - Uttaradit - Sra Kaeo - Bentong Raub ocean
Bangong-Co ocean
Indus-Zangbo ocean
India
Lhasa
Qiangtang
Indochina
Sibumasu
P-T arc
Gangdese arc

(a)

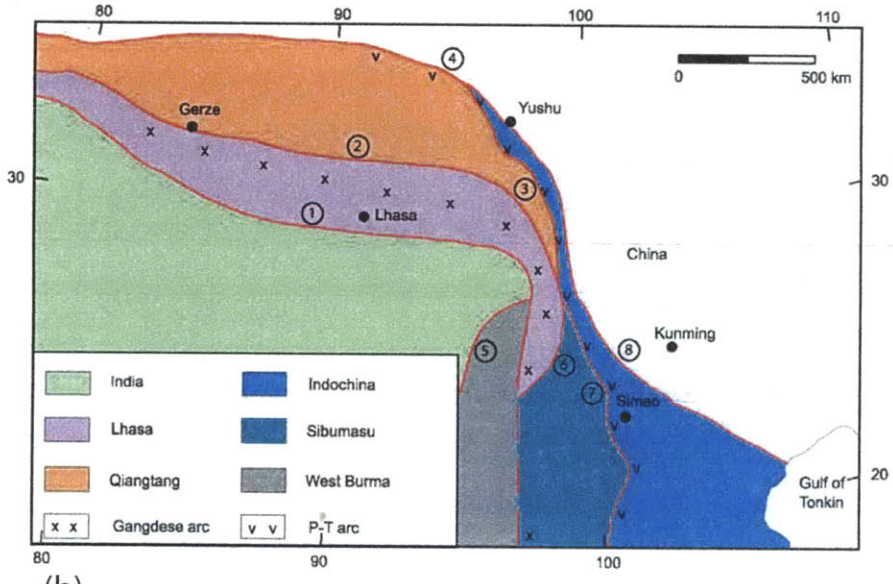
80
90
100
110
30
20
0
500 km
Gerze
Yushu
Lhasa
China
Kunming
Simao
Gulf of Tonkin
India
Lhasa
Qiangtang
Gangdese arc
Indochina
Sibumasu
West Burma
P-T arc

(b)

FIGURE 22

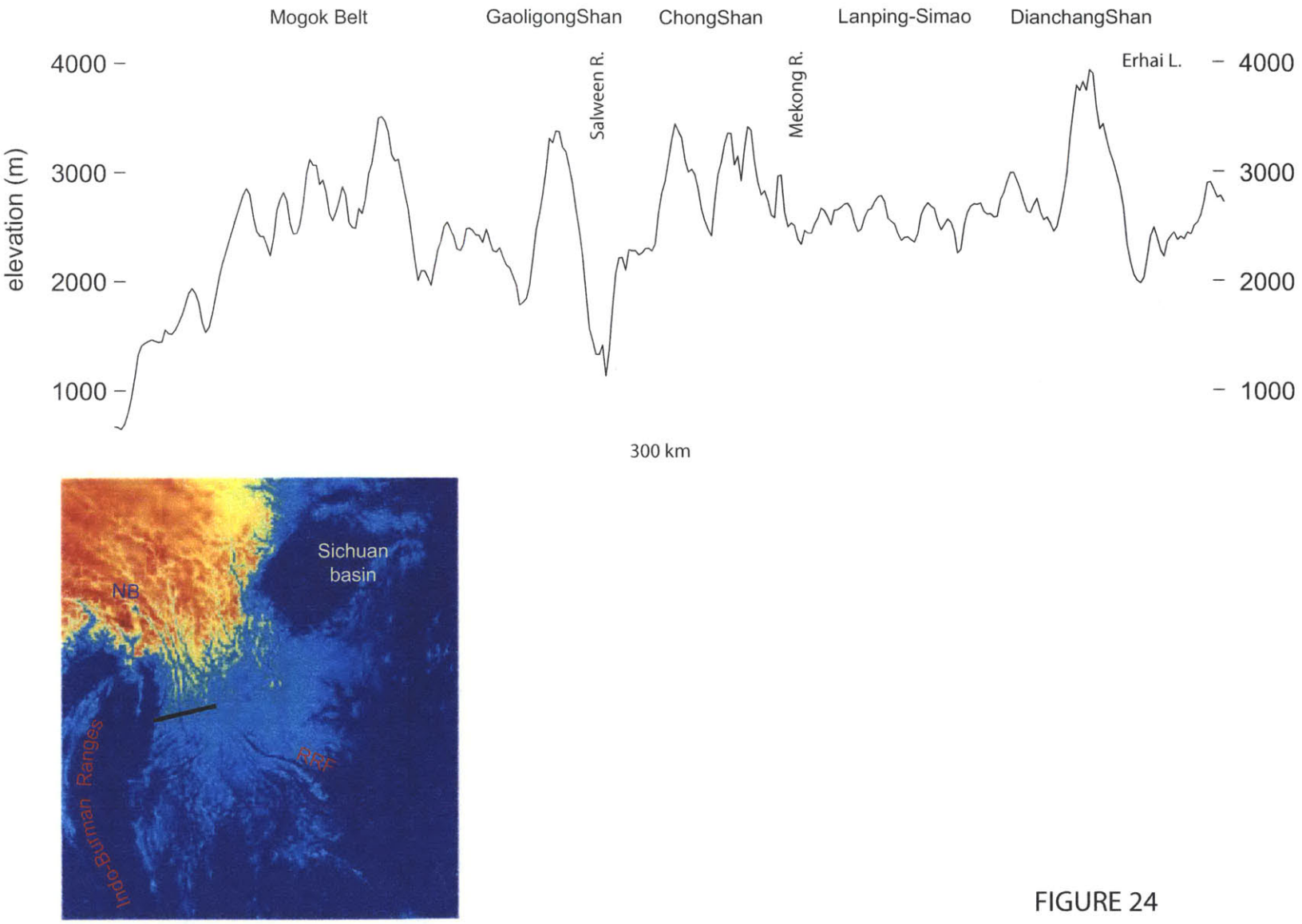
Mogok Belt
GaoligongShan
ChongShan
Lanping-Simao
DianchangShan
Salween R.
Mekong R.
Erhai L.
elevation (m)
4000
3000
2000
1000
300 km
Sichuan basin
NB
RRF
Indo-Burman Ranges

FIGURE 24

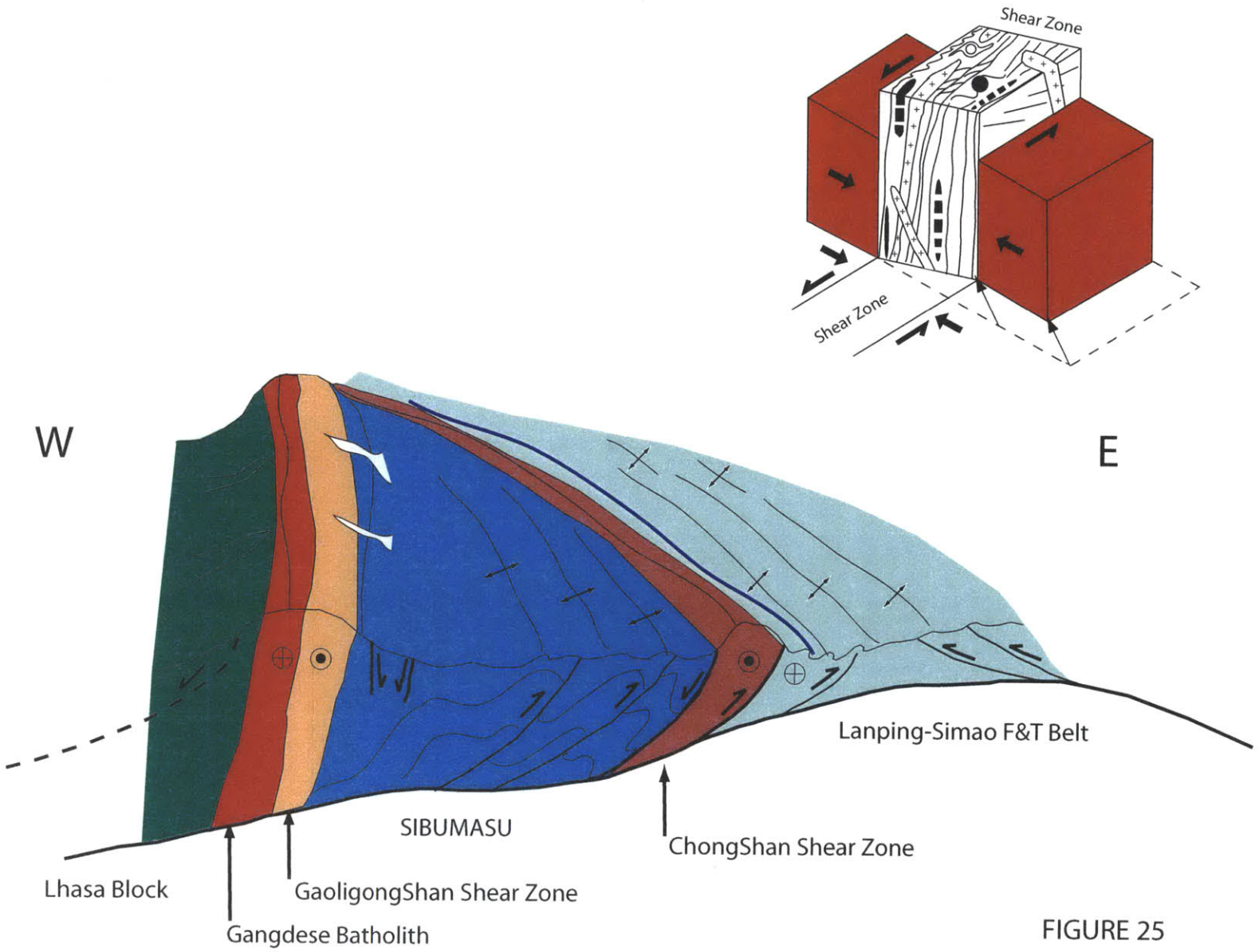
Shear Zone
Shear Zone
W
E
Lanping-Simao F&T Belt
SIBUMASU
ChongShan Shear Zone
Lhasa Block
GaoligongShan Shear Zone
Gangdese Batholith

FIGURE 25

Table 1. U-Pb isotopic data.

Sample (a)	Weigh (µg) (b)	U (ppm)	Pb (ppm)	Th / U (c)	Pb_c (pg) (d)	$^{206}Pb/^{204}Pb$ (e)	$^{208}Pb/^{206}Pb$ (f)	$^{206}Pb/^{238}U$ (f)	% err (g)	$^{207}Pb/^{235}U$ (f)	% err (g)	$^{207}Pb/^{206}Pb$ (f)	% err (g)	corr. coef.	$^{206}Pb/^{238}U$ age (h)	$^{207}Pb/^{235}U$ age (h)	
00JN25.1 foliated leucogranite																	
m1b	4.4	3517	77.8	9 55	15.9	404	2.91	0.006186	0.09	0.037910	0.27	0.044449	0.24	0.44	39.8	**37.78 ± 0.10**	-
m1a	3.6	4321	84.9	8.90	2.8	2124	2.67	0.006070	0.09	0 036658	0 13	0.043804	0.09	0 71	39.0	**36.56 ± 0.05**	-1
m2a	3.7	5203	97.0	9.18	5.0	1412	2.71	0.005674	0.08	0.033650	0.14	0.043013	0.12	0.59	36.5	**33.61 ± 0.05**	-1
m2b	8.7	4541	74.6	7.40	13.4	1091	2.23	0.005702	0.05	0.034436	0.10	0.043804	0.08	0.57	36.7	**34.38 ± 0.03**	-1
m3a	1.3	10624	261 4	11.27	3.4	1704	3.43	0.006313	0.09	0.038639	0.16	0.044394	0.13	0.62	40.6	**38.49 ± 0.06**	-
m3b	1.3	8475	239.1	12 35	4 3	1148	3.77	0.006705	0.11	0.041207	0.16	0.044576	0.11	0.70	43.1	**41.00 ± 0.06**	-
m3c	1.6	5616	157 6	12 44	3.0	1280	3.80	0.006637	0.13	0.040826	0.18	0 044611	0.12	0.75	42.6	**40.63 ± 0.07**	-
m4a	1 3	6787	173.5	10.81	2 2	1817	3.25	0.006838	0 13	0.041462	0.16	0.043976	0.10	0.79	43.9	**41.25 ± 0.07**	-1
98JL18.4 unfoliated leucogranite																	
m1	1.3	16991	187.4	6.28	7.2	903	1 83	0 004382	0.27	0.025465	0.32	0.042147	0.17	0.84	28.2	**25.53 ± 0.08**	-2
m3	1 6	49370	427.0	3 34	7 0	3509	1.01	0.004826	0 07	0.029392	0.16	0.044172	0.14	0 48	31.0	**29.41 ± 0.05**	-1
m4	1.3	12569	148 7	7.26	9.6	479	2.14	0.004113	0.12	0.024241	0.25	0 042750	0.22	0.52	26.5	**24.32 ± 0.06**	-1
98JU27.1 unfoliated leucogranite																	
m1	2 3	17079	248.6	7.54	85.8	149	2.19	0 004462	0.15	0.025894	0.56	0.042092	0.53	0.36	28.7	**25.96 ± 0.15**	-2
m2	3.1	10090	125.8	7.52	18.5	488	2.16	0.004330	0.20	0.024848	0.39	0.041620	0.32	0.57	27.9	**24.92 ± 0.10**	-2
m3	1.6	4773	63.2	8 61	2.7	806	2.42	0.004345	0.23	0.024434	0 39	0.040784	0.31	0.62	28.0	**24.51 ± 0.10**	-3
m4	2.1	14674	156.7	6.09	5.2	1651	1.77	0 004339	0.11	0 025203	0.22	0.042129	0.19	0.52	27.9	**25.27 ± 0.06**	-2
00JN21.4 cross-cutting leucogranite																	
m2b	1.6	7396	53.7	6 18	2.6	844	1.84	0 002853	0.23	0 016945	0 35	0.043068	0.26	0.68	18.4	**17.06 ± 0.06**	-1

(a) m1a, m1b, m2a etc. correspond to labels on concordia diagrams. Fractions are composed of single monazite fragments; letters following the same number are fragments from the same grain.

(b) Sample weights are estimated to within 20% using measured grain dimensions and density

(c) Model Th/U ratio calculated from radiogenic 208Pb/206Pb ratio and 207Pb/206Pb age.

(d) Total weight of common Pb.

(e) Measured ratio corrected for spike and fractionation only. Mass fractionation correction of 0.20%/amu ± 0.04%/amu (atomic mass unit) was applied to single-collector Daly analyses (based on daily analysis of NBS-981) and a correction of 0.12%/amu ± 0.04% was applied to dynamic Faraday-Daly analyses.

(f) Corrected for fractionation, spike, blank, and initial common Pb. All common Pb was assumed to be procedural blank U blank was <0.1 pg. Measured laboratory blank composition: 206Pb/204Pb = 19.10 ± 0.1, 207Pb/204Pb =15.71 ± 0.1, 208Pb/204Pb = 38.65 ± 0.1 (2 sigma).

(g) Errors are 2 sigma, propagated using the algorithms of Ludwig (1980).

(h) Age calculations are based on the decay constants of Steiger and Jager (1977) Error in the 207Pb/206Pb age is 2 sigma.

Chapter 5: Sibumasu tectonic element: Its sutures and their role in the Cenozoic evolution of continental SE Asia

Sinan Akciz[1]*
B. Clark Burchfiel[1]
James L. Crowley[1]
Yin Jiyun[2]
Chen Liangzhong[2]

[1]Massachusetts Institute of Technology, Dept. of Earth, Atmospheric and Planeary Sciences, 77 Massachusetts Ave., Cambridge, MA 02139

[2]Yunnan Institute of Geological Sciences, 131 Baita Rd., Kunming, Yunnan, China.

*E-mail: akciz@mit.edu

ABSTRACT:

Three major ductile strike-slip shear zones, the Gaoligongshan, the Chongshan and the Ailaoshan shear zones in Yunnan, China, have played a major role in accommodating the indentation of India into Asia until ~18 Ma. The close spatial correlation between these shear zones and the pre-Cenozoic suture zones suggest that suture zones have been very important in the localization of deformation in the region during early to middle Cenozoic time. Our knowledge of these suture zones, particularly the ones that bound the Sibumasu tectonic element, is limited. The aim of this study is to review the currently available geological data from the Bangong-Nujiang and Lancangjiang-Raub suture zones and to re-interpret the relations of these suture zones to the younger shear zones along the northernmost section of the Sibumasu tectonic element based on our field and laboratory studies. The re-interpretation arrives at several important conclusions that include: 1) the Sibumasu tectonic element pinches out in western Yunnan, and does not continue into Tibet, 2) the Nujiang ocean separated the Sibumasu and the Qiangtang crustal fragments, 3) the Bangong Co ocean separated the Qiangtang and Lhasa crustal fragments, 4) Cenozoic right-lateral shearing along the Gaoligongshan shear zone, which re-activated the Nujiang suture and the southern section of the Bangong suture, caused their alignment, and 5) Cenozoic shearing related to indentation of India into Eurasia has caused segments of these suture zones be become cryptic. A better documentation of the exact location of the various segments of these suture zones by detailed fieldwork and determination of the duration of their deformational histories by detailed geochronological studies will undoubtly vastly improve our understanding of the Cenozoic tectonic evolution of SE Asia.

INTRODUCTION

Interpretations of the Cenozoic tectonic evolution of the eastern part of the Tibetan Plateau lying east of the India indenter have been varied and controversial. Some authors (Cobbold and Davy, 1988; Dewey et al., 1989; England and Molnar, 1990) suggest the region east of the eastern syntaxis has been undergoing broad, right-lateral shear and clockwise rotation along left-lateral faults throughout the development of the collision zone. Probably the most influential conceptual model for development of this region, however, is the two-phased "extrusion model" (Tapponnier et al., 1982, 1986) which hypothesizes the eastward extrusion of Indochina during the first phase, immediately after the India – Eurasia collision, followed by the

eastward extrusion of the region bounded by the Altyn Tagh and the Red River faults for the last 5 – 10 Ma (Figure 1).

Wang and Burchfiel (1997) and Wang et al. (1998) documented that from at least 2-4 Ma to present, the deformational style is dominated by the clockwise rotation of crustal material around the eastern Himalayan syntaxis, bounded by the Xianshuihe-Xiaojiang-Dien Bien Phu fault system to the east. Rotation around the syntaxis is confirmed, at least in the short term, by GPS data (King et al., 1997; Chen et al., 2000), raising concerns regarding the second phase of the extrusion model. And in chapters 2,3 and 4, I have documented 2 additional strike-slip shear zones during the first phase of extrusion, the Gaoligongshan (GSSZ) and Chongshan shear zones, contemporaneous with the Ailaoshan Shear Zone (ASSZ), and argued that even though the region between the GSSZ and the ASSZ did extrude to the southeast, this extrusion happened within the right-lateral accommodation zone of the India indenter, and did not move Indochina from a region in front of the India indenter in order to accommodate India's penetration into Eurasia. This alternative interpretation, based on new field and geochronological data from a previously little known region, has major implications for the tectonic evolution of continental southeast Asia for the last ~50 Ma and requires new discussions on the origins and the significance of these major strike-slip shear zones.

Jackson (1990) proposed the idea that most of the faults within the continental crust are reactivated from older faults, though the relevance and importance of older suture zones affecting SE Asian Cenozoic tectonics has been downplayed by others (e.g. Tapponnier et al., 1986). East of the eastern Himalayan syntaxis, continental SE Asia consists of several accreted crustal fragments separated by sutures that in places contain the remnants of oceanic rocks or in other places are sheared so that the evidence for oceanic rocks is missing and become cryptic.

The observation that all three of these strike-slip shear zones are positioned within or close to pre-Cenozoic suture zones is indisputable (Figure 2). The GSSZ lies along the Bangong-Nujiang suture zone, the CSSZ follows the northern continuation of the Changning-Menglian suture zone (which is part of the Lancang Jiang - Changning-Menglian - Nan-Uttaradit – Sra Kaeo – Chantaburi - Bentong -Raub sutures), and finally the ASSZ follows the Song Da – Anding suture zone (Sengor et al., 1988).

We, therefore, follow Jackson (1980) and suggest that these suture zones form crustal anisotropies that were reactivated during Cenozoic collision and subsequent penetration of India into Eurasia, so long as they were appropriately oriented. In chapters 2 and 3, for example, we have argued that the GSSZ reactivated the Bangong Co-Nujiang suture during the early Tertiary, but after 18 Ma, the motion along it terminated as it was no longer properly oriented to accommodate the indentation of India. Therefore, the location and history of these suture zones becomes additionally important in understanding the Cenozoic tectonic evolution of SE Asia east of the eastern Himalayan syntaxis. In this chapter, we review the present knowledge regarding the suture zones bounding the Sibumasu continental fragment, as defined by Metcalfe (1984, 1988), which was reactivated as the GSSZ and the CSSZ during the Tertiary times.

Regionally, the Sibumasu fragment, lies within an amalgamated complex of microcontinents, or crustal fragments, in SE Asia that consists of the Lhasa, Qiangtang, Western Burma, IndoChina, and South China (Figure 2) fragments. The Sibumasu fragment (also known as the Shan-Thai block or Sinoburmalaya block) is an elongated fragment of continental crust that extends from northwestern Sumatra in the south through western Malaysia, Peninsular Thailand and Peninsular Burma, northwest Thailand, the Shan State of Burma and to Bijiang, western Yunnan, China, in the north. It is bounded by the Lancangjiang-Changning-Menglian-

Nan-Uttaradit-Bentong-Raub suture zone on the east, and by the Gaoligongshan shear zone, Shan boundary Fault and the Andaman Sea on the west. Between these boundaries the Sibumasu fragment contains a characteristic latest Proterozoic to late Mesozoic assemblage of sedimentary and magmatic rocks that, to the best of our knowledge, has no continuation farther north (and west).

The boundaries of these continental fragments and the age and location of through-going sutures that separate them remain controversial, largely because of lack of information owing to geographic remoteness, extreme landscape conditions, as well as cultural and political barriers. As a result, first order questions, such as the names of the various tectonic units, the location of their boundaries and their geological evolution are still controversial. The suture boundaries and evolution of the Sibumasu and adjacent fragments are no exception, in fact they are among the geologically least known in SE Asia. Aiding in the identification of the suture zones that bound the Sibumasu fragment are the products of subduction formed during closure of the surrounding oceanic regions, such as remnants of oceanic crust, accretionary prisms and forearc and arc rocks. A review these rocks and their possible continuations through this region is necessary to define the major paleogeographic and tectonic boundaries within the area of investigation.

Lancang Jiang - Changning-Menglian – Nan-Uttaradit – (Chiang Mai?) – Sra Kaeo – Chantaburi - Bentong -Raub Suture

The suture that bounds the east side of the Sibumasu fragment consists of a discontinuous belt of suture zone and associated subduction derived rocks. In our interpretation it can be traced

discontinuously from the north in the Lancang Jiang suture south through southern China into Bentong-Raub suture in Malaysia (Figure 3). The discontinuous suture fragments consist of the Changning-Menglian - Nan-Uttaradit – Sa Kaeo – Chantaburi - Bentong -Raub sutures.

Lancang Jiang suture zone:

The Lancang Jiang suture is exposed in southern Tibet where it forms the boundary between the Qamdo-Simao (Indochina) and the eastern Qiangtang continental fragments (Figure 2). The suture zone rocks include Devonian and Carboniferous turbidites, ocean-floor and basic magmatic rocks of Permian age and Carboniferous-Permian mélange (Chen & Xie, 1994). Scattered outcrops of ultramafic rocks occur in the Muta region of Tibet and in Qinghai provinces (Chen & Xie, 1994). Carboniferous-Permian island arc rocks are developed along the west side of the suture (Wang & Tan, 1994). These suture zone rocks are unconformably overlain by very thick Jurassic sediments in the Tanggula Range. (Chen & Xie, 1994).

Changning-Menglian suture zone:

South from Deqqin in Tibet suture zone rocks are not exposed for ~300 km having been severely disrupted by the Cenozoic, post-collisional Chong Shan shear zone. The Changning-Menglian suture in southern Yunnan (Figure 3) we interpret as the continuation of the Lancang Jiang suture because it forms the eastern boundary of the Sibumasu crustal fragment. However, the relations between the Qiangtang and Sibumasu fragments which lies west of the Lancang Jiang and Chengning-Menglian sutures are complex; we interpret them as two separate crustal fragments, but bounded by the same suture zone, a relationship that will be discussed in more

detail. In this part of Yunnan the Changning-Menglian suture separates the Sibumasu fragment from the Mesozoic strata of the Lincang granitic batholith and associated metamorphic rocks as well as the Lanping-Simao- Qamdo basin, which are assigned to the Indochina tectonic unit. The suture zone contains dismembered ophiolites and associated deep water sedimentary rocks along with some volcanic rocks. In the Menglian area, the volcanic sequence consists of dominantly undeformed pillowed lavas (Wu et al., 1985). Unfortunately, there are no reliable radiomentic ages for the volcanic rocks. Oceanic ribbon chert-shale sequences have yielded graptolites, conodonts and radiolarians indicating ages that range from early Devonian to Middle Triassic (Duan et al., 1982; Qin et al., 1980;Wu and Li, 1989; Liu et al., 1991; Fang, et al., 1994). Limestone blocks and lenses found mostly within basaltic rocks have yielded fusulinids indicative of Middle Carboniferous to Late Permian ages (Duan et al., 1982; Wu et al., 1985).

The suture is truncated to the north of Changning by the CSSZ, but we agree with Metcalfe (l996) that its continuation to the north is the Lancang Jiang suture exposed west of Deqqin. The southern extension of the Changning-Menglian, however, is problematic. The suture can be traced to the China-Myanmar border, but its extension into Myanmar and Thailand has not been convincingly documented, and thus remain to be controversial. Until recently, it was generally thought that the southern continuation of the Changning-Menglian suture was the Nan-Uttaradit suture that were offset by a cryptic left-lateral strike-slip fault Metcalfe (1996). However, recent discoveries in north-western Thailand suggest that the Chiang Mai accretionary complex might be the southern continuation, with the Nan-Uttaradit representing a back-arc marginal basin (Metcalfe, 2002).

Nan-Uttaradit:

The accretionary complex of the Nan-Uttradit suture zone (Figure 3) contains serpentinite, blueschists (Barr et al., 1985; Barr and Macdonald, l987), Early-Middle Permian limestone blocks and Middle - Late Triassic radiolarian cherts (Hada et al., 1997). Suture zone rocks are overlain by Upper Triassic to Cretaceous redbeds (Ridd, 1980) and post-Triassic(?) intraplate continental basalts (Panjasawatwong&Yaowanoiyothin, 1993).

Chiang Mai:

The accretionary complex in the Chiang Mai-Chiang Doi area of northwestern Thailand (Figure 3) contains pillow basalts, Devonian, Carboniferous, Permian and Triassic radiolarian cherts (Caridroit et al., 1990; Sashida et al., 1993; Sashida and Igo, 1999)and pelagic limestone, mudstone and turbidites. Thick, but laterally restricted bodies of shallow marine fusulinid limestones dated as Early Carboniferous to Late Permian north of Chiang Mai (Ueno and Igo, 1997) are interpreted as seamount caps.

Bentong-Raub suture:

The Bentong-Raub suture is a narrow north-south trending zone extending from Thailand through Bentong and Raub (Figure 3). It is approximately 13 km wide and contains melange, oceanic sediments (mainly cherts), schist, and discontinuous, narrow bodies of serpentinised mafic and ultramafic rocks (Hutchison, 1975, 1989; Tjia 1987, 1989). Limestone clasts in the melange have yielded Early and Late Permian ages (Metcalfe, 1989). Deep-marine bedded cherts within the suture zone range in age from Late Devonian to Late Permian (Metcalfe, 1992;

Spiller&Metcalfe, 1993, 1995; Metcalfe&Spiller, 1994). The Khorat Group, equivalent of the Late Triassic Tembeling Formation (Gobbett&Hutchison, 1973), consists of fluvial-deltaic-lacustrine strata that rest unconformably on Permian strata (Ichikawa et al., 1966). These data suggest collision of Sibumasu with Indochina in the latest Triassic (Sengor (1984). The continuation of the suture along the eastern side of the Sibumasu fragment to south remains controversial. A continuation into Sumatra has been suggested by Hutchison (1993). In this region, the precise age of suturing is still poorly constrained, but a latest Permian - earliest Triassic suturing is generally accepted (e.g. Metcalfe, 1996).

Bangong – Nujiang Ocean

The Sibumasu crustal fragment is bounded on the west by what is called the Bangong-Nujiang suture (Figure 3), even though interpretations regarding the nature of the suture zone vary. Early interpretations considered it as a major suture zone (Pan and Zheng, 1983; Girardeau et al., 1985). However, pre- and post-collisional deformation are minor (Coward et al., 1988; Dewey et al., 1988) and magmatism related to its closure is absent (Dewey et al., 1988), which has led some workers to interpret it as a strike-slip pull-apart rift (Yu et al., 1991). In Tibet the Bangong suture lies ~300 km north of the Indus-Tsangpo suture and separates the Lhasa crustal fragment on the south from the Qiangtang block on the north (Figures 2 and 3). To the southeast the suture is not exposed because of extreme Cenozoic deformation, but the Lhasa crustal fragment continues to the south into Myanmar as the Tengchong tectonic element. The Palaeozoic sequence of the Tengchong tectonic element is distinctly different from the Baoshan section of the Sibumasu continental fragment (Jin, 1994) and as a result, we interpret this

contrast to indicate that the Bangong suture continued south between these two fragments to connect with suture fragments assigned to the Nujiang suture in SW Yunnan and northern Myanmar.

Data from this suture zone is extremely limited and it is best studied segment is exposed near the Donqiao-Gyanco area in eastern Tibet (Figure 3). Here, Upper Palaeozoic low-grade metamorphic gray limestone, quartzite, and shale, containing radiolarians of Early and Late Jurassic age (Wang, 1980; Li Hongshang, 1986), are tectonically interleaved with well-developed ophiolites. Both the Upper Palaeozoic metasediments and the ophiolites were thrust southward above Middle-Upper Jurassic flysch (Hutchison, 1989), and all these rocks were then uncoformably overlain by Aptian-Albian red clastic strata and volcanic rocks (Girardeau et al., 1984). North of Dongqiao the ophiolites are covered transgressively by shallow water marine detrital sediments with foraminifers and algae indicating a Late Jurassic-Early Cretaceous age (Chang et al., 1981, Chang et al., 1989). Closure of the suture in Late Jurassic-Early Cretaceous time was followed by widespread deposition of Orbitolina-bearing late Early Cretaceous (Albian) limestones (Bally et al., 1980).

To the southeast, the Bangong suture zone is interpreted to turn abruptly southward around the eastern syntaxis of the Himalaya to follow the course of the Nu Jiang even though the suture zone itself is not well preserved and is cryptic due to intense shearing along the Gaoligong Shan shear zone in the Cenozoic. In the Luxi area of western Yunnan (Figure 3)Triassic flysch and ultramafic rocks are present and blanketed Middle Jurassic age strata (Bureau, 1990). These data gathered from very limited outcrops are interpreted to be the remnants of the Nujiang suture, the southern continuation of the Bangong suture. The data also indicate that Nujiang ocean was open during the Triassic, but was closed earlier than the Bangong suture to the north.

In Myanmar, a thick folded sequence of basaltic andesite and basalt pillow lava, named the Mawgyi Andesites (Mitchell, 1993), show similarities to the Donqiao ophiolite. Farther to the south the suture is interpreted to continue into the Mandalay region (Şengör and Natal'in, 1996). Further to the south, the suture is difficult to identify, though it is generally thought to follow the Sagaing fault and continue offshore along the eastern margin of the Andaman Sea (e.g. Metcalfe 1984, 1988). Alternatively, Min et al. (2001) have suggested the suture continues into the Gulf of Thailand, based on the sporadic occurrence of Triassic aged turbidites and pelagic sediments on the 1:250 000 geological map of Thailand.

DISCUSSION AND IMPLICATIONS TO ASIAN TECTONICS:

East and SE Asia is a giant jigsaw puzzle of continental fragments which have been multiply deformed due to the numerous collisions and post-collisional deformation that have affected the region, the last of which was the collision and the continued northward movement of India relative to Eurasia. The Sibumasu continental fragment (Metcalfe, 1984, 1986) represents the eastern part of the Cimmerian continent of Sengor (1979, 1984), but its extent, due to the difficulty in tracing its bounding suture zones, has remained ambiguous. The following interpretations regarding the definition of the Sibumasu continental fragment are based on the data reviewed and also our detailed field work carried along the GSSZ and the CSSZ, within the Baoshan section of the intervening Sibumasu tectonic element, as well as regional reconnaissance field work conducted along all accessible roads around the eastern Himalayan syntaxis.

(1) The Sibumasu tectonic element does not continue farther north than west-central Yunnan, and is not part of the Qiangtang tectonic element.(e.g. Metcalfe, 2002). The sedimentary rocks of the Baoshan section of the Sibumasu tectonic element, pinch out just south of Bijiang, in between the GSSZ and CSSZ, and have no continuation to the north (figure 2, 3 and 4).

(2) The southward continuation of the Changning-Menglian suture zone remains problematic and clearly requires additional detailed field work, however, the available data can be interpreted in at least three possible ways: (a) The Chiang Mai accretionary complex (Figure 3) is the southern continuation and the Nan-Uttaradit is back-arc marginal basin (Metcalfe, 2002). (b) The Nan-Uttaradit suture zone is the southern continuation (Figure 3), and the present left-lateral offset is due to a triple junction migration (Figure 5). In this interpretation, we assume that the Lancangjiang-Raub ocean, in the area south of the Changning-Menglian section, was subducting both to the east and the west, as suggested by Hutchison (1989) in order to explain the Permo-Triassic granites on both sides of the Nan-Uttaradit suture zone. We also assume that the Permo-Triassic aged Lincang granites were formed as a result of the easterly subduction of the more northerly Changning-Menglian segment of the same ocean. Once the section of the Uttaradit-Raub segment of the Lancangjiang-Raub ocean located in between the two subduction zones was consumed, the triple junction migrated to the west, offsetting the suture zone, but keeping the granitic batholiths, associated with the arc aligned. (c) The region between the Changning-Menglian-Chiang Mai and the Lincang granites in Yunnan and its southern continuation in Myanmar and Thailand, is a wide accretionary prism (the ruled area in Figure 3). This

wide accretionary prism was cut off in Cenozoic time by the CSSZ to the north, and cannot be followed to the north passed the Sibumasu continent. If this interpretation is correct, the accretionary prism, consists of rocks belonging mainly to the Sibumasu continental fragment. The accretionary prism cannot be followed south of the Three Pagodas Fault, after which it connects with the Sra Kaeo segment of the suture.

(3) The Lancangjiang segment of the Lancangjiang-Raub suture, and the Jinshajiang suture are probably the remnants of the same ocean, within a series of continental fragments and island arcs located in between (Figure 4).

(4) The Bangong-Nujiang ocean, which is probably a short-lived, fairly narrow sea embayment floored with an oceanic crust, bounds the Sibumasu tectonic element to the west, separating it from the Qiangtang, Lhasa and Burma tectonic elements (Figure 4). The Bangong section of this suture zone separated the Lhasa and the Qiangtang tectonic elements. The Nujiang section, however, separated the Qiangtang tectonic element, from the northernmost section of the Sibumasu tectonic element. These two suture zones, which separated different tectonic fragments lined up in the Cenozoic times, as a result of the right-lateral shearing along the GSSZ

This review summarizes our current knowledge of the suture zones bounding the Sibumasu continent, and puts constraints on its northern termination, and introduces a triple-junction migration hypothesis in explaining the possible separation of the Changning-Menglian and Nan-Uttaradit suture zones, if they indeed turn out to be continuous. Additional constraints on the extent of these suture zones may come from the extensive arc-associated granitic batholiths present in the area. These batholiths, which have been the focus of numerous geochemical studies, due to their tin content, are actually not well-documented

geochronologically. The northern continuation of the Lincang granites, which we interpret to be associated with the eastward subduction of the Lancangjiang-Menglian segment of the Lancangjiang-Raub ocean, and the southern continuation of the Gangdese granites, which are interpreted to be associated with the northward subduction of the Indus-Tsangbo ocean, need to be documented geochronoligically, which would also put additional constraints on the duration of subduction and its possible termination. However, regardless of these ambiguities, the close spatial correlation of these suture zones with the three Tertiary strike-slip shear zones, the GSSZ and the CSSZ (this thesis) and the ASSZ (e.g. Harrison et al., 1992; Leloup et al., 1993, 1995; Schärer et al., 1994, 1996; Harrison et al., 1996; Gilley et al., 2003) indicate that these pre-existing zones of weaknesses have played an important role on the collisional and post-collisional tectonics of Asia during the last 50 myr.

A better understanding of the location of the major and minor structures that were active during and following the various continent-continent collisional events, similar to the India-Eurasia collision, would place important constraints on the style of tectonic development of the region and also the types of processes that might have produced them. This requires the determination of at least the first order tectonic units, their boundaries, and the evolution of these boundaries through time, which has not been very easy to accomplish in Asia, not only because of the logistical problems such as political instabilities, lush vegetation, and deep chemical weathering, or very strong Cenozoic overprinting due to India – Eurasia collision, but also because of the uncoordinated scientific efforts that have not appreciated the regional relevance and the importance of the tectonic evolution of the regions they were studying. In our interpretation, crustal anisotropies, such has suture zones and volcanic arcs, will likely, but not necessarily reactivate after a continent-continent collision if they are also properly oriented. For

example, following the India-Eurasia collision, the Sibumasu and the Indochina tectonic elements were extruded to the southeast along the GSSZ, CSSZ and the ASSZ , all of which follow closely old suture zones. Continued indentation changed the original orientation of these shear zones, and caused the termination of shearing along them by ~18 Ma. There is no indication that these presently active structures, such as the Xianshuihe – Xiaojiang fault system (Wang and Burchfiel, 1997, Wang et al., 1998) has followed the older suture zones, or the Tertiary strike-slip shear zones, as zones of weakness. These faults, instead, are mostly new and oriented obliquely to the present trends of the suture zones and the strike-slip shear zones. The reasons for not taking advantage of the pre-existing zones of weaknesses within the crust can be numerous, which include: (1) unfavorable orientation of the zones of weaknesses within the stress regime, (2) the change of boundary conditions in eastern Asia with the collision of the Australian an Philippines Sea plates, (3) significant changes in the rheological properties of the deforming crust due to the progressive development of a weak lower crust (Royden et al., 1997; Clark, et al., 2004), that flowed from beneath Tibet, possibly resulting in the formation of a decoupling zone in the mid- to lower crust.

In conclusion, suture zones of Palaeozoic and Mesozoic age have likely caused the localization of deformation in the broad accommodation zone east of India indenter during early to mid-Cenozoic time. During late Cenozoic time, however, these suture zones have played a much more limited role in localizing deformation in the region east of the Eastern Himalayan syntaxis. Documentation of their exact location by detailed fieldwork, determination of the duration of their deformational histories by detailed geochronological studies would undoubtly vastly improve our understanding of the Cenozoic tectonic evolution of SE Asia.

Figure Captions

Figure 1. Schematic map of Cenozoic extrusion tectonics and large faults in Eastern Asia (modified after Tapponnier et al., 1986). Heavy lines indicate major faults or plate boundaries. Small arrows show senses of finite motion on strike-slip faults. Open arrows represent the sense of motion from Eocene until mid-Miocene. Shaded areas represent the regions affected by the different extrusion phases. Large open arrows represent the major block motions with respect to Siberia since the Eocene. Boxed area refers to Figure 2.

Figure 2. Location of the four major tectonic elements within the Three Rivers area and the three ductile strike-slip shear zones: T = Tengchong (Lhasa); Q = Qiangtang; LS = Lanping/Simao; B = Baoshan (Sibumasu) Dashed line within the Baoshan element is the Late Palaeozoic Changling-Mengliang suture. Strike-slip shear zones are shown in black with white stripes. The stripes orientation does not refer to the orientation of the fabrics observed within all three of these shear zones. Abbreviations: ASSZ = Ailao Shan Shear Zone; CSSZ = Chong Shan Shear Zone; DSSZ = Dianchang Shan Shear Zone; GSSZ = Gaoligong Shan Shear Zone; XS = Xuelong Shan; M = Mangkang; S = Simao. Inset map shows location of Figure 2, in relation to the India/Eurasia collision zone and the major tectonic blocks that form Eurasia. Abbreviations: SG = Songpan – Garze flysch belt, BNS = Bangong-Nujiang suture zone, LS = Lanchangjiang suture zone, SAS = Song Da – Anning suture zone; Y = Yidun volcanic arc; GL = Garze-Litang suture zone.

Figure 3. A map of SE Asia highlighting the location of the Sibumasu tectonic element and showing our current knowledge of its suture zones. Major active structures and major rivers are also shown. Each small box summarizes schematically the field observations at those particular sites, though the dip of the fault contacts may or may not represent the observed orientation. Abbreviations are: SF – Sagaing Fault, XF – Xianshuihe fault, XJF – Xiaojiang fault, RRF – Red River fault.

Figure 4. (a) A schematic map view diagram that shows the locations of the various tectonic elements that formed southeastern Eurasia prior to intense Cenozoic deformations. The segment of the main Paleo-Tethys ocean from Changning to Raub is the name of the ocean that separated Sibumasu from Indochina. Jinshajiang and Lancangjiang oceans likely refer to the

same, westernmost part of the same ocean separating mainland Eurasia from the Qiangtang block. Island arcs (e.g. the Yidun arc) and small continental fragments existed between the two. Nujiang suture is the suture between the Sibumasu and the Qiangtang blocks, and not a direct continuation of the Bangong suture. .(b) Traces of the major sutures in Tibet and western Yunnan (modified after Jin, 1994). 1- Indus-Tsangbo, (2) Bangong, (3) Lancangjiang, (4) Jinshajiang, (5) Indo-Burma, (6) Nujiang, (7) Changning-Menglian, 8) Song Da – Anding..

Figure 5. A simple diagram that shows the migration of a triple junction, that connects three subduction zones. Continued subduction brakes the zone into two segments and offsets the main trace of the subduction zone and the associated volcanic arc sequences left-laterally.

REFERENCES:

Bally, A.W., Allen, C.R., Geyer, R.B., Hamilton, W.B., Hopson, C.A., Molnar, P.H., Oliver, J.E., Opdyke, N.D., Plafkar, G., Wu, F.T., 1980. Notes on the Geology of Tibet and Adjacent Areas - Report of American Plate Tectonic Delagation to the People's Republic of China. U.S. Geological Survey open file report 80-501.

Barr, S.M., Macdonald, A.S., Yaowanoiyothin, W., Panjasawatwong, Y., 1985. Occurrence Of blueschist in the Nan River mafic-ultramafic belt, northern Thailand. Warta Geologi, 11, 47-50.

Barr, S.M., Macdonald, A.S., 1987. Nan river suture zone, northern Thailand. Geology, 15, 907-910.

Bureau of Geology and Mineral Resources of Yunnan Province, 1990, Regional Geology of Yunnan Province: Beijing, Geological Publishing House, 728 p.

Caridroit, M., Fontaine, H., Jongkanjanasoontorn, Y., Suteethorn, V., Vachard, D., 1990, First results of paleontological study of northwest Thailand. CCOP Technical Secretariat, p. 337-350.

Chang Cheng Fa, Pan, Yu Sheng, 1981. A brief discussion on the tectonic evolution of Qinghai-Xizang plateau. Proceedings of Symposium on Qinghai-Xizang(Tibet) Plateau, v. 1, p. 1-18.

Chang Chen Fa , Pan Yu-Sheng, Sun Yi-Ying, 1989. The tectonic evolution of Qinghai-Tibet Plateau; a review. In: Sengor, A. M. C. , Yilmaz, Y., Okay, A. I., Gorur, Naci (eds.), Tectonic evolution of the Tethyan region, NATO ASI Series. Series C: Mathematical and Physical Sciences , 259, p. 415-476.

Chen Bingwei and Xie Guanglian, 1994, Evolution of the Tethys in Yunnan and Tibet: Journal of Southeast Asian Earth sciences, v. 9, p. 349-354.

Chen, H., Dobson, J., Heller, F., Jie Hao, 1995, Paleomagnetic evidence for clockwise rotation of the Simao region since the Cretaceous: A consequence of India-Asia collision: Earth and Planetary Science Letters, v. 134, p. 203-217.

Chen, Z., Burchfiel, B.C., Liu, Y., King, R.W., Royden, L.H., Tang, W., Wang, E., Zhao, J., Zhang, X., 2000, GPS measurements from eastern Tibet and their implications for India/Eurasia intracontinental deformation, Journal of Geophysical Research, v. 105, p. 16,215–16,227.

Coward, M.P., Kidd, W.S.F., Pan, Y., Shackleton, R.M., Zhang, H., 1988, The structure of the 1985 Tibet geotraverse, Lhasa to Golmud. Philosophical Transactions of the Royal Society of London, Series A: Mathematical and Physical Sciences, 327 , p. 307-336.

Curray, J.R., Moore, D.G., Lawver, L.A., Emmel, F.J., Raitt, R.W., Henry, M., Kieckhefer, R., 1979, Tectonics of the Andaman sea and Burma, in Watkins, T.S. et al., eds., Geological and geophysical investigations of continental margins: AAPG Memoir no. 29, p.189-198.

Cobbold, P.R., and Davy, P., 1988, Indentation tectonics in nature and experiment 1. Central Asia: Geological Institute, University of Uppsala, v. 14, p. 129-141.

Dewey, J.F. , Shackleton, R.M., Chang C., Sun Y., 1988. The tectonic evolution of the Tibetan Plateau. In: The geological evolution of Tibet; report of the 1985 Royal Society - Academia Sinica geotraverse of the Qinghai-Xizang Plateau, Philosophical Transactions of the Royal Society of London, Series A: Mathematical and Physical Sciences, 327 , p. 379-413.

Dewey, J., Cande, S., and Pitman, W.C., III, 1989, Tectonic evolution of the India-Eurasia collision zone: Eclogae Geologicae Helvetiae, v. 82, p. 717-734.

Duan, Y., Xiao, Y., Hong, Y., Liu, Y., Zhao, Z., 1982. 1:200,000 scale geological map (Menglian) and technical report (in Chinese).

Girardeau, J., Marcoux, J., Allegre, C. J., Bassoullet, J. P., Tang Youking, Xiao Xuchang, Zao Yougong, Wang Xibin, 1984, Tectonic environment and geodynamic significance of the Neo-Cimmerian Donqiao Ophiolite, Bangong-Nujiang suture zone, Tibet: Nature (London), v. 307 , p. 27-31.

Gobbet, D.J., Hutchison, C.S., 1973. Geology of the Malay Peninsula, Wiley, Interscience, New York, p. 483.

Hada, S., Bunopas, S., Ishii, K., Yoshikura, S., 1997. Rift-drift history and the amalgamation of Shan-Thai and Indochina/East Malaya blocks. Proceedings of the international conference on Stratigraphy and tectonic evolution of Southeast Asia and the South Pacific , p. 273-286.

Hutchison, C.S., 1975. Ophiolite in SE Asia, Geological Society of America Bulletin, v. 86, p. 797-806.

Hutchison, C. S., 1989. Geological evolution of South-east Asia, Oxford Monographs on Geology and Geophysics, Clarendon Press, Oxford, pp. 368.

Hutchison, C. S., 1993. Gondwana and Cathaysian blocks, Palaeotethys suture and Cenozoic tectonics in South-east Asia. Geologische Rundschau, 82, 388-405.

Ichikawa, K., Ishii, K., Hada, S., 1966. On the remarkable unconformity at the Jengka Pass, Pahang, Malaya. J. Geosci. Osaka City Univ., 9, p. 123-130.

Jackson, J.A., 1980, Reactivation of basement faults and crustal shortning in orogenic belts: Nature, v. 283, p. 343-346.

Jin Xiaochi, 1994, Sedimentary and paleogeographic significance of Permo-Carboniferous sequences in western Yunnan, China. Geologisches Institut der Universitat zu Koln, Sonderveroefentlichungen, 136 p.

King, R.W., Shen, F., Burchfiel, B.C., Royden, L.H., Wang, E., Chen, Z., Liu, Y., Zhang, X.Y., Zhao, J.X. , Li, Y., 1997, Geodetic measurements of crustal motion in southwest China: Geology, v. 25, p. 179-182.

Li Hongsheng, 1986. Upper Jurassic (early Tithonian) radiolarians from Southern Banggong Lake, Xizang. Acta micropal. Sinica, 3, p. 297-315.

Liu Benpei, Feng Qinglai, Fang Nianqiao, 1991. Tectonic evolution of the Palaeo-tethys in Changning-Menglian Belt and adjacent regions, Western Yunnan. Journal of China University Geosciences, 2, p. 18-28.

Metcalfe, I. 1986. Late Palaeozoic palaeogeography of Southeast asia: Some stratigraphical, palaeontological and palaeomagnetic constraints. Geological Society of Malaysia Bulletin, 19, p. 153-164.

Metcalfe, I., 1988, Origin and assembly of South-East Asian continental terranes, in Audley-Charles, M.G., and Hallam, A., eds., Gondwana & Tethys, Geological Society of London Special Publication No. 37, p. 101-118. Oxford University Press.

Metcalfe, I. 1989. Triassic sedimentation in the central Basin of Peninsular Malaysia. In: Thanasuthipitak, T. & Ounchanum, P. (Eds.) Proceedings of International Symposium on Intermontane Basins. Geology and Resources. Chiang Mai University, Thailand, 173-186.

Metcalfe, I. 1992. Ordovician to Permian evolution of Southeast Asia terranes: NW Australian Gondwana connections. In: Webby, A. D. & Laurie, J. R. (Eds.) Global Perspectives on Ordovician geology.(Proceedings Sixth International Symposium on the Ordovician System.) A. A. Balkema, Rotterdam, 293-305.

Metcalfe, I. 1996 Gondwanaland dispersion, Asian accretion and evolution of Eastern Tethys. Australian Journal of Earth Sciences, Vol. 43, No. 6., 605-623.

Metcalfe, I., Spiller, F.C.P. 1994. Correlation of the Permian and Triassic in Peninsular Malaysia: New data from conodont and radiolarian studies. In, Angsuwathana, P., Wongwanich, T., Tansathian, W., Wongsomsak, S. and Tulyatid, J. (eds) Proceedings of the International Symposium on Stratigraphic Correlation of Southeast Asia, p. 129, Dept. Min. Res. Bangkok, Thailand.

Min Myo, Khin Khin Lin, Feng Qinglai, Chongpan Chonglakmani, Meischner, D., Ingavat-Helmke, R., Helmke, D., 2001. Tracing disrupted outer margin of Paleoeurasian continent through Union of Myanmar. Journal of China University of Geosciences, v. 12, p. 201-206.

Mitchell, A, H. G., 1993. Cretaceous-Cenozoic tectonic events in the western Myanmar (Burma)-Assam region. Journal of the Geological Society of London, 150, 1089-1102.

Pan, G., Zheng, H., 1983, A preliminary study on Bangong Co – Nujiang suture: Contributions to the Geology of Qinghai-Xizang (Tibet) Plateau, v. 12, p. 229-242.

Panjasawatwong, Y., Yaowanoiyothin, W., 1993. Petrochemical study of post-triassic basalts from the Nan Suture, northern Thailand. Journal of Southeast Asian Earth Sciences, 8, p. 147- 158.

Qin, D., He, C., Yang, J., Li, H., Chen, K., Yang, Z., Wnag, Z., Wang, J., 1980. 1:200,000 scale geological map (Baoshan) and technical report (in Chinese).

Ridd, M.F., 1980. Possible Palaeozoic drift of SE Asia and Triassic collision with China. Journal of the Geological Society of London, 137, Part 5, p. 635-640.

Royden, L.H., Burchfiel, B. C., King, R. W., Wang, E., Chen Zhiliang, Shen Feng, Liu Yuping, 1997, Surface deformation and lower crustal flow in eastern Tibet: Science, v. 276, p. 788-790.

Sashida, K., Igo, H., 1999. Occurrence and tectonic significance pf Paleozoic and Mesozoic radiolarian in Thailand and Malaysia. In: Metcalfe, I. (Ed.). Gondwana dispersion and

Asian Accretion. Final results Volume for IGCP Project 321A. A. Balkema, Rotterdam, pp/ 175-196.

Sashida, K., Igo, H., Hisada, K., Nakornsri, N., Ampornmaha, A., 1993, Occurrence of Paleozoic and early Mesozoic radiolarian in Thailand (preliminary report). Journal of Southeast Asian Earth Science, v. 8, p. 97-108.

Şengör, A.M.C., 1984, The Cimmeride orogenic system and the tectonics of Eurasia: Geological Society of America, Special paper 195, xi+82 pp.

Şengör, A.M.C., Altiner, D., Cin, A., Ustaomer, T., and Hsu, K.J., 1988, Origin and assembly of the Tethyside orogenic collage at the expense of Gondwanaland, in Audley-Charles, M.G., and Hallam, A., eds, Gondwana and Tethys: Geological Society Special Publications, no. 37, p. 119-181.

Şengör, A.M.C. and Natalin, B.A., 1996, Palaeotectonics of Asia: fragments of a synthesis: In Yin, A. and Harrison, T.M. (Eds.), The tectonic evolution of Asia. Cambridge University Press: p. 486–640.

Spiller, F.C.P. and Metcalfe, I. 1993. Late Palaeozoic radiolarians from the bengtong-Raub suture zone, Peninsular Malaysia – initial findings. In: Third International Symposium of 321 Gondwana dispersion and Asian accretion. Abstracts of Papers. 67-69.

Spiller, F.C.P. and Metcalfe, I. 1995. Late Palaeozoic radiolarians from the Bentong-Raub suture zone and Semanggol Formation, Peninsular Malaysia - Initial findings. Jour. Southeast Asian Earth. Sci. 11, 217-224.

Tapponnier, P., Peltzer, G., Le Dain, A.Y., Armijo, R., Cobbold, P., 1982, Propagating extrusion tectonics in Asia: new insights from simple experiments with plasticine: Geology, v. 10, p. 611-616.

Tapponnier, P., Peltzer, G., Armijo, R., 1986, On the mechanics of the collision between India and Asia: Coward, M.P., and Ries, A.C., eds., Collision Tectonics: London, Geological Society, Geological Society Special Publication, no. 19, p. 115-157.

Tjia, H. D. 1987. The Bentong Suture. In: Situmonang, B. (ed) Proceedings Regional Conference on Mineral Hyd. Resources of SE Asia. 73-85.

Tjia, H. D. 1989. Tectonic history of the Bentong-Bengkalis Suture. Geologi Indonesia, 12, 89-111.

Ueono, K., Igo, H., 1997, Late Paleozoic foraminifers from the Chiang Dao area, northern Thailand: geologic age, faunal affinity, and Palaeobiogeographic implications. Proceedings of the 13th International Congress on the Carboniferous and Permian, Krakow, Poland, 1997, pp. 339-358.

Wang, E., Burchfiel, B.C., 1997, Interpretation of Cenozoic tectonics in the right-lateral accommodation zone between the Ailao Shan shear zone and the Eastern Himalayan Syntaxis: International Geology Review, v. 39, p. 191-219.

Wang, E., Burchfiel, B. C., Royden, L. H., Chen Liangzhong, Chen Jishen, Li Wenxin, and Chen Zhiliang, 1998, Late Cenozoic Xianshuihe-Xiaojiang, Red River, and Dali fault systems of southwestern Sichuan and central Yunnan, China: Geological Society of Ameica Special Paper, no. 327, 108 p.

Wang Nai-Wen, 1980. Qingzang-India paleocontinent and its welding to Cathaysia. In: Li Guang-Cen, Mercier, J.L. (eds), Sino-French Cooperative Investigation in Himalayas, Geological Publishing House, Beijing, 1984, p. 39-58 (in Chinese).

Wang Zuguan, Tan Xuechun, 1994, Palaeozoic structural evolution of Yunnan: Journal of Southeast Asian Earth Sciences, 9 (4), p. 345-348.

Wu Haoruo, Boulter, C. A., Ke Baojia, Stow, D. A. V., Wang Zhongcheng, 1995. The Changning-Menglian suture zone; a segment of the major Cathaysian-Gondwana divide in Southeast Asia, Tectonophysics, 242, p. 267-280.

Wu Haoruo, Li, H., 1989. Carboniferous and Permian Radiolaria in the Menglian area, western Yunnan. Acta Micropalaeontol. Sinica, 6, p. 337-343 (in Chinese with English abstract).

Yu G., Wang, C., Zhang, S., 1991, The characteristic of Jurassic sedimentary basin of Bangong Co – Dengqen fault belt in Xizang. Bulletin of Chengdu Institute of Geology and Mineral Resources, v. 13, p. 33-44 (in Chinese).

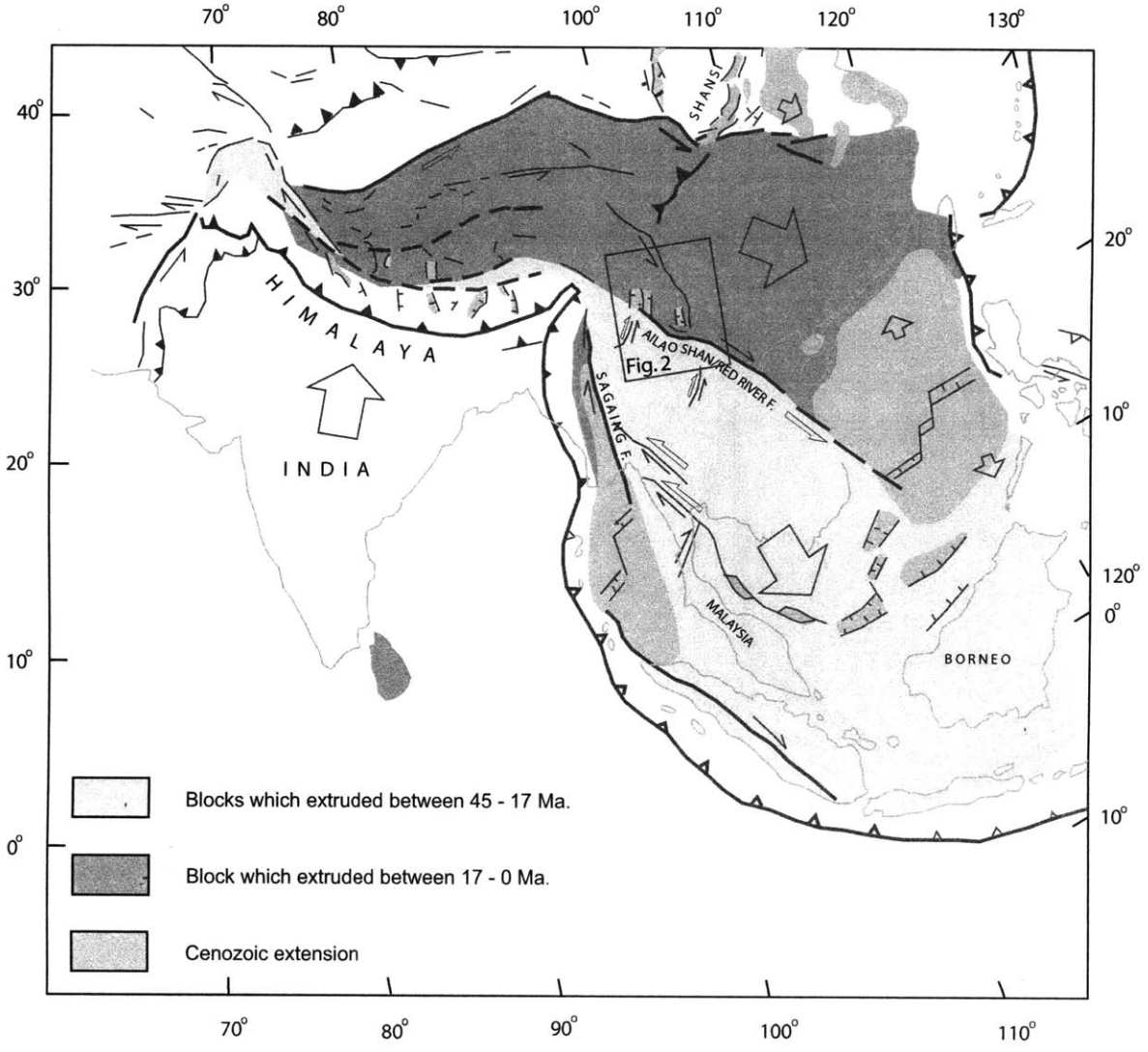
70°
80°
100°
110°
120°
130°
40°
30°
20°
10°
0°
20°
10°
120°
0°
10°
SHANSI
HIMALAYA
INDIA
AILAO SHAN-RED RIVER F.
Fig. 2
SAGAING F.
MALAYSIA
BORNEO
Blocks which extruded between 45 - 17 Ma.
Block which extruded between 17 - 0 Ma.
Cenozoic extension
70°
80°
90°
100°
110°

FIGURE 1

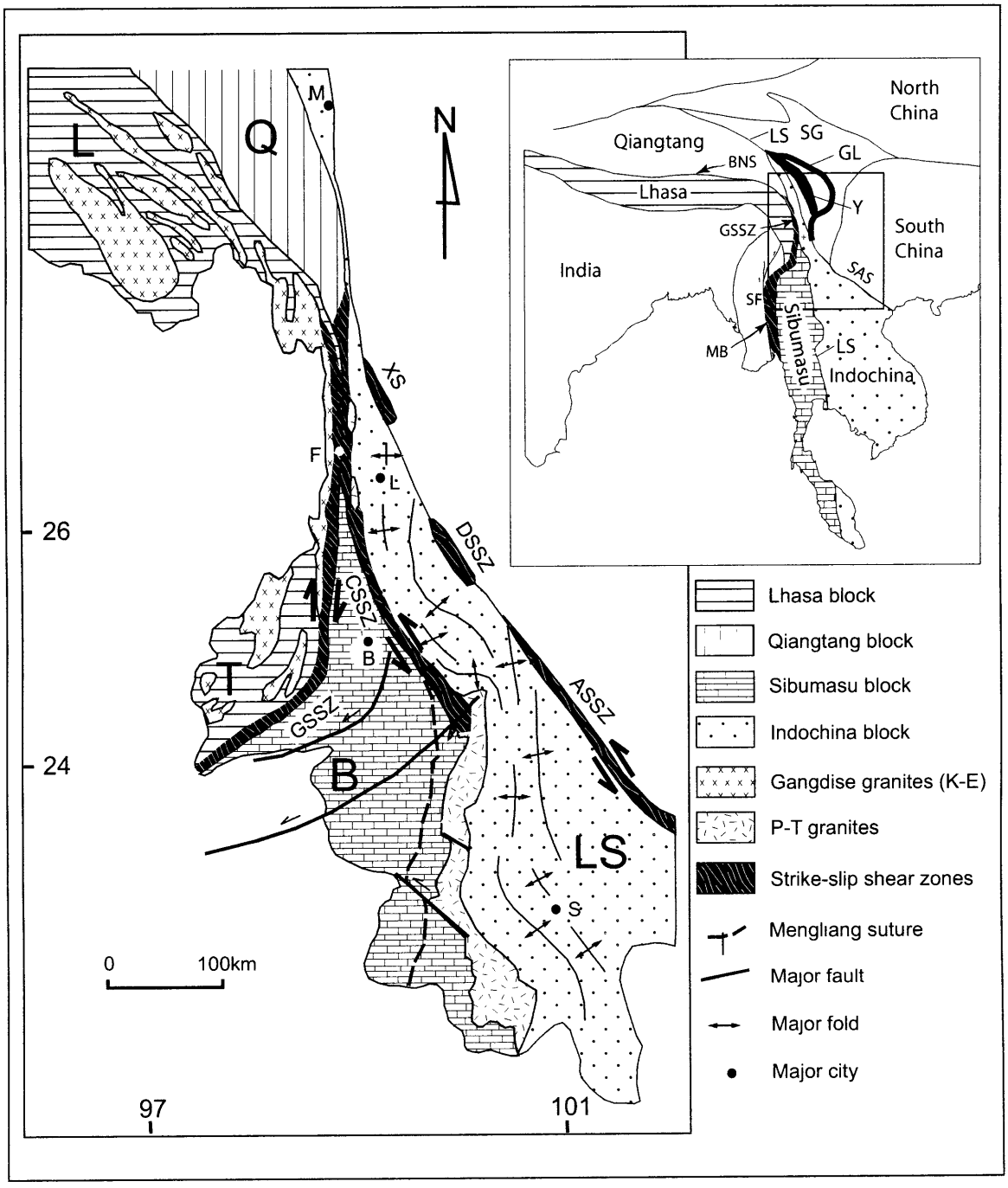
L
Q
M
N
XS
F
L
DSSZ
CSSZ
B
T
GSSZ
ASSZ
B
LS
S
26
24
0
100km
97
101
North China
Qiangtang
LS
SG
GL
BNS
Lhasa
Y
GSSZ
South China
India
SAS
SF
Sibumasu
MB
LS
Indochina
Lhasa block
Qiangtang block
Sibumasu block
Indochina block
Gangdise granites (K-E)
P-T granites
Strike-slip shear zones
Mengliang suture
Major fault
Major fold
Major city

FIGURE 2

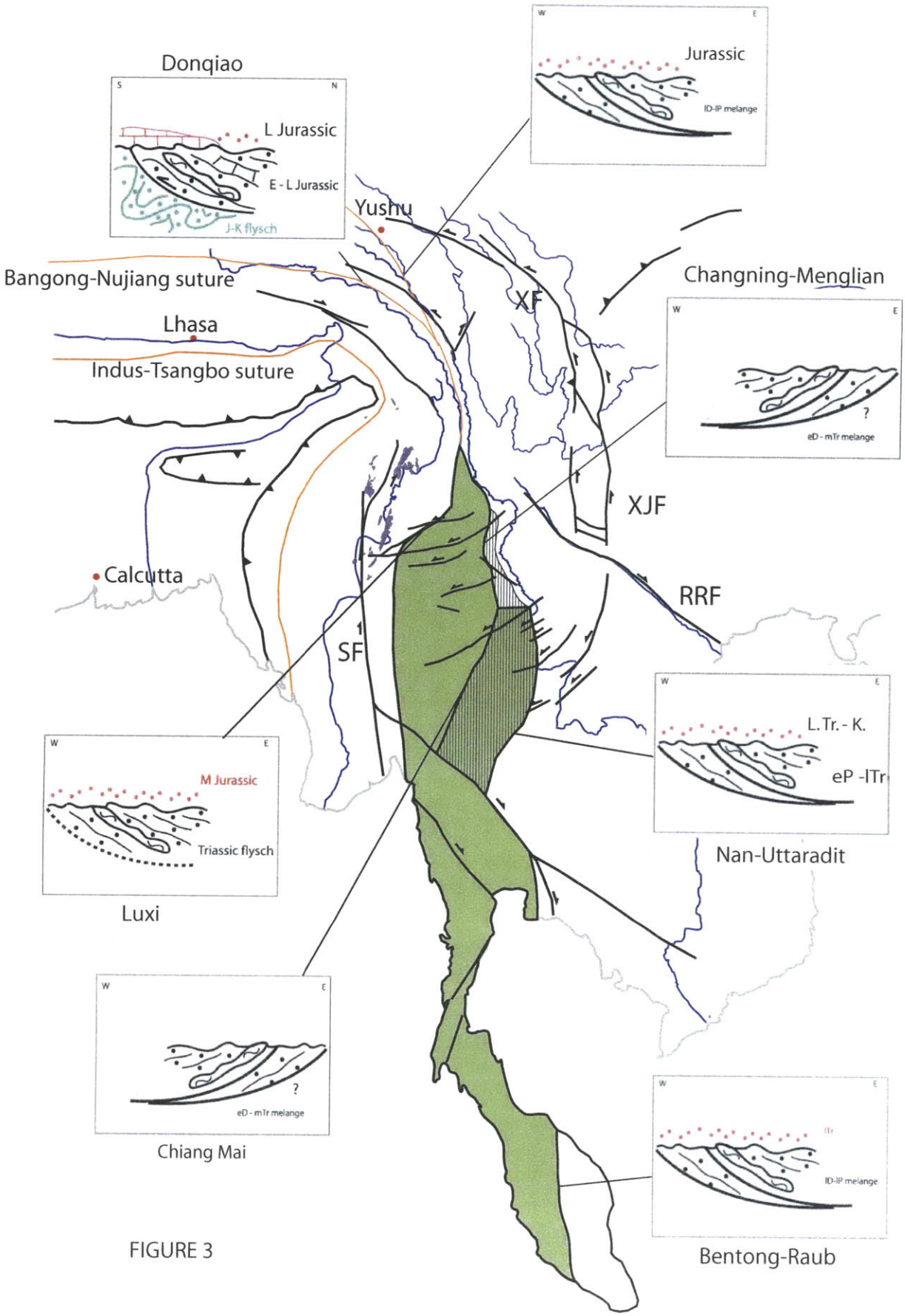
Donqiao
S
N
L Jurassic
E - L Jurassic
J-K flysch
W
E
Jurassic
ID-IP melange
Yushu
Bangong-Nujiang suture
Lhasa
Indus-Tsangbo suture
XF
Changning-Menglian
W
E
?
eD - mTr melange
XJF
Calcutta
RRF
SF
W
E
M Jurassic
Triassic flysch
Luxi
W
E
L.Tr. - K.
eP -lTr
Nan-Uttaradit
W
E
?
eD - mTr melange
Chiang Mai
W
E
lTr
ID-IP melange
Bentong-Raub

FIGURE 3

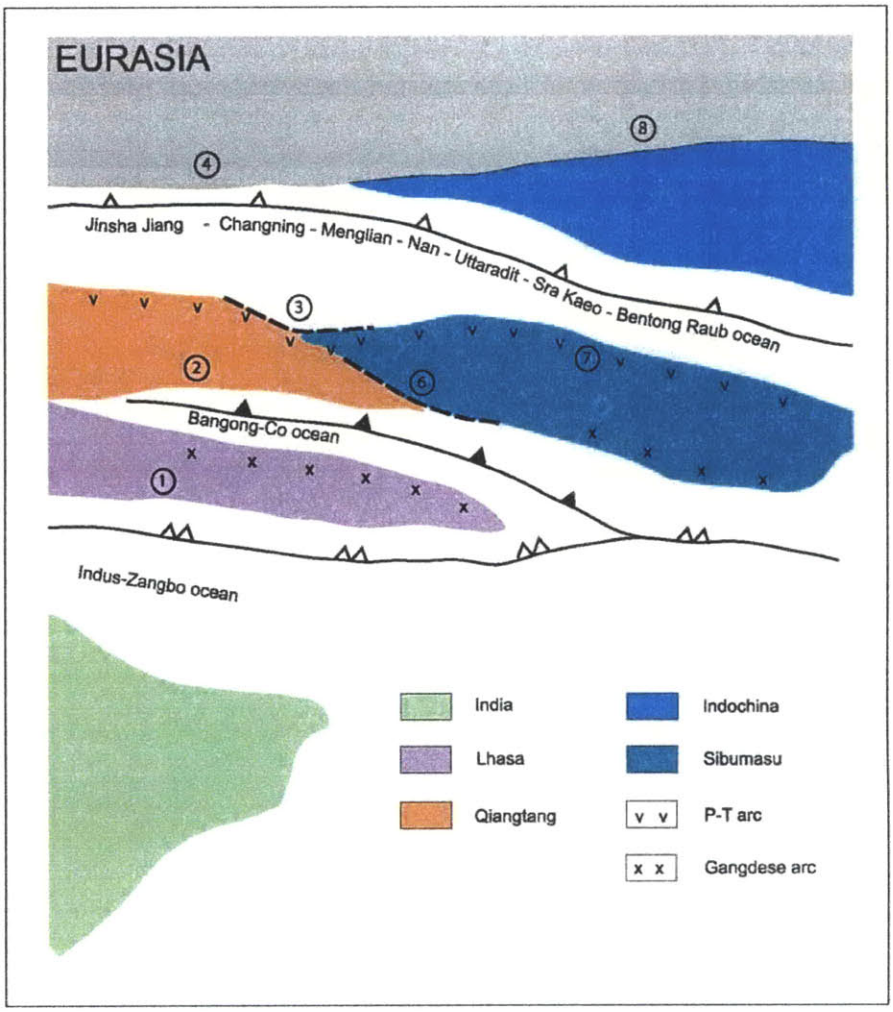
EURASIA
Jinsha Jiang - Changning - Menglian - Nan - Uttaradit - Sra Kaeo - Bentong Raub ocean
Bangong-Co ocean
Indus-Zangbo ocean
India
Lhasa
Qiangtang
Indochina
Sibumasu
P-T arc
Gangdese arc

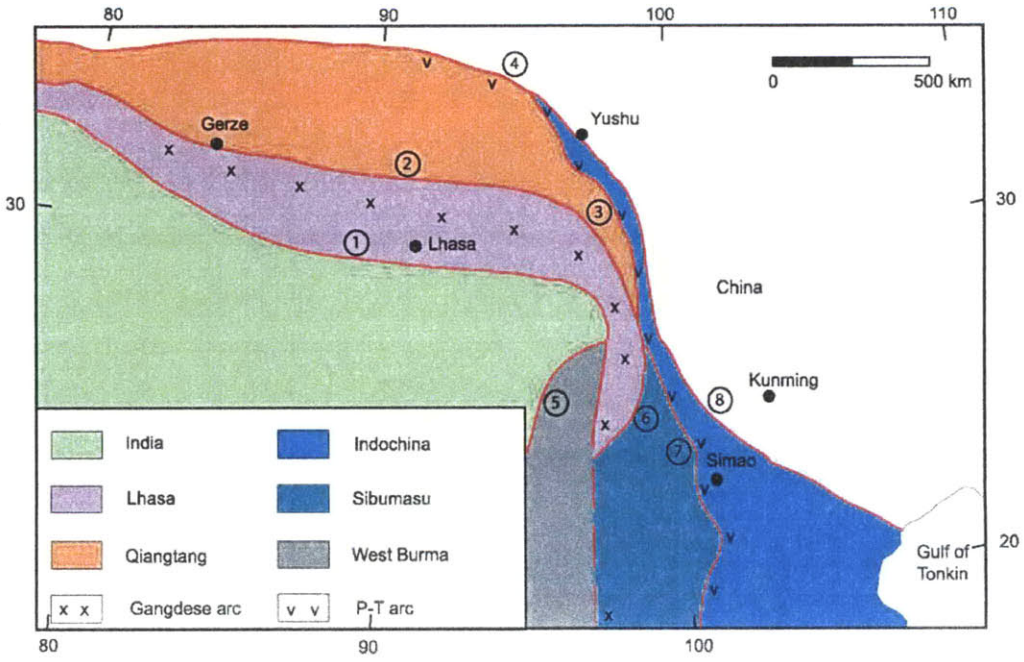
80
90
100
110
30
20
0
500 km
Gerze
Yushu
Lhasa
China
Kunming
Simao
Gulf of Tonkin
India
Lhasa
Qiangtang
Gangdese arc
Indochina
Sibumasu
West Burma
P-T arc

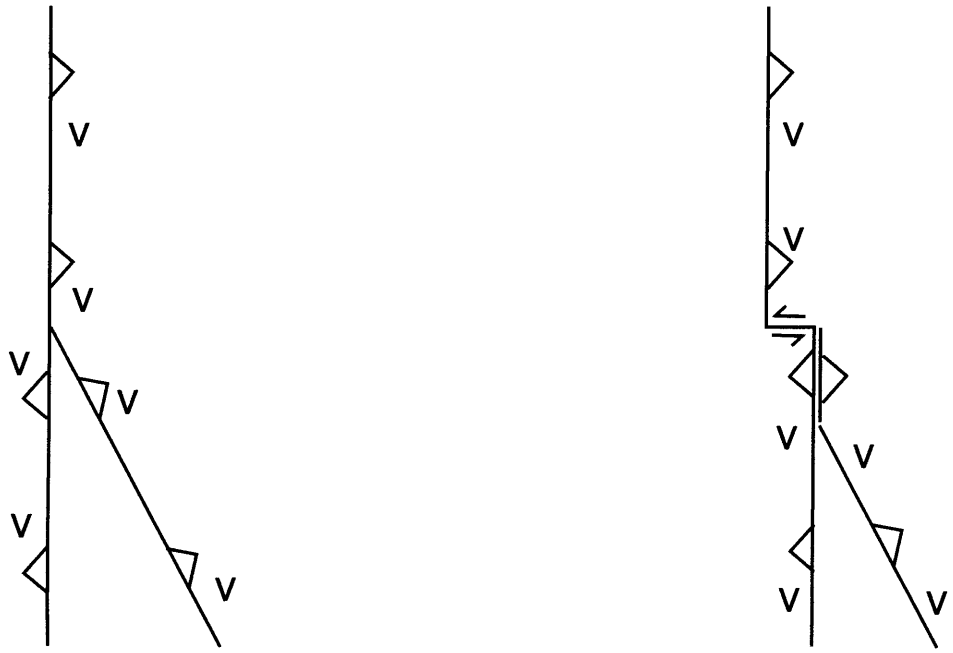

FIGURE 5

Chapter 6. CONCLUSIONS

The geology of the region between the eastern Himalayan syntaxis and the Ailao Shan Shear Zone (ASSZ) records part of the post-collisional Cenozoic motion between India and South China and our studies provide some of the best constraints yet for when, where and how India's penetration into Eurasia has been accommodated. Our primary conclusions are:

1- The GSSZ is not a belt of Precambrian metamorphic rocks as previously suggested (Bureau of Geology and Mineral Resources of Yunnan Province, 1990), but is an important dextral Cenozoic (and possibly latest Mesozoic) shear zone that accommodated some of the post-collisional indentation of India into Eurasia at least during the late Miocene (until ca. 18Ma). The presently inactive GSSZ appears to be the only right-lateral shear zone with the appropriate orientation to accommodate major pre- ca. 11 Ma northward movement of India relative to Eurasia. Cession of movement on the GSSZ was probably due to deformation of the shear zone by bending and displacement by oblique right-lateral strike slip faults.

2- The previously unknown Chong Shan shear zone (CSSZ) is a long (>300 km) and wide (10-20 km) metamorphic belt containing an assemblage low- to high-grade rocks from possibly several tectonic units which contain a prominent sub-vertical foliation and a sub-horizontal stretching lineation. CSSZ is mainly a left-lateral shear zone of regional importance during early Cenozoic extrusion.

3- During the early Cenozoic the crustal rocks within the map area has undergone both shortening and horizontal shear. Evidence for the shortening is the internal folding and thrusting within each tectonic element and the juxtaposition of mid-crustal rocks in the shear zone with essentially unmetamorphosed adjacent rocks. The vertical component of motion is also expressed by boudins with subhorizontal axes. However, the magnitude of vertical motion has been overwhelmed by large magnitude of horizontal shear that dominates the rocks fabrics. Many of the horizontal shear zones in the region show a similar relationship.

4- The motion along the CSSZ was contemporaneous with movement on the left-lateral Ailao Shan and the right-lateral Gaoligong Shan shear zones. Data presented in this thesis indicate that while the region between the GSSZ and ASSZ extruded to the southeast, it did not extrude as a single rigid block, but rather it was dismembered into at least two major crustal fragments.

5- The Baoshan crustal fragment, separated by the GSSZ and CSSZ pinches out to the north in NW Yunnan and does not have an equivalent in Tibet. The Baoshan fragment continues south into Indochina where it forms part of the larger Sibumasu crustal fragment. The kinematics of the CSSZ indicate the Baoshan fragment moved to the SE relative to the Lanping-Simao fragment that lies to the NE. Where the two shears zones merge, the CSSZ contains right-lateral shear sense indicators along its western side, suggesting that shearing in the GSSZ influenced the CSSZ after they merged and shows the complexity of movements between these two crustal fragments during extrusion.

6- This thesis documents the dextral GSSZ as the conjugate pair to the sinistral ASSZ, and thus constrain the limits of the crustal fragments that extruded to the southeast. Based on our reinterpretations of the geological maps of Tibet and the Three Rivers area, however, we propose that the extruded crustal material originated east of the easternmost corner of the Indian indentor, and did not create space for the penetration of India by getting out of the way. While at least limited extrusion did occur, there is no compelling geological evidence to indicate large-scale eastward movement of crustal material from directly north of the India indentor.

7- The northern continuations of the GSSZ, the CSSZ and the ASSZ, still remain enigmatic. We propose that all three of the strike-slip shear zones pass into and terminate within the Bangong-Nujiang suture zone. The Sibumasu and the Indochina tectonic elements would need to move eastward more than 1,500 km along the Bangong-Nujiang suture and the GSSZ and the ASSZ, in order to play a significant role in accommodating the indentation of India into Eurasia, but presently there is no geological evidence to indicate that such large movements took place.

8- According to our new kinematic interpretation deformation within the Sibumasu/Lanping-Simao tectonic element began in late Eocene time, shortly after the

India-Eurasia collision. NE-SW shortening and both right-lateral and left-lateral strike slip deformation began in western Yunnan. During Oligocene to approximately middle Miocene time, the region between the GSSZ and the ASSZ was shortened and displaced to the southeast relative to South China and parts of eastern Tibet. The continued indentation, however, modified the extruding tectonic elements, as well as their margins, and the deformation within both the Sibumasu and Indochina crustal fragments was heterogeneous. The Sibumasu fragment was dismembered it into numerous rhomb-shaped crustal blocks, bounded mainly by strike-slip faults, which ultimately was partly responsible for the bending and distortion of the GSSZ. These blocks formed in response to the rotation and bending of the Sibumasu/Indochina tectonic element as it moved around the eastern Himalayan syntaxis. By ~18 Ma, the northern part of the GSSZ rotated until it was no longer favorably oriented to accommodate India's continued northward movement. At that time a new fault, the northern part of the Sagaing fault, broke immediately west of the mylonitic GSSZ.

Once southeastward extrusion of the Sibumasu/Indochina composite tectonic unit ceased, a new style of deformation began to affect the region, east of the Eastern Himalayan Syntaxis. Since at leastPliocene time, the Xianshuihe – Xiaojiang and Zongdian fault systems and their probable southward continuations bounded on the east by the Dien Bien Phu fault, gradually became the dominant structures accommodating indentation by the clockwise rotation of the southeastern Tibetan plateau (Wang and Burchfiel, 1997; King et al., 1997; Wang et al., 1998; Chen et al., 2000). Although the right-lateral Red River fault developed in late Miocene or Pliocene time, along part of the older left-lateral Ailao Shan shear zone, the amount of right-lateral displacement has been small, perhaps no larger than ~ 40 km (Allen et al., 1984; Replumaz et al., 2000; Wang et al., 1998; Schoenbohm 2004). Thus the amount of late Cenozoic eastward movement of the region between the Red River fault and the Altyn Tagh fault as proposed by Tapponier et al. (1982, l986) may be small and the large-scale extrusion of a large part of Tibet on individual faults may not occurred. Rather, the right-lateral movement on the Red River fault was result of the counterclockwise rotation of the ASSZ and differential extension north and south of the fault (Wang et al., 1998; Schoenbohm, 2004).

9- The Cenozoic Gaoligong Shan, Chong Shan and Ailao Shan strike-slip shear zones are located either along or close to the Bangong – Nu Jiang, Lanchang Jiang, Jinshajiang and Song Da - Anding suture zones, respectively. Any dynamic model which deals with the Cenozoic deformational history of the India – Eurasia collisional zone, therefore, must take into account the pre-existing heterogeneities of the crust and lithosphere before collision of a continental crustal fragments such as Sibumasu or India, as well as their complex fragmentation and deformation and the temperal change in crustal rheology. However, our present knowledge of these suture zones are very limited.

10- Much more detailed mapping and radiometric dating of rocks from within the suture zones and also the shear zones need to be done. Future geochronological studies conducted in this area must BSE image every grain, produce chemical maps of selective grains based on the BSE images, and date fragments corresponding to each domain. Such detailed geochronological studies are necessary to interpret important, but complicated, geochronological data similar to the those presented in this thesis.

REFERENCES:

Allen, C.R., Gillespie, A.R., Han Yuan, Sieh, K.E., Zhang Buchun, Zhu Chengman, 1984, Red River and associated faults, Yunnan Province, China: Quaternary geology, slip rates, and seismic hazard: Geological Society of America Bulletin, v. 95, p. 686-700.

Bureau of Geology and Mineral Resources of Yunnan Province, 1990, Regional Geology of Yunnan Province: Beijing, Geological Publishing House, 728 p.

Chen, Z., Burchfiel, B.C., Liu, Y., King, R.W., Royden, L.H., Tang, W., Wang, E., Zhao, J., Zhang, X., 2000, GPS measurements from eastern Tibet and their implications for India/Eurasia intracontinental deformation, Journal of Geophysical Research, v. 105, p. 16,215–16,227.

Leloup, P. H., Lacassin, R., Tapponnier, P., Zhong Dalai, Liu Xiaohan, Zhang Lianshang, Ji Shaocheng, Phan Trong Trinh, 1995, The Ailao Shan-Red River shear zone (Yunnan, China), Tertiary transform boundary of Indochina: Tectonophysics, v. 251, p. 3-84.

Schoenbohm, L., 2004, Cenozoic tectonic and geomorphic evolution of the Red River region, Yunnan Province, China [PhD Thesis] Boston, Massachusetts Institute of Technology, 235 p.

Tapponnier, P., Peltzer, G., Le Dain, A.Y., Armijo, R., Cobbold, P., 1982, Propagating extrusion tectonics in Asia: new insights from simple experiments with plasticine: Geology, v. 10, p. 611-616.

Tapponnier, P., Peltzer, G., Armijo, R., 1986, On the mechanics of the collision between India and Asia: Coward, M.P., and Ries, A.C., eds., Collision Tectonics: London, Geological Society, Geological Society Special Publication, no. 19, p. 115-157.

Wang, E., Burchfiel, B.C., 1997, Interpretation of Cenozoic tectonics in the right-lateral accommodation zone between the Ailao Shan shear zone and the Eastern Himalayan Syntaxis: International Geology Review, v. 39, p. 191-219.

Wang, E., Burchfiel, B. C., Royden, L. H., Chen Liangzhong, Chen Jishen, Li Wenxin, Chen Zhiliang, 1998, Late Cenozoic Xianshuihe-Xiaojiang, Red River, and Dali fault systems of southwestern Sichuan and central Yunnan, China: Geological Society of America Special Paper, no. 327, 108 p.

Appendix A:

1:350,000 Geological map of the Salween River Gorge.

Appendix A: Geologic map of the study area along the Salween River. Insets are Schmidt diagrams (lower hemisphere) that show mylonitic foliations and stretching lineations in mylonitic gneisses of the (a) northern GSSZ, north of Lisadi, (b) CSSZ along the Shidu section, (c) CSSZ along the LiShiNerHe section, (d) CSSZ along the Bijiang section, (e) central GSSZ in between Lisadi and Bijiang, and (f) southern GSSZ, south of Bijiang.

98°36'0"E
98°42'0"E
98°48'0"E
98°54'0"E
99°0'0"E
99°6'0"E
27°6'0"N
26°30'0"N
26°24'0"N
26°18'0"N
26°12'0"N

(e)

n = 402

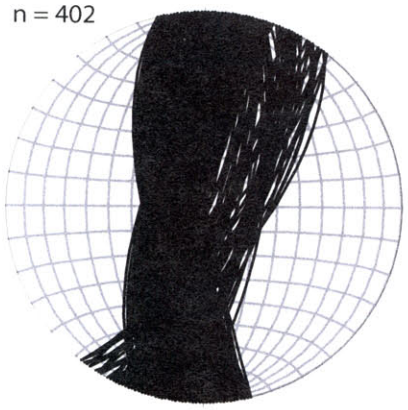

n=181

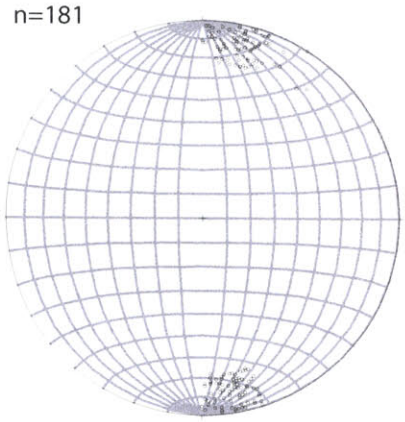

(f)

n=361

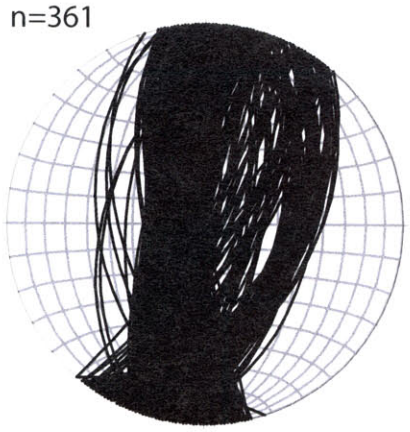

n=323

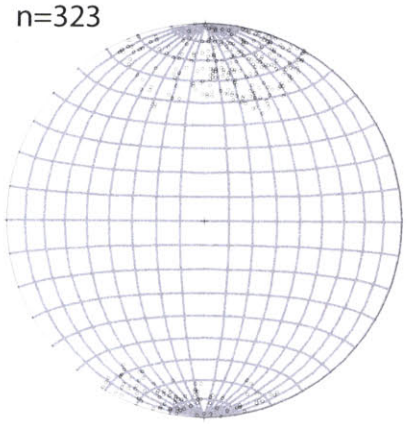

(d)

(n = 63):

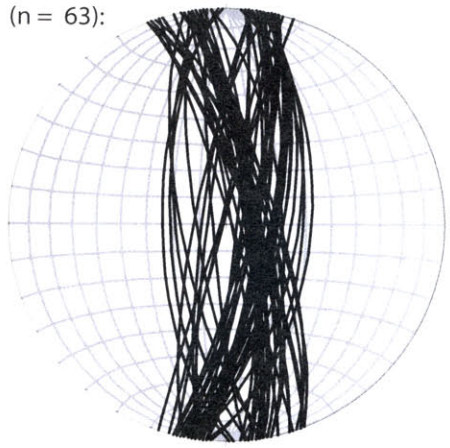

(n = 31):

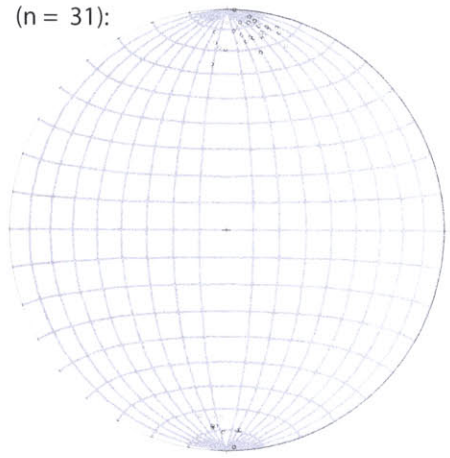

Fugong

Bijiang sect.

Bijiang

72 72 79 83 87 89 72 80 60 86 89 74 72 74 82 67 72 74 79 76 75 87 83 88 83 76 77 74 69

Geological map of the Salween River Gorge
1:350,000

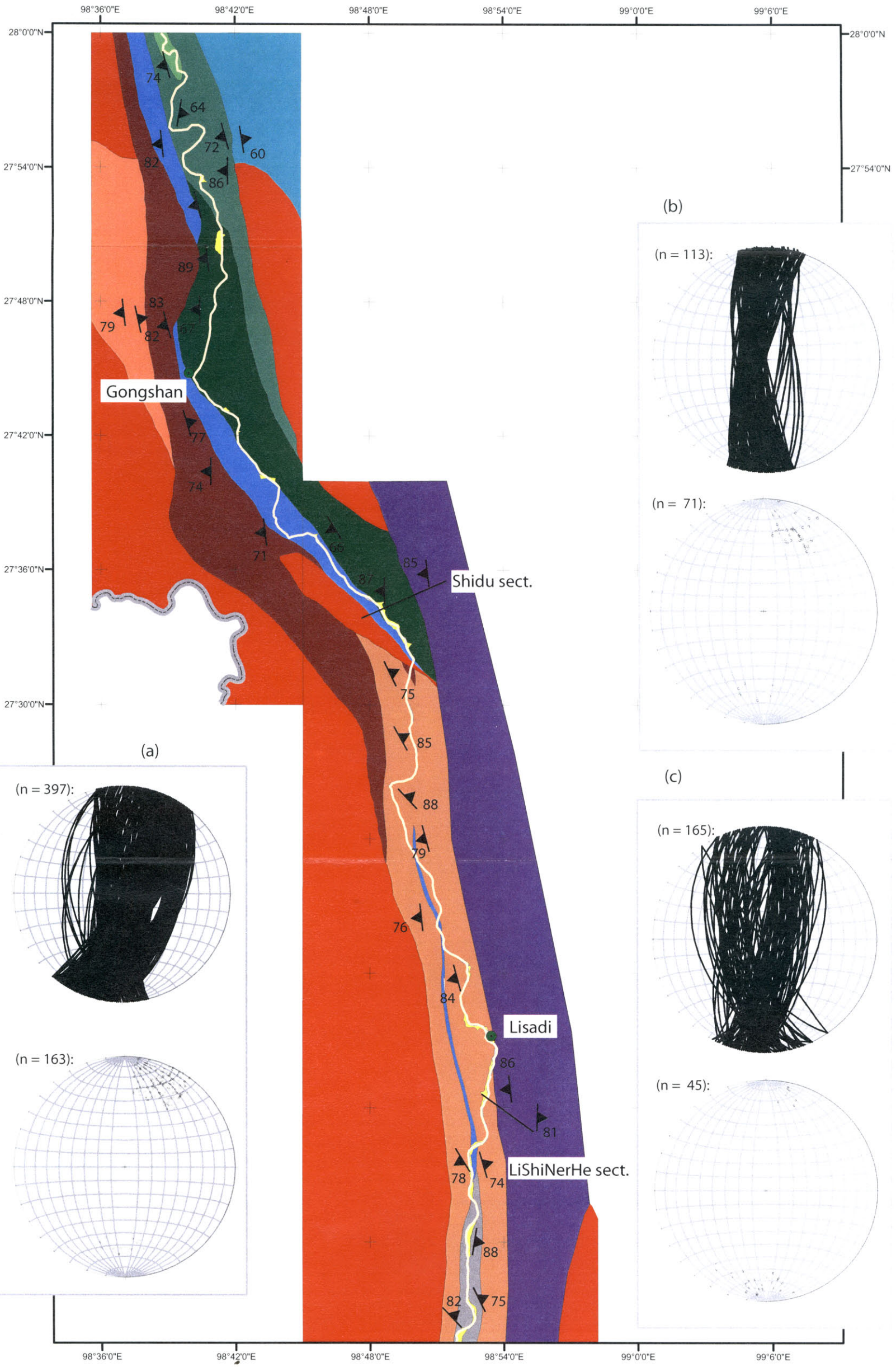

Appendix B. Geography of western Yunnan

"As a young man, my fondest dream was to become a geographer. However, while working in the customs office I thought deeply about the matter and concluded it was too difficult a subject. With some reluctance I then turned to physics as a substitute."

> Duane F. Marble (Professor Marble wrote the quote and put it on his office door at SUNY at Buffalo in response to the cool welcome received by the geography department which had taken over part of the physics building).

Geography

Figure 1 Geographic map showing the location of the Yunnan Province along with its major towns and rivers.

Yunnan (in Chinese, *South of the Clouds*), with a population of 40 million, is the eighth largest province in China, has an area of 394,000 square kilometers (Figure 1). It borders Guizhou Province and Guangxi Autonomous Region on the east, reaches north to Sichuan Province and the Tibetan Autonomous Region. On the west and the south it borders Myanmar, Laos and Vietnam.

Kunming is the capital of Yunnan. Kunming is known to the world as "Spring City" for its spring like climate-winters without bitter cold and summers without scalding heat. It is also a major industrial base in southwest China. Major industries of the city include: machinery, electronics, tobacco, medicine, perfume, metallurgy, and phosphorous chemical industry.

Yunnan is a part of the Yunnan-Guizhou plateau where the average elevation is 2,000 meters above sea level. From north to south, the height gradually drops from 6,700 meters at the peak of Meili Snow Mountain to 76 meters in the south close to Vietnam. The whole geographical feature of Yunnan mountain is a big slope inclining from the northwest to the southeast and are cut by four famous rivers (Salween, Mekong, Yangtze, and Red River) (Figure 2). Salween (Nu Jiang) and Mekong (Lancang Jiang) follow major north-south trending structural lineaments, which is the focus of this thesis work, and traverse the whole of western Yunnan (Figure 1). The Yangtze (Jinsha Jiang), runs southward in its upper reaches, parallel to the Salween and the Mekong, cuts accross the Lanping - Simao folded redbeds to take its easterly course to the Pacific. The Red River begins near Dali and runs along the seismically active Red River Fault along its entire course until it reaches the South China Sea.

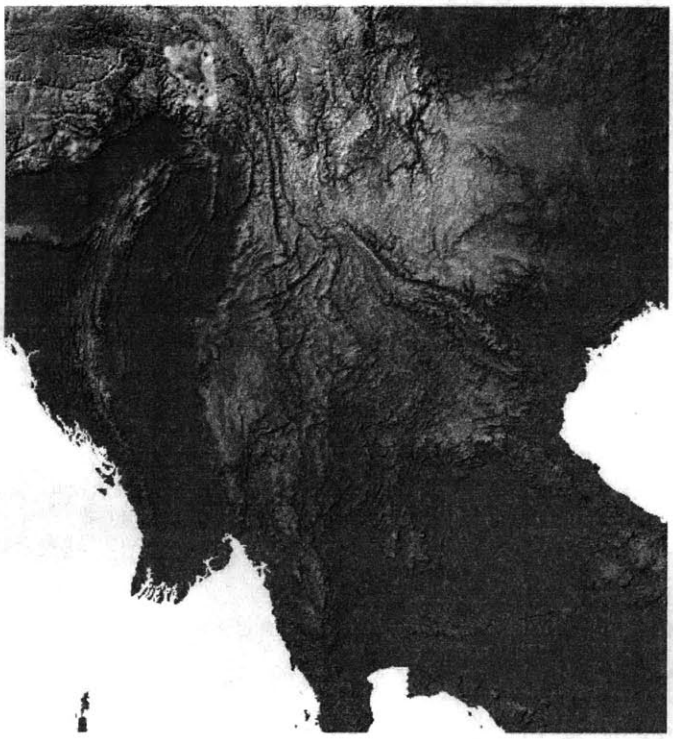

Figure 2 A Digital Elevation Model (DEM) reduced from GTOPO30 data showing the big inclined topography between the Tibetan Plateau and the SE Asia lowlands.

The eastern half of the province is a limestone plateau with karst scenery and a network of rivers flowing through deep mountain gorges, whereas, the western half is characterized by mountain ranges and rivers running north and south (Figure 3).

In mountainous areas, forests not only provide wood for fuel and timber for building houses and making furniture, but also are main sources of food, livestock feed, and cash income. In the period of short supply of grains, farmers pick up variety of wild shoots, leaves, flowers, fruits and roots in forests in order to meet family needs. In the rainy season, they collect mushrooms in forests for family consumption or being sold at local market. In many places of Yunnan, there are some examples that farmers benefit and become rich by planting medicinal plants or mushroom in forests, or managing cash trees gardens. Because of traditional cropping methods, poor information and transportation, and rapid increase of population have resulted in the exhaustion of forest resources, environment deterioration, and decline in farmers' living standards in most mountainous areas.

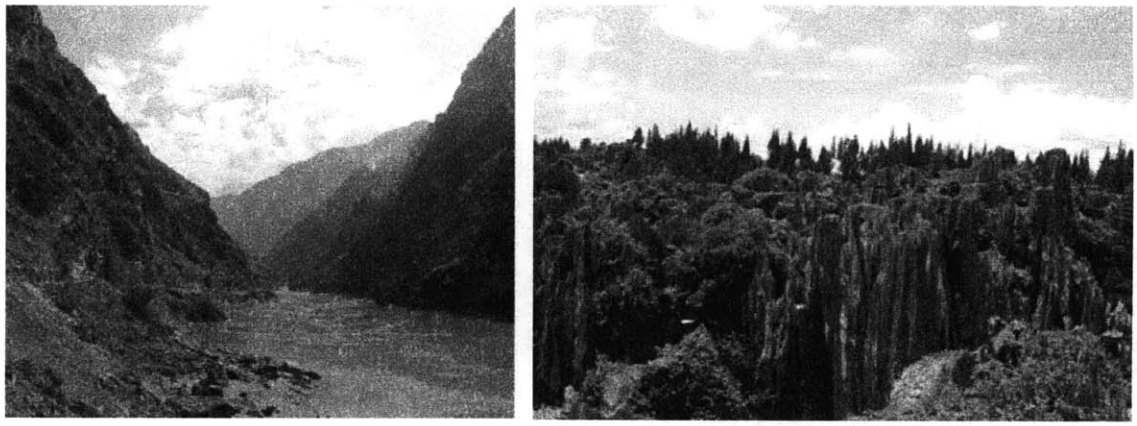

(a) (b)

Figure 3. Two major morphological features of the Yunnan Province. (a) Salween (Nu) river is one of the four major rivers which cut deep into the bedrock and form deep gorges. (b) The eastern half of the province is a limestone plateau with beautiful karst scenery.

The rugged, vertical terrain produces a wide range of flora and fauna, and the province has been called a natural zoological and botanical garden. Agriculture is restricted to the few upland plains, open valleys, and terraced hillsides. Rice is the main crop, but corn, wheat, sweet potatoes, soybeans (as a food crop), tea, sugarcane, tobacco, and cotton are also grown. On the steep slopes in the west livestock is raised and timber is cut (teak in the southwest). However, Yunnan's chief source of wealth lies in its vast mineral resources. It is the country's leading tin producer. Other deposits include iron, coal, lead, copper, zinc, gold, mercury, silver, antimony, and sulfur.

Yunnan has sufficient rainfall and many rivers and lakes. The annual water flow originating in the province is 200 billion cubic meters, three times that of the Yellow River. The rivers flowing into the province from outside add 160 billion cubic meters, which means there are more than 10,000 cubic meters of water for each person in the province. This is four times the average in the country. The rich water resources offer abundant hydro-energy.

In order to fuel its ever-expanding industrial growth China is in need of more electricity, and its latest plan involves harnessing the power of the Nu river to build 13 hydro-electric dams. It will rank along side similar developments by China on the Yangtze and Mekong rivers.

Road and railroad traffic has been recently improved and Kunming is now a transportation center of the province. Traveling to Fugong, from Kunming is not very easy and can be very adventuresome north of LiuKu. Deforestation and heavy rainfall cause numerous landslides on the steep banks of the Nujiang valley. Flashfloods, overfilled tributaries and raised levels of the Salween river often cause sections of this one and only road to be obstructed. The road goes as far north as the town named BinZhongLuo, just north of Gongshan. The section of the road from LiuKu to BiFuQiao is on the west side of the river, whereas the section from BiFuQiao to Gongshan is on the east side. From Gongshan to BinZhongLuo, the road is again on the east bank of the river. Bridges are an inseparable part of the Nujiang valley road. Turbulent waters, however, mean most bridges are suspension bridges other than the two big ones where the road goes across the river. Locals, in general, have no choice but to use rope bridges and cables to cross the river, in order to avoid walking long distances to reach these bridges.

Climate & Population

The mixed influences of the topography, Indian monsoon and the Pacific monsoon, create a distinct climatic condition where nearly all types of climates from the tropical to pole can be found in the province. To the west, the valley floors and lower slopes of this mountainous area enjoy warm humid weather, while a temperate zone stands between 2,000 to 3,000 metres, and ice and snow envelop the high summits. In general, most areas in Yunnan have subtropical

weather featuring two seasons: the dry season in Winter and Spring and the wet season in Summer and Autumn, in south part of province and some river valleys, there exist tropical climate types. It is diverse topography and weather conditions that provide different habitats for various vegetation types and animals. It is almost impossible to find a dry field season at the Salween gorge, though August and September are known to be the rainiest. January is drier, though the high peaks get a lot of snow, and cover most of the best exposed sections of the mountains.

With a population of 40 million, Yunnan has the most nationalities in the great family of China. There are 24 minority nationalities, that include over 12 million people, constituting one third of the province's total population and one sixth of China's total minority population. From ancient times the Chinese invaders gradually pushed the aboriginal tribes into mountain localities, where today, retaining their distinct languages and culture, they populate eight autonomous districts. The Miao, Yao, Lolo, Lao, Shan, Thai, and Lisu are some of the larger tribes; there is also a considerable Tibetan minority. They display their rich and distinctive features, such as the vastly different styles of buildings, the various colorful costumes and ornaments, the folk songs and dances brimming with idyllic flavors and very interesting marital customs. The predominate group is the Han as in China as a whole. While many languages are spoken and written by the different minorities Mandarin is the official language. A very interesting but totally different from Chinese characters is the written language still practiced by the Naxi of Lijiang (Figure 4a).

The town of Fugong and the villages between Binzhongluo and LiuKu are dominantly inhabited by the Lisu people (Figure 5a). The Lisu people mainly engage in agriculture and hunting. In the past, the Lisu people worshiped many gods, nature and a multitude of other things. Religious professionals made a living by fortune-telling and offering sacrifices to ghosts. In early 20th century, however, Christianity was introduced to the Lisu in the Dehong and Nujiang regions by western missionaries who also created a written language consisting of upsidedown latin alphabet letters, and published the only book in this language, the Bible (Figure 4b).

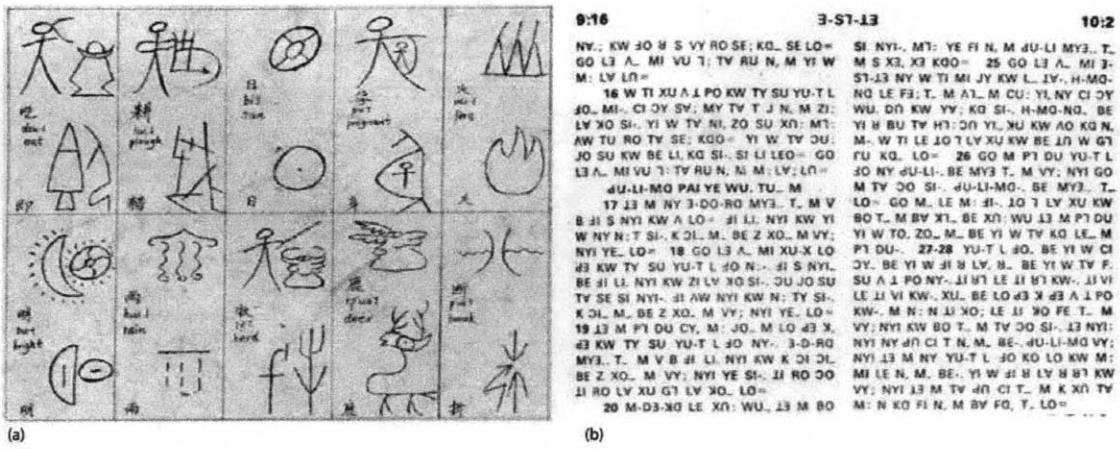

Figure. 4. Examples of two very interesting written alphabets used by the minorities in the Yunnan Province. (a) Naxi writing. (b) The Bible is the only published book in the Lisu language.

Durong people live in a remote area which can only be reached by hiking for about 60 kilometres northwest of Gongshan. The Durong have very distinctive costumes that include draping a decorated hemp cloth over their shoulders. Men and women have particular ways of wearing the cloth: men put them sideways across the back and tie a knot in front while women wear two square cloths that go down to the knees. Every male Durong is a good hunter, and wild ox and goat horns are hung in front of every house. Tradition says that the more horns there are the more courageous and successful the hunter is. The Durong also live off the fish in the Durong River.

The Durong are one of the very few Chinese minorities to have customary tattooing of the face (Figure 5b). Most interesting is that only women middle-aged or older have tattoos. Lines are drawn between the eyebrows, on the nose bridge, the cheeks and around the mouth with black ash from the cooking stove. Then a needle is used to prick along the lines, and black ashes rubbed on. Three to five days later, the designed pattern will appear in deep blue.

There are several interpretations of this custom. One holds that tattoos are symbols of beauty; another has it that tattoos can scare off evil spirits; still another says tattoos serve as distinguishing marks of clans or tribes.

(a) (b)

Figure 5 Salween river is inhabited by mainly two minorities. (a) Lisu, and (b) Durong people who tattoo their face (http://www.expo99km.gov.cn).

Brief History

Though the plains of Yunnan were originally the home to numerous aboriginal tribes, Chinese invasions over several centuries pushed them into mountainous areas, where many ethnic groups, direct descendants of those original tribes live today. The powerful Tai kingdom of Nanchao held sway over Yunnan for 247 years, during the Tang dynasty (AD 618-907), but was replaced by the Dali Kingdom in 937AD. For 300 years, Dali ruled supreme until, in 1253, it was over-run by Kublai Khan's Mongol hordes and assimilated into his growing empire. The take-over turned out to have many positive effects. The capital was moved to Kunming, trade with the rest of the empire stimulated the local economy, living standards improved, and ethnic relations improved. Kunming had become a prosperous city by the time Marco Polo arrived, and was renowned for its skilled craftsmen.

During the 14th century, several hundred thousand troops, civilians, and officials were dispatched to the province by the Ming Court to set up military outposts and reclaim land. Agriculture, mining, and social development all benefited from the influx of expertise. In the

mid-17th century, Manchurian troops occupied most of the central areas of China, and the Qing Dynasty took the reigns of power in Yunnan.

China's national power was weakened after it lost the Opium War in 1840, and Yunnan yielded to British and French imperialism - the French building the Hanoi-Kunming railway line to exploit the province's resources. The British occupied territory in northwestern Yunnan, and forced China to concede territory in what is now the Myanmar state of Kachin.

During the Sino-Japanese War (1937-1945), manufacturing, education, and government bodies moved to Kunming, promoting the growth of industry and the development of natural resources. Kunming became major US Air Force base during WWII, and the "Flying Tigers" earned their reputation flying military supplies and equipment into this province. On October 1, 1949, Mao Tse Tung announced the founding of the People's Republic of China and Yunnan was peacefully taken over by Red Army troops under General Lu Han on December 9, 1949. In March 1950, the People's Government of Yunnan Province was established.

The Cultural Revolution and the Second Indochina War were both trying times for the province. But since then, large-scale economic development has taken place and great efforts have been made to increase trading capacity, stabilize prices, and enhance living standards in both urban and rural areas.